Spatial and Temporal Variability in the Ridge and Runnel Morphology along the North Lincolnshire Coast

by
Selma Tamara van Houwelingen

Doctoral Thesis

Submitted in partial fulfilment of the requirements
for the award of
Doctor of Philosophy of Loughborough University

February 2005

I dedicate this thesis with immense gratitude and all my love to my father, my mother, my brother and my Lucho

ABSTRACT

Ridges and runnels are low-amplitude, shore-parallel bars and troughs in the intertidal zone of macrotidal sandy beaches. Ridge and runnel beaches are very common in the United Kingdom, particularly in the vicinity of large river outlets. Hence, an understanding of its dynamics will increase our understanding of British coastal processes, which may be useful in national coastal management plans.

A number of studies have focussed on the morphodynamics of ridges and runnels, however, the main shortcoming of these previous studies is that the morphodynamics have generally been considered at limited spatial and temporal scales. This research investigates the ridges and runnels on a variety of scales and is innovative in the sense that small-scale morphodynamic behaviour is attempted to be linked to large-scale and long-term dynamics. The study area is the north Lincolnshire coast, east England, where generally 3–5 well-developed ridges and runnels are present.

A detailed DEM obtained by LIDAR showed that the largest ridges occur around MSL and that the spacing of drainage channels was directly related to the amount of water that needs to be drained during the falling tide. Along parts of the study area, a wide intertidal flat and salt marsh is present in the upper intertidal zone, and here the ridges are more frequently dissected by drainage channels.

Ridges and runnels are very dynamic, particularly on an intra-annual time-scale. A distinct seasonal variation in forcing conditions is reflected in the ridge and runnel morphology, resulting in fewer ridges during the winter. This 'resetting' of the intertidal profile inhibits the tracking of individual ridges from year to year, so any inter-annual variability is difficult to detect. It was clear though that ridge and runnel morphology is a permanent feature along the north Lincolnshire coast, but that individual ridge and runnel couplets are not permanent.

Monthly morphological changes reveal the importance of longshore sediment transport and the ridges migrate alongshore at a rate up to 1 m a day. Onshore and offshore migration of individual bar crests is clearer on a daily to weekly time scale and migration rates range from insignificant to 1.6 m per tidal cycle. The morphological responses over these shorter timescales are mainly accomplished by swash and surfzone processes. Although these two types of wave processes induce similar rates of morphological change, the action of surfzone bores tend to be dominant in controlling

the onshore or offshore migration of bars crests, simply because of longer residence times over a tidal cycle.

The ridges, the runnels and the drainage channels form three distinct sub-environments on a ridge and runnel beach, each with different hydrodynamic processes, sediment transport patterns and bed morphology. The ridges are subject to the most diverse range of wave-processes, often experiencing swash, surf and shoaling wave processes, whereas the runnels are characterised by the prevalence of long-shore currents. The degree of tidal control on the long- and cross-shore current velocities varies across the intertidal zone and with varying wave-energy conditions. The presence of drainage channels established a seaward flow of water and sediment directly from one runnel to a seaward-lying runnel and this may reduce onshore migration rates of the ridges.

Energetics- and acceleration-based sediment transport models were not able to predict the complex patterns of sediment transport and they need further adjustment to enhance the capacity to predict morphological change for ridge and runnel morphology.

Finally, the morphological response of the intertidal bar morphology is considered to be a combination of forcing-, relaxation time- and feedback-dominated response and observations are compiled into a proposed morphodynamic model.

KEYWORDS

Ridges and runnels; intertidal bars; beach morphodynamics; macrotidal beach; LIDAR; waves; currents; tide; north Lincolnshire.

ACKNOWLEDGEMENTS

This research is funded by NERC grant NER/M/S/2000/00281 ('Spatial and Temporal, Variability in Ridge and Runnel morphology') and the Faculty of Social sciences of Loughborough University. Sea level, wave buoy and meteorological data were provided by the British Oceanographic Data Centre, the British Meteorological Office and the British Atmospheric Data Centre, whereas long-term beach profile data and aerial photographs were made available by the Anglian Regional office of the Environment Agency and the Aerial Photography section of the Unit for Landscape Modelling of Cambridge University. The Geography Department of Utrecht University, the Netherlands, kindly offered the use of their hydrodynamic equipment. Thanks to Dr Aart Kroon in particular, for helping to arrange that. Thanks as well to John Walker, assistant site manager for English Nature, and the RAF Donna Nook to 'open' the beach for research.

Thanks to Dr Edward J. Anthony and Dr Paul Wood for being the examiners of my thesis.

I would like to express my sincere gratitude to my principal supervisor, Dr Gerhard Masselink, for his support and contributions, and for offering me the framework to carry out this project. Gerd, you always said that doing a PhD was a process with a steep learning curve. Well indeed, when I look back I have learned tremendously! I have benefited from your professional guidance, your constructive advice and, not least, from your enthusiasm to investigate coastal processes. I also would like to thank you on a more personal level, particularly for your understanding and patience during a period of prolonged illness. I hope I made up the delay by providing you real Dutch liquorice from time to time!

A big thanks to my other supervisor, Dr Joanna Bullard, for her indispensable advice and her encouragement. Also thanks to Professor Helen Rendell, my Director of Research. I would like to thank Professor Ian Reid, Head of Department, to arrange financial support after my 3-year research period had finished. Thanks as well to all the other staff and postgraduate students in the department for providing a well-organised and friendly working atmosphere.

A very big thanks to everyone that helped me in the field and in the lab: Aafke Tonk (thanks for reading parts of this thesis too!), Judith Snepvangers, Susanne Quartel, Petra Dankers, Darren Evans, Martin Austin and many undergraduate students of which I'd especially like to thank Duncan, Kirsty, Ian and Kathy. You helped me from sunny summers to stormy winters and from dawn to dusk and yes...even in the middle of the night! The team spirit was high and you never let me down, not even in moments that the last place to be was the beach. Your hard work and participation made our teamwork very efficient and resulted in the collection of a very comprehensive data set. Thanks!

Finally a very warm 'thank you' to all the people that supported me personally. Papasee, Mam, Titus and Ka, I could not wish for a nicer family, thanks for your love and care. Also thanks to my in-laws, Family Rivera, I am so touched by your warm attitude and encouragement. Dunja, Han, Arjen, Kini, RJ and Pauline, your support has been unconditional and I am amazed how our friendships gained so much more depth, regardless of the North sea extending between us! Thanks as well to my 'new' friends in Loughborough: Pablo, Fer, Yubiri, Alberto, Aafke, Cyriel, Ben and many more. Each one of you made my time in England so much more fun! Lucho, mi amor, you are last in my list, but definitely not least! Your love, support, understanding and attitude is so amazing. Many times you gave me the energy to keep going in a happy way. :o)

CONTENTS

LIST OF FIGURES

LIST OF TABLES

Chapter one

Introduction

1.1 MOTIVES AND SCOPE OF STUDY

On many wave-dominated sandy beaches, the unconsolidated sediments are arranged into nearshore bars, both in the intertidal and subtidal zones. Nearshore bars develop under a wide range of hydrodynamic conditions and are one of the most dynamic elements of the nearshore profile. They play an important role in protecting the subaerial beach from storm erosion, but most research into their dynamics has focussed on subtidal bar systems. The topic of the present study is intertidal bar systems. In low- to medium-wave energy, macrotidal coastal settings, it is common for the intertidal zones of low-gradient, sandy beaches to be characterised by a series of shore-parallel bars and troughs (Figures 1.1 and 1.2). Such multiple intertidal bar morphology is referred to as 'ridge and runnel topography' (King and Williams, 1949) or 'low-amplitude ridges' (Wijnberg and Kroon, 2002).

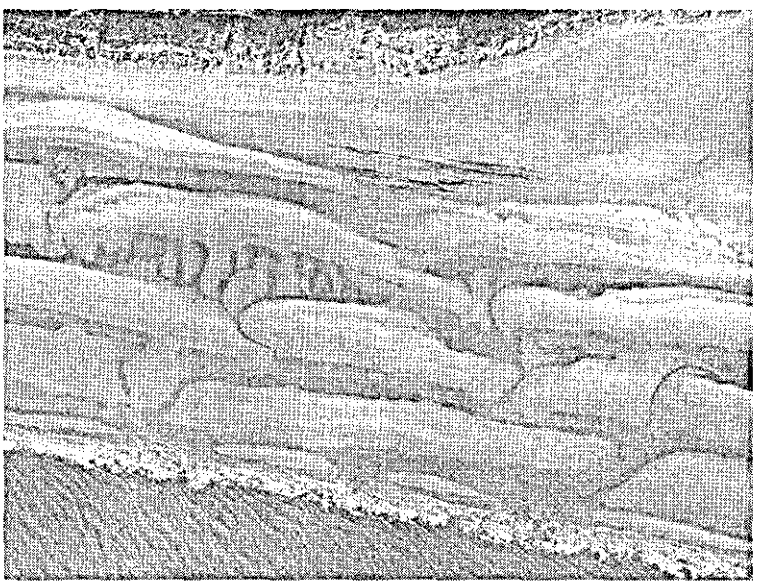

Figure 1.1 – Aerial photograph of ridges and runnels along the north Lincolnshire coast. The width of the ridge and runnel zone is c. 450 m.

In this study, the term 'ridges and runnels' is applied as defined originally by King and Williams (1949), i.e., for the shore-parallel morphological highs and intervening lows that have formed in the *intertidal* zone of low-energetic macrotidal beaches. North American scientists have used the same nomenclature for onshore migrating nearshore bars that have formed in the *subtidal* zone during storm-recovery beach profile adjustments (e.g., Hayes, 1967; Hayes and Boothroyd, 1969). The North American

convention, however, is a descriptive term, whereas the original terminology has genetic implications (Orford and Wright, 1978; Orme and Orme, 1988).

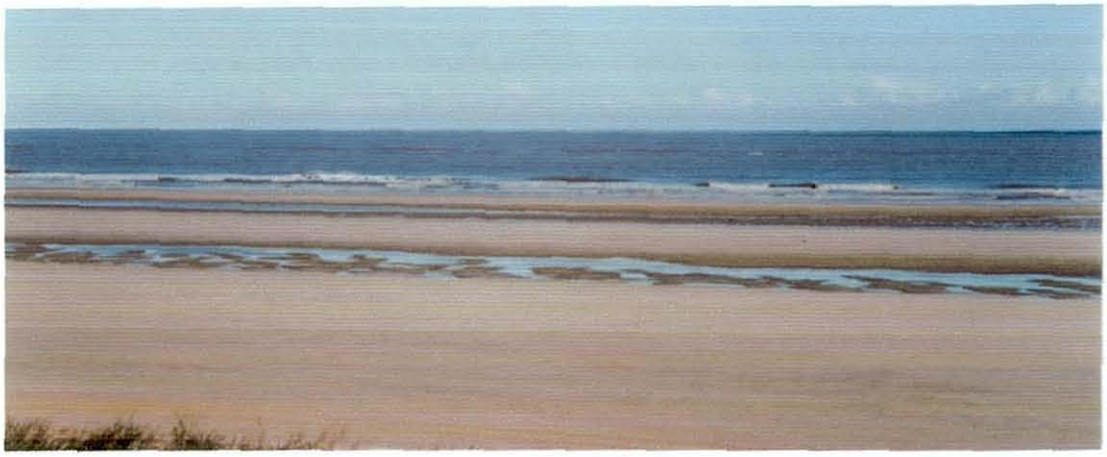

Figure 1.2 – Beach view of ridge and runnel morphology, Mablethorpe, north Lincolnshire.

Ridge and runnel morphology is very common in the United Kingdom (Figure 1.3 and Table 1.1). Long stretches (> 5 km) with well-developed ridges and runnels occur on beaches characterised by a large tide range (TR > 6 m), low wave energy conditions (H_{10} < 0.5 m) and a location in the vicinity of estuaries (e.g., Ribble, Mersey, Humber), whereas the occurrence of small coastal stretches (< 5 km) with ridge and runnel morphology are less restricted to specific tidal and wave-energy conditions. Ridge and runnel morphology is mostly backed by natural dunes, either with or without a transition zone in the form of a sand flat, but they have also been observed on beaches with small engineering structures, such as seawalls, groins and piers. Table 1.1 further suggests that sandy beaches subject to smaller tidal ranges and/or larger waves tend to be characterised by the presence of just one distinct intertidal bar.

Ridges and runnels are subject to continuously altering hydrodynamic conditions and therefore form a very dynamic morphological system. Semi-diurnal tidal water level variations are commonly larger than 3 m and result in a significant oscillation of the waterline and littoral zones across the intertidal beach (Masselink, 1993). The tidal variation over a lunar tidal cycle and the effects of changing wave-energy conditions influence the behaviour of ridges and runnels on larger temporal scales.

As ridge and runnel beaches are very common in the United Kingdom, the present study increases the understanding of coastal processes and morphological change along the British coast. Additionally, more than 70% of the world's sandy coastlines have been undergoing net erosion over the past decades (Bird, 1985) and to counter this erosion, adequate coastal defence strategies are necessary, based on a sound understanding of coastal sediment transport processes. This study contributes to this understanding by investigating nearshore processes and morphology along a stretch of coastline characterised by ridge and runnel morphology.

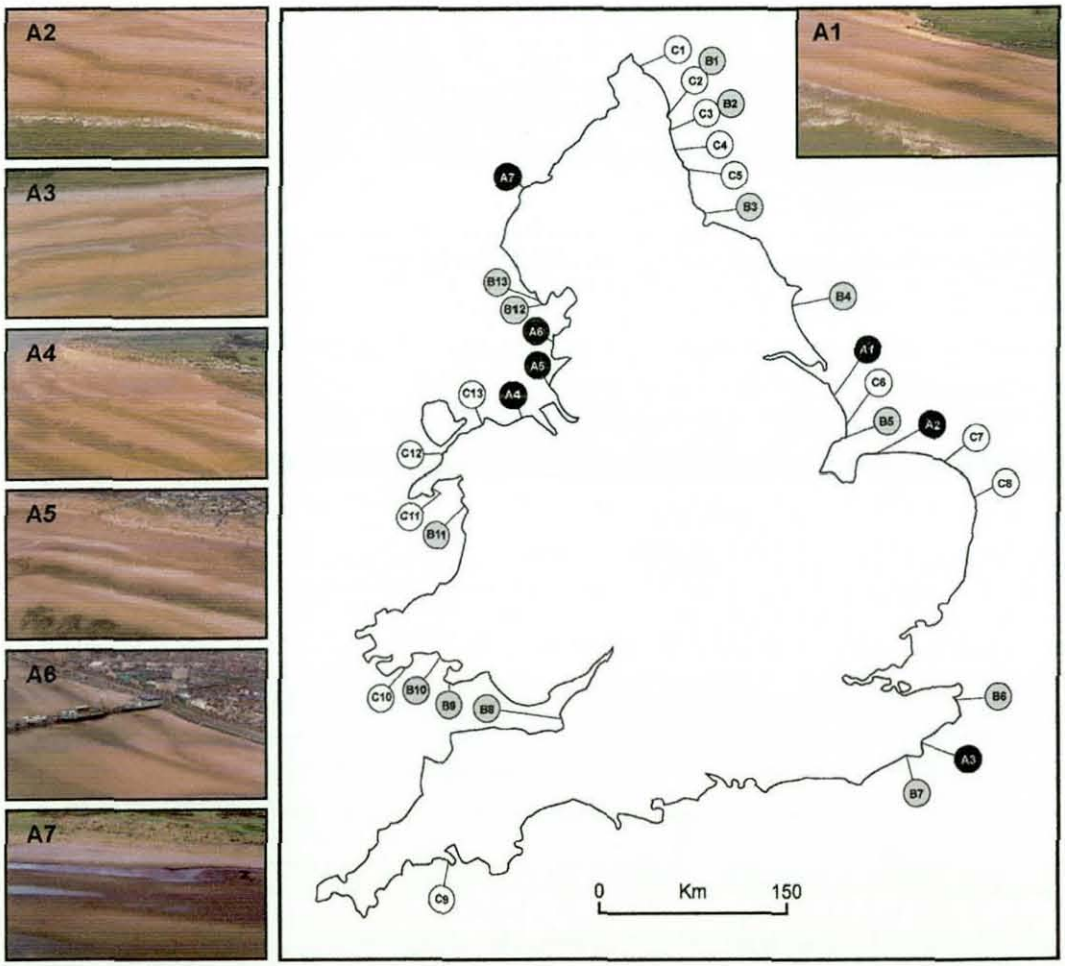

Figure 1.3 – Beaches with intertidal bar morphology along the coast of England and Wales: (A) extensive stretch of coast with multiple intertidal bars (black); (B) limited stretch of coast with multiple intertidal bars (grey); and (C) extensive stretch of coast with single intertidal bar (white). Data are derived from a video of the whole coastline of England and Wales (taken as part of DEFRA's Futurecoast project; Burgess et al., 2002), complemented by aerial photographs and field visits For more information on the intertidal bar locations refer to Table 1.1.

Table 1.1 – Characteristics of beaches with intertidal bar morphology along the coast of England and Wales as observed in early 2001: number of bars (N), length of barred coast (L in km), type of landward transition (Tr: d = dunes, f = tidal flat, c = cliff, i = inlet and s = seawall), 10% exceedence significant inshore wave height (H_{10} in m; derived from the Wave Climate Atlas of the British Isles (Draper, 1991) and mean tidal range (T in m; derived from the Admiralty Tide Tables (2004)). For location of sites refer to Figure 1.3.

	Location	N	L	Tr	H_{10}	TR		Location	N	L	Tr	H_{10}	TR
A1	North Lincolnshire	3	18	d	0.25	6.1							
A2	Northwest Norfolk	3	32	dcs	0.3	5.9	B11	Barmouth	2	1-2	d	0.75	4.4
A3	Dymchurch	4	8	s	0.6	6.7	B12	Piel Island	3	1-2	-	0	8.2
A4	Rhyl	4	15	d	0.25	7.5	B13	Barrow-in-Furness	3	1-2	d	0	8.2
A5	Formby Point	3	18	f	0.5	8							
A6	Blackpool	3	7	s	0.5	7.9	C1	Cheswick Black Rocks	1	3	f	0.5	4.2
A7	Silloth	2	9	d	0.4	8.1	C2	Alnmouth Bay	1	5	d	0.75	4.2
							C3	Druridge Bay north	1	5	d	0.75	4.2
B1	Alnmouth Bay	2	1-2	i	0.75	4.2	C4	Blyth	1	5	dc	0.75	4.2
B2	Druridge Bay south	3	1-2	d	0.75	4.2	C5	Whitley Bay north	1	3	s	0.75	4.3
B3	Hartlepool	2	1-2	d	0.75	4.6	C6	Sandilands-Skegness	1	17	s	0.25	6.1
B4	Hilderthorpe	2	1-2	d	0.75	5	C7	Cromer	1	6	c	0.5	4.4
B5	Gibraltar Point	2	1-2	d	0.25	6.1	C8	Hemsby	1	5	d	0.5	2.6
B6	Sandwich flats	2	1-2	d	0.5	5	C9	Whitsand Bay, Freathy	1	5	c	0.75	4.5
B7	Rye Bay	2	1-2	d	0.7	6.8	C10	Giltar Point	1	3	d	0.5	7.5
B8	Burnham on Sea	3	1-2	d	0.3	11	C11	Abersoch	1	4	d	0.6	4.3
B9	Llangennith	2	1-2	d	1	7.5	C12	Abermenai Point	1	7	i	0.5	4.1
B10	Cefn Sidan Sands	4	1-2	d	0.5	7.2	C13	Conwy-Llandudno	1	4	c	0.1	6.9

1.2 THEORETICAL APPROACHES TO UNDERSTANDING GEOMORPHIC SYSTEMS

The general approach to investigate coastal behaviour is to consider the coast as a geomorphic system. Such systems consist of a hierarchy of compartments, each with its own temporal and spatial scale according to the primary scale relationship (Kroon, 1994). A close coupling exists between the temporal and spatial scales so that both are small at lower-order compartments and large at higher-order compartments (Figure 1.4). Hydrodynamic processes, sediment transport and morphology at corresponding scales interact mutually and morphodynamic systems can be identified within each compartment (Figure 1.5). Hydrodynamic processes (waves and currents) result from the energy input by wind, tides, sea level and offshore waves and subsequently convert part of their energy into sediment transport. Gradients in sediment transport result in morphological change, which in turn influences the hydrodynamics. These interactions are often non-linear. For example a threshold value of a hydrodynamic variable must be exceeded in order to mobilise the sediment (Shields, 1936), however, once initiated, the sediment flux is proportional to the cube of the flow velocity (e.g., Bailard and Inman, 1981). In addition, a time lag between a change in hydrodynamic conditions and

morphological response is common. The time lag can be subdivided into the reaction time, the interval between the change in the force and the start of morphological change, and the relaxation time, the interval over which the morphology adjusts to the hydrodynamics (Kroon, 1994). The reaction time may often be neglected in high-energy coastal systems with sandy sediments. The relaxation time is proportional to the morphologic inertia within a system and is a function of the intensity of hydrodynamic processes and the volume of sediment involved in the morphological adjustment.

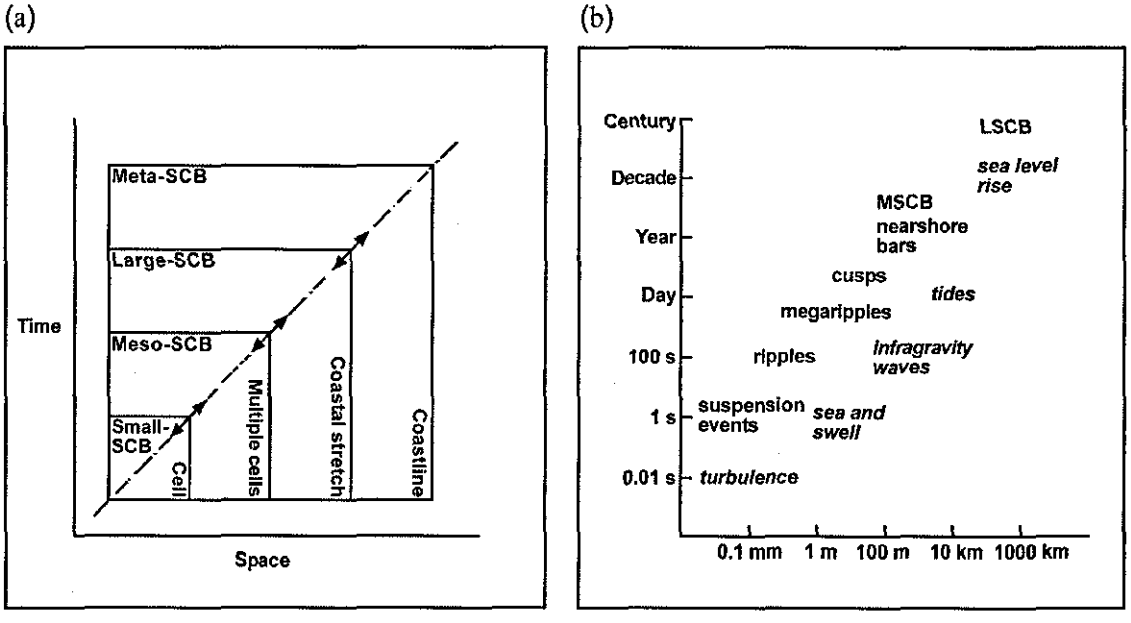

Figure 1.4 – Primary scale relationship: (a) coastal geomorphic system with hierarchy of compartments (after Kroon, 1994); and (b) temporal and spatial scales of hydrodynamics (italic) and morphology (normal) (after Ruessink, 1998). 'SCB' stands for '[...]-scale coastal behaviour', for instance meso-scale coastal behaviour (labelled in (b) as MSBC) or large-scale coastal behaviour (labelled in (b) as LSBC).

Feedback mechanisms between morphology and hydrodynamics are essential in a morphodynamic system and have a critical role in determining the evolution of a system (Phillips, 1992). A negative feedback reinforces the system to maintain a state of equilibrium, however, the tendency for coastal systems is that this state is rarely reached as the variations in the hydrodynamic forcing often occupy a smaller time span than the duration of the relaxation time of the morphology. This effect is more important at larger scales, where process-response relations are slow and long-term, than at small scales, where a dynamic equilibrium may be attained.

The relationships between the compartments are often difficult to determine as the scale dimensions between one level and the next differ too much to recognize obvious links. To upscale the morphodynamic behaviour of a smaller compartment to a larger compartment, Kroon (1994) suggests defining a new coastal parameter at each successive compartment that schematises all the process variables and explains the morphological behaviour at that level. Another approach may be the upscaling to larger-scale processes by filtering the processes at small scales (Terwindt and Battjes, 1990). The theoretical approaches to understanding geomorphic systems are discussed in further detail in Chapter 8.

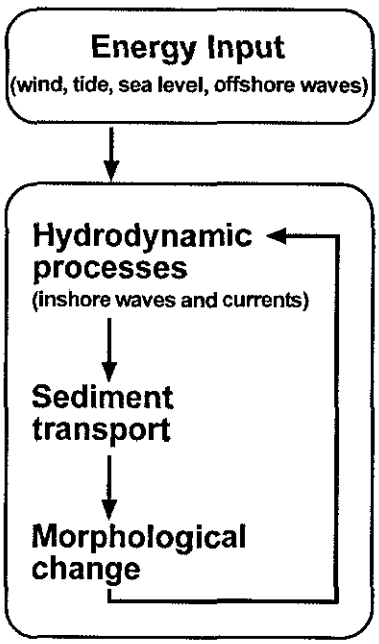

Figure 1.5 – Coastal morphodynamic system.

1.3 DYNAMICS OF RIDGES AND RUNNELS – PREVIOUS RESEARCH

In a recent review of barred beaches, Wijnberg and Kroon (2002) indicated that little is known about the generation, evolution and decay of ridges and runnels, and in fact, our understanding of such bar systems is derived from only a few investigations. King and Williams (1949) provided the first comprehensive description of ridges and runnels and proposed that the ridges are formed by swash processes, rather than breaking waves, and that they represent swash bars that have survived tidal submersion. Further studies by King (1972a) also adhered to a swash origin of the ridges and suggested that their formation is promoted by macrotidal conditions, fetch-limited waves, a low-gradient

beach and a surfeit of sediment. It was argued that the ridges are mainly found at locations on the intertidal profile where relatively stationary water levels prevail (allegedly the mean tidal levels) and that ridge height increases in the seaward direction. Additionally, ridges were considered to be relatively static features that build up under calm conditions and are flattened during storms. Although the findings by King and co-workers have become entrenched in coastal literature to represent the morphodynamic characteristics of ridge and runnel beaches, several subsequent studies (e.g., Parker, 1975; Mulrennan, 1992; Levoy et al., 1998; Sipka and Anthony, 1999; Masselink and Anthony, 2001; Kroon and Masselink, 2002; Anthony et al., 2004) have revealed characteristics and behaviour of ridges and runnels that contradict the observations by King (1972a). In fact, King's early findings are now considered site-specific (Mulrennan, 1992; Masselink and Anthony, 2001), rather than universal.

Table 1.2 summarises the environmental settings, characteristics and dynamics of several previously-investigated ridge and runnel beaches. Based on this compilation of studies, the following paragraphs review the occurrence and behaviour of ridges and runnels to evaluate and complement King's postulations. Note: this section only generally addresses the current knowledge, more specific findings are described in Chapters 3–7.

Ridges and runnels are found on beaches with tidal ranges varying from mesotidal (Mulrennan, 1992) to megatidal (Anthony et al., 2004), the latter term indicating a mean spring tidal range exceeding 8 m (Levoy et al., 2000). They tend to occur on relatively sheltered coasts where wave energy is low to intermediate and wind direction is predominantly offshore or alongshore. Ridges and runnels have also been observed, however, in more energetic and storm wave environments (Anthony et al., 2004). In Europe, ridge and runnel morphology is a common feature of sandy beaches bordering the Irish sea, the North sea and the English Channel. These beaches are all characterised by a gentle beach slope ($\tan\beta = 0.006$–0.018) and consist of fine to medium sand. The sediment budgets of ridge and runnel beaches are not necessarily characterised by accretion. For example, the erosive coast at Formby Point, northwestern England, exhibits up to 4 well-developed ridges (Parker, 1975).

Table 1.2 – Environmental conditions and morphological characteristics of previously investigated ridge and runnel beaches. Position of ridges and runnels is expressed relative to the mean spring and neap tidal levels: Mean High Water Spring (MHWS); Mean High Water Neap (MHWN); Mean Low Water Neap (MLWN); and Mean Low Water Spring (MLWS)

Research	Location	Beach conditions and characteristics					Ridge and runnel morphology						Morphological change	
		Spring (and neap) tidal ranges (m)	Wave height (m) and period (s)	Wind (-)	Beach slope (tanβ)	Grain size (μm)	Number (-)	Ridge height (m)	Ridge width (m)	Spacing of ridge crests (m)	Seaward slope (tanβ)	Position (-)	Migration	Seasonal or yearly
King and Williams (1949)	Blackpool, U.K.	8.1	-	-	0.007	-	2–6	0.6–1.1	70–183	113–226	0.02–0.03	MLWS–MHWN	Insignificant	Fair-weather: build-up; Storm: flattening
King and Barnes (1964)	Skegness-South, U.K.	-	-	Offshore	0.007	-	4	0.6–1.0	45–70	75–125	0.01–0.09	MLWN–MHWS	-	-
King and Barnes (1964)	Gibraltar Point, U.K.	-	-	Offshore	0.006	Fine (200 μm)	3	0.8–1.0	45–75	125	0.001–0.04	MLWN–MHWS	-	-
King (1972a)	Blackpool, U.K.	-	-	-	0.008	Medium (220 μm)	2–4	0.20–0.80	45–70	55–155	0.01–0.04	-	Insignificant	Fair-weather: build-up; Storm: flattening
King (1972b)	Skegness-South, U.K.	-	0.6–0.9; 6	Offshore	0.018	'sandy'	2	-	-	142	0.06	MLWN–MHWN	80 m per *year* (due to longshore sediment transport)	Fair-weather: build-up; Storm: flattening
Parker (1975)	Southwest Lancashire, U.K.	8.2	0.6–1.0; 4.0–4.5	Alongshore	-	-	3–4	0.5–1.2	-	100–120	-	-	-	-
Wright (1976)	Ainsdale, Merseyside, U.K.	-	0.6;-	-	0.01	Fine (203 μm)	3–4	0.3–1.2	45–120	75–150	0.01–0.04	MLWN–MHWN	1–2 m per tidal cycle	Fair-weather: build-up; Storm: flattening but further no yearly trend
Mulrennan (1992)	Portmanock barrier, Ireland	3.9	0.65; 4.0	Variable	0.009–0.011	-	3–4	1.25	15–110	50–125	0.01–0.03	MLWN–MHWS	10 m a month Less migration during storm recovery period	Fair-weather: build-up; Storm: flattening
Voulgaris et al. (1996, 1998)	Nieuwpoort aan Zee, Belgium	6.4; (2.7)	0.5–1.0; 4–12	Oblique onshore and alongshore	0.012	Fine (183 μm)	4	0.3–0.9	30–95	75–130	0.03–0.05	MLWS–MHWS	0.6–1.2 m per tidal cycle	-
Levoy et al. (1998)	Merlimont, France	7; (5.5)	0.3–0.5; 4–5 and 15–18	-	0.010	Fine to medium (250 μm)	3	0.80	60–105	145–160	0.02–0.06	-	Insignificant (0.3 m in two weeks)	-
Sipka and Anthony (1999)	Leffrinkoucke, France	5.6; (3.5)	0.25–1.5; 3–6	-	0.013	Fine	6	0.4–1.2	25–40	25–75	0.02–0.04	MLWN–MHWS	Insignificant	-
Chauhan (2000)	Siloth, U.K.	10	1.0 ($H_{10\%}$)	Alongshore	0.003	Fine to medium	2–3	0.1–0.4	40–85	125–150	0.01–0.04	-	-	-
Navas et al. (2000)	Dundrum, Northern Ireland	4.6	Low to moderate	Offshore	0.012	Fine to course (116–643 μm)	5–6	0.8	50–75	90–140	0.01–0.03	-	-	Storm: flattening
Masselink and Anthony (2001)	Leffrinkoucke, France	5.6	0.25–1.5; 3–6	Oblique onshore	0.015	Fine to medium (190–280 μm)	4	0.5–0.7	25–50	60–85	0.01–0.03	MLWN–MHWN	-	-
Masselink and Anthony (2001)	Blackpool, U.K.	7.9	0.4; 2–4	Alongshore	0.007-0.012	-	2–3	0.1–1.0	40–105	80–175	0.02–0.04	MLWN–MHWN	-	-
Masselink and Anthony (2001)	North Lincolnshire, U.K.	6	0.5; <4	Offshore	0.012–0.017	Fine (160–210 μm)	3–4	0.1–1.5	20–45	70–135	0.02–0.05	MLWN–MHWS	-	-
Kroon and Masselink (2002)	North Lincolnshire, U.K.	6	0.5; <4	Offshore	0.015	Fine (160–210 μm)	6	0.6–1.1	10–40	20–90	0.01–0.04	MLWS–MHWS	8 m over fair-weather lunar cycle	-
Reichmüth and Anthony (2002)	Côte D'Opale, France	5.6–7.2	0.25–1.5; 3–6	Oblique onshore and alongshore	0.01	Fine to medium (170–320 μm)	3–6	0.5–1.2	30–60	50–100	0.02–0.04	MLWN–MHWS	15 and 30 m per month for, resp., summer and winter	Most migration when successive storm events occur
Buscombe (2002)	Blackpool, U.K.	7.6	0.4; 2–4	Oblique onshore	0.007	Medium (220–240μm)	3–5	-	50–110	-	-	-	No migration over three month fair-weather period	Fair-weather: build-up
Reichmüth (2003)	Côte D'Opale, France	5.6–8.5	0.5–1.5; 6	Oblique onshore and alongshore	0.012–0.019	Fine to medium	2–5	0.3–0.8	25–60	50–110	0.01–0.05	MLWN–MHWS	0–40 m per month	Fair-weather: build-up; Storm: flattening
Anthony et al. (2004)	Merlimont, France	5	0.6; 4–9	Onshore	0.012	Fine to medium (200–400 μm)	2	1	75–100	140	0.02–0.03	MLWS–MHWN	Insignificant (over 10-day period)	Daily change same order of magnitude under fair-weather and storm

Between 2 and 6 bar-trough systems have been observed on the various ridge and runnel beaches. Ridge height rarely exceeds 1.5 m and hence ridges are small compared to subtidal bars. The seaward slope of the ridge is wide and steep with gradients up to 0.062, whereas the landward slope is generally narrow and often features a slipface. Masselink and Anthony (2001) used a large number of beach surveys collected from three localities to investigate whether the positioning of intertidal bars is related to mean tidal water levels and they determined that intertidal bars occur over the entire intertidal zone. Furthermore, there was some indication that the most pronounced bar systems are located around the mid-tide position, i.e., where the water level is least stationary, and that the smallest ridges are found low in the intertidal profile. These findings confirm the observations by Wright (1976), Mulrennan (1992), Levoy et al. (1998), Sipka and Anthony (1999) and Reichmüth and Anthony (2002), and in fact King (1972a) was the only one to suggest a seaward increase in ridge size. The spacing of the ridges is determined by a complex combination of beach gradient, tidal translation rate, breaker height, relaxation time and the degree of protection of inner ridges by outer ridges (Orford and Wright, 1978), and hence varies significantly between the various beaches (25–175 m). Also, the mobility of ridges and runnels is remarkably variable as they seem relatively static features on some beaches (King, 1972a; Wright, 1976; van den Berg, 1977; Navas et al., 2001), but migrate significantly on others (Mulrennan, 1992; Kroon and Masselink, 2002; Reichmüth and Anthony, 2002).

A number of mainly hydrodynamic field studies have recently been conducted (Voulgaris et al., 1996, 1998; Levoy et al., 1998; Sipka and Anthony, 1999) and although these investigations have contributed to our understanding of wave-current processes on ridge and runnel beaches, they have provided limited insight into the morphodynamics of the intertidal bar systems. Subsequent work by Kroon and Masselink (2002), however, addressed the morphodynamic roles of swash action and surf zone processes (breaking waves and bores). They examined the morphological response of ridges and runnels over a spring-to-spring tidal cycle under low-wave conditions and coupled the observed morphological change to the local tidal water level variations and related residence times for swash and surf zone processes. The latter played the major role in the onshore migration of the intertidal bars and it was concluded that ridges can not be considered swash bars. Most recently, Anthony et al. (2004) investigated ridge and runnel morphology over a 10-day period under both, high-

and low-wave conditions. They observed that the spatial pattern of morphological change was poorly correlated with wave energy level and tidal residence times, but reflected local morphodynamic feedback effects due to breaks in slope associated with the bar-trough morphology. They also alluded to the importance of strong flows in the runnels potentially inhibiting cross-shore migration of the ridges.

A significant limitation to previous investigations of ridge and runnel dynamics is the lack of information regarding their large-scale (> 1 km) characteristics and long-term (> month) behaviour. Most studies have focussed on a single beach transect, or at most a number of transects, and not much is known about the longshore morphological variability of the ridges and runnels. Similarly, the factors controlling morphological changes over single and lunar tidal cycles may be reasonably well understood (Kroon and Masselink, 2002; Anthony et al., 2004), but the intra- and inter-annual behaviour of ridge and runnel morphology is less clear. On a smaller scale, the fate of sediment once swept over a ridge crest and the relevance of drainage channels in controlling sediment transport pathways has not been addressed. What is equally unclear is how sediment transport processes operating over shorter time scales are linked to morphological changes occurring over longer time scales (cf., Terwindt and Battjes, 1990). As pointed out by Wijnberg and Kroon (2002), long-term bar behaviour can only partly be explained by meteorological and oceanographic forcing, and additional knowledge of the role of relaxation time and morphological feedback is needed. Furthermore, the lack of knowledge concerning the initial formation of ridges and runnels has been intriguing and although recent speculations are increasingly well-substantiated (Masselink and Anthony, 2001; Kroon and Masselink, 2002; Reichmüth, 2003; Masselink, in press), the issue remains unsolved due to the lack of in-situ measurements during ridge formation.

1.4 OBJECTIVES AND OUTLINE OF THESIS

The aim of the present study is to investigate the morphodynamics of ridge and runnel morphology at a range of nested spatial and temporal scales, drawing upon Kroon's (1994) concept of a coastal geomorphic system with a hierarchy of compartments (Figure 1.6). More specifically, the objectives are:

(1) to document the longshore morphological variability in ridge and runnel morphology along a coastal stretch (Figure 1.6, level D);

(2) to improve insight into the inter- and intra-annual behaviour of the ridges and runnels (Figure 1.6, respectively level C and E);

(3) to describe and explain temporal and spatial variability in ridge and runnel dynamics under varying tidal and wave-energy conditions (Figure 1.6, level A and B); and

(4) to yield additional insight into the controlling processes for maintenance and evolution of ridge and runnel topography.

The investigation of the mechanisms underlying the initial formation of ridge and runnel morphology is beyond the scope of this thesis.

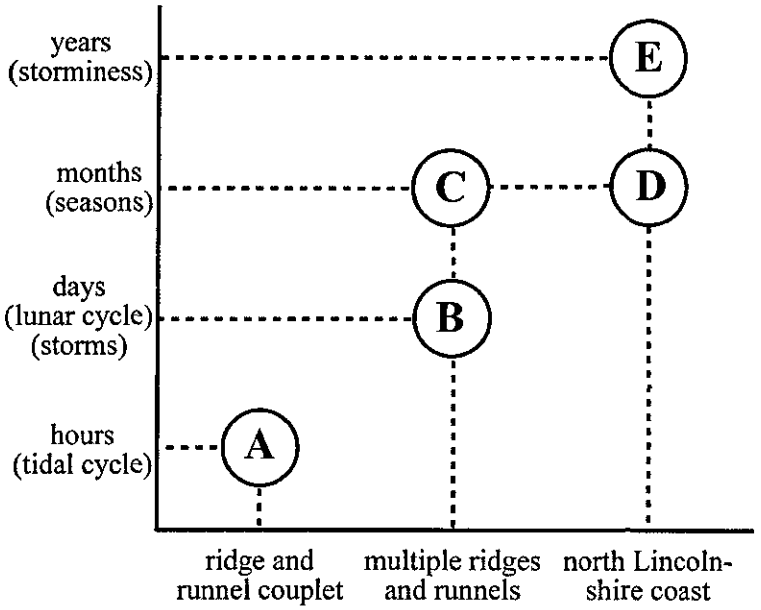

Figure 1.6 – Primary scale relationship diagram for present study.

The outline of the thesis is visualised in Figure 1.7. The thesis first describes the oceanography and coastal geomorphology of the north Lincolnshire coast where the study was conducted (Chapter 2). This is followed by a description of the longshore variability of the intertidal bar geometry using a digital elevation model of the intertidal area obtained by LIDAR (Chapter 3). Inter-annual ridge and runnel behaviour at three selected sites is discussed next, based on annual aerial photographs and twice-yearly beach profiles (Chapter 4). This is followed by an analysis of monthly beach profiles for the same selected sites to investigate the degree of seasonal variability in the morphology (Chapter 5). The results of two field campaigns during which wave, currents and morphology were monitored intensely at a single location are then described to discuss the ridge and runnel dynamics over a lunar (Chapter 6) and single

(Chapter 7) tidal cycle. The thesis concludes by a synthesis to compile the observations at the various spatial and temporal scales (Chapter 8).

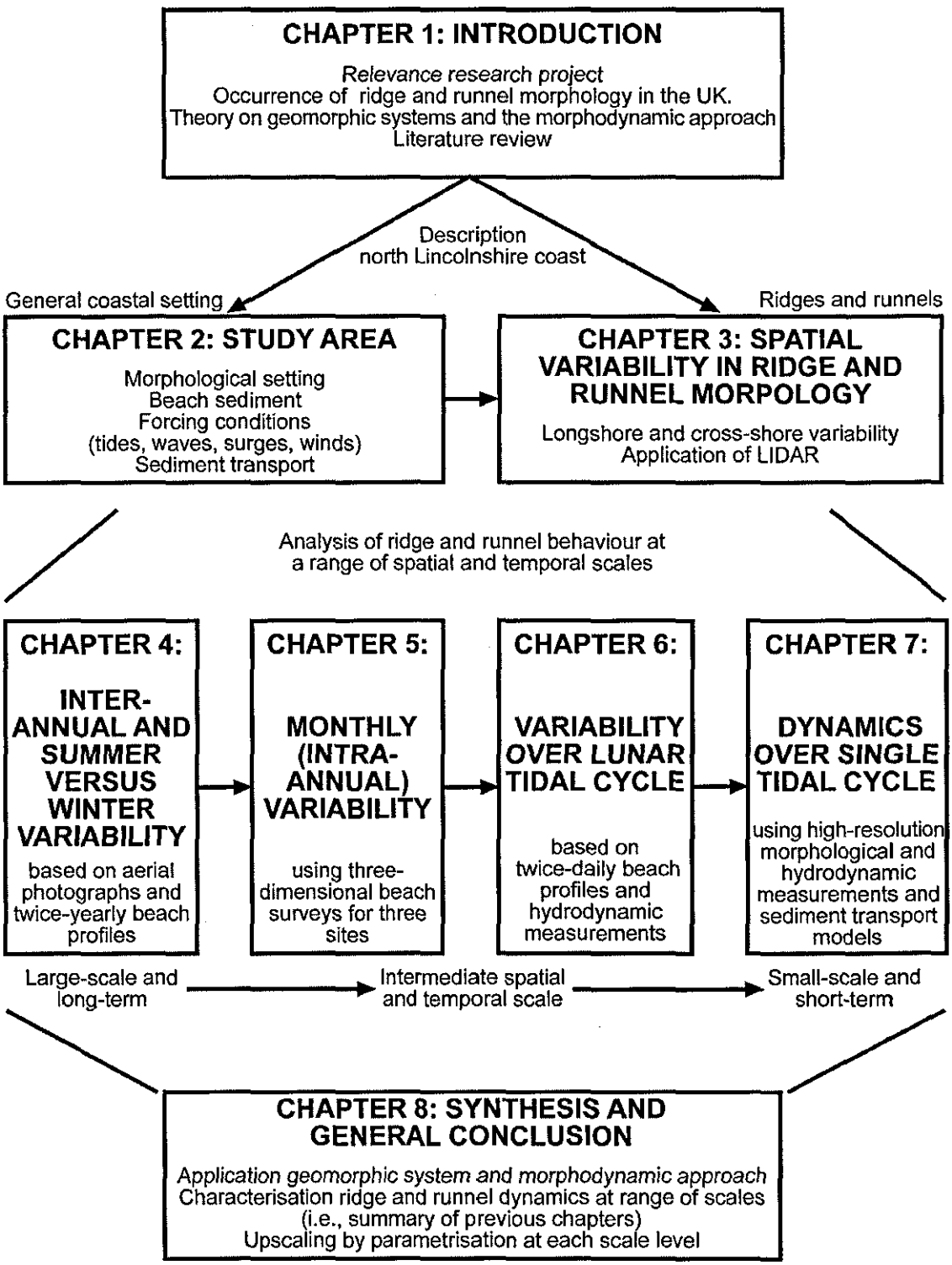

Figure 1.7 – Map showing outline of thesis

Chapter two

The North Lincolnshire Coast

2.1 MORPHOLOGICAL SETTING

The north Lincolnshire coast, extending c. 16 km from Donna Nook in the north to Mablethorpe in the south (Figure 2.1), is one of the longest coastal stretches with ridge and runnel morphology in the United Kingdom. It can be considered the southern part of the ebb-tidal delta of the Humber and represents an area of long-term accretion (Pethick, 2001). Offshore sand banks act as a sediment source for the beaches (Halcrow, 1988) and beach extension coincides with a steepening of the intertidal profile as the high-water mark advances more rapidly than the low-water mark, particularly between Donna Nook and Saltfleet (Posford Duvivier, 1996).

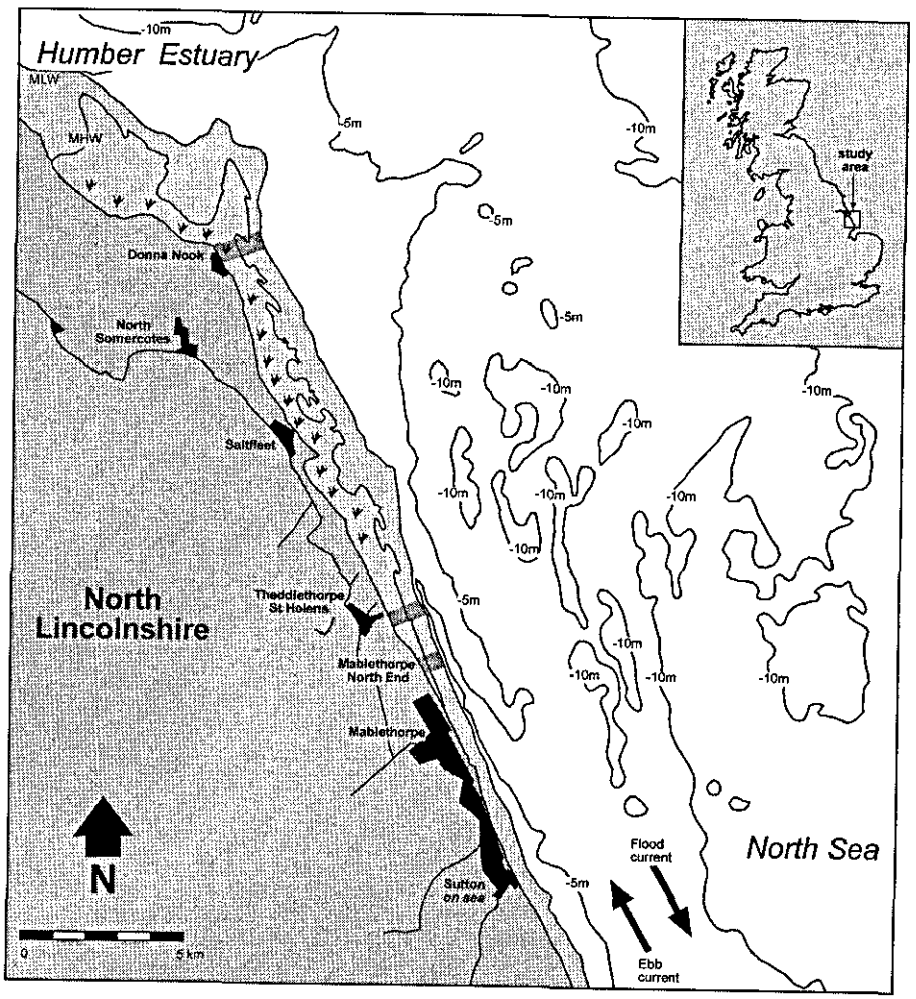

Figure 2.1 – Location map of the study area. The light-grey patch represents the intertidal zone and the rectangular patches indicate the study sites (from north to south: Donna Nook, Theddlethorpe and Mablethorpe North End). The occurrence of salt marshes is marked using vegetation symbols. MHW and MLW are the mean high water and mean low water lines, respectively. Subtidal bathymetry is indicated with the –5 and –10 depth contours

The region is characterised by pronounced multiple intertidal bar morphology along its entire length. In any one year, 3–5 intertidal bars are present with a typical height and spacing of 1 m and 100 m, respectively (Masselink and Anthony, 2001). The intertidal gradient is 0.01–0.015, but the seaward slopes of the bars are significantly steeper and have gradients up to 0.05.

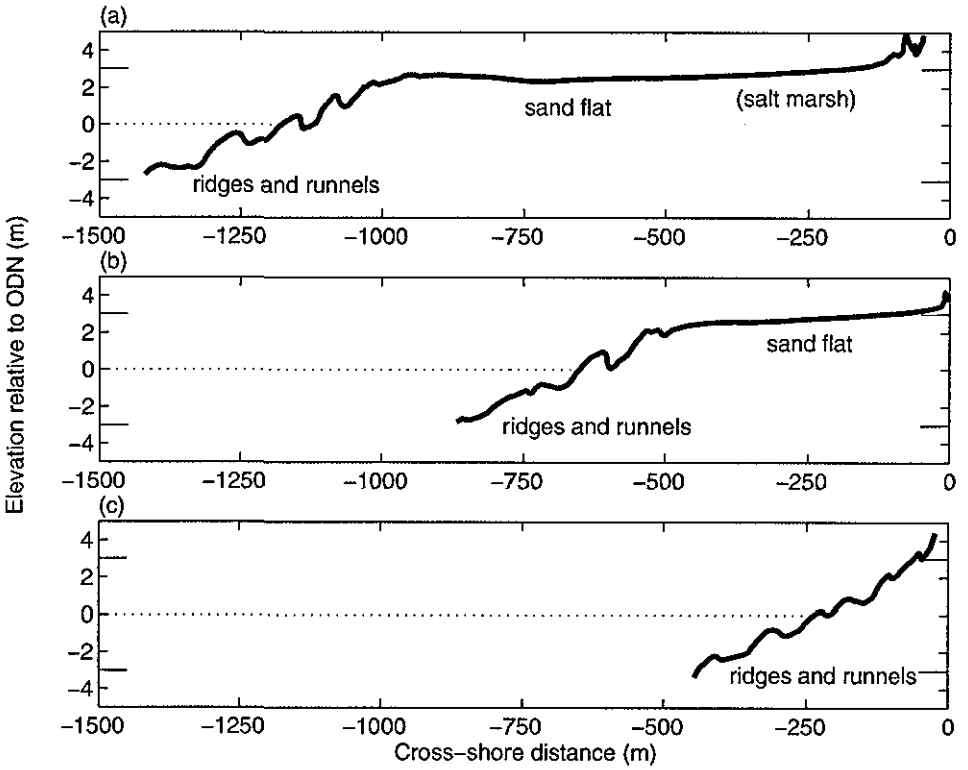

Figure 2.2 – Beach profiles along the north Lincolnshire coast at: (a) Donna Nook; (b) Theddlethorpe; and (c) Mablethorpe. The horizontal dotted line represents mid-tide level (MSL) and the small horizontal lines indicate MHWS (top) and MLWS (bottom).

This investigation is concerned with the entire north Lincolnshire coast, but attention is focussed on three locations in particular: Donna Nook, Theddlethorpe and Mablethorpe North End (Figure 2.1). All sites are characterised by pronounced intertidal bar morphology, but differences exist between the three localities (Figure 2.2). Specifically, the gradient of the ridge and runnel zone at Donna Nook ($\tan\beta = 0.012$) is less than at Theddlethorpe ($\tan\beta = 0.013$) and Mablethorpe ($\tan\beta = 0.015$). The width of the ridge and runnel zone decreases concurrently with the steepening of the intertidal zone from 460 m at Donna Nook to 410 m at Mablethorpe. The ridges and runnels are backed by an almost horizontal sand flat, although in the south they directly front foredunes. The

width of the sand flat at Donna Nook and Theddlethorpe is 1 km and 500 m, respectively, and the upper parts of the sand flat immediately north and south of Donna Nook exhibit well-developed salt marshes. The coastline is devoid of coastal engineering structures.

2.2 BEACH SEDIMENT

The beach is composed of fine to medium sand, but spatial variations in the textural characteristics exist. Sediment samples of the upper 0.02 m of the beach surface were collected from the intertidal zone to determine the spatial and temporal variability in sediment size, and included:

(1) samples taken along nine cross-shore transects at Theddlethorpe (September 2001) to document intra-site spatial variability;

(2) samples from the crests of ridges, the runnels and the sand flats along three cross-shore transects at, respectively, Donna Nook, Theddlethorpe and Mablethorpe (February 2001) to examine inter-site spatial variability; and

(3) monthly samples from the crests of ridges and from the runnels along one cross-shore transect at Theddlethorpe over the period February 2001 till January 2002 to investigate seasonal variability.

The sediment samples were rinsed with water to remove salt and wet-sieved through a 63 μm sieve to isolate sand from mud. The sand fraction of the samples was analysed using a settling tube and the fall velocities from the analysis were converted to grain sizes applying the equations of Hallermeier (1981) and Pettijohn et al. (1987). The mud fraction was not analysed as it was noticed during sampling that the accumulation of mud was highly irregular due to the occurrence of local depressions such as the troughs of ripples and dunes.

The grain size D_{50} ranged from 160 to 275 μm across the intertidal zone at Theddlethorpe, and the average grain size below MSL (190 μm) was found to be finer than above MSL (230 μm) (Figure 2.3a). This textural break was also observed by Kroon and Masselink (2002) during a field study in summer 2000. In addition, sediments in the runnels were 20–30 μm finer than those on the ridges and the coarsest sediments on the ridge occured just seaward of the crest. As opposed to the distinct

cross-shore variation, the intra-site alongshore variability at Theddlethorpe was insignificant. On the inter-site scale, however, alongshore variability was larger and sediment size at Donna Nook (D_{50} = 205 μm) was found to be significantly finer than at Theddlethorpe (D_{50} = 225 μm) and Mablethorpe (D_{50} = 215 μm) (Figure 2.3b). As at Theddlethorpe, a textural break at MSL occurred at the other sites and the ridges tended to be coarser than the runnels, especially below MSL. The sediments on the sand flats were relatively coarse, in particular for Theddlethorpe where the sand flat was even coarser than the ridges. A seasonal variation in grain size was not distinct from monthly sediment samples over 2001. The textural break at MSL, however, was present throughout the year.

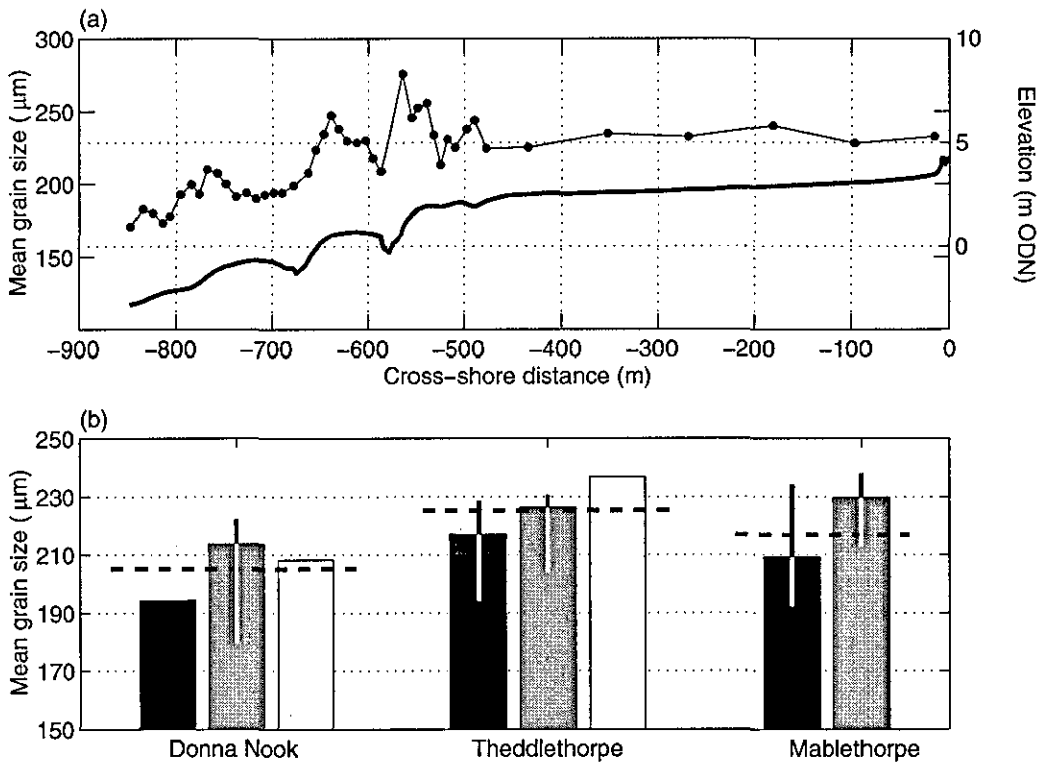

Figure 2.3 – Spatial variability in sediment size: (a) Cross-shore variation in D_{50} at Theddlethorpe, September 2001 (thin line with marks). The thick line represents the beach profile. (b) Average D_{50} at Donna Nook, Theddlethorpe and Mablethorpe. The thick, dashed horizontal lines represent the average of all samples taken at one site, whereas the black, grey and white bars symbolise the runnels, the ridges and the sand flats, respectively. Vertical lines are used to differentiate between the ridges and runnels above MSL and below MSL: white and black lines represent the difference between the mean of all the ridges (or runnels) and the mean of only those below MSL or above MSL, respectively.

2.3 TIDAL, WIND, SURGE AND WAVE CONDITIONS AND SEDIMENT TRANSPORT PROCESSES

The north Lincolnshire coast is characterised by macrotidal, semi-diurnal tides (Davies, 1964) and low to medium wave-energy conditions. The mean spring and neap tide ranges are 6 m and 2.85, respectively, and the tidal levels are: MLWS = –2.85 m, MLWN = –1.25 m, MHWN = 1.55 m and MHWS = 3.15 m (all relative to Ordnance Datum Newlyn (ODN), which is approximately mean sea level) (Admiralty Tide Tables, 2004, standard port Immingham, secondary port Skegness). Figure 2.4a shows an example of predicted water level variation over two lunar tidal cycles, the second cycle including the largest predicted tides of the year during the equinoxes in March. The tidal wave along the north Lincolnshire coast is slightly asymmetric with flood times being shorter than ebb times, except during neap tide conditions (Figure 2.4b). The average flood and ebb times are 5.9 and 6.5 hours, respectively.

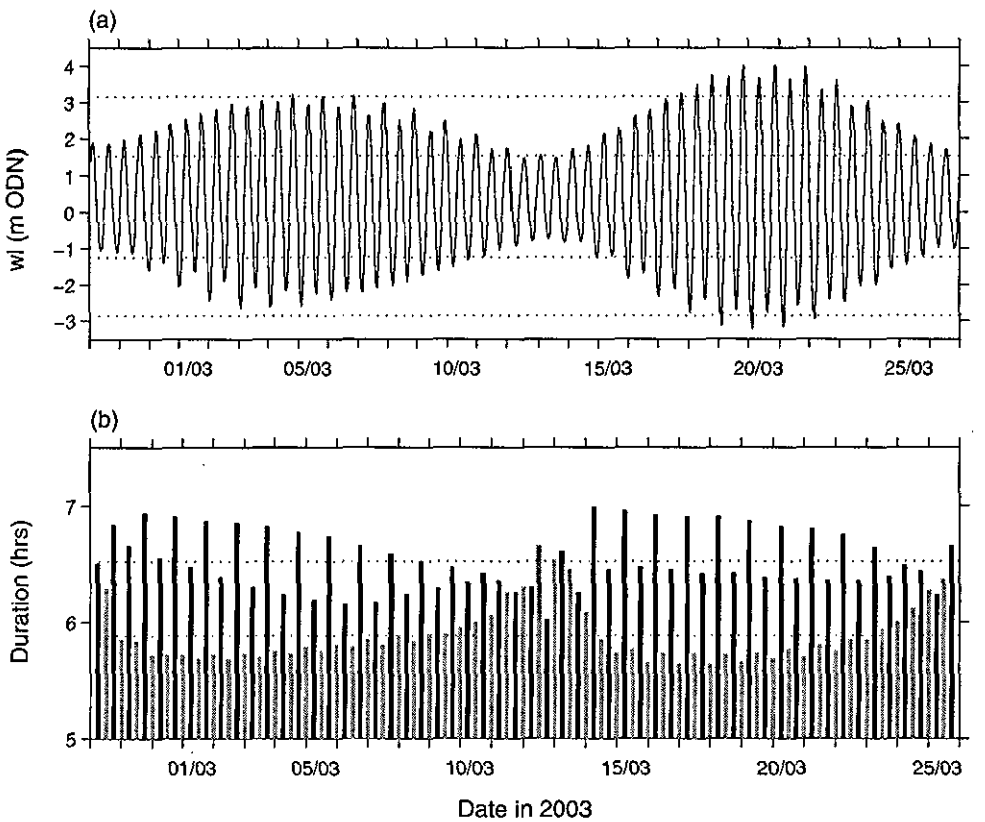

Figure 2.4 – Tidal conditions for Skegness (20 km south of study area) over two lunar tidal cycles: (a) predicted tidal water level; (b) ebb- (black) and flood (grey) durations.

Tidal currents flow southward during the flood and northwards during the ebb and the tidal residual current is directed to the south (Motyka, 1986). Residual currents are, however, weaker in summer than in winter (Simpson, 1994). Tidal currents in and out of the Humber estuary complicate the current regime at Donna Nook, particularly during the ebbing tide when the Humber outflow collides with the open coast currents. In the Humber Estuary itself, flood flows dominate the southern side of the estuary, whereas ebb channels tend to form at the north side (ABP, 1996).

Winds are predominantly from the southwest (Pye, 1995) and hence are mainly offshore (Figure 2.5a). During the winter months, however, the development of high pressure systems over northern Europe can lead to prolonged northwesterly to easterly winds (Odd et al., 1995). Wind speed varies between 3.4–7.9 m s^{-1} the majority of the time, although northerly winds in particular tend to be relatively strong (> 13.9 m s^{-1}). The wind climate at the Lincolnshire coast is very consistent from year to year (Figure 2.5b).

Occasionally, the area experiences large surges in water level and the 1 in 50 year storm surge residual is c. 2.5 m (Southgate and Beltran, 1998). Storm surges normally develop as deep low pressure systems tracking eastward toward the North Sea and moving around the North Sea basin in an anticlockwise circulation. This causes increased surge levels along the east coast of England due to the funnelling effect as the surge travels south.

Offshore wave conditions along the Lincolnshire coast are characterised by a 50% exceedence significant wave height of 0.5 m and a modal wave period of less than 4 s (Draper, 1991). Wave roses are shown for three locations along the north Lincolnshire coast, illustrating the wave climate at c. 3 km offshore (Figure 2.6). The 1 in 1 year and 1 in 100 year significant wave heights have been calculated applying statistical techniques on wind data from an offshore light vessel, taking into account the effect of the sea bed on the waves as they approach the coast (Posford-Duvivier, 1996). The wave roses indicate that the exposure of the coastline to wave energy increases to the south and that the largest waves approach from the north-east, i.e., with the longest fetch.

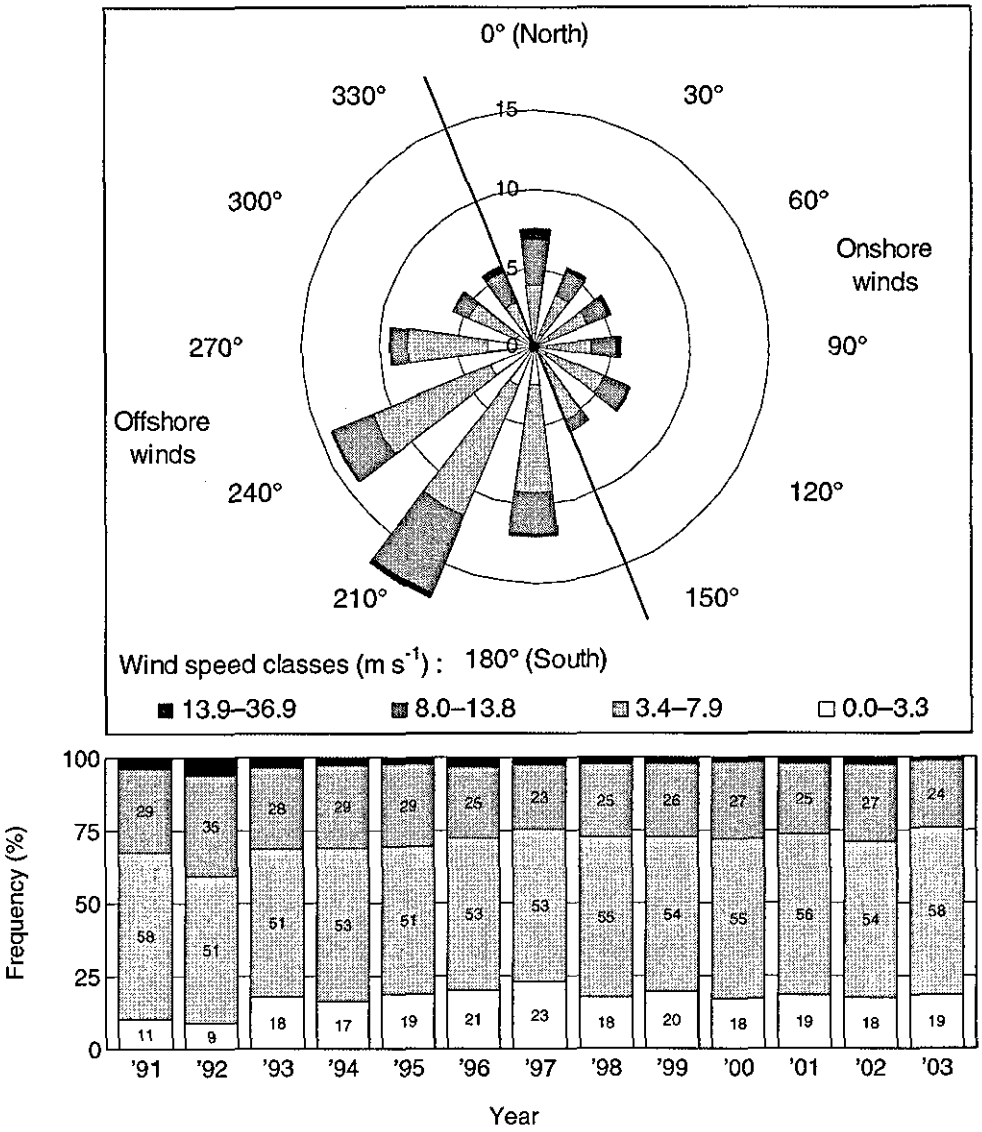

Figure 2.5 – Wind conditions for Donna Nook for the period 1991–2003: (top panel) wind rose; and (bottom panel) annual wind speed frequencies. Wind speed classes are defined according to the scale of Beaufort: 0–2 (0.0–3.3 m s^{-1}), 3–4 (3.4–7.9 m s^{-1}), 5–6 (8.0–13.8 m s^{-1}) and 7–12 (13.9–36.9 m s^{-1}). Wind data was provided by the British Atmospheric Data Centre.

The wave conditions on the beach, however, are thought to be affected by the subtidal bathymetry and concurrent inshore and offshore wave data were collected over a period of a month to investigate this influence. Hourly wave data measured 130 km offshore were made available by the National Data Buoy Centre and instrument stations were deployed at Donna Nook, Theddlethorpe and Mablethorpe to gather inshore wave measurements. Two self-logging instrument stations equipped with a pressure sensor were deployed just above mean low water spring level and sampled water level at 2 Hz

for half an hour at three-hour intervals. As only two stations were available for three sites, the data were collected in two stages: (1) at Donna Nook and Theddlethorpe from 5-11-2002 to 16-11-2002; and (2) at Theddlethorpe and Mablethorpe from 17-11-2002 to 3-12-2002. Halfway through the second deployment, the data collection instruments at Theddlethorpe failed, shortening the time series available. Mean water depth (tide level) and current velocity were computed for each of the data segments representing shoaling and deep-water waves ($H/h < 0.35$; Thornton and Guza, 1982; Ruessink et al., 1998). Significant wave height H_s was estimated by $H_s = 4\sigma$ (Aagaard and Masselink, 1999), where σ is the standard deviation of the detrended 30-min pressure records. The significant wave height was corrected for depth attenuation using linear wave theory (Bishop and Donelan, 1987).

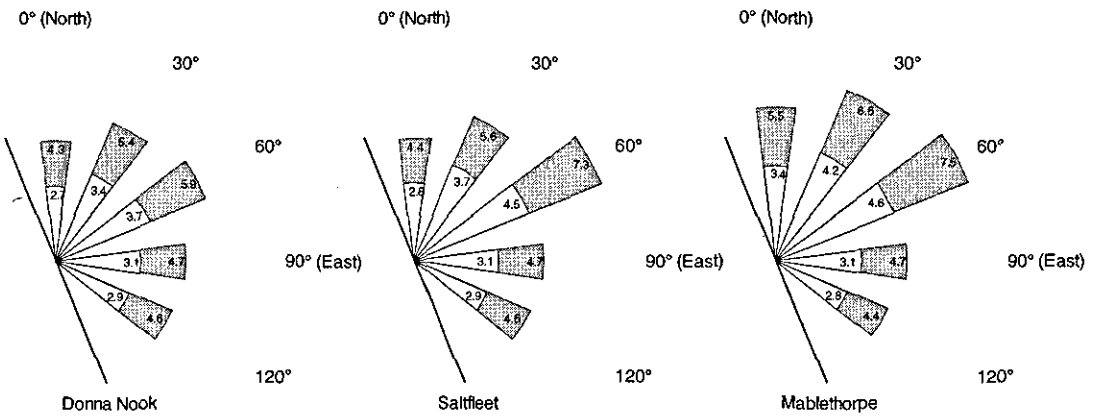

Figure 2.6 – Offshore wave roses for Donna Nook, Saltfleet and Mablethorpe illustrating the 1 in 1 year (white) and 1 in 100 year (grey) significant wave height (in m) for directions between 0-120° (modified from Posford-Duvivier, 1996).

The inshore wave height appears 2–3 times smaller than the offshore wave height (Figure 2.7). Correspondence between the offshore and onshore data was smaller during the first half of the period than during the second half. The degree of correlation relies on wind direction, as the offshore wave buoy measured waves approaching from all quadrants, whereas the inshore measurements only included waves approaching from the east. A least-squares analysis between concurrent inshore wave data collected at Donna Nook, Theddlethorpe and Mablethorpe indicates that the wave height at Theddlethorpe was approximately 20% higher than at the other two localities (Figure 2.8). The proportionality factors between the significant wave height at Theddlethorpe and the wave height at Donna Nook and Mablethorpe are 0.71 and 0.78, respectively, with correlation coefficients r^2 greater than 0.95. Differences in offshore bathymetry

explain the variation in wave energy along the north Lincolnshire coast. A subtidal bank is present in the southern part of the study area, whereas a low gradient shelf fronts the intertidal zone in the northern part of the study area (Figure 2.1). The influence of the subtidal bank at Theddlethorpe is smaller than at Mablethorpe because the bank system at Theddlethorpe is more subdued and located further offshore, hence the larger wave energy conditions at this locality.

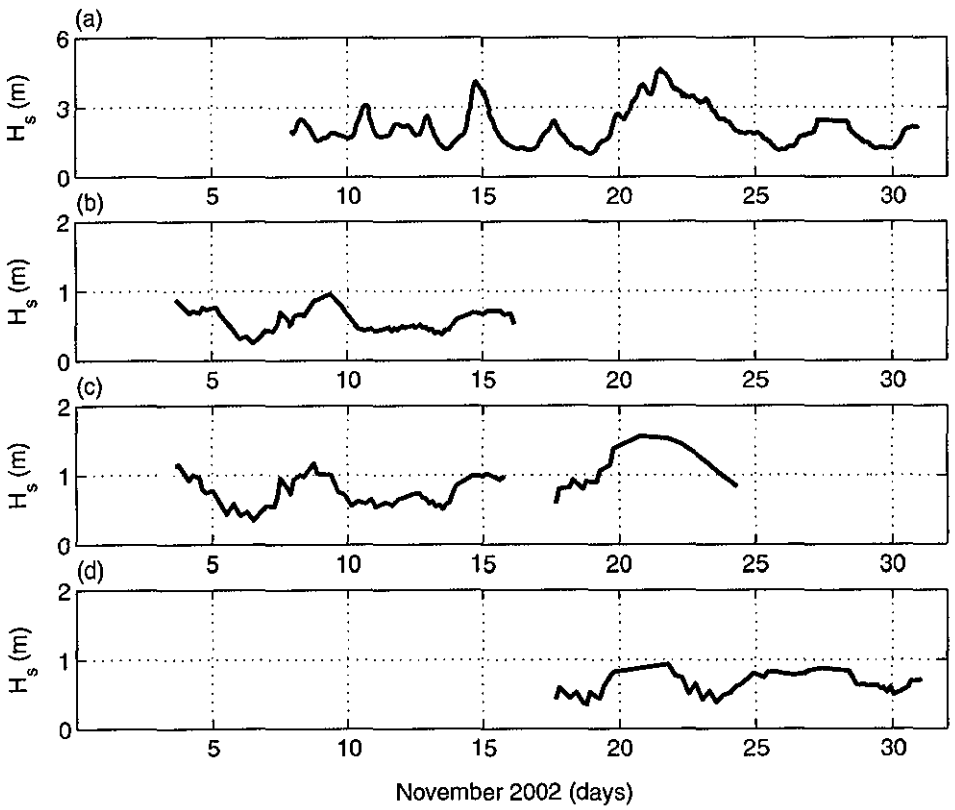

Figure 2.7 – Offshore and inshore significant wave height H_s over the period 5-11-2002 to 3-12-2002 for: (a) a wave buoy located 130 km offshore; (b) Donna Nook; (c) Theddlethorpe; and (d) Mablethorpe. (Note: data plotted after the 30th November represent the 1st–3rd December).

Longshore sediment transport is primarily wave-driven and wave-energy calculations suggest that beach sediments are commonly transported southward from Donna Nook, though the mean direction can vary from year to year (Halcrow, 1988). An early sea bed drifter experiment by Robinson (1968) found similar results as drifters released on the subtidal banks just north of the Humber Estuary were transported down the Lincolnshire coast. Drifters, however, were also recovered from the south shore of the Humber,

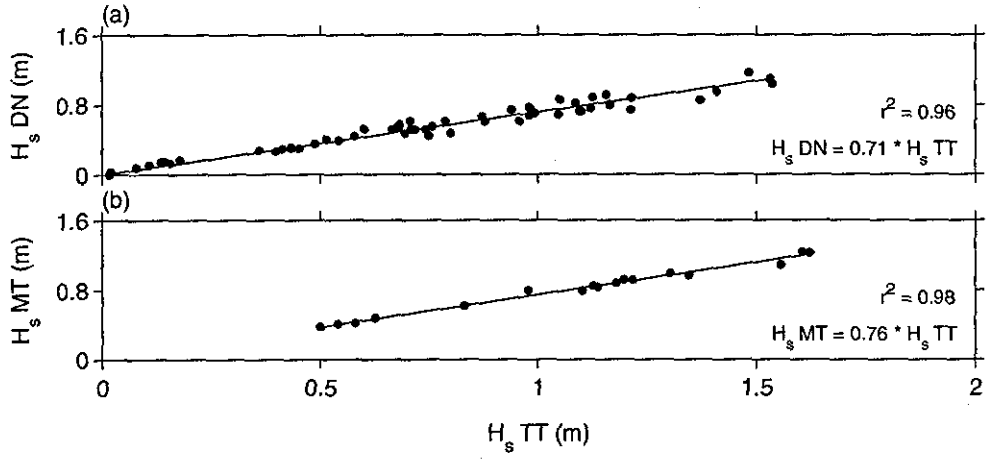

Figure 2.8 – Least square analysis of the significant wave height measured at Theddlethorpe (H_s *TT*) and the significant wave heights measured at (a) Donna Nook (H_s *DN*); and (b) Mablethorpe (H_s *MT*).

suggesting that Donna Nook is a longshore drift diversion point. The sediment at Donna Nook is being supplied from the offshore area (Robinson, 1968) and the residual southward sediment transport is in fact subordinate to this cross-shore movement of sediment (Halcrow, 1988). The long-term accretion of the coast between Donna Nook and Mablethorpe is therefore thought to be the result of abundant onshore sediment transport (ABP, 1996) rather than of a direct sediment supply from further north (the eroding cliffs along the Holderness coast). Sediment transport studies in the southern North sea have further shown that suspended sediment transport rates are some 2 orders of magnitude higher than those of bedload transport, and that suspended sediment concentrations are higher in winter than in summer (ABP, 1996).

Chapter three

Spatial Variability in Ridge and Runnel Morphology

3.1 COASTAL MAPPING USING AIRBORNE TOPOGRAPHIC LIDAR

A range of techniques exists today that can be applied to obtain elevation data. Until recently, morphological coastal studies have been based on a combination of ground surveys, maps and aerial photographs, but during the last decade airborne remote sensing methods have matured, resulting in significant new capabilities that are enabling cost-effective and large-scale quantitative topographic mapping. LIDAR (Light Detecting And Ranging) is one of these methods. It makes use of a scanning laser mounted in a small aircraft that transmits laser pulses toward the land surface (Figure 3.1) and the energy reflected back toward the airborne platform is continuously recorded to develop a LIDAR waveform (Wehr and Lohr, 1999). This technology allows rapid and accurate surveys of land elevations (Sallenger et al., 1999) and a major advantage of LIDAR is the high spatial density of data collection, with ground elevation measurements every square metre (Brock et al., 2002). It also enables a detailed survey of areas that are otherwise inaccessible and/or would be damaged by conventional methods (e.g., through trampling).

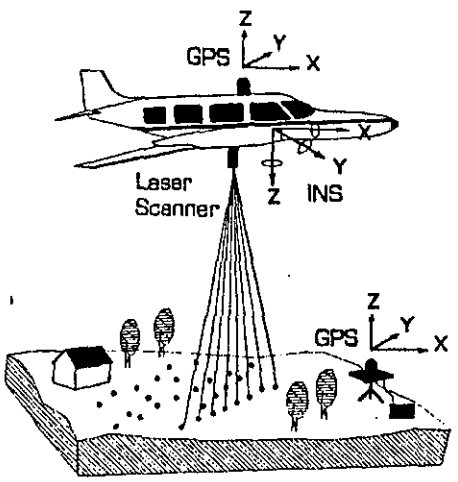

Figure 3.1 – Scanning the surface by LIDAR (From TU Delft, 1997)

The potential of LIDAR for monitoring coastal areas was recognised soon after the development of the first LIDAR data acquisition systems by NASA (Krabill et al., 2002) and the Institute of Photogrammetry at the University of Stuttgart (Ackerman, 1999) and LIDAR has been used for regular mapping of coastal change over the last ten years (NOAA-USGS, 2004). The recent development of commercial LIDAR data acquisition systems has led to a further increase in its application to a wide range of coastal scientific investigations.

In general, two types of laser systems are used for coastal studies: bathymetric LIDARs that penetrate the water and provide measurements of water depth, and topographic LIDARs that only measure subaerial topography. Bathymetric LIDAR mapping has been a fully operational hydrographic survey system since 1994 and survey projects varied from the study of tidal inlets and navigation projects to beach nourishment projects and monitoring (Parson et al. 1997; Irish and Lillycrop, 1997, 1999; Irish and White, 1998; Lillycrop et al., 1999; Buonaiuto and Craus, 2003). Topographic LIDAR on the other hand has proven to be a useful tool for the large-scale mapping of shoreline changes, beach erosion, overwash deposition, soft-cliff erosion and even dune scarping (e.g., Huising and Vaessen, 1997; Hampton et al., 1999; Cracknell, 2000; Adams and Chandler, 2002; Revell et al., 2002; Stockdon et al., 2002; Mitasova et al., 2003; White and Wang, 2003). When compared with ground survey data, topographic LIDAR has a root-mean-square vertical error of about 0.15 m (French, 2003; Sallenger et al., 2003; Woolard and Colby, 2002) and numerous recent studies have demonstrated that this is sufficient to resolve the magnitude of changes observed during severe storms and post-storm recovery on beaches (e.g., Brock et al., 2002; Stockdon et al., 2002; Zhang et al., 2003). LIDAR is therefore now frequently used for emergency-response surveys after severe storms and hurricanes (Irish and White, 1998). Furthermore, in their study on spatial characterisation and volumetric change of coastal dunes, Woolard and Colby (2002) presented a successful use of LIDAR for smaller scale coastal features. This research also explored the influence of spatial resolution and they suggested an optimal spatial resolution of 1–2 m to provide the most reliable representation of coastal dunes.

Aim and objectives Chapter 3

The purpose of this chapter is to introduce airborne topographic LIDAR as a tool to document the large-scale spatial characteristics of ridge and runnel morphology along the north Lincolnshire coast. LIDAR has not been used previously to map intertidal features and this innovative application of the technique to provide a Digital Elevation Model (DEM) for such low-amplitude morphology utilises the LIDAR at its limit in terms of vertical resolution. More specifically, research questions are:

(1) Does a DEM obtained from LIDAR accurately represent ridges and runnels?

(2) Does the ridge and runnel morphology show any systematic longshore variability?

(3) Similarly, does the ridge and runnel morphology show any cross-shore variability?

(4) Does the ridge and runnel morphology of the north Lincolnshire coast exhibit any relationships between morphometric variables, for instance:
- are the number of ridges related to the width of the ridge and runnel zone? and
- is the steepness of ridges dependent on the beach gradient?

3.2 LIDAR SURVEY PROCEDURE AND EVALUATION OF ITS USE FOR RIDGE AND RUNNEL TOPOGRAPHY

The LIDAR survey, including the data processing to a 'user-friendly' product, was carried out by the Environment Agency Technology Group (EATG), formerly known as the National Centre for Environmental Data and Surveillance. Their topographic LIDAR system operates on the same basic principle as many other such systems, by emitting a laser pulse toward the ground, detecting its return and using the return travel time to compute the slant distance between the aircraft and the point on the ground (e.g., NCEDS, 1997; Ashkenazi et al., 2000). As a result of the scanning mechanism used by EATG and the along track motion of the aircraft, the LIDAR scan pattern was not a regular strip perpendicular to the direction of flight, but a 'zig-zag' pattern with ground separation distances typically between 1 and 4 metres. The aircraft position was recorded simultaneously by an onboard GPS receiver and in combination with the concurrently collected signals of a GPS ground base station, the exact aircraft flight trajectory was determined. The aircraft locations were subsequently combined with the record of slant distances to compute the precise coordinates for each point scanned by LIDAR.

Further data processing was carried out to transform coordinates to the desired local (map) coordinate system and to compute a digital elevation model with a regular grid. The conversion from the GPS to the local Ordnance Survey coordinate system involved two separate processes: (1) the translation of the plan (E, N) coordinates; and (2) the conversion from the ellipsoidal GPS-height to an orthometric height above ODN (Ashkenazi et al., 2000). The coordinate transformations were followed by the conversion of the 'zig-zag' scan pattern to a regular gridded set of elevations. The first step in the generation of a 'raw' DEM was to divide the survey area into a regular grid of bins and each scanned point was subsequently assigned to one bin. The remaining empty bins were then filled using the 'inverse distance' interpolation technique (Nick

Holden, 2001, pers. comm.). Initial bin size is typically 1 by 1 m, but the DEM grid was later resized to 2 by 2 m. The final step of data processing was to separate the ground points from non-ground points such as buildings and vegetation. This step converted the raw DEM to the final product: a Digital Terrain Model (DTM).

The claimed accuracies of a LIDAR DTM generated by EATG, are 0.11–0.25 m and 1.08–1.45 m for, respectively, the vertical and horizontal accuracy (Ashkenazi et al., 2000). Errors and deviations found in the DTM are mainly the result of the imprecision of the LIDAR system (LIDAR instrument and GPS system) and vertical and horizontal claimed accuracies for the system itself are respectively, 0.09–0.15 m and 1.08–1.44 m. Although the EATG carries out ground-truthing surveys to establish the precision and accuracy of the LIDAR system during each flight, they do not supply information concerning the precision and accuracy of each final DTM product. Therefore the first part of the analysis in this chapter focuses on the quality of the LIDAR data and its ability to accurately reproduce the ridge and runnel topography.

The LIDAR survey was carried out at the daylight low tide of the 21/08/2001 under spring tide conditions. A detailed ground survey of nine cross-shore transects at 50-m intervals was carried out simultaneously at Mablethorpe North End using a laser total station that was accurate to ± 3 mm. The transects started in the dunes and extended nearly 500 m across the entire width of the ridge and runnel zone. The beach height was measured on the breaks in slope, with a maximum spacing of 10 m between observations. A local Environment Agency benchmark was used to link the profiles to a known level above ODN. Additionally, the locations of 4 to 6 points per transect were recorded with a hand-held GPS to facilitate the extraction of LIDAR heights corresponding to each transect. The 'raw' DEM, i.e., without removal of buildings and vegetation, was used for evaluation and analysis in this chapter.

The LIDAR DEM reproduces ridge and runnel topography in great detail, distinctly showing the bars and troughs and also intersecting drainage channels (Figure 3.2). Figure 3.3 shows a three-dimensional presentation of the ridges and runnels at Mablethorpe to compare results of the total station ground survey with those obtained from LIDAR and it demonstrates that the beach profiles match very well. All five ridges

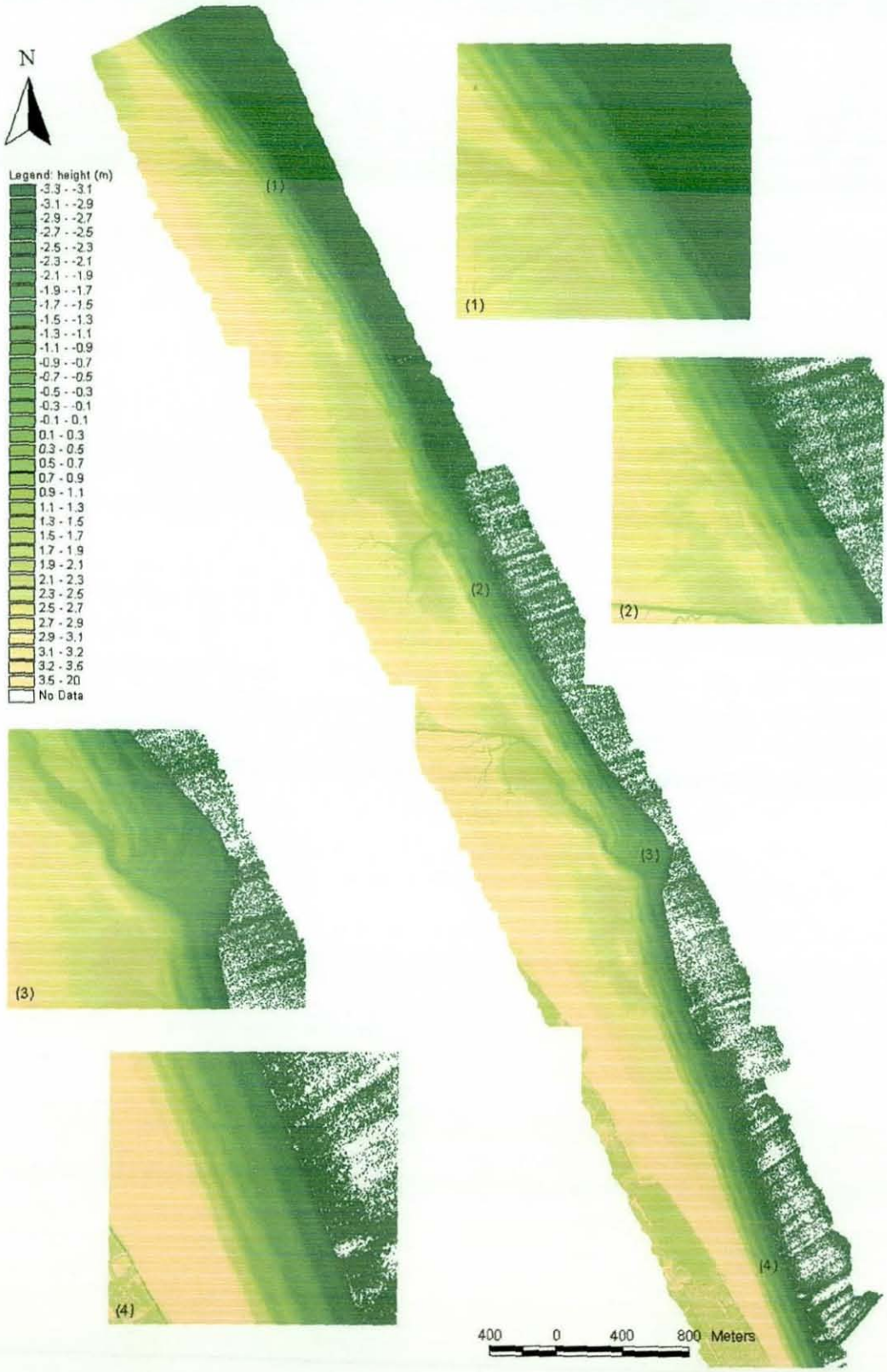

Figure 3.2 – Digital Elevation Model for the north Lincolnshire Coast derived from LIDAR (21/08/2001). The water surface on the right-hand side can be distinguished from sub-aerial data by the presence of missing values (white pixels). Enlargements show the ridges and runnels in more detail for four selected areas, indicated by coinciding numbers in the plot.

present at the time, irrespective of size, are accurately presented by LIDAR and even the shape of the ridges and runnels is well reconstructed in most cases. A quantitative comparison of the elevations obtained from LIDAR and the total station survey reveals that the values obtained by LIDAR are generally 0.02–0.05 m higher (Figure 3.3a). The RMS (vertical) error is 0.096 m and 95 % of the LIDAR data fall within ± 0.18 m of the corresponding total station survey data. The RMS error for this survey is smaller than reported in previous studies (0.15 m; Mason et al., 2000; French, 2003; Sallenger et al., 2003; Woolard and Colby, 2002) and is even below the most optimistic claimed vertical accuracy for LIDAR (0.11m). This is attributed to the lack of vegetation on the beach.

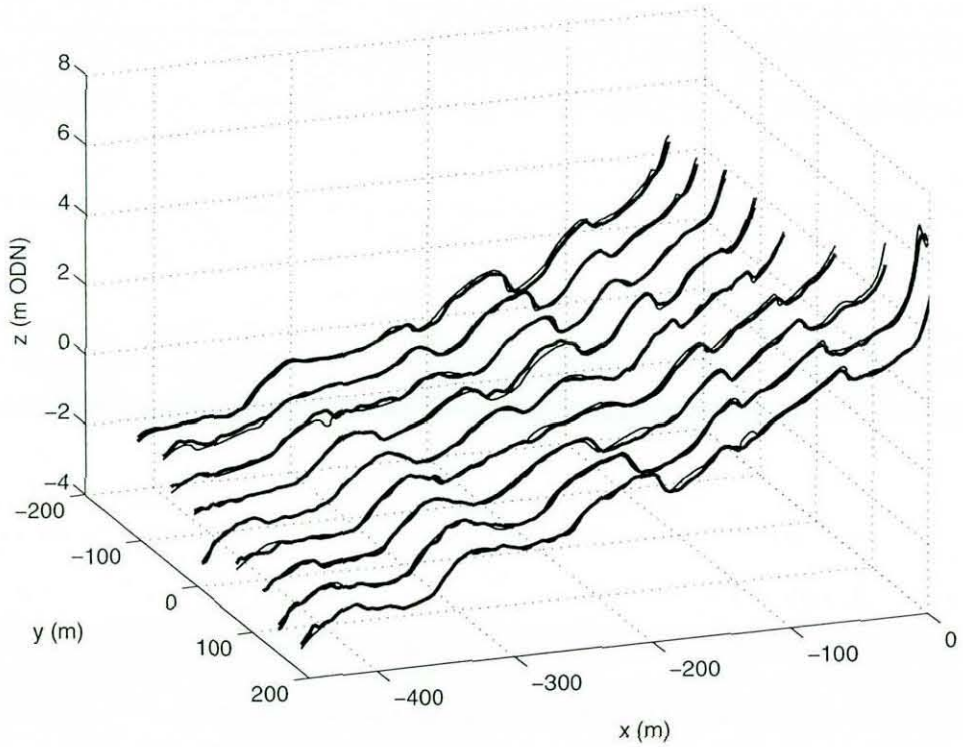

Figure 3.3 – Beach profiles for Mablethorpe derived from airborne LIDAR (thick solid line) and total station ground survey (thin solid line). On *x*- and *y*-axis are cross-shore distance and alongshore distance, respectively. Direction of view is towards the southwest.

Cross-shore variation in the deviation is insignificant and errors are similar on the different ridges, irrespective of their size (Figure 3.4b). The largest deviations, however, systematically occur on slipfaces that are narrower than the spatial resolution of the DEM, and in runnels where standing water might have distorted the proper return of the laser pulses. The close correspondence between LIDAR and total station elevations is statistically confirmed by least-squares analysis, resulting in a correlation coefficient r^2 of 0.98 (Figure 3.4c).

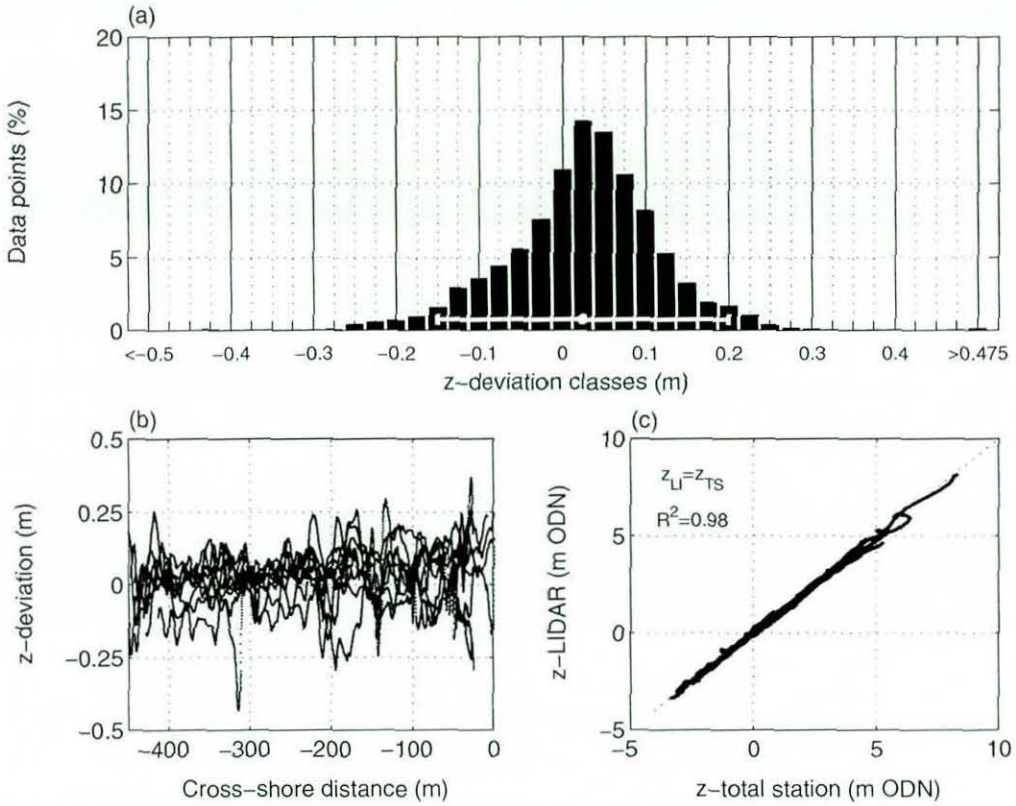

Figure 3.4 – Comparison of elevations obtained from LIDAR and total station survey: (a) frequency of elevation deviations per 0.025 m-intervals. Positive deviations indicate that LIDAR values are larger than those from the ground survey. The white line at the bottom shows the statistical 95% confidence interval. (b) cross-shore variability in elevation deviation; and (c) total station (Z_{TS}) versus LIDAR (Z_{LI}) elevations.

It should be mentioned that the differences between LIDAR and total station elevations are not only due to inaccuracies of the LIDAR system and data processing procedures, but also by imprecision in the total station survey and the linking to ODN-level through a local benchmark. In addition, the extraction of exactly identical cross-shore transects from the LIDAR data set is unlikely due to the inaccuracies involved in recording locations with the hand-held GPS (1–10 m). Nevertheless, the results show that the spatial and vertical resolution of LIDAR is sufficient to generate a DEM that features ridges and runnels and that the data used in this study was accurate enough to reproduce in detail the ridge and runnel morphology along the north Lincolnshire coast.

3.3 SPATIAL CHARACTERISATION OF THE RIDGES AND RUNNELS: METHODOLOGY

The LIDAR data set was supplied in a series of ascii-files and comprised 16 blocks of data, each covering a 2-by-2 km area. These data were directly imported into the software package ARCVIEW to visualise the DEM (Figure 3.2) The data set covers an area extending longshore from Donna Nook to Mablethorpe and across-coast from landward of the dunes to seaward of the spring low water line. Initially, a set of multiple individual cross-shore beach profiles was used for further analysis as an in-depth analysis of the data set as a whole was not achievable at this stage because the data set was several orders of magnitudes larger than that for which the available GIS tools were designed.

A total of 70 cross-shore profiles were extracted from the data at a constant longshore spacing of 250 m, using a specially-designed LIDAR toolbox in ARCVIEW. This toolbox makes the DEM very versatile in that profiles can be constructed having any desired orientation, yet the procedure is time-consuming since it can only be executed manually. The spring low tide mark was taken as the seaward limit of the extracted profiles, whereas the landward limit coincided with the upper boundary of the ridge and runnel zone. The variation in the ridge and runnel morphology was subsequently investigated applying a ridge-by-ridge analysis, analogous to a wave-by-wave analysis of a time series of water surface elevation. For that, the profiles were linearly interpolated to 0.1 m and second-order polynomial curves were fitted to the ridges and runnels using least-squares analysis (Figure 3.5). The fitted curves represent the concave-upward beach profiles on which the ridge and runnel morphology is superimposed. The curves were subtracted from the profiles to yield the residual intertidal profile, whereby positive and negative residuals represent, respectively, the ridges and the runnels. This enabled objective selection of individual bars and consistent measurements of ridge and runnel characteristics. Definitions for various morphometric parameters are summarised in Table 3.1.

Although the LIDAR DEM is of sufficient resolution and accuracy to reproduce the ridges and runnels (section 3.2), it is noted that the minimum ridge height computed from multiple profile analysis is c. 0.15 m larger than observed in the field, where the

smallest ridges were approximately 0.1 m. A visual check of each profile revealed that the smaller ridges were in fact present in the LIDAR data, but that they were lost in the subsequent analysis using second-order polynomial curves to define ridge height. It was decided to manually add the left-out ridges, as many of these were in fact clear ridges and runnels covering a significant part of the cross-shore beach profiles. The heights of these ridges were set to equal zero and only other characteristics such as number, width and crest spacing were included in further analysis.

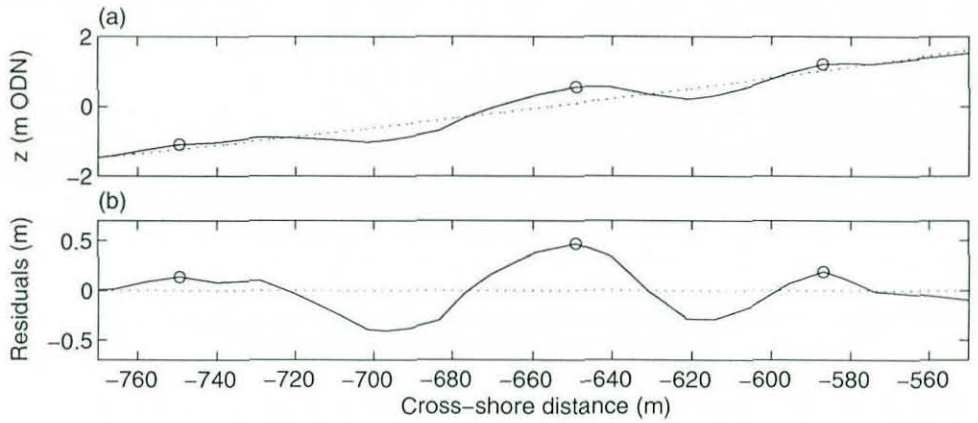

Figure 3.5 – Utilisation of a residual profile: (a) beach profile (solid line) with fitted second order polynomial curve (dashed line); and (b) profile residual. The open circles indicate the positions of ridge crests.

The LIDAR analysis was supplemented in a later stage, when a more sophisticated personal computer became available and with it the possibility to analyse the LIDAR data using the software package MATLAB. The full data set was imported and the strip of data representing the ridge and runnel zone was extracted and prepared for further analysis. As the LIDAR data is organised according to Northing ('longshore') and Easting ('cross-shore') coordinates, 'cross-shore' profiles extracted from the data are not perpendicular to the NNW–SSE orientated coastline. To correct for this, the Easting coordinates of the profiles were re-scaled using the shoreline orientation and since the shoreline orientation varies along the coast, each 'cross-shore' profile was individually adjusted. The length of the profiles was fixed to 400 m to facilitate comparison. The total length of the strip of LIDAR data representing the ridge and runnel zone is 15.6 km and includes 7,800 cross-shore intertidal profiles at 2-m intervals, i.e., the resolution of the data set. Again a second-order polynomial was fitted to each of the profiles to yield the residual profiles.

Table 3.1 – Definitions of parameters to characterise ridge and runnel morphology from residual profiles.

	Parameter	Definition
1	Number of ridges (-)	Number of intervals with positive residuals
2	Width of ridge and runnel zone (m)	Distance between seaward and landward boundaries of ridge and runnel zone (see text for definition boundaries)
3	Slope of ridge and runnel zone (tan β)	Height difference between seaward and landward boundaries of ridge and runnel zone divided by the width of the ridge and runnel zone.
4	Relative ridge position (-)	Distance of ridge crest to seaward boundary of ridge and runnel zone divided by the width of the ridge and runnel zone. Crest position is defined as the location where the (positive) value of the residuals is maximum.
5	Elevation of ridge (m ODN)	Elevation of the data point that represents the crest derived from the LIDAR profile.
6	Ridge height (m)	Twice the value of the residual of the data point that represents the crest
7	Ridge width (m)	Distance between (two) intersections of the LIDAR profile and polynomial, with positive residuals in between the intersections.
8	Ridge volume (m^3m^{-1})	Sum of residuals between (two) intersections with positive residuals in between the intersections (corrected for interpolation resolution)
9	Slope seaward ridge face (tan β)	Height difference between seaward ridge boundary intersection en crest divided by the distance between these points.
10	Ridge asymmetry (ln(-))	Natural logarithm of the distance between seaward ridge boundary intersection and crest divided by the distance between crest and landward ridge boundary intersection.
11	Ridge crest spacing (m)	Distance between the crests of two adjacent ridges.
12	Relative runnel position (-)	Distance of runnel to seaward boundary of ridge and runnel zone divided by the width of the ridge and runnel zone. Runnel position is defined as the location where the (negative) value of the residuals is minimum.
13	Runnel depth (m)	Twice the value of the residual of the data point that represents the runnel position
14	Runnel width (m)	Distance between (two) intersections of the LIDAR profile and polynomial, with negative residuals in between the intersections.

Spectral analysis was subsequently used to quantify spatial patterns in the ridge and runnel morphology. A raw spectrum was computed for each residual cross-shore profile and the wave number k associated with the spectral peak was used to identify the dominant cross-shore spacing (reciprocal of k) of the intertidal bars and troughs. The prominence of the bars was quantified using parameter Q_p indicating the sharpness of the spectral peak (Darras, 1987):

$$Q_p = \frac{2}{m_0^2} \int_0^\infty kS(k)^2 dk$$

where m_0 is the 0th spectral density moment and $S(k)$ is the spectral density. The peakedness factor is commonly used to characterise ocean waves, but has been deployed by Coco et al. (2000) to quantify the prominence of beach cusp morphology. The larger Q_p, the narrower the spectrum and the more pronounced the morphology.

3.4 SPATIAL CHARACTERISATION OF THE RIDGES AND RUNNELS: RESULTS

Figure 3.6 shows the residual morphology of the intertidal bar zone along the north Lincolnshire coast. The ridge and runnel morphology is very clearly depicted with 3–5 ridges present at most locations. The ridges and runnels display a remarkable longshore continuity and some individual ridges can be followed longshore for more than 4 km. There are three sections where the ridge and runnel morphology is interrupted; at y = 5.2–6.3 km a large tidal creek (Saltfleet) cuts through the ridges and runnels, whereas at y = 9.5–11.3 and 13.6–14.1 km a number of tidal creeks are present. The ridges are also dissected by smaller drainage channels approximately every 500 m and small deltas occur where the channels discharge into the troughs. The orientation of most of the drainage channels reflects a southward nearshore sediment transport direction.

The 70 beach profiles that were extracted from the LIDAR data set are visualised in Figure 3.7. This set of profiles was used to determine characteristics of the beach morphology, such as the number of ridges and runnels, and their amplitude, size and spacing. Table 3.2 summarises the values of various such morphometric parameters, averaged for the entire North Lincolnshire coast. It shows that the average ridge height along this coast is c. 0.7 m and that the ridges tend to be wider than the runnels. The asymmetry factor indicates that the ridges are generally skewed landward.

The longshore variation in the spectral shape of the intertidal profiles is shown in Figure 3.8 and indicates that stretches of coast with prominent ridges and runnels are characterised by $Q_p > 2$ and a peak at $k \approx 0.01$ m^{-1}. The dominant cross-shore length scale of the ridge and runnel morphology is therefore c. 100 m, in agreement with the

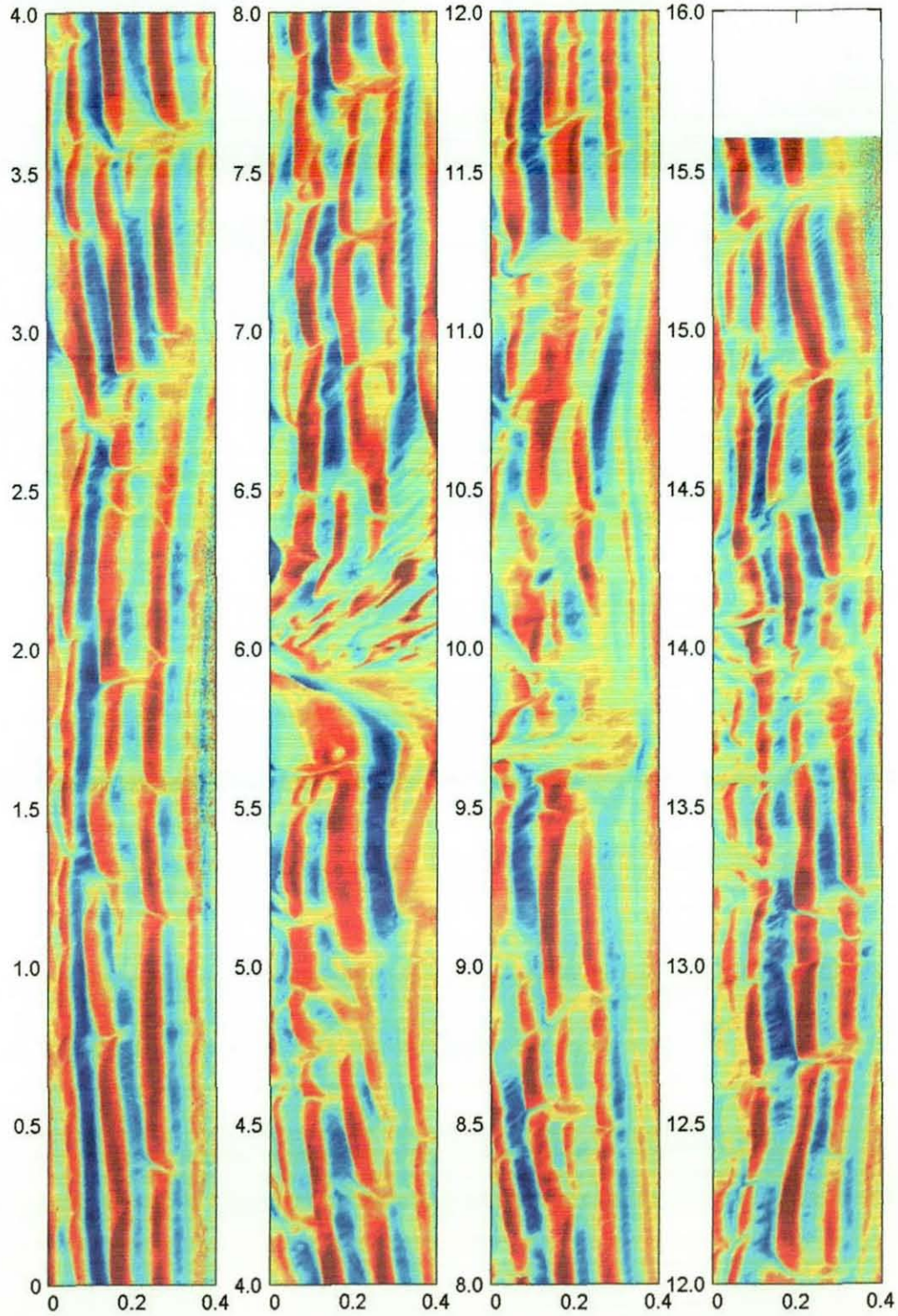

Figure 3.6 – Residual intertidal morphology along the north Lincolnshire coast obtained from LIDAR data (21/08/2001). Positive residuals represent ridges (dark red = +0.5 m), negative residuals represent runnels (dark blue = –0.7 m). The longshore *y*-coordinate runs in a northward direction from Mablethorpe (*y*= 0 km) to Donna Nook (*y* = 16 km). The cross-shore *x*-coordinate (in km) runs in a seaward direction.

findings presented in Table 3.2. The peakedness factor is very sensitive to the presence of even relatively modest drainage channels and fluctuates widely alongshore. Its values are higher and less variable in the southern part of the study region compared to that in the north. This suggests that the ridges and runnels in the south are more prominent and/or less frequently dissected by drainage channels than in the north.

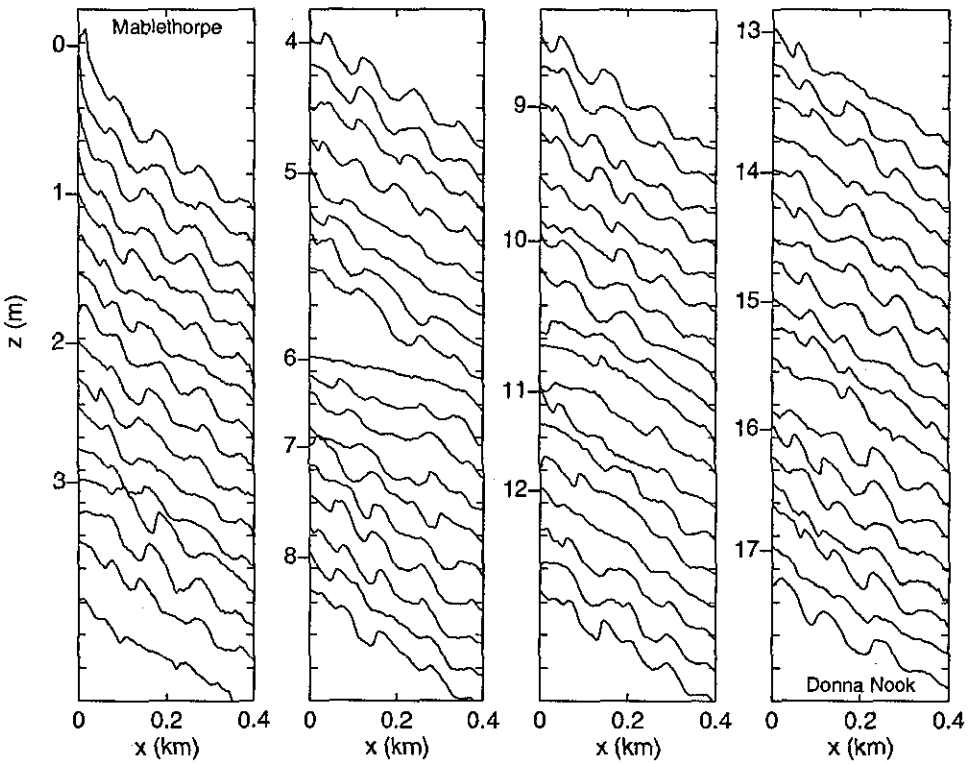

Figure 3.7 – Beach profiles for the north Lincolnshire coast derived from LIDAR data. The profiles have been stacked with an offset of 1.5 m. Vertical spacing between tickmarks is also 1.5 m. Labelling of the profiles, expressed as the distance from Mablethorpe (in km), is shown on the left hand side of the panels.

Table 3.2 – Mean ridge and runnel characteristics for the north Lincolnshire coast. Positive and negative values for ridge asymmetry indicate, respectively, landward- and seaward-skewed ridges.

Number of ridges (-)	5.19	Ridge volume ($m^3\ m^{-1}$)	11.21
Width ridge and runnel zone (m)	494.89	Ridge asymmetry (ln (-))	0.23
Slope ridge and runnel zone (tanβ)	0.011	Slope seaward ridge face (tanβ)	0.025
Ridge height (m)	0.67	Spacing ridge crests (m)	92.2
Ridge width (m)	51.49	Runnel width (m)	43.74

These findings are supplemented with the results of the ridge-by-ridge analysis and again it is shown that the southern area differs from the northern part, with the Saltfleet tidal creek as the division between the two zones (Figure 3.9). The area between Saltfleet and Mablethorpe is characterised by a narrowing and hence steepening of the intertidal zone and interestingly this coincides with a steepening of the seaward faces of the ridges as well. Ridge spacing is rather regular along the coast except for the locations with tidal creeks, where spacing is larger due to a wider intertidal zone and/or a fewer number of ridges and runnels.

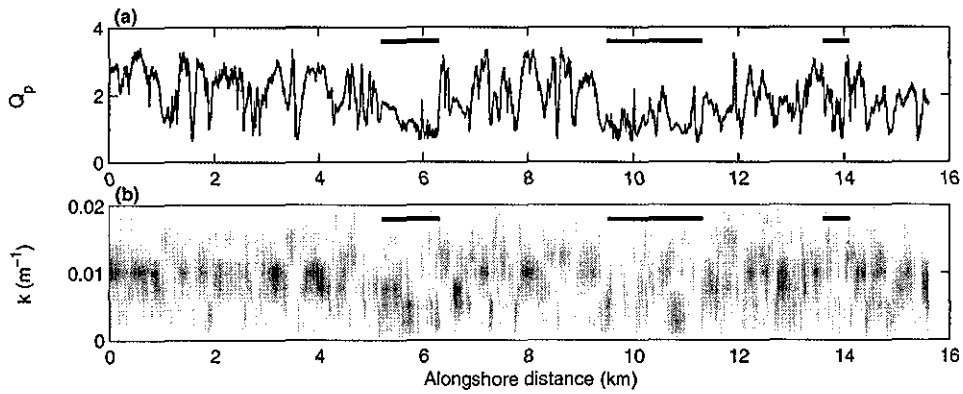

Figure 3.8 – Longshore variation in the energy spectrum of the intertidal cross-shore profiles: (a) sharpness of the spectral peak Q_p; and (b) spectral energy as a function of the cross-shore wave number k. In (b), the spectral energy level is represented by the grey scale such that the dark patches in the diagram represent the largest energy levels. Horizontal lines indicate sections with pronounced tidal drainage channels.

The crest elevation of all selected ridges is plotted against their associated longshore distance in Figure 3.10 to examine the longshore variability in drainage channels density in more detail. The presence of drainage channels dissecting the ridges is indicated by a decrease in the crest elevation. As noted previously, 3–5 ridges and runnels are present at most locations and individual ridges can be traced over large distances. The distance between the drainage channels appears larger in the southern part of the study area than in the northern part. There is also a tendency for the channels dissecting the upper ridges to be closer together than those cutting through the middle ridges. There are relatively few drainage channels present in the lower part of the intertidal zone, although data from this part of the profile are limited.

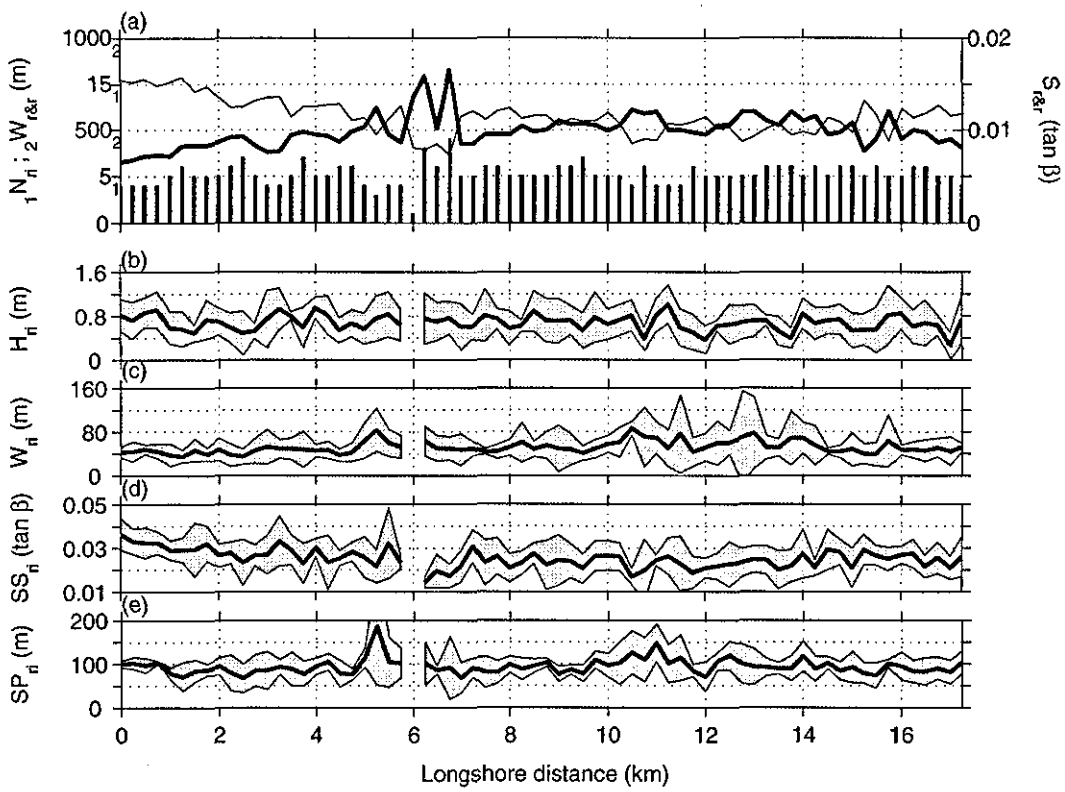

Figure 3.9 – Longshore variation in ridge and runnel morphology: (a) number of ridges (bars, left *y*-axis, subscript 1), width of the ridge and runnel zone (thick line, left *y*-axis, subscript 2) and gradient of the ridge and runnel zone (thin solid line, right y-axis); (b) ridge height; (c) ridge width; (d) gradient of seaward ridge face; and (e) spacing between ridge crests. Panels (b-d) present the cross-shore average (thick solid line) with their corresponding ± one standard deviation-envelopes (grey patches).

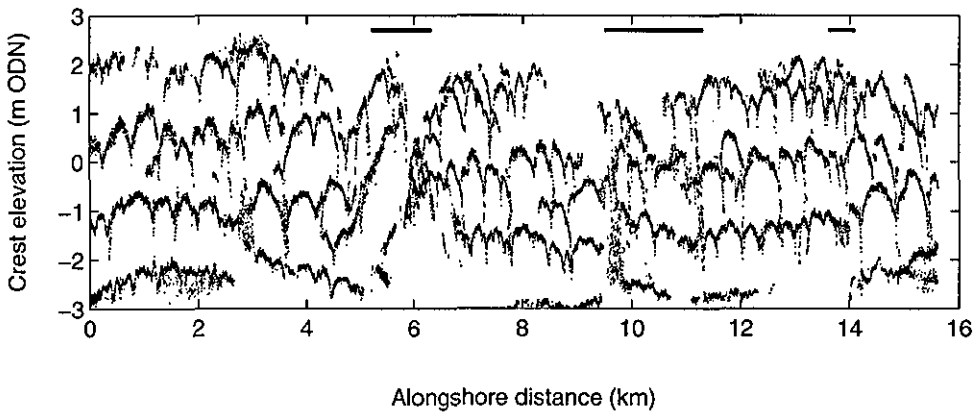

Figure 3.10 – Longshore variation in crest elevation of the ridges.

To investigate the cross-shore variation in the ridge and runnel morphology, the selected ridges were grouped on the basis of their crest elevation relative to ODN in 0.4-m wide classes. The ridges present in the three regions with significant tidal drainage channels were excluded from the analysis. For each crest elevation class, the number of ridges and various morphometric parameters, such as average ridge height and volume, were computed. In accordance with a similar analysis by Masselink and Anthony (2000), the ridges along the north Lincolnshire coast are distributed fairly evenly across the intertidal profile (Figure 3.11a). The average height of the ridges is 0.5–0.8 m on the upper part of the profile and considerably less (0.2–0.5 m) on the lower part of the profiles (Figure 3.11b). Whilst ridge height stays relatively constant above 0 m ODN, the ridge volume shows a different trend. The largest ridges (in terms of volume per unit meter width) are found around mid-tide level and the smallest ridges occur on the lower part of the profile (Figure 3.11c). Above 0 m ODN, ridge volume decreases onshore, implying that the upper ridges are less wide than the mid-intertidal ridges. This tendency coincides with a decreased spacing between the upper ridges (Figure 3.11d). The seaward slope of the ridges seems to steepen landward with average gradients between 0.02–0.025 (Figure 3.11e), whereas the ridge asymmetry does not vary significantly across the intertidal zone (Figure 3.11f). The dominance of positive asymmetry values indicates that the ridges are generally skewed toward the land, i.e., the landward slopes are narrower than the seaward slopes.

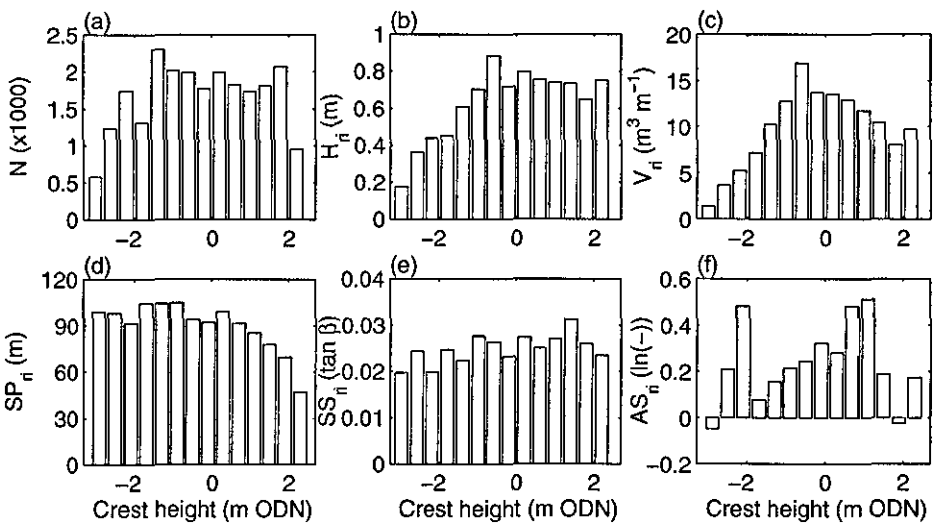

Figure 3.11 – Histograms showing cross-shore variation in ridge and runnel morphology: (a) number of ridges; (b) average ridge height; (c) average ridge volume; (d) ridge crest spacing; (e) average gradient of seaward ridge face; and (f) ridge asymmetry.

The LIDAR enabled the analysis of a significantly larger set of cross-shore profiles than would have been possible from any type of ground survey. This resulted in a large data set of ridge and runnel characteristics that was not only used to quantify spatial variability, but also to investigate the mutual correlations between parameters. Table 3.3 summarises the Pearson's correlation coefficients between various morphometric parameters and some of these correlations are visualised in Figure 3.12. One of the strongest correlations (R^2=0.97) is that between relative cross-shore position of the ridge crest and elevation of the ridge crest relative to ODN (Figure 3.12a), justifying the earlier use of the latter parameter as a surrogate for cross-shore position to facilitate direct comparison to mean tidal levels. Other strong correlations, for instance between width and slope of the ridge and runnel zone or ridge volume and height, are rather obvious and for this reason Figure 3.12b-i focuses on correlations that are weaker, yet more interesting.

Table 3.3 – Correlation Table between various morphometric parameters characterizing the ridge and runnel morphology: (1) number of ridges and runnels; (2) width of the ridge and runnel zone; (3) slope of the ridge and runnel zone; (4) cross-shore position of the ridge crest; (5) elevation of the ridge crest relative to ODN; (6) ridge height (7) ridge width; (8) ridge volume; (9) gradient of the seaward ridge face; (10) ridge asymmetry; (11) spacing of ridge crests; (12) cross-shore position of the runnel; (13) runnel depth; and (14) runnel width. The values within the left-hand box represent the correlation coefficient between a ridge and the landward-lying runnel or ridge, whereas the right-hand box represents the correlation between a ridge and the seaward-lying runnel or ridge. Correlation values above ±0.5 are in bold.

		1	2	3	4	5	6	7	8	9	10	11	12	13	14
		No_{ri}	$W_{r\&r}$	$S_{r\&r}$	Pos_{ri}	$Elev_{ri}$	H_{ri}	W_{ri}	V_{ri}	SS_{ri}	AS_{ri}	Sp_{ri}	Pos_{ru}	D_{ru}	W_{ru}
1	No_{ri}		-	-	-	-	-	-	-	-	-	-	-	-	-
2	$W_{r\&r}$	**0.62**		-	-	-	-	-	-	-	-	-	-	-	-
3	$S_{r\&r}$	-0.42	**-0.88**		-	-	-	-	-	-	-	-	-	-	-
4	Pos_{ri}	0.00	-0.05	0.06		-	-	-	-	-	-	-0.10	**0.98**	-0.05	-0.22
5	$Elev_{ri}$	0.02	0.02	0.00	**0.97**			-	-	-	-	-0.07	**0.93**	-0.02	-0.19
6	H_{ri}	-0.11	-0.04	0.05	0.22	0.29		-	-	-	-	0.22	0.06	0.27	0.10
7	W_{ri}	-0.14	0.14	-0.16	0.15	0.21	0.40		-	-	-	0.32	0.01	-0.04	-0.05
8	V_{ri}	-0.17	0.01	-0.01	0.23	0.31	**0.77**	**0.76**		-	-	0.25	0.09	0.14	0.05
9	SS_{ri}	-0.27	-0.37	0.35	0.16	0.19	0.37	-0.24	0.06		-	-0.15	0.02	0.41	0.15
10	AS_{ri}	0.20	0.11	-0.07	0.07	0.07	0.05	-0.14	-0.14	-0.31		0.29	-0.02	0.09	0.05
11	Sp_{ri}	-0.22	0.13	-0.15	-0.33	-0.28	0.07	0.35	0.18	-0.05	-0.35		-	-	-
12	Pos_{ru}	0.01	-0.11	0.12	**0.98**	**0.94**	0.28	0.09	0.22	0.34	0.15	-0.22		-	-
13	D_{ru}	-0.14	-0.14	-0.01	-0.05	-0.06	0.19	0.12	0.12	0.03	0.11	0.43	0.00		-
14	W_{ru}	-0.27	0.01	-0.03	-0.39	-0.39	-0.04	0.11	0.00	-0.09	-0.19	**0.77**	-0.29	**0.60**	

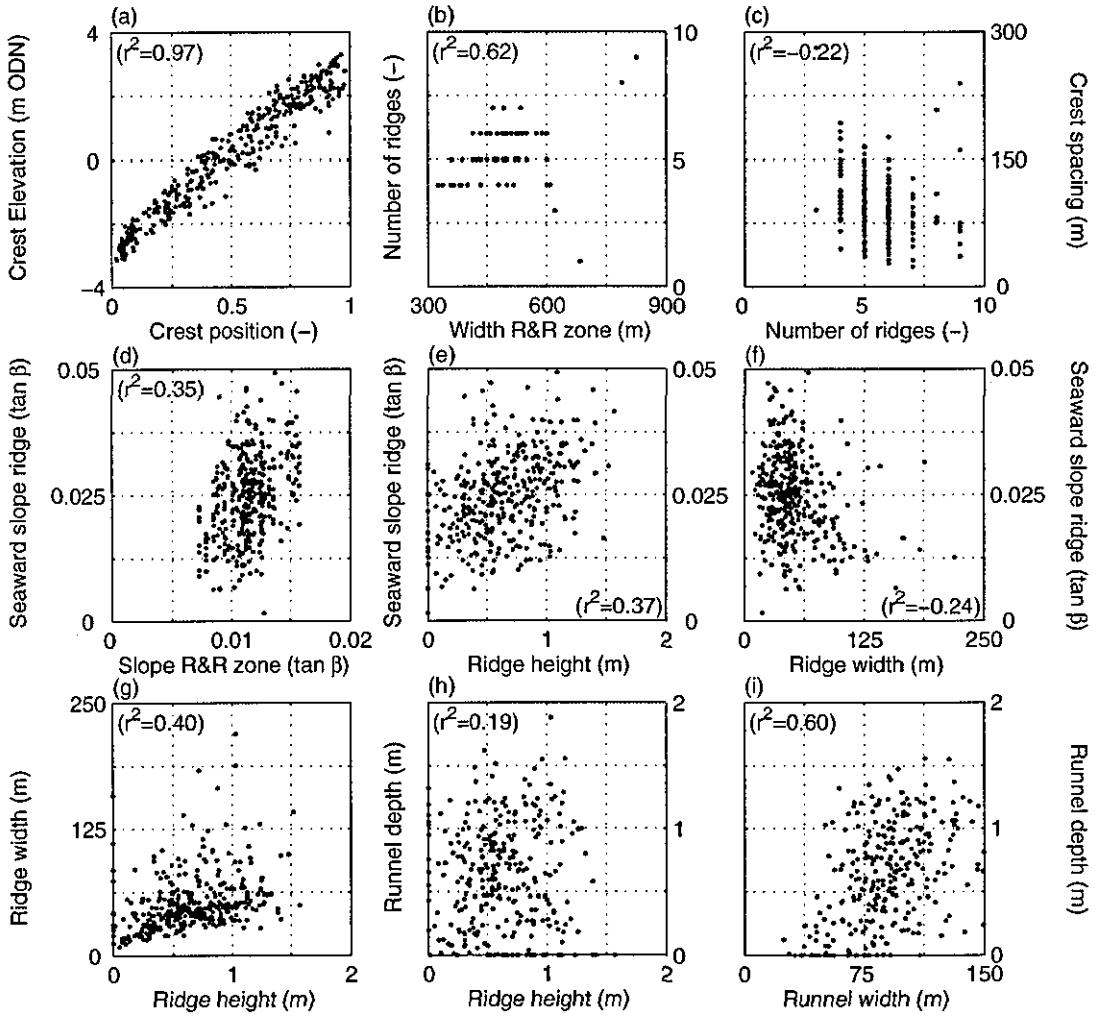

Figure 3.12 – Correlation plots between various morphometric parameters characterizing the ridge and runnel morphology

It appears that a wider ridge and runnel zone features more ridges with a smaller spacing between them (Figure 3.12b-c) and that on steeper intertidal zones also the gradient of the seaward ridge face tends to be larger (Figure 3.12d). Additionally, the seaward slope of the ridge depends on the ridge height and ridge width in such a way that steep slopes tend to occur on high and/or narrow ridges (Figure 3.12e-f). Steeper ridges also appear to have a smaller landward asymmetry and as seaward-skewed ridges are hardly observed, this implies that these ridges tend to be symmetrical. Ridge height is furthermore positively correlated to width of the ridge (Figure 3.12g) and also wider runnels tend to be deeper (Figure 3.12i). Finally, the correlation of ridge parameters

versus characteristics of respectively the landward-lying and seaward-lying runnels are characterised by similar correlation coefficients (Table 3.3).

3.5 DISCUSSION

Investigation of the cross-shore variation in the dimensions of the intertidal bars clearly demonstrates that the largest bars (in volume) occur around MSL, whereas the smallest bars are found in the lower intertidal zone. The height of the upper intertidal bars is similar to those found around MSL, but they are considerably narrower. This provides confirmation of the tentative result obtained by Masselink and Anthony (2001), but contrasts with King (1972a), who argued that the height of the intertidal bars increases in the seaward direction. Additional observations of the seaward decrease in ridge height were provided by Sipka and Anthony (1999), Navas and Malvarez (2002) and Reichmüth and Anthony (2002). King (1972a) further suggested preferred locations of ridge development at the mean spring and neap tidal levels, where the water level was assumed to be stationary for the longest period of time. The ridges and runnels along the north Lincolnshire coast, however, are distributed fairly evenly across the intertidal profile, in accordance with several other studies that reported that ridges occurred most frequently between MLWN and MHWN levels (e.g., Wright, 1976; Orford, 1985; Mulrennan, 1992; Masselink and Anthony, 2001). This investigation further shows that the spacing between the ridges is constant on the lower beach, but decreases landward above MHWN level. Similarly, ridge spacing decreases onshore at Dundrum beach in Northern Ireland (Navas et al., 2001; Navas and Malvarez, 2002). The opposite is observed, however, at Nieuwpoort aan Zee in Belgium (Voulgaris et al., 1996 and 1998). Navas and Malvarez (2002) also reported that the ridges become steeper onshore. This is partially in agreement with the findings for the Lincolnshire coast, as here the gradient of the seaward slopes only increase till MHWN level and decrease again higher on the beach.

Inspection of the longshore variation in intertidal morphology suggests that the north Lincolnshire coast can be subdivided into three areas based on the appearance and/or absence of ridges and runnels: (1) the beaches north of the tidal creek delta near Saltfleet; (2) the delta itself; and (3) the area south of the delta until Mablethorpe. The beach morphology near Saltfleet is dominated by the presence of the tidal creek and

shore-parallel ridges and runnels are replaced by tidal levees perpendicular to the shore. Ridges and runnels recur, however, immediately north and south of the delta and the morphology at both sides of the delta differs in that spacing of the drainage channels that dissect the ridges appears related to the amount of water that needs to be drained during the falling tide. A wide upper intertidal flat and salt marsh region is present in the northern part of the study area and here, drainage channels frequently dissect the ridges, resulting in a distinctly three-dimensional morphology. In the southern part of the study area, where the ridges and runnels are directly backed by dunes, the drainage channels are less numerous and the morphology is more two-dimensional. Hence, the longshore variability in the ridge and runnel morphology is dominated by the variation in drainage channel density rather than any longshore variability in number, size, volume or slope of ridges and runnels. Quantification of the longshore variability is scarce in previous studies, although Reichmüth and Anthony (2003) noted little longshore variability for the ridges and runnels at Dunkerque-west in France, whereas Mulrennan (1992) reported significant longshore variation in the gradient of the ridge and runnel profile and ridge dimensions due to the close presence of an active ebb tidal delta system.

Previous studies have not reported relations and correlations between various morphometric ridge and runnel parameters and hence the results of the correlation analysis presented in Table 3.3 stand on their own. The main findings of the correlation analysis presented in this chapter were: (1) the positive relation between the width of the ridge and runnel zone and the number of ridges; (2) despite a widening of the zone, the larger amount of ridges goes together with a decrease in the spacing; (3) the slope of the seaward ridge face depends on the overall slope of the ridge and runnel zone, with steeper ridges on steeper profiles; (4) ridge height is positively correlated to ridge width; and, similarly, (5) deeper runnels tend to be wider.

The overall characterisation of the ridge and runnel morphology in this study (Table 3.2) reveals that on average more ridges and runnels are present along the north Lincolnshire coast than on other beaches. Leffrincoucke beach in France, though, is another site with a large number of ridges and runnels, with, for instance, up to 6 ridges and runnels during the field study of Sipka and Anthony (1999). The average height of the ridges (c. 0.7 m) is comparable to the ridge height at most other beaches, although

significantly larger ridges were observed at Portmanock Barrier in Ireland (c. 1.2 m) (Mulrennan, 1992). Ridge spacing is generally smaller than elsewhere. It should be noted, however, that the LIDAR data provided a snap-shot of the ridge and runnel morphology at one moment, just as the results in other studies are based on a relatively small set of cross-shore profiles surveyed over a particular period.

The accomplishment of additional LIDAR surveys of the north Lincolnshire coast is strongly advised. This not only enables a sediment budget analysis for this coastal stretch, but also the detailed investigation of the temporal variability in ridge and runnel morphology. The use of repetitive topographic LIDAR surveys has provided fine-resolution and accurate quantifications of volume change in numerous coastal studies (e.g., Mitasova et al., 2003; Sallenger et al., 2003), yet, sediment budget analysis for ridge and runnel beaches has only been based on data from ground surveys (King 1972a; Mulrennan, 1992, Reichmüth and Anthony, 2002).

3.6 CONCLUSIONS

- The ability of LIDAR to rapidly survey long, narrow strips of terrain has been very valuable in various coastal applications, particularly in the monitoring of short- and long-term coastal change. LIDAR has not been previously applied, however, to map intertidal features such as ridges and runnels.
- A LIDAR-derived DEM of the intertidal zone along the north Lincolnshire coast is of sufficient resolution and quality to accurately reproduce ridges and runnels. The DEM has provided unprecedented insight into the spatial variability of the ridge and runnel morphology.
- Longshore variability in the ridge and runnel morphology is dominated by the variation in drainage channel density. The spacing of the drainage channels appears related to the amount of water that needs to be drained during the falling tide and density of the drainage channels is therefore significantly larger in the northern part of the study area, where the ridges and runnels are backed by wide tidal flats.
- The ridges and runnels along the north Lincolnshire coast, are distributed fairly evenly across the intertidal profile, and the largest bars (in terms of volume) occur

around MSL. The spacing between the ridges is constant on the lower beach, but decreases landward above MHWN level

- On average, five ridges and runnels are present along the north Lincolnshire coast, and this is generally more than on other ridge and runnel beaches. The average ridge height was c. 0.7 m (similar to ridge height elsewhere).
- Correlation analysis between various morphometric parameters showed: a positive relation between the width of the ridge and runnel zone and the number of ridges; a dependence of ridge steepness on the beach gradient; and that ridge height is positively related to ridge width.

Chapter four

Inter-annual and Intra-annual (summer versus winter) Variability in Ridge and Runnel Morphology

4.1 INTRODUCTION

After a description of the large-scale spatial variability in ridge and runnel morphology in Chapter 3, this chapter focuses on the long-term dynamics of the ridges and runnels, as it is thought that insight on these large spatial and temporal scales provides an essential framework for understanding the behaviour of ridges and runnels on smaller scales (Chapters 5–7).

Although ridge and runnel topography has been the subject of an increasing number of morphodynamic studies (e.g., Mulrennan, 1992; Kroon and Masselink, 2002; Reichmüth and Anthony, 2002; Anthony et al., 2004), the investigation of long-term variability in ridge and runnel morphology has been limited. Profile data for ridge and runnel beaches rarely extend up to 5 years and in fact many previous monitoring projects have only lasted 1–3 years (King and Williams, 1949; Wright, 1976; Mulrennan, 1992; Reichmüth, 2003). The few studies that have described ridge and runnel characteristics over longer periods are King (1972a) for the south Lincolnshire coast, UK (1958–1968), van den Berg (1977) for Schouwen beach, the Netherlands (1962–1975) and Masselink and Anthony (2001) for the north Lincolnshire coast, UK (1991–1999) and Blackpool beach, UK (1980s–1999).

Ridges and runnels are permanent features on most beaches (King and Williams, 1949; King, 1972a; Wright, 1976; Chauhan, 2000), although some authors refer to the semi-permanency of the ridge and runnel topography as ridges tend to be well-developed during calm weather and flattened or destroyed by storm waves (van den Berg, 1977; Mulrennan, 1992; Sipka and Anthony, 1999). For example, Masselink and Anthony (2001), describing profile data for the north Lincolnshire coast, UK and Leffrincoucke beach, France, noted that all summer beach profiles and most of the winter profiles were characterised by ridge and runnel morphology, but that fewer ridges were generally present in winter and that they were also less pronounced than in summer. Van den Berg (1977) noted a long-term increase in the number of ridges and runnels on Schouwen beach, the Netherlands, as an average of 1.2 ridges were present from 1962 to 1967, increasing to 3.1 ridges from 1972 to 1975.

Research on the dynamics of subtidal bars has been more common and numerous studies have examined the long-term behaviour of such bars, for example along the Holland Coast, the Netherlands (Kroon, 1994; Wijnberg, 1995; Wijnberg and Terwindt, 1995), the coast of Terschelling (Ruessink, 1998; Ruessink and Kroon, 1994), the Wanganui coast in New Zealand (Shand et al., 1999) and at Duck, U.S.A. (Lippmann et al., 1993; Plant et al., 1999). These coasts are characterised by double or multiple subtidal bar systems and show long-term cyclic behaviour. From datasets, covering 30 years for the Dutch coast, and 15 years for the study at Duck, it was observed that the subtidal bars pass through three stages during their existence: generation close to the shoreline; net seaward migration through the surf zone; and decay at the outer margin of the nearshore zone (Figure 4.1). This systematic formation, migration and destruction of bars results in cyclic behaviour so that after each cycle the same bar topography can be observed. The characteristic duration of the cycle differed between the beaches and was even found to change dramatically along a stretch of coast. For example, Ruessink (1998) and Ruessink and Kroon (1994) described the cyclic behaviour at Terschelling, the Netherlands, and they found a cycle duration of 12 years. Further south, along the Holland coast, however, Kroon (1994) and Wijnberg (1995) found durations of 15 years and 4 years, with the change occurring across opposite sides of a jetty, despite similar external forcing and geologic conditions.

Aim and objectives Chapter 4

The aim of this chapter is to improve insight into the long-term characteristics and inter-annual variability of ridge and runnel morphology. Additionally, seasonal variation (summer versus winter) will be examined. Specifically, the following research questions were formulated:

(1) Are ridges and runnel permanent features along the north Lincolnshire coast?
(2) What are the average number and dimension of the ridges and runnels over the last decade?
(3) Do the ridges and runnels show a distinct long-term variability in number, dimension and shape?
(4) How significant is the long-term variability in relation to any seasonal variability?
(5) Can the morphological changes be linked to variations in external forcing?

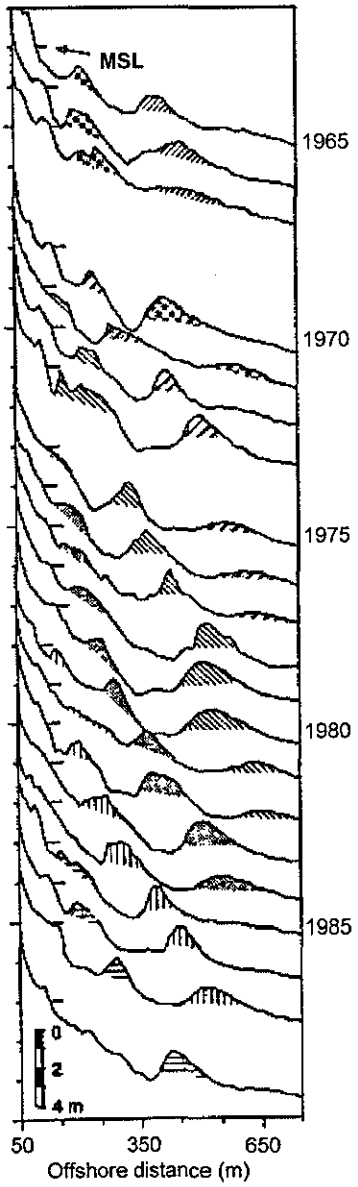

Figure 4.1 – Migration of a subtidal bar system (Modified from Wijnberg, 1996).

4.2 METHODOLOGY

A qualitative, as well as a quantitative analysis of the inter- and intra-annual variability in ridge and runnel morphology was carried out using aerial photographs and twice-yearly beach profiles for three localities along the north Lincolnshire coast: Donna Nook, Theddlethorpe and Mablethorpe. Annual aerial photographs were collected to enable the qualitative comparison of the appearance of ridges and runnels from year to year. The aerial photographs were provided by the Anglian Regional

Office of the Environment Agency, UK, and cover the period 1991–2003. The photographs were taken between July and October (generally in August) and represent the summer state of the ridge and runnel morphology. Additionally, aerial photographs, taken in July 1977 and May 1983 were included and these were made available by the Aerial Photography section of the Unit for Landscape Modelling of Cambridge University, UK. For each beach, and each year, an area of 375 m (longshore) by 450 m (cross-shore) was extracted from the photographs, using distinctive landmarks as dune paths, car parks and bombing targets to identify identical areas.

Twice-yearly beach profile data (summer and winter) for Donna Nook, Theddlethorpe and Mablethorpe were used to complement the annual photographs. Surveys were conducted from 1991 to 2003, however, a significant number of the beach profiles for Donna Nook and Mablethorpe do not extend to MLWS and do not include all the ridges and runnels present at the time. A quantitative analysis of the morphological change was therefore only carried out for Theddlethorpe.

The profiles were cross-correlated to each other to quantify the degree of similarity between successive profiles. The time interval between profiles was half a year, but additionally cross-correlation coefficients between profiles with larger time lags were calculated to investigate how often the beach profile 'resets', so that individual ridges cannot be tracked from one profile to the next. The beach profiles were further used to determine morphometric characteristics of the ridge and runnel morphology, such as number of ridges, and their amplitude, shape, size and spacing. Elevation data for the ridges and runnels were extracted from each profile, taking the seaward limit of the profile as the lower boundary of the ridge and runnel zone and defining the landward boundary visually. The shortened profiles were then linearly interpolated to 0.1 m and a second-order polynomial curve was fitted through the ridges and runnels to yield the residual profile (refer to Figure 3.4). Ridge amplitude, shape, size and spacing were calculated for each ridge in the residual profile in a similar way as presented in Chapter 3, for the analysis of multiple beach profiles obtained from LIDAR (refer to Table 3.1 for definitions of morphometric parameters). The data were further reduced by averaging in the cross-shore direction so that one value was obtained for each parameter, for each year. This value was directly used to compare

the profiles from year to year and to detect any long-term trends in the development of the ridges and runnels. The surveyed profiles were regularly found to be incorrectly linked to ODN level and this was manually corrected for by assuming that the level of the sand flat between consecutive profiles, i.e., over 6 months, was constant. The correction did not have any effect on the quantification of long-term morphometric characteristics, however, the adjustments in beach level did alter the sediment-budget calculations. Even if the corrected profiles would deviate 0.01 m from the real value this would result in significant variations in the sediment budget. Because many profiles are also too short to include MLWS, it was decided not to include long-term sediment budget analysis in this chapter.

Time series of wind and surge covering the period 1991–2003 were used to relate the morphological development of the ridges and runnels to the long-term external forcing. Hourly measurements of wind speed and direction at Donna Nook and hourly sea level observations for Cromer were supplied by, respectively, the British Meteorological Office/British Atmospheric Data Centre (UK Metoffice) and the UK National Tidal Gauge Network/British Oceanographic Data Centre (BODC). The wind data were converted into a wind rose (Figure 2.5) and annual wind speed frequencies were calculated whereby wind speed classes were defined using the scale of Beaufort as a basis (Figure 2.5). The data were subsequently reduced from hourly observations to daily averages and a distinction was made between the occurrence of onshore and offshore winds. Surge was defined as the elevation of tidal level on top of the predicted astronomical tide and was used as an indicator for storminess. Hourly sea level predictions for Cromer were extracted from the Admiralty Tide Tables (2001) and surge data were then computed by subtracting the sea level predictions from the sea level observations. Although Cromer is located 90 km south of the study site, these surge data were assumed to be representative for the north Lincolnshire coast as well. The hourly surge time series was used to determine the frequency of storm surge events over the 90-day periods before beach profiles were taken. Additionally, storm surges in combination with onshore winds were identified.

4.3 RESULTS

Figure 4.2 shows the development of the beach at Donna Nook, Theddlethorpe and Mablethorpe over the period 1991–2002. Interesting changes were observed in the dune area, particularly at Donna Nook and Theddlethorpe. An incipient foredune developed at Donna Nook between 1991 and 1997, that accreted further between 1997 and 2002. The dune development at Theddlethorpe is characterised by the growth of the existing dunes. The wide sub-horizontal sand flats at these two beaches underwent some accretion, but generally morphological change here was small. Additionally, the profiles reveal that the cross-shore position of the ridge and runnel zone was stationary.

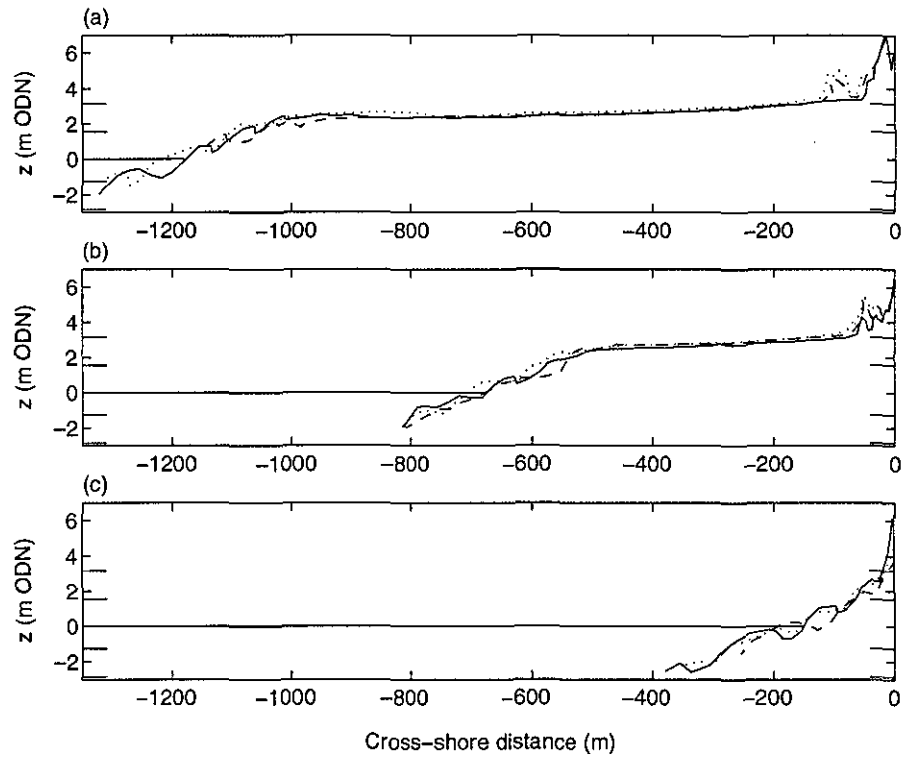

Figure 4.2 – Summer beach profiles for 1991 (solid lines), 1997 (dashed lines) and 2002 (dotted lines) at: (a) Donna Nook; (b) Theddlethorpe; and (c) Mablethorpe. The horizontal solid line represents MSL, and the small horizontal lines refer from bottom to top to MLWS, MLWN, MHWN and MHWS.

Annual aerial views of the ridges and runnels at Donna Nook, Theddlethorpe and Mablethorpe, covering the period 1991–2003, are presented in Figures 4.3–4.5. Photographs taken in 1977 and 1983 are also shown. The key observation of these series of aerial photographs is that a clear pattern of ridges and runnels is visible in all

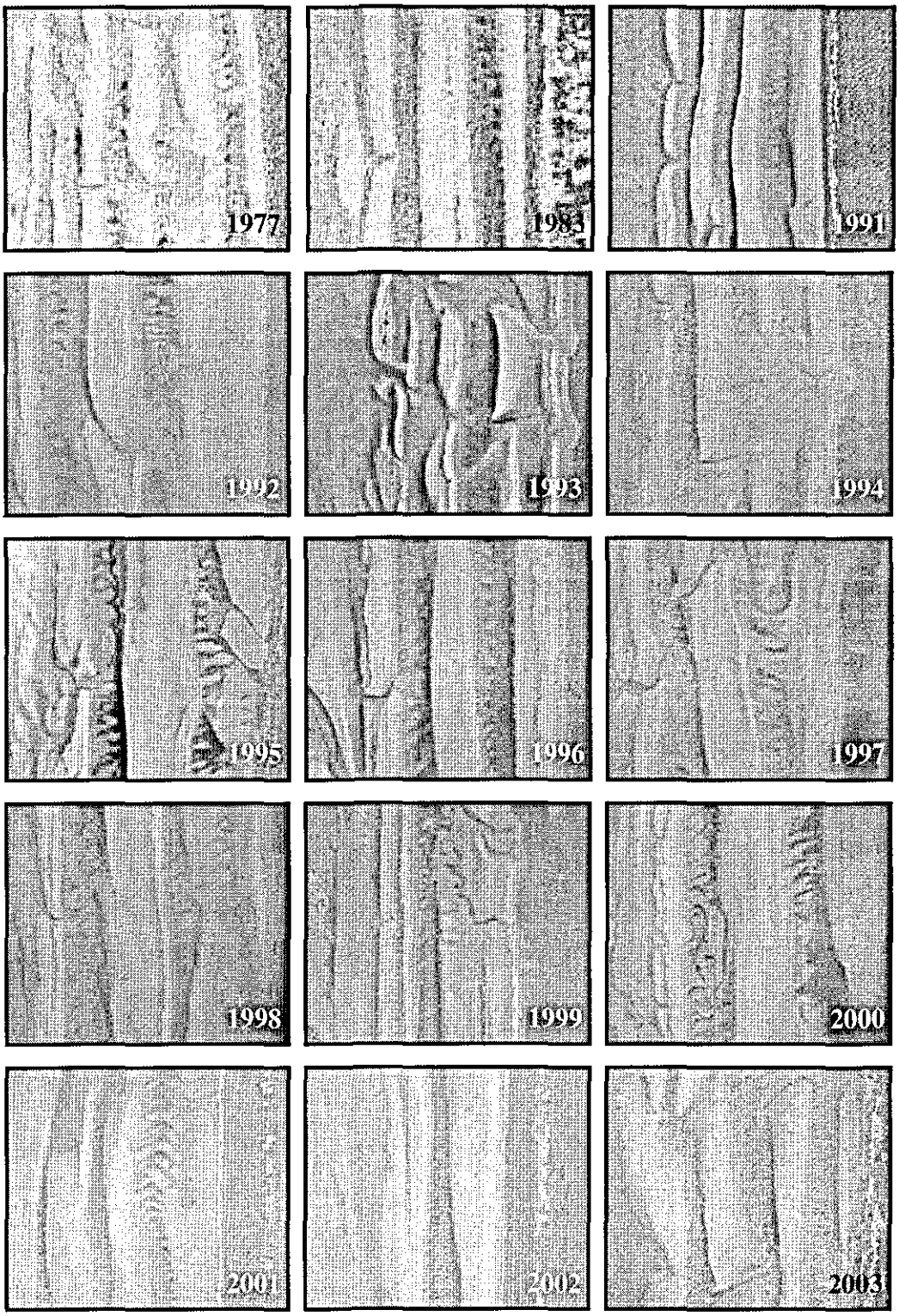

Figure 4.3 – Aerial photographs of the ridges and runnels at Donna Nook from the years 1977, 1983 and 1991–2003. For each photo, the sea is displayed on the right-hand side and the region with ridges and runnels merges with the sand flat on the left-hand side.

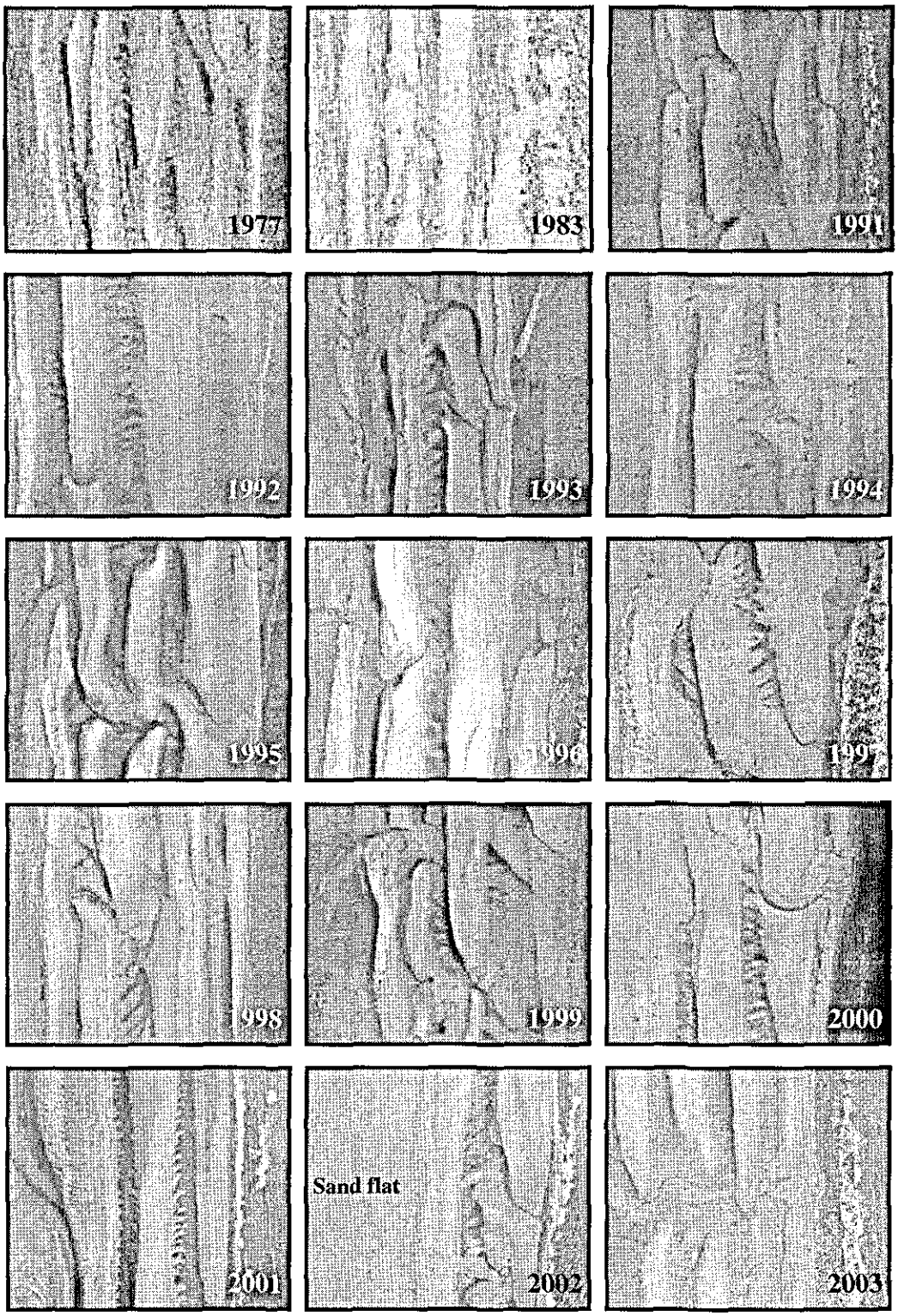

Figure 4.4 – Aerial photographs of the ridges and runnels at Theddlethorpe from the years 1977, 1983 and 1991–2003. For each photo, the sea is displayed on the right-hand side and the region with ridges and runnels merges with the sand flat on the left-hand side. (Note: the 2002 photograph represents an area slightly more landward and only shows the upper part of the ridge and runnel zone.

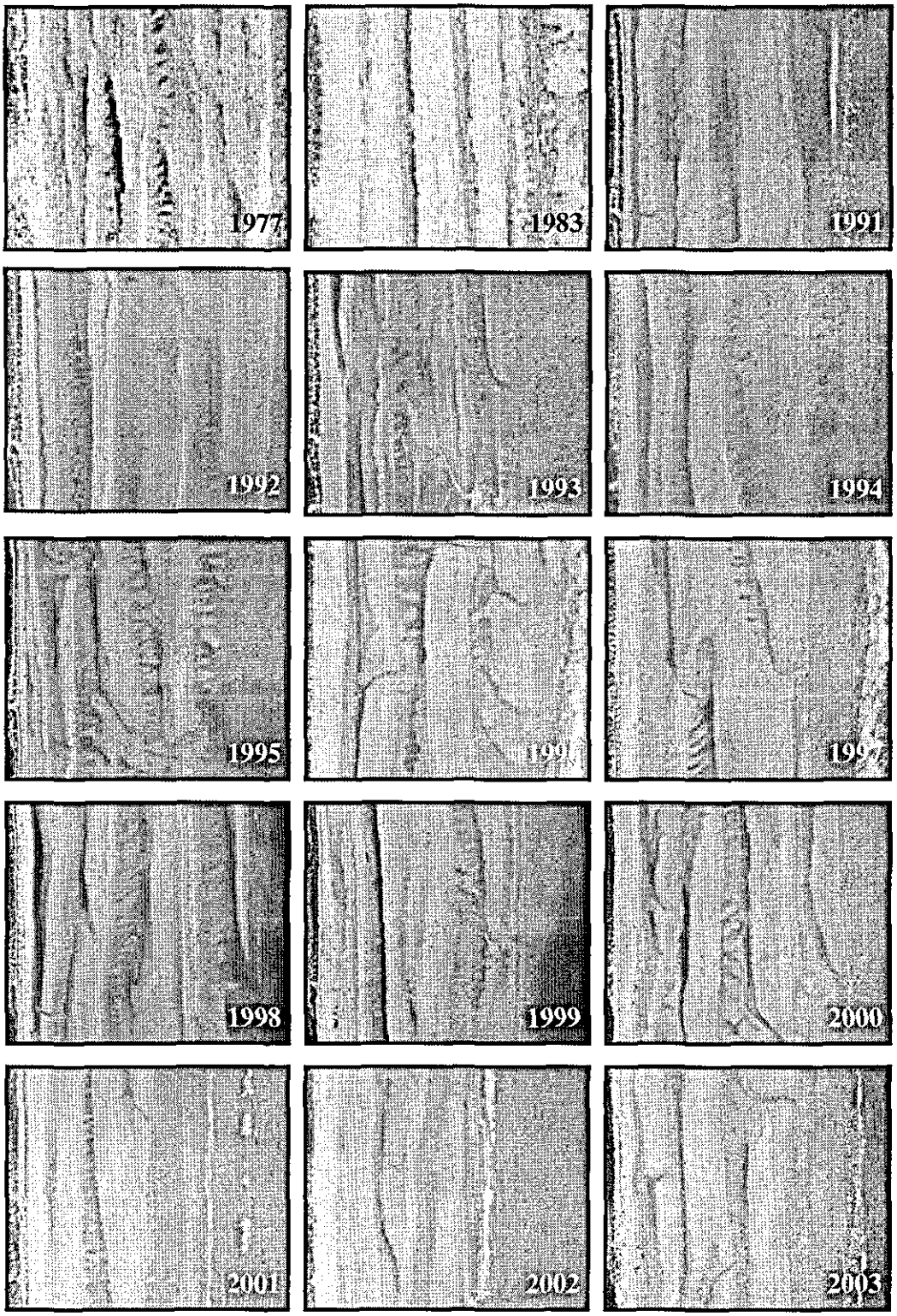

Figure 4.5 – Aerial photographs of the ridges and runnels at Mablethorpe from the years 1977, 1983 and 1991–2003. For each photo, the sea is displayed on the right-hand side and the region with ridges and runnels is backed by dunes on the left-hand side.

photographs. This is very convincing evidence that ridges and runnels are permanent features of the intertidal beach along the north Lincolnshire coast, not only on a time scale of years, but over decades. The number of ridges was 3–6 at Donna Nook, 3–5 at Theddlethorpe and 2–5 at Mablethorpe, with an average number of 4 ridges at Donna Nook and Theddlethorpe and 3 ridges at Mablethorpe (Table 4.1). The configuration of the ridges and runnels was very dynamic and precludes the tracking of individual ridges from year to year. The low coherence in ridge configuration between consecutive photographs may be the result of large cross-shore and longshore ridge migration rates and/or major re-arrangement of the ridge configuration as a whole (e.g., the formation of a new ridge, infilling of a runnel or development of a new drainage rip). Annual changes in the morphology were compared between the three different sites, but the spatial coherence was limited. For example, on Theddlethorpe beach, the ridge and runnel morphology was highly three-dimensional in 1993, 1995 and 1999, but this was not the case on the other two beaches. For all three sites, however, it was noted that the widest ridge was generally one of the middle ridges (cf., Masselink and Anthony, 2001) and only 2–4 of the 15 aerial photographs that were investigated per site showed that the lowest ridge was widest (cf., King and Williams, 1949; King, 1972a).

Table 4.1 – Ridge and runnel characteristics for Donna Nook, Theddlethorpe and Mablethorpe, based on the visual analysis of aerial photographs: (1) number of ridges; (2) location of the widest ridge (referring to the lower (low) and middle (mid) ridge and runnel zone); and (3) ridge configuration (minor (–), intermediate (+/–) or mayor (+) distortion by drainage channels).

	Donna Nook			Theddlethorpe			Mablethorpe		
Year	Num-ber	Widest Ridge	Config-uration	Num-ber	Widest Ridge	Config-uration	Num-ber	Widest Ridge	Config-uration
1977	6	mid	–	5	-	+/–	5	-	+/–
1983	5	mid	–	4	mid	–	3	mid	–
1991	4	low	–	4	mid	+	3	low	–
1992	4	mid	+/–	3/4	mid	–	4	mid	–
1993	5	mid	+	4	mid	+	3	equal	+
1994	4	mid	+	4	mid	+	3	mid	+/–
1995	4	mid	+/–	5	mid	+/–	3	mid	+/–
1996	4	low	–	4	mid	+/–	3	mid	+/–
1997	3	mid	–	3	equal	+	2	low	+
1998	3/4	mid	–	4	mid	+/–	4	mid	–
1999	3/4	low	–	4	mid	+	3	mid	+
2000	3	mid	–	3	low	–	4	mid	+/–
2001	4	mid	–	4	mid	–	3	mid	–
2002	3	low	–	-	-	+/–	3	equal	+/–
2003	4	mid	+	4	equal	+/–	4	mid	–

The permanency of the ridges and runnels is further confirmed by analysis of the twice-yearly beach profiles and it is also observed that the winter profiles tend to be flatter with fewer, but often wider, ridges (Figure 4.6). The profiles show furthermore that the ridges regularly exhibited well-developed slipfaces in summer, but generally not in winter.

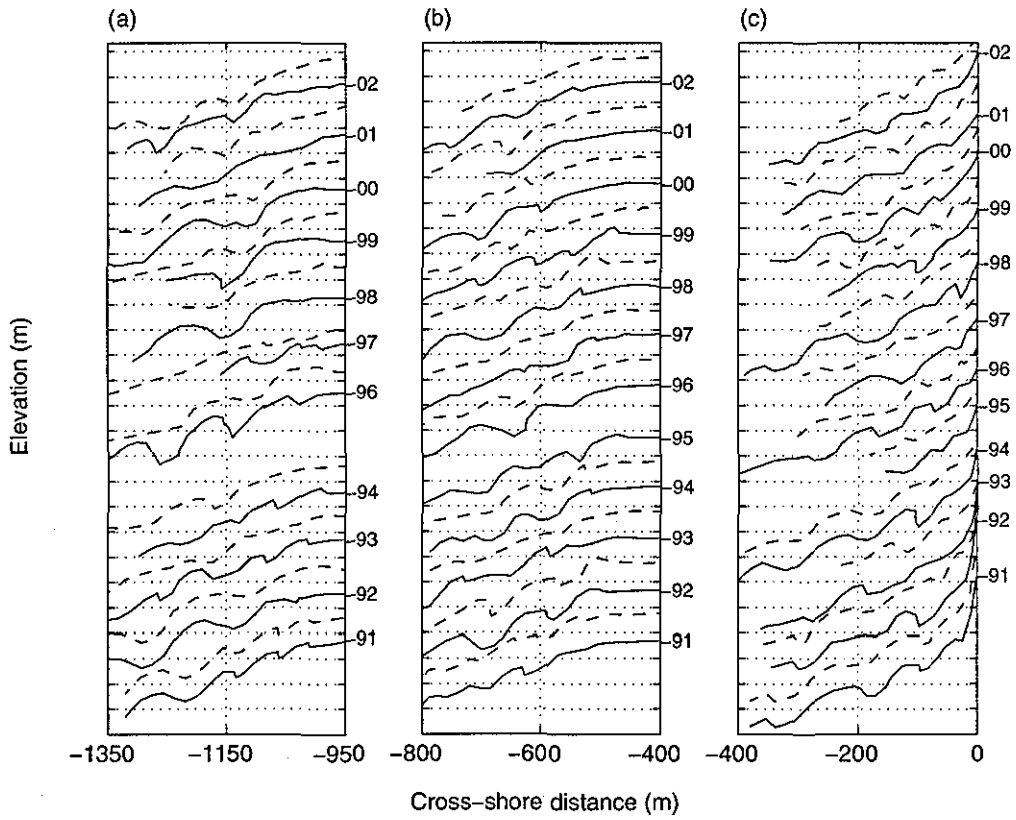

Figure 4.6 – Summer (solid lines) and winter (dashed lines) profiles of the ridge and runnel zone at (a) Donna Nook, (b) Theddlethorpe, and (c) Mablethorpe over the period 1991–2003. The profiles have been stacked with an offset of 1.5 m. The vertical spacing between gridlines is also 1.5 m.

Cross-correlation between successive profiles indicates that the degree of resemblance between summer and winter is similar to that between winter and summer (Figure 4.7a). The degree of resemblance was defined as the maximum correlation coefficient from cross-correlation analysis and values are on average c. 0.65 for both the summer-to-winter and the winter-to-summer correlations, with standard deviations of c. 0.3. The fairly low correlation coefficients indicate that morphological change over half a year is significant, but that complete 'resetting' of the beach profile did not occur. The lag distance corresponding to the maximum correlation coefficient is interpreted as an indicator for ridge migration rate (provided

that the lag distance is smaller than the average ridge spacing) and it appears that ridges migrated on average c. 5 m offshore from summer to winter and c. 20 m onshore from winter to summer (data not shown). Beach profiles surveyed more than 6 months apart display less similarity, as suggested by lower correlation coefficients and larger standard deviations for profiles with larger time intervals between them (Figure 4.7b).

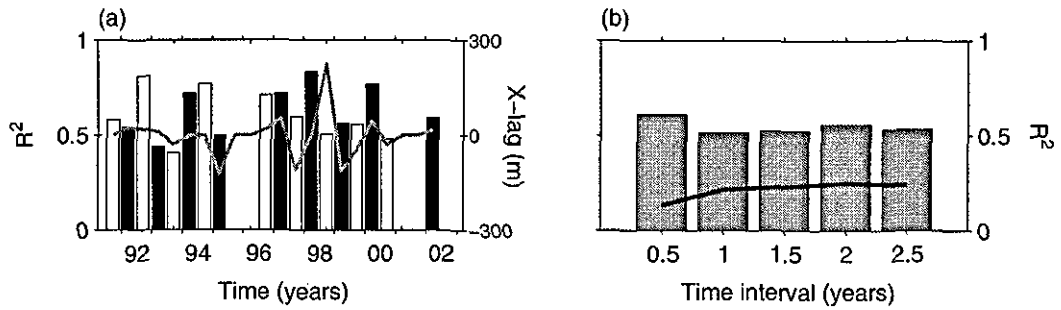

Figure 4.7 – Results from cross-correlation between beach profiles: (a) maximum correlation coefficients from summer to winter (white bars) and winter to summer (black bars). The right-hand axis refers to the corresponding distance lag (grey solid line); (b) maximum correlation coefficient in relation to time interval between profiles. Plotted are the average values for each time interval (bars), together with their standard deviations (line).

Ridge-by-ridge analysis further complements the investigation to quantify long-term morphological change and Table 4.2 summarises average values for various characteristics of ridge and runnel morphology. It is noted that the overall averages for the period 1991–2003 are remarkably similar to the results obtained from the LIDAR DEM in Chapter 3. The main difference is that the number of ridges and runnels appears lower from the present profile analysis. Over long-term, an average of 3.5 ridges and runnels were present at Theddlethorpe and more ridges tended to be present in summer than in winter. It is further revealed that ridge spacing increased between summer and winter and that ridge shape altered concurrently from being landward-skewed in summer to seaward-skewed in winter.

Figure 4.8 shows the bi-annual variability of some of the morphometric parameters listed in Table 4.2, whereby the grey areas around the curves indicate the degree of variation amongst individual ridges in the profile. The most notable observation is that intra-annual (summer versus winter) variation in the ridge and runnel

morphology is more significant than the inter-annual variation and that a clear long-term trend in number, dimensions and shape of the ridges and runnels is not obvious.

Table 4.2 – Morphometric characteristics for the ridge and runnel morphology at Theddlethorpe over the period 1991–2003. The different columns present the averages of, respectively, all profiles, the summer profiles and the winter profiles. Positive and negative values for ridge asymmetry indicate, respectively, landward- and seaward-skewed ridges.

Parameter	All	Summer	Winter
Number of ridges	3.5	3.8	3.2
Ridge height (m)	0.6	0.6	0.6
Ridge width (m)	57	53	62
Ridge volume ($m^3\ m^{-1}$)	9.5	9.9	9.1
Ridge asymmetry (ln(-))	0.01	0.06	-0.06
Gradient seaward ridge face (tanβ)	0.024	0.024	0.024
Spacing ridge crests (m)	92	85	102
Runnel width (m)	42	39	45

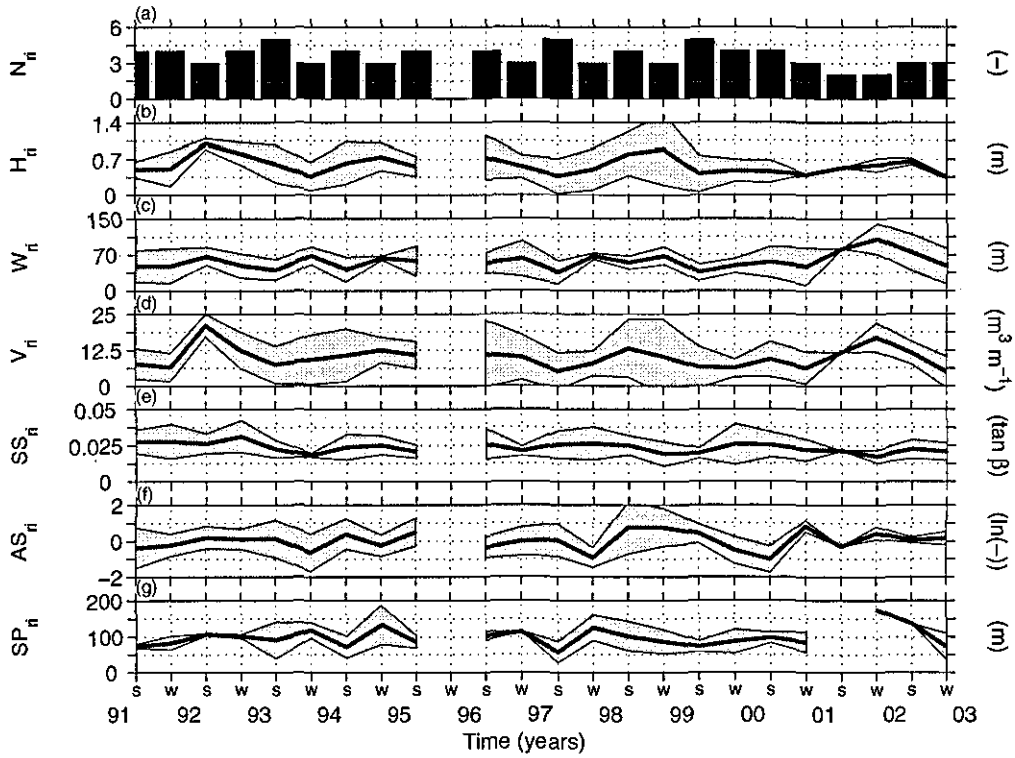

Figure 4.8 – Variability in ridge and runnel morphology from summer 1991 to winter 2002/2003: (a) number of ridges; (b) ridge height; (c) ridge width; (d) ridge volume; (e) gradient of seaward ridge face; (f) ridge asymmetry; and (g) ridge crest spacing. The solid lines in (b–g) represent the cross-shore average of the profiles and the grey envelopes indicate the ± one standard deviation

Wind and surge conditions from 1991 to 2003 are plotted in Figure 4.9 to obtain an indication of the long-term storminess over this period. It appears that wind conditions were rather similar from year to year (Figure 4.9a) and that annual wind speed frequencies were remarkably constant as well (Figure 2.6). Surge levels also show a low inter-annual variability, but seasonal variability was more significant and clearly shows that storm surge events tended to occur in winter (Figure 4.9b). The number of summer surge events increased, however, considerably after 1999 (note: the large number of onshore storm surges in summer 2001 was due to the inclusion of autumn storms as profile measurement was delayed for 2 months till November). Extreme surges (> 1.5 m) occurred just before the profiles were taken in winter 1999 and winter 2002, but the effect on the morphology may have been limited as these surges coincided with offshore winds. The surge events in combination with onshore winds were generally between 0.5 and 1 m and large storm surge events (> 1 m) with onshore wave attacks were rare (Figure 4.9d).

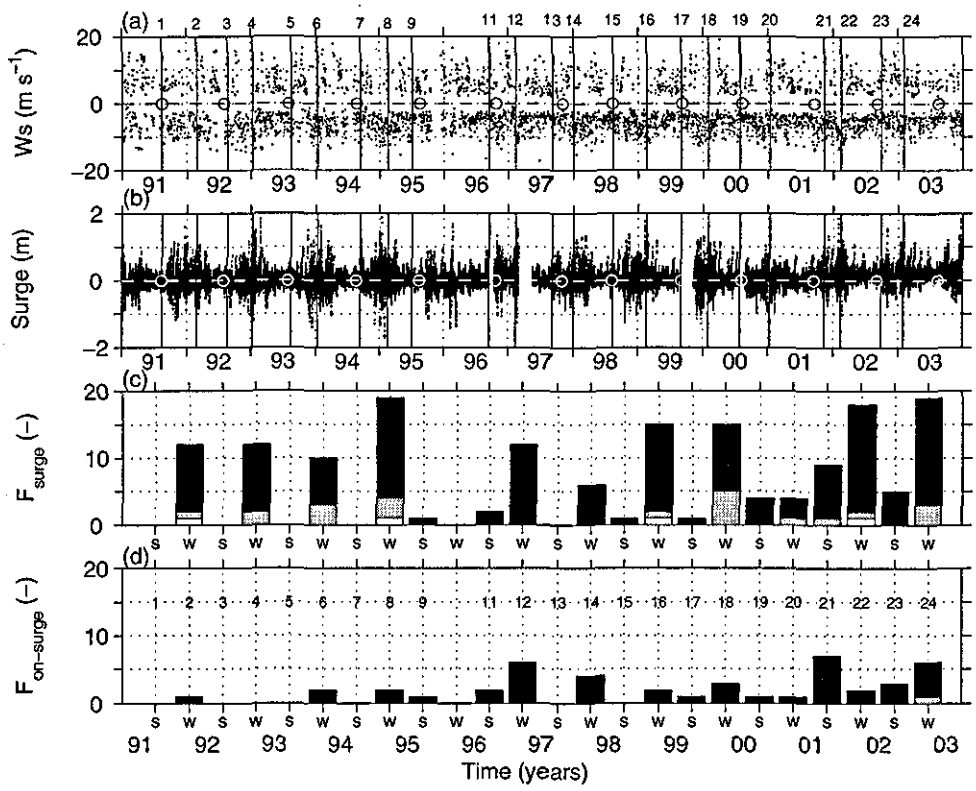

Figure 4.9 – Wind and surge conditions from 1991 to 2003: (a) onshore (positive values) and offshore (negative values) wind speeds > 7.5 m s^{-1}; (b) surge level; (c) frequency of surges with levels of 0.5–1 m (black bars), 1–1.5 m (grey bars) and > 1.5 m (white bars); and (d) frequency of surges with onshore wind. Timing of beach surveys and annual aerial photographs are indicated in the upper two panels by, respectively, vertical lines and circles.

The variability in external forcing conditions agrees with the observed morphological variation to the extent that a distinct long-term trend is absent and that changes show a strong seasonal variation. The increase in storm surge events during the summer months after 1999 did not clearly manifest itself in a decrease of the ridges and runnels, although the lower number of ridges and runnels in summer 2000 and summer 2001 may be explained by this.

4.4 DISCUSSION

Ridges and runnels appear to have been permanent features of the intertidal beach along the north Lincolnshire coast for at least the last 50 years. King (1972a) was the first to report ridge and runnel morphology along this stretch of coast and surveyed some beach profiles at Theddlethorpe and Mablethorpe in 1953 that clearly featured the ridges and runnels. Noteworthy, these profiles were taken just after an extreme storm surge event in February 1953. Ridges and runnels were subsequently observed in 1957 (also by King, 1972a), 1977, 1983 and annually from 1990 until present.

Ridge and runnel morphology also seems permanent on other coasts, as beaches that were studied tens of years ago (e.g., King and Williams, 1949; King and Barnes, 1964; Parker, 1975; Wright, 1976) still feature well-developed ridges and runnels today (refer to Figure 1.3). Furthermore, the semi-permanent, also referred to as quasi-permanent, character of the ridges and runnels in other studies (Wright, 1976; van den Berg, 1977; Mulrennan, 1992) was attributed to the flattening or destruction of individual ridges and in fact complete destruction of the ridge and runnel topography has never been observed. From this it may be concluded that ridge and runnel morphology as a whole tends to be a permanent characteristic of a beach, whereas individual ridges and runnels are not permanent. The life span of an individual ridge and runnel couplet is directly related to the occurrence of storms (magnitude and frequency) and the relaxation time involved in morphological adjustment, and is therefore not only dependent on the volume of the ridges but also on their position in the cross-shore profile.

The qualitative beach profile analysis presented in this chapter is unfortunately only based on single beach profiles surveyed at Theddlethorpe, as the available data set

was of inadequate quality to incorporate accurate and complete profiles for Donna Nook and/or Mablethorpe. Incorrect linking of beach profiles to ODN level further inhibited detailed analysis of sediment budgets. Accretive or erosive beach states have been suggested previously to play an essential role in the occurrence and behaviour of ridges and runnels (King 1972a; Reichmüth and Anthony, 2003), but the present study lacks data from which to comment on this issue.

Nevertheless, the beach profiles could be used for visual inspection of the long-term morphological development of the coast and the most remarkable change is the accretion in the dune area. This resulted in significant growth of the present foredune at Theddlethorpe and even led to the formation of a new one at Donna Nook. So, even with prevailing offshore winds along the coast, significant amounts of sediment have been transported towards the dunes during episodes of onshore winds. The dunes at Mablethorpe, however, did not change significantly. The differential behaviour between the sites is attributed to the presence of a sand flat at Donna Nook and Theddlethorpe. When these sand flats are exposed, they function as a source for aeolian sediment transport and since they form the upper part of the intertidal zone they are sub-aerial for the majority of the lunar tidal cycle. The dunes at Mablethorpe not only lack the sand flat as a source of aeolian sediment, but also as a buffer under high wave-energy conditions. The dunes here are under direct wave-attack during storms, resulting in regular scarping of the dune face.

Studies of multiple subtidal bars on low-tidal beaches (tidal range < 3 m), have suggested the occurrence of long-term cyclic behaviour, with bars forming, migrating and decaying over periods varying from 4 to 15 years (e.g., Kroon, 1994; Wijnberg, 1995; Ruessink, 1998). They further indicate that a strong interdependence exists between the bars and that the most outward bar plays the determinative role (Ruessink and Kroon, 1994; Shand et al., 1999). For example, as soon as the outer bar starts to decay, the inner bar(s) starts to migrate offshore, making space near the shoreline for a new bar to form. To reveal such long-term behaviour was only possible because the used data sets covered the duration of at least two complete cycles. A similar long-term behaviour may be present on ridge and runnel beaches, but the profile data from 1991 to 2003 for the north Lincolnshire coast may be too limited to reveal a clear long-term variation in the ridge and runnel morphology.

Additionally, intertidal bars are only under the influence of hydrodynamic processes during part of a tidal cycle and this may possibly result in even longer cycle durations (if long-term behaviour is cyclic in the first place).

The current data set, nonetheless, resulted in an extended insight into the long-term development of ridge and runnel morphology along the north Lincolnshire coast. From 1990 to 2003, on average 3.4 ridges and runnels were present, with an average ridge height and width of, respectively, 0.6 m and 60 m. Intra-annual (summer versus winter) appeared more significant than inter-annual variation. Specifically, more ridges were generally present in summer than in winter (cf., King, 1972a; Mulrennan, 1992; Masselink and Anthony, 2001) and the variation in number of the ridges and runnels consistently coincided with a change in ridge dimension and shape. The ridges and runnels seemed very dynamic with the morphology 'resetting' itself almost every 6 months. Individual ridges could therefore not be tracked from year to year and systematic cross-shore bar migration trends were not apparent. In that respect, the inter-annual variability in ridge and runnel morphology along the north Lincolnshire coast is very different from those described from the above-mentioned subtidal bar systems, where it is generally possible to track individual bars and identify trends in offshore (Ruessink and Kroon, 1994; Wijnberg, 1996; Shand et al., 1999; Plant et al., 2001) and onshore (Aagaard et al., 2004) bar migration.

Examination of long-term wind and surge conditions revealed that external forcing is characterised by a strong seasonal variability, with higher waves and more storms in winter. Hence, the large intra-annual (summer versus winter) variation in the ridge and runnel morphology seems strongly related to the external forcing conditions. This suggests that on a summer versus winter time-scale, a ridge and runnel system can be considered forcing-responsive. The large change in beach configuration between the twice-yearly profiles may further be attributed to longshore migration of the ridges, but this is investigated in greater detail in Chapter 5.

4.5 CONCLUSIONS

- Ridge and runnel morphology has characterised the intertidal beach of the north Lincolnshire coast for at least the last 50 years. Ridges and runnels are also permanent features on numerous other beaches in Britain, for example at Formby Point, Blackpool and Gibraltar Point.
- Individual ridge and runnel couplets, however, are not permanent as they tend to flatten or even disappear during periods of relatively high-wave energy conditions. The life span of an individual ridge and runnel is directly related to the occurrence of storms (magnitude and frequency) and the relaxation time involved in the morphological adjustment.
- From 1990 to 2003, on average 3.4 ridges and runnels were present along the north Lincolnshire coast, with an average ridge height and width of, respectively, 0.6 m and 60 m. A distinct long-term change in the ridge and runnel dimensions was not observed.
- Intra-annual (summer versus winter) morphological variability is more significant than inter-annual variation. More ridges were generally present in summer than in winter and the ridge and runnel configuration changes to such extent that individual ridges can generally not be tracked from year to year.
- Ridges and runnels can be considered forcing-responsive on a summer versus winter time-scale, indicated by the reflection of the external forcing conditions.
- Profile data for at least 20 years is essential to further investigate whether ridge and runnel morphology is subject to long-term change, as observed elsewhere for subtidal bars.

Chapter five

Intra-annual (monthly) Variability in Ridge and Runnel Morphology

5.1 INTRODUCTION

In Chapter 4 it was shown that pronounced summer-winter variability in ridge and runnel morphology is significantly related to seasonally-driven changes in meteorological and oceanographic forcing. Intra-annual variability is further investigated in this chapter using monthly beach surveys. Dynamics of ridges and runnels on this intermediate time-scale have not been investigated previously for the north Lincolnshire coast and such research has also been limited for other ridge and runnel beaches. The earliest profile measurements over periods larger than a month date back more than 25 years (King and Williams, 1949; King, 1972a; Wright, 1976) and it was observed that intra-annual variability in ridge and runnel morphology is generally characterised by a build-up of ridges during fair-weather periods, followed by a flattening of the relief under high-energy conditions. These early studies, however, did not link morphological change to external forcing conditions due to the lack of wave- and wind measurements. Mulrennan (1992) and Reichmüth (2003) presented more comprehensive studies on the medium-term morphodynamic behaviour of ridges and runnels and the following two paragraphs summarise their results.

Mulrennan (1992) found a distinct relationship between ridge development and prevailing wave conditions along the meso-tidal coast of Portmanock Barrier, east Ireland. She examined the monthly variability in ridge and runnel morphology based on a series of beach profiles covering a twelve-month period. Wave climate over the study period was characterised by moderate sea states from October to December, rough seas between January and April and calm conditions from May to September. As a result, ridges and runnels were best-developed between September and November, flattened in the following winter and then re-established during the spring- and summer months. Ridge migration rates were c. 10 m per month during the phase of moderate wave conditions, but decreased to 0.5 m per month throughout the recovery period. The ridges generally migrated onshore year-round. The study further indicated that ridge development was independent of beach volume change. For example, it was shown that a net aggradation of the beach was not by definition associated with ridge growth, as postulated earlier by King (1972a).

Reichmüth (2003) studied the variability of ridge and runnel morphology along the Côte d'Opale, northern France, and related morphological change to the intra-annual variation in wind conditions. Monthly profiles collected over a one-year period showed that the ridges and runnels along this coast were very dynamic. Various ridges formed and disappeared within the year and average migration rate was c. 10 m per month. Ridge construction prevailed from spring to mid-autumn (Figure 5.1) and coincided with moderate wind conditions. Ridge destruction was dominant during winter. The ridge and runnel morphology seemed further to adapt to internal forcing processes, since a significant spatial variability in morphological response was observed, despite identical external forcing conditions. Ridge development was not related to volumetric changes, as described before by Mulrennan (1992).

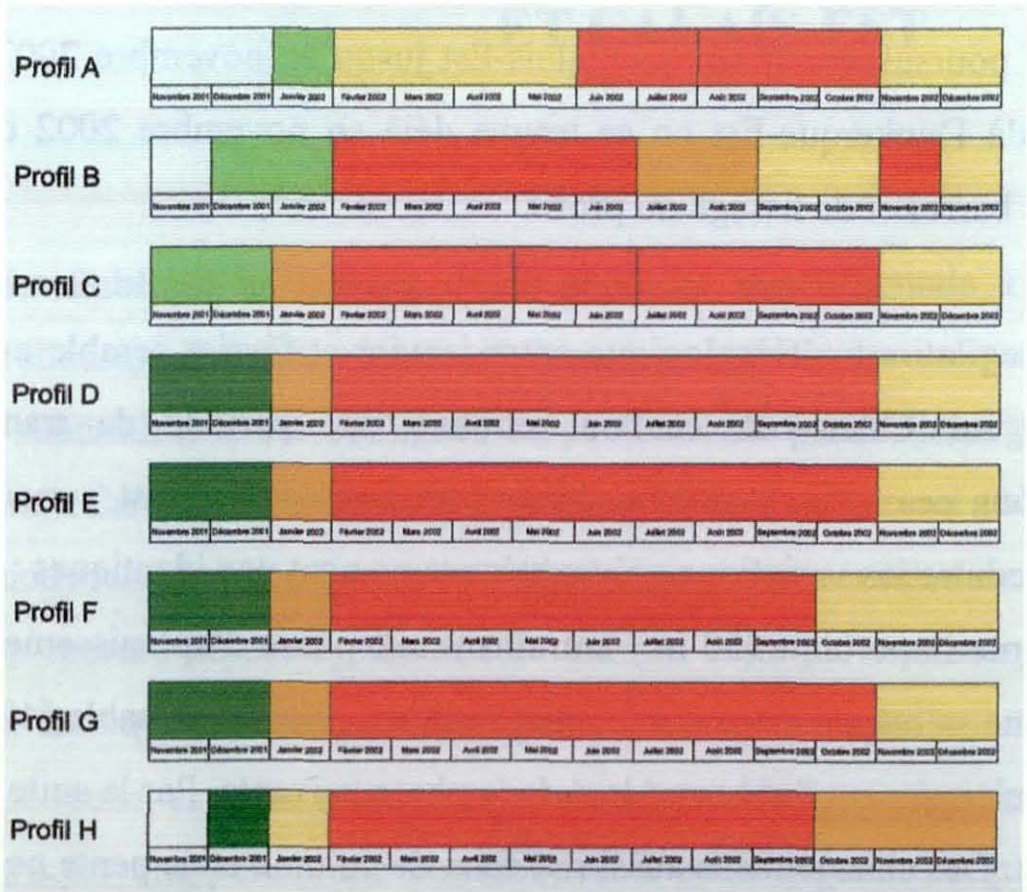

Figure 5.1 – Ridge and runnel development at Dunkerque, northern France, over a 1-year monitoring period (November 2001 to December 2002). Colouring indicates periods of destruction (yellow), transition (orange) and construction (red). The green on the left indicates the state of the morphology at the start of the monitoring period with darker green for more pronounced morphology (modified from Reichmüth, 2003).

Corbau et al. (1999) investigated beach change along the same stretch of coast in northern France, but noticed limited construction and migration during the summer fair-weather period, whereas significant migration of the ridges and runnels occurred over a winter and spring period with frontal winds (heavy swell).

Aim and objectives Chapter 5

The aim of this chapter is to gain insight into the intra-annual (seasonal and monthly) variability in ridge and runnel morphology. For this, beach configuration was monitored over a time span of one year at three different sites along the north Lincolnshire coast. The following research questions were formulated:

(1) Does ridge and runnel morphology change on the time-scale of a month?

(2) Is there a seasonal variability in the ridge and runnel morphology?

(3) Can morphological changes be linked to external forcing conditions?

(4) Are there any indications for feedback-dominated response?

5.2 METHODOLOGY

Monthly beach surveys were conducted at Donna Nook, Theddlethorpe and Mablethorpe between February 2001 and January 2002, although he surveys at Donna Nook were delayed until April 2001 due to restricted beach access (outbreak of foot and mouth disease). The forcing conditions during the survey period represented an average year, with wind speed frequencies of 3.4–7.9 m s^{-1} the majority of the time (refer to Figure 2.5), average offshore wave conditions of 1.6 m and surge levels that were generally < 1 m (refer to Figure 4.9c).

At each site, nine transects with a spacing of 50 m were surveyed and the measurements were related to a permanent benchmark in the dunes with known elevation in m ODN. Surveys were carried out using a laser total station and the vertical and horizontal accuracy of the measurements is estimated at ±1 cm and ±10 cm, respectively. Beach height was measured on the breaks in slope and with a maximum spacing of 10 m between observations. Sediment samples were collected for one cross-shore transect during each survey to determine the temporal variability in the sediment size of the beach (refer to Section 2.2).

Digital elevation models (DEMs) were computed from the monthly beach profiles and these are used to assess the spatial and temporal variation in the ridge and runnel morphology. The longshore resolution of the DEMs was set to 10 m, whereas cross-shore resolution was 1 m to include smaller-scale morphological features (e.g., slipfaces). Elevation changes were calculated from February to August and August to January by overlaying the consecutive DEMs and creating differential maps. The residual morphology was computed by subtracting a planar trend surface from the three-dimensional morphological data (Figure 5.2) and served as a basis for further analysis. This methodology enabled objective distinction between ridges (positive residual relief) and runnels (negative residual relief) (cf., Masselink et al., 1997; Brander and Cowell, 2003).

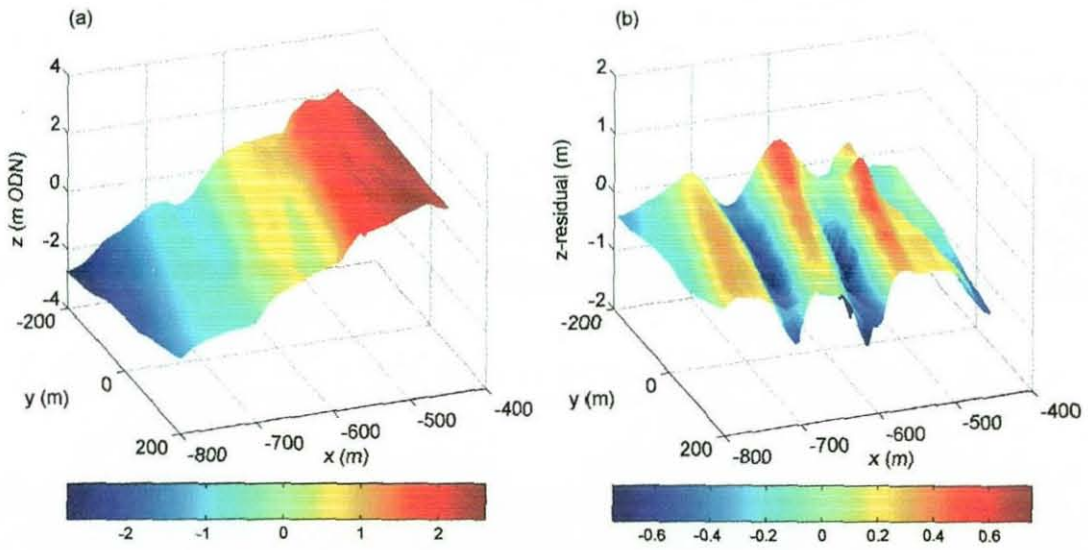

Figure 5.2 – Ridge and runnel morphology (a) before and (b) after subtraction of a planar trend surface, i.e., (b) represents the residual morphology. Legends (colour bars) are in m.

The residual morphology was used to determine the monthly changes in ridge configuration (number of ridges and prominence) and ridge migration. Ridge migration rate was defined as the cross-shore displacement of the ridge crest between monthly surveys, whereby crest positions correspond to local maximums in the residual surface. The correlation coefficient r^2 between the residual topography and the planar trend surface was used as a measure of the prominence of the ridge and runnel morphology. The smaller r^2, the more the morphology deviates from a planar surface and the more pronounced is the ridge and runnel morphology. Volume change

of the ridge and runnel zone was calculated in relation to the volume in April, as this was the first month that data was collected for all three sites.

Climatic and hydrodynamic conditions for the period 1-1-2001 till 31-01-2002 were made available by the British Atmospheric Data Centre and the UK National Tidal Gauge Network (as part of the British Oceanographic Data Centre) and included:

(1) hourly measurements of wind speed and direction at Donna Nook;

(2) hourly significant wave height and period, measured at a wave buoy located 120 km offshore; and

(3) hourly sea level observations for Cromer, 90km south of study area.

The wind data were used to calculate wind roses and wind speed frequencies over the survey period. As wave-conditions in fetch-limited environments are strongly controlled by the prevailing wind direction, i.e., onshore winds reinforcing waves and offshore winds suppressing waves, a distinction was made between on- and offshore winds using a coastline orientation of 160°–340°. A storm wave analysis was carried out using the offshore significant wave height data (cf., Lemm, 1999), whereby storms were defined as events with maximum offshore significant wave height exceeding 5 m. Duration of the storm was taken as the period over which the hourly significant wave height remained in excess of 4 m. Sea level observations and sea level predictions, the latter extracted from the Admiralty Tide Tables (2001), were used to compute surge level. Surge was used as another indicator for storminess.

5.3 MONTHLY CHANGE IN RIDGE AND RUNNEL MORPHOLOGY: RESULTS

Figure 5.3 shows DEMs of the ridges and runnels at Donna Nook, Theddlethorpe and Mablethorpe and illustrates the elevation change over the survey period. On average, 4–5 ridges and runnels were present at all three localities (note: the lowest ridge is not included in the DEM). The best-developed ridges were generally located around MSL and the orientation of most ridges was parallel to the shoreline. The intra-site long-shore variability was largest at Theddlethorpe, where the ridges in the northern part were significantly more pronounced than in the south. Despite some spatial variability, elevation change patterns at Donna Nook and Theddlethorpe reveal that the seaward slopes of the ridges eroded from spring to summer and that the released

sediment was deposited on the ridge crest and in the runnels, implying an (onshore) migration of the ridges. Elevation change between summer and winter suggests an opposite tendency, with erosion of the ridge crests and accretion of the seaward slopes.

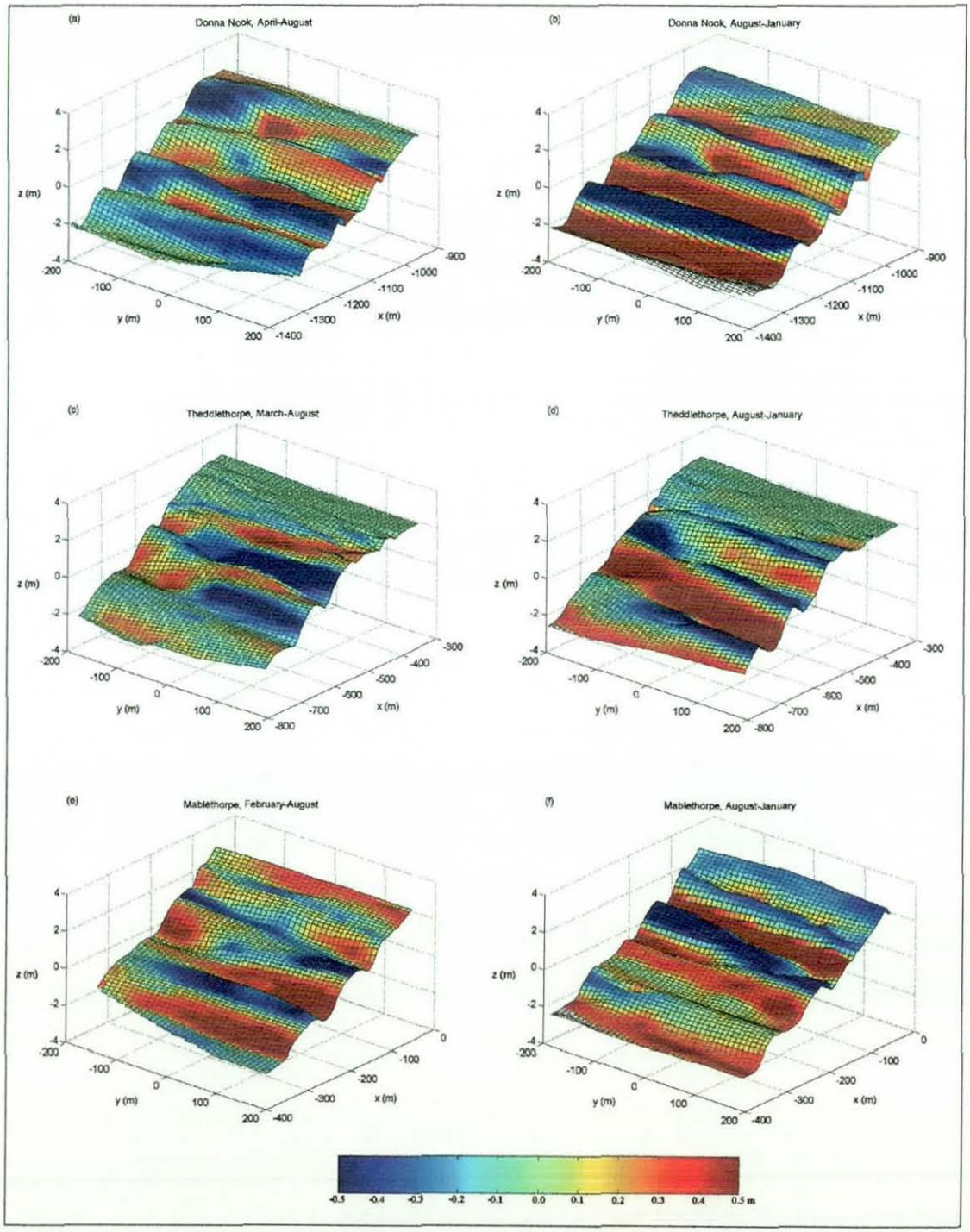

Figure 5.3 – Elevation change from spring to summer (left) and summer to winter (right), 2001–2002, for Donna Nook (top), Theddlethorpe (middle) and Mablethorpe (bottom). Elevation change is plotted on top of the DEMs of spring (left) and summer (right). The *y*-axis runs northward.

The monthly variation in ridge number was determined by counting the ridges in each cross-shore transect, for each monthly survey (Figure 5.4 top panels). The number of ridges varied between 2 and 5 at Theddlethorpe and between 3 and 7 at Donna Nook and Mablethorpe. All sites showed a seasonal variation with more ridges in summer than in winter. The prominence of the ridges, as quantified by r^2, is comparable between the three sites, but varies in time (Figure 5.4 bottom panels). A distinct summer versus winter difference is observed for Mablethorpe, where the ridges were more pronounced in winter than in summer. The ridge and runnel morphology at Donna Nook and Theddlethorpe was most prominent in December and January, respectively. It should be kept in mind that r^2 is also affected by the presence of drainage channels in the monitoring area, which results in higher r^2 values and possibly larger monthly variations. This may explain the inter-site variability in r^2.

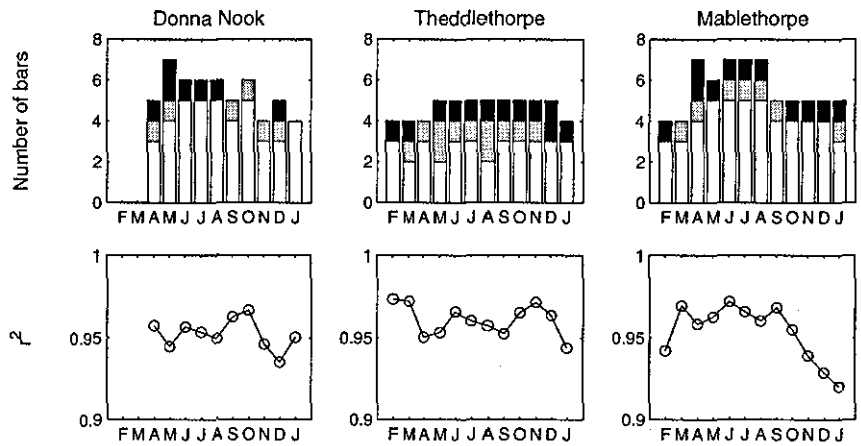

Figure 5.4 – Monthly variation in ridge number (top panels) and prominence (bottom panels). The white, grey and black bars in the top panels represent the minimum, the average and the maximum number of ridges, respectively. The middle panels show the Pearson's correlation coefficient r^2 associated with fitting a planar trend surface to the morphology. The smaller r^2, the more pronounced are the ridges and runnels.

Figure 5.5 shows monthly cross-shore profiles to study the development of individual ridges in more detail. The ridge and runnel morphology appears very dynamic and only in some cases is it possible to trace the development of individual bars over the 1-year survey period. The lowest ridge at Donna Nook, for example, can be tracked from profile to profile and indicates a strong onshore migration. It is further noticed that from May onwards, an extra ridge was present in the upper ridge and runnel zone at Theddlethorpe and that profile change at Mablethorpe was limited except for the increased number of ridges in summer.

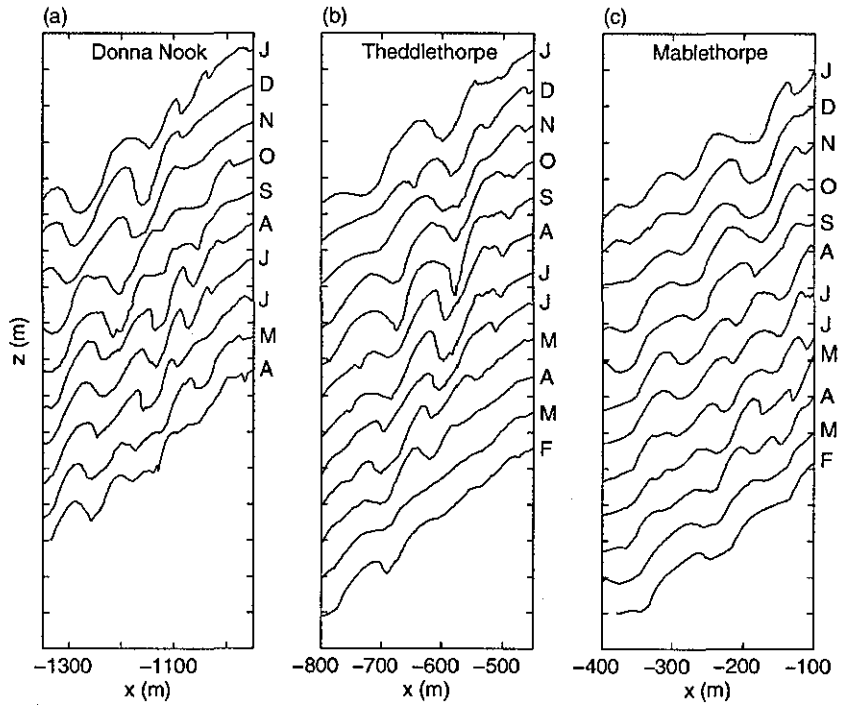

Figure 5.5 – Monthly beach profiles for the central transect at: (a) Donna Nook; (b) Theddlethorpe; and (c) Mablethorpe. The profiles are vertically offset by 1 m.

The investigation of 27 cross-shore profiles (nine at each site) reveals a range of ridge responses that are illustrated in Figure 5.6 for one of the profiles at Donna Nook. The most common observations are onshore and offshore ridge migration, build-up, flattening, appearance and disappearance. In a few cases, two ridges seemed to merge into one single ridge, whereas the opposite, bifurcation, was also observed. The positions of bar crests identified from the residual morphology were mapped over time and migration rates were averaged using information from different cross-shore transects. Ridge migration rates were subsequently used to demonstrate the movement of the ridges over the monitoring period (Figure 5.7). The pattern of ridge crest displacement is complex and exhibits a large spatial (between sites and across the intertidal) and temporal variability. Some general trends can, however, be identified. For the first part of the survey period (until August), most ridges migrated onshore with rates of up to 10 m per month. After that, the lower ridges at Donna Nook and Mablethorpe continued to migrate onshore, while the upper ridges were either stationary or migrated offshore. The ridges at Theddlethorpe showed an opposite trend with the upper ridges persisting their onshore movement, whereas the lower ridges migrated offshore.

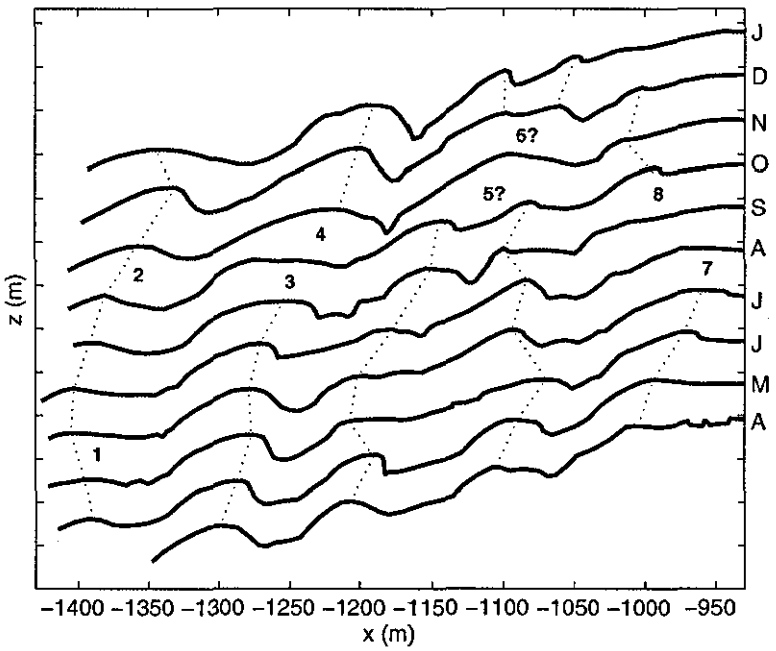

Figure 5.6 – Stacked monthly profiles for Donna Nook to illustrate ridge responses: (1) offshore migration; (2) onshore migration; (3) flattening; (4) build-up; (5) merging; (6) bifurcation; (7) disappearance; and (8) appearance. Dotted lines indicate cross-shore ridge crest displacement.

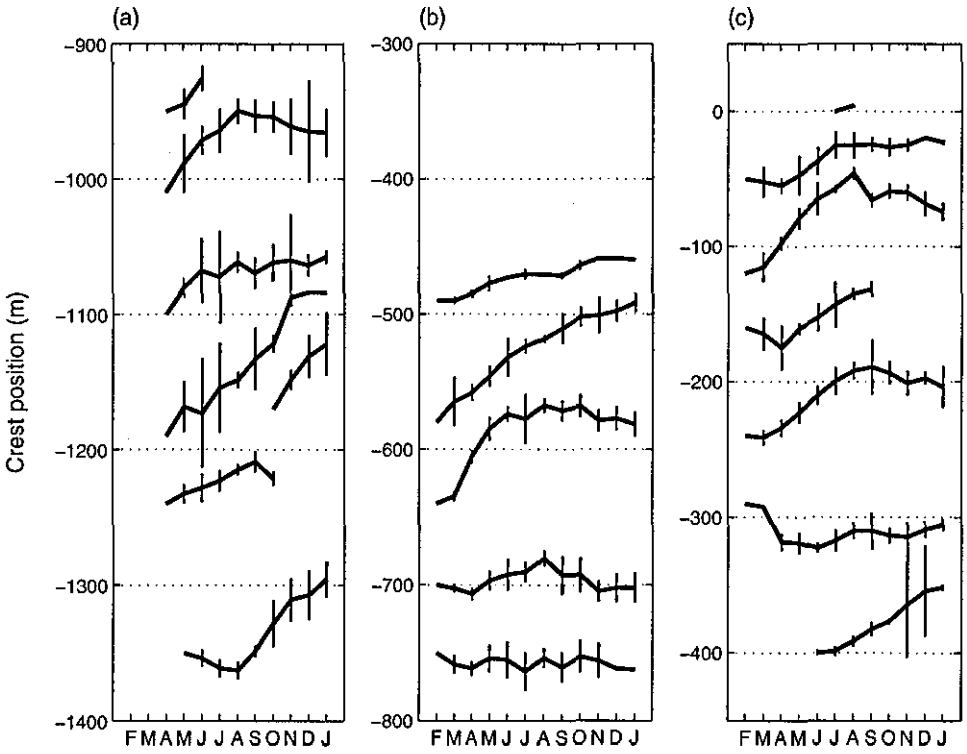

Figure 5.7 – Average cross-shore location of ridge crests for: (a) Donna Nook; (b) Theddlethorpe; and (c) Mablethorpe. The error bars represent ± one standard deviation associated with the computation of the mean location of the crests.

The survey data were also used to determine changes in the sediment volume (Figure 5.8). At each of the study sites, the maximum monthly change was similar to the net change over the 1-year monitoring period and was in the order of 30 m^3 per m beach width. No obvious seasonal trends in the sediment volume were present. The sediment volume changes can be converted to bed level changes by dividing the volumetric change (in m^3) by the surface area of the control region. The net change was c. –0.1 m for Donna Nook and Theddlethorpe (i.e., negative sediment budgets) and c. +0.1 m for Mablethorpe (i.e., positive sediment budget). These changes were significantly larger than the vertical accuracy of the survey data (±0.01 m).

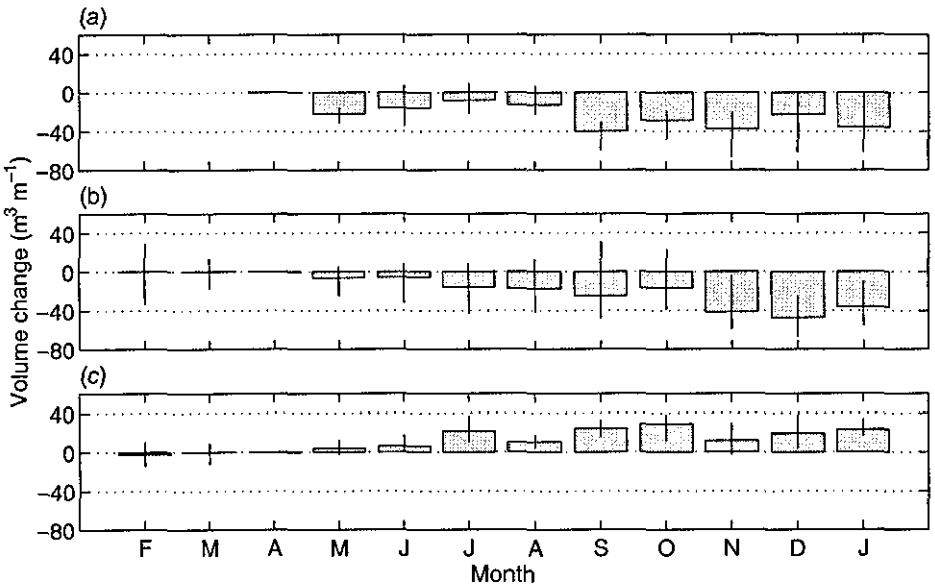

Figure 5.8 – Average volume change relative to April 2001 for: (a) Donna Nook; (b) Theddlethorpe; and (c) Mablethorpe. The error bars represent ± one standard deviation associated with the computation of the mean volume change.

Figure 5.9 shows the residual ridge and runnel morphology for Donna Nook, Theddlethorpe and Mablethorpe over the 1-year monitoring period. The plots reveal a dominant longshore migration of the morphology as indicated by the lengthening of intertidal bars and the migration of drainage channels. This movement was most evident at Theddlethorpe (e.g., from May to August). Longshore migration was directed southwards and its rate is estimated at 1 m per day. It is difficult to separate the ridge response into longshore and cross-shore components, but the appearance and disappearance of ridges is usually related to the longshore migration of the morphology. For example, the appearance of the middle ridges in the cross-shore

profile measured at Theddlethorpe in April (refer to Figure 5.5b) can directly be attributed to the migration of two ridges past the $y = 0$ m line. The most seaward ridge at Theddlethorpe, on the other hand, shows a flattening at the start of winter that appears more related to a cross-shore exchange of sediment.

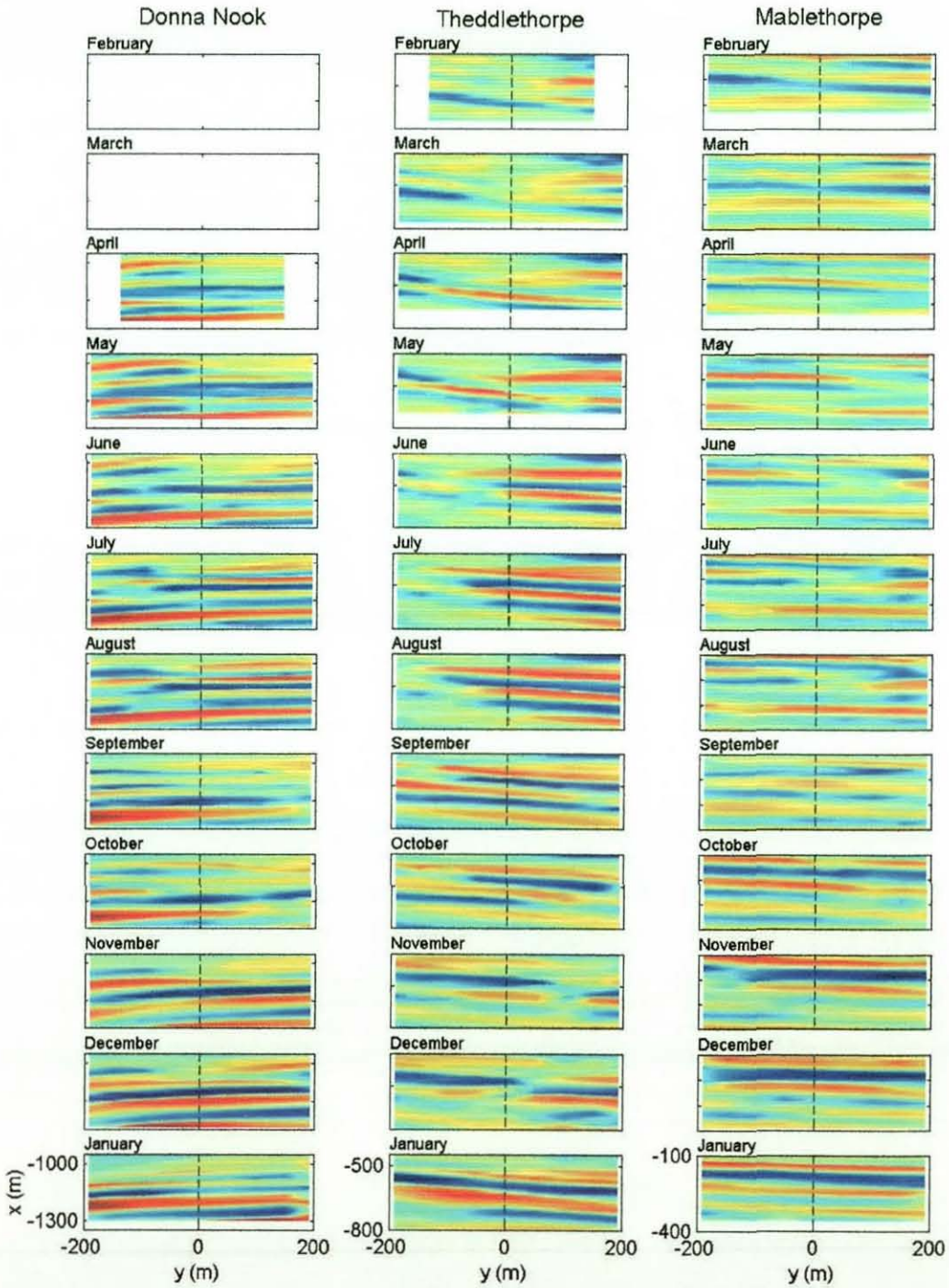

Figure 5.9 – Monthly variation in residual ridge and runnel morphology from February 2001 to January 2002. The colour bar runs from –0.6 m (dark blue = runnels) to +0.6 m (dark red = ridges) and the dashed vertical line represents the position of the central profile (refer to Figure 5.3). The *y*-axis runs from south to north.

5.4 WIND, WAVE AND SURGE CONDITIONS OVER THE 1-YEAR MONITORING PERIOD

The Lincolnshire coast was characterised by a pronounced seasonality in the meteorological and oceanographic forcing over the 1-year monitoring period. Wind data measured at Donna Nook indicate that wind speeds were modest (< 8 m s^{-1}) for most of the time, particularly in summer (Figure 5.10). Stronger winds occurred in spring and autumn. Figure 5.10 further shows monthly wind roses from February 2001 to March 2002, with a division between onshore and offshore winds based on the shoreline orientation (160-340°). The prevailing wind direction was offshore, especially in the autumn and winter months. March and May were the only months with predominant onshore winds. The wind roses also show that the strongest winds (> 13.9 m s^{-1}) generally came from the northerly quadrants.

The offshore wave height (measured 120 km offshore) also displayed a clear seasonality, with wave conditions during winter being significantly more energetic than during summer (Figure 5.11a, b). Typical peak and monthly-averaged significant offshore wave heights during winter months were 6 m and 2.5 m, respectively, whereas summer wave heights were about half that (Note: inshore significant wave height was 2–3 times smaller than the offshore significant wave height; Section 2.3). A storm wave analysis, carried out using the offshore wave data, showed that storm events occurred throughout the year, except for summer (Figure 5.11c). Severe storms took place in the 2001/2002 winter when the mean storm significant wave height was in excess of 5 m for many days. Surge level was used as an alternative indicator for storminess and also displays a clear seasonal variability with surge events being higher and more frequent in winter than in summer (Figure 5.11d). The positive surge level rarely exceeded 0.2 m in summer, but was often larger than 0.5 m in winter.

5.5 DISCUSSION

Monthly surveys over a 1-year period at three beaches along the north Lincolnshire coast have provided an unprecedented insight into the ridge and runnel dynamics on the intra-annual time-scale. Ridge and runnel morphology appeared very dynamic and

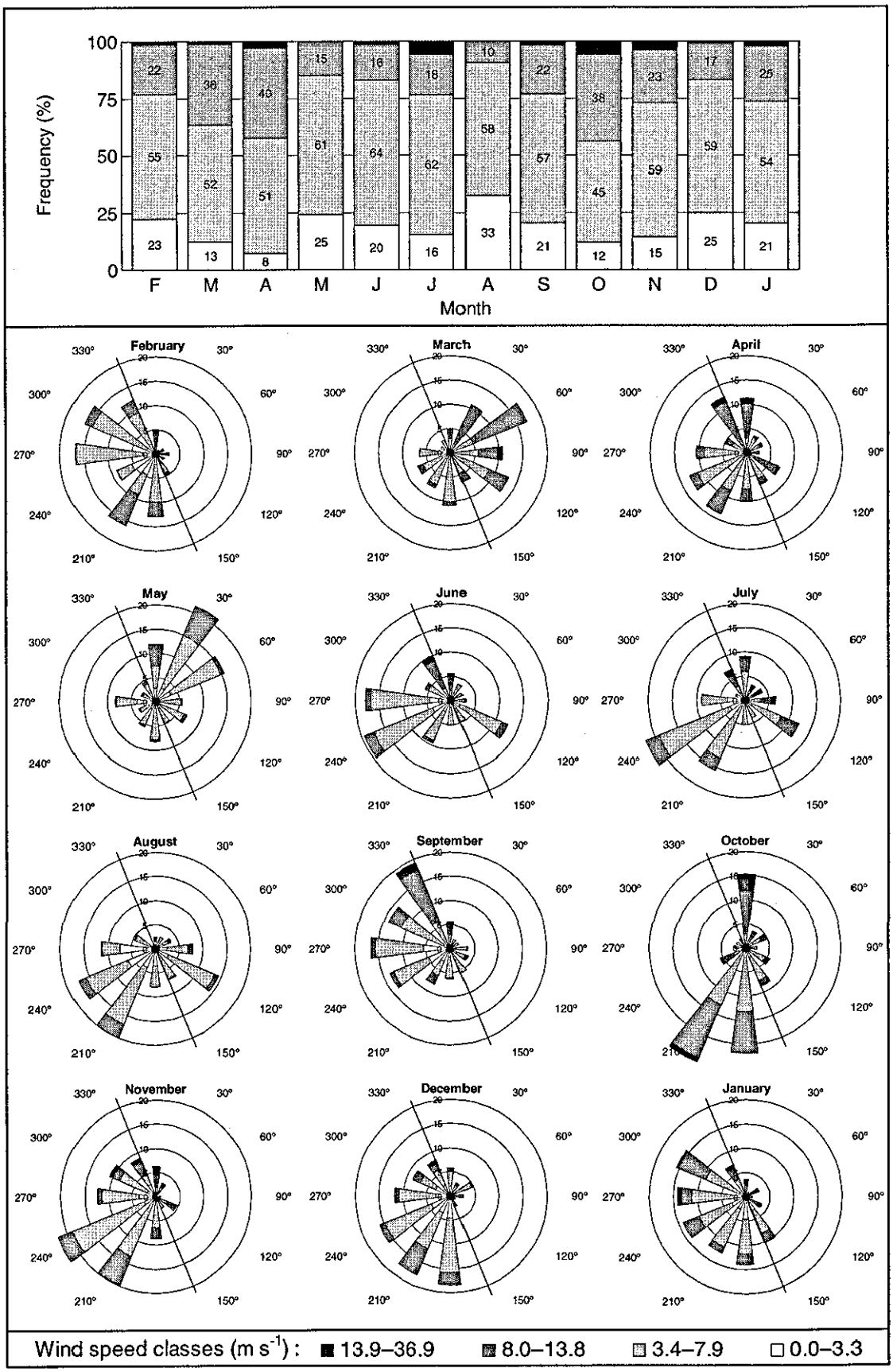

Figure 5.10 – Monthly wind speed frequencies (top panel) and wind roses (bottom panel) for the North Lincolnshire coast from February 2001 to January 2002.

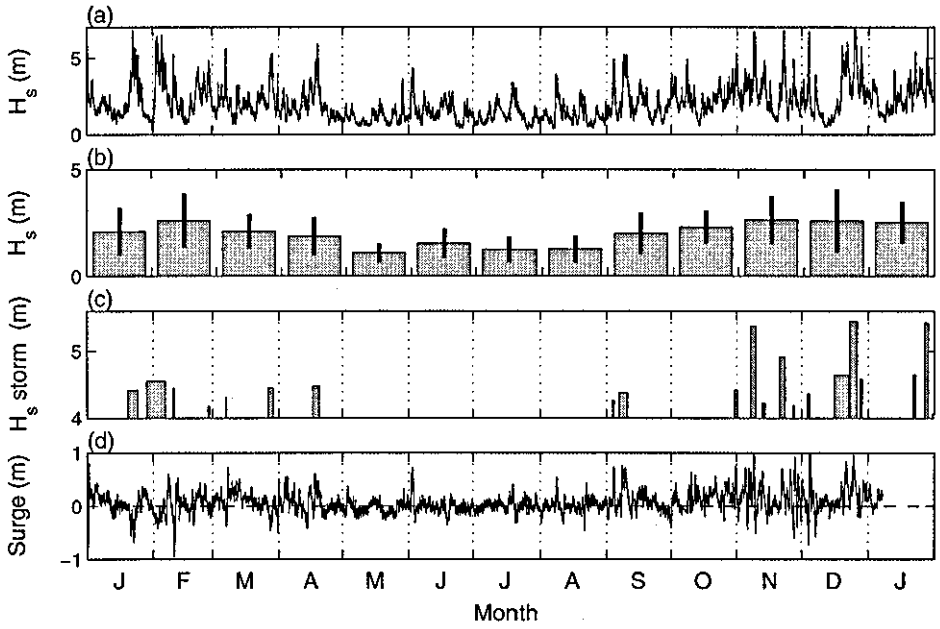

Figure 5.11 – Wave and surge conditions from January 2001 to January 2002: (a) offshore significant wave height; (b) monthly-averaged offshore significant wave height; (c) occurrence of storms; and (d) surge level. The error bars in (c) represent ± one standard deviation associated with the computation of the mean significant wave height. The bar height in (d) represents the mean significant wave height during the storm and the bar width indicates storm duration (the first storm lasted 11 hrs).

its configuration changed from month to month. A range of responses has been observed, including migration (onshore and offshore), build-up, flattening, appearance and disappearance. Ridge behaviour exhibited a significant inter-site spatial variability, particularly between Mablethorpe, the most southern beach, and Donna Nook and Theddlethorpe. The main difference between those beaches is the presence of an upper tidal flat at the northern two beaches. The ridge and runnel morphology at Donna Nook and Theddlethorpe was further characterised by a negative sediment budget over the monitoring period, whereas the beach at Mablethorpe underwent accretion. The response of ridges and runnels also showed intra-site spatial variability. Particularly, ridge migration rates and directions varied across the intertidal zone and systematic cross-shore ridge migration trends were therefore not apparent. Rather, one of the dominant forces driving the ridge and runnel dynamics at the monthly time-scale was longshore sediment transport. The time series of three-dimensional residual topography indicated that the ridges moved alongshore at a rate of up to 1 m per day in a southward direction. This longshore

migration accounted for the local appearance and disappearance of individual ridges and runnels and resulted in a significant alongshore spatial variability of the ridge dynamics within the study sites. Longshore ridge migration can easily be misinterpreted as cross-shore movement (e.g., King and Barnes, 1964) and advanced data analysis techniques should be implemented to unequivocally separate the two components (e.g., Van Enckevort and Ruessink, 2003a,b).

The factors wind strength, wave height and surge level are considered the most relevant in external forcing of ridge and runnel morphology and these environmental conditions exhibited a distinct seasonality between January 2001 and January 2002. Conditions were calm between May and August, whereas higher energy conditions occurred during the other months of the year. This seasonal trend in external forcing was reflected in the ridge and runnel morphology, particularly in the prominence of the ridges and runnels. Ridge size at Donna Nook and Theddlethorpe generally increased during spring and summer and this was followed by a flattening of the ridges and runnels in response to the higher energy conditions in autumn. At the end of autumn, ridge and runnel morphology started to build-up again. This seemed contradictory at first because the external forcing conditions indicated high *offshore* significant wave heights and the frequent occurrence of storms. The wind roses from November to January, however, indicated that offshore-directed winds prevailed over this period and hence, the *inshore* wave climate was probably significantly different to that further offshore. Strong offshore winds countering incident wave heights or generating waves that are highly refracted may have caused a relatively calm period in terms of wave height and this would explain the increase in ridge and runnel prominence. The intra-annual variation in ridge size at Mablethorpe seemed further affected by the appearance and disappearance of individual ridges. The decreased ridge size in summer coincided with the existence of an additional ridge from April to August and this implies that the formation of the extra ridge was the result of cross-shore sediment re-distribution amongst all the ridges rather than of supply from alongshore or from the subtidal zone.

Although the changes in the ridge and runnel morphology over the 1-year monitoring period seem clearly due to the seasonal variation in wave-, surge- and wind-conditions, there are a few factors that should be kept in mind:

(1) One aspect that could have affected the interpretation of morphological change in relation to external forcing conditions is the timing and frequency of monthly surveys. Particularly, the timing of a monthly survey in relation to the occurrence of individual storms is important as this would result in different profiles before or after a storm. In Chapter 6 it will be shown that the morphological change during a twelve-hour storm event can be similar to the change over a whole month with fair-weather conditions. Furthermore, ridge migration rates could have been calculated more accurately with smaller survey intervals.

(2) The correlation coefficient between the residual ridge and runnel morphology and a planar trend surface as a measure of the prominence is only reliable when it is ensured that the changes in ridge and runnel morphology were not affected by the presence of drainage channels in the monitoring area. Drainage channels were observed to move alongshore at rates up to 1 m a day and it was a matter of coincidence that a drainage channel was located in a survey transect than that it indicated a change in the ridge and runnel prominence.

(3) Inshore wave measurements are essential to link morphological change to incident wave-energy levels.

The observations in this study are partially in agreement, but also partially in disagreement, with earlier findings on intra-annual ridge and runnel dynamics (e.g., Mulrennan, 1992; Corbau et al., 1999; Reichmüth, 2003). Ridge migration rates, for instance, were similar to those found by King (1972b), Mulrennan (1992) and Reichmüth, 2003, and were c. 10 m per month for onshore migration and c. 5 m per month for offshore migration. The short-term investigation by Kroon and Masselink (2002) also implied significant migration rates at the north Lincolnshire coast. They observed an onshore ridge migration of 7–8 m over a single lunar tidal cycle. In further agreement with Mulrennan (1992) and Reichmüth (2003), specific ridge responses such as build-up, flattening and migration, appeared independent of volume change. For instance, ridge flattening and/or destruction did not necessarily go together with erosion, or vice versa. It should be noted, however, that a direct relationship between morphological and volumetric change may be masked by shorter-term and/or local profile changes and that the role of declining or increasing sediment budget should be viewed over longer time intervals. The investigation of Mulrennan (1992) further showed a clearer link between external forcing conditions

and ridge response, in particular ridge migration. She noted ridge build-up and largest (onshore) migration rates in summer (low-wave energy conditions), whereas ridge destruction and lowest migration rates were observed during winter (rough sea states). In this study, trends in ridge migration patterns were very complex and seemed not to be linked to the external forcing conditions.

The degree of coherence between external forcing and morphological response may be reduced by feedback-dominated processes. A feedback-dominated response, however, is difficult to convincingly demonstrate, as a weak correlation between forcing and morphological response may be because the link between forcing and response is complex and not all processes are accounted for. Nevertheless, some observations in this study are believed to suggest feedback-dominated behaviour. Cross-shore ridge migration trends, for example, vary greatly depending on the ridge location and also between different beaches. Despite a similar offshore wave forcing, some ridges migrated onshore, whilst other remained stationary or even migrated in the offshore direction. Longshore migration patterns are also expected to play a role here, but a significant component of the disparate behaviour of the different ridges may be attributed to feedback effects, in particular the effect of the lower ridges on the wave conditions higher on the beach (Masselink, in press). The dominant behaviour on the monthly time-scale was, however, the longshore migration of ridges and this response is considered to be forced by the littoral drift induced by the prevailing northeasterly waves. The monthly variation in number of ridges and prominence is also believed to be mostly a forced response and is related to the seasonal variation in the incident wave energy.

Finally, it was observed that intra-annual variability in the ridge and runnel morphology along the north Lincolnshire coast is very different from that described from multi-bar systems on low-tidal beaches (tidal range < 3 m), where most (if not all) bars are subtidal. On such beaches, it is generally possible to identify clear trends in offshore or onshore bar migration (e.g., Ruessink and Kroon, 1994; Shand et al., 1999; Aagaard et al., 2004) and morphological response resembles changes in the external forcing conditions to a much greater extent (e.g. Hayes and Boothroyd, 1969; Davis et al., 1972). Nearshore bars systems in the Magdalen Islands, for example, show destruction, re-formation and development of the bars that is directly associated

with the occurrence of storms (Owens and Frobel, 1977). At ridge and runnel beaches, individual ridges also flatten, and even disappear, as a result of high-energy wave-conditions, but a complete flattening of the ridge and runnel morphology as a whole does not occur, as concluded earlier in Chapter 4.

5.6 CONCLUSIONS

- Ridge and runnel morphology is very dynamic and its configuration changes from month to month due to ridge migration, build-up, flattening, appearance and disappearance.
- The dominant morphologic behaviour on the intra-annual time-scale is the longshore migration of the ridges, whereas cross-shore redistribution of sediment is of secondary importance. Longshore migration rate is estimated at 1 m per day.
- The monthly variability in the ridge and runnel morphology is moderately related to the seasonally-driven changes in the meteorological and oceanographic forcing. Ridge and runnel prominence clearly exhibited a seasonal change, but cross-shore migration rates trends did not reflect the external forcing conditions.
- The morphological change of ridges and runnels at the intra-annual timescale is a combination of forcing- and feedback-dominated response.

Chapter six

Ridge and Runnel Dynamics over Lunar Tidal Cycles

6.1 INTRODUCTION

After the description of the ridge and runnel dynamics on the inter- and intra-annual timescale in Chapters 4 and 5, this chapter scales down further to describe the morphodynamic behaviour of ridges and runnels over lunar tidal cycles. On this time-scale, ridge and runnel morphology is subject to fluctuations in hydrodynamic conditions due to varying high- and low-tide levels, wave-energy and meteorological conditions. Wind speed and direction are particularly important as, for example, strong onshore winds induce storm surges. Surges up to 1 m are common in the North Sea (Komar, 1998), but the coincidence of an extreme storm surge coupled to a high spring tide may add as much as 2–3 m to predicted tidal levels (Carter, 1988). Masselink and Anthony (2001) described the non-stationary water levels as one of the most important characteristics of the hydrodynamic regime in a ridge and runnel environment and showed that the degree of non-stationarity varies significantly across-shore, with largest rates of tidal change at MSL. This variation in water level, induces rapid cross-shore migration of different hydrodynamic zones across the wide intertidal profile (Masselink, 1993) and the ridge and runnel morphology is subject to a mixture of swash, surf and shoaling wave processes during submergence (Kroon and Masselink, 2002).

The most commonly described morphological changes over a lunar tidal cycle are the onshore migration of ridges under low wave-energy conditions (Parker, 1975; van den Berg, 1977; Voulgaris et al., 1998; Kroon and Masselink, 2002) and the flattening of ridges and runnels during storms (King and Williams, 1949; King, 1972a; Wright, 1976; Levoy et al, 1998). Onshore migration rates under fair-weather conditions (Figure 6.1) have been observed to vary between 0.4 and 1.2 m per tidal cycle and depend on the cross-shore position of the ridge. For instance, King and Williams (1949) and Voulgaris et al. (1998) found that the upper ridges were migrating onshore, whereas the lower ridges remained stationary. Davis et al. (1972) directly related ridge migration rate to the tidal range and postulated that ridges migrate slower when subject to large tidal regimes, as then, waves are only acting on the ridges and runnels for a limited amount of time. Onshore migration is accomplished by the transfer of sediment from the seaward to the landward slope of the ridge (Kroon and Masselink, 2002) and this localised erosion and accretion

generally constitutes the only distinct bed level change under low wave-energy conditions. Sipka and Anthony (1999) found that vertical changes were commonly smaller than 0.01 m per day, whereas Levoy et al. (1998) observed changes of 0.05 m per day, but only limited to short sections of the cross-shore profile. Anthony et al. (2004), however, showed that daily fluctuations were higher under low to moderate wave-energy conditions and found that maximum bed level changes occurred on the landward slopes of the ridges and in the runnels (up to ±0.3 m).

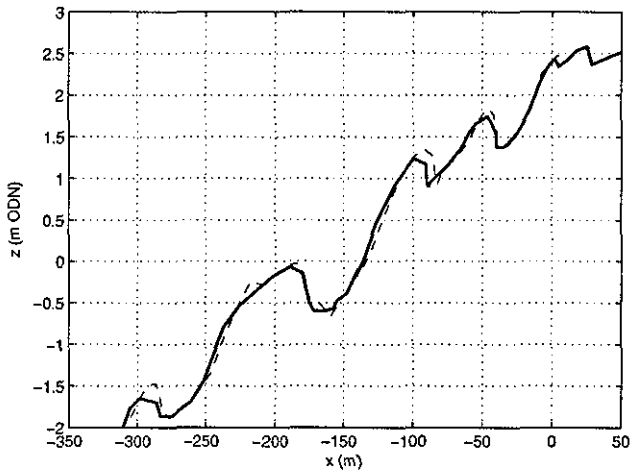

Figure 6.1 – Morphological change of a ridge and runnel profile over a lunar tidal cycle under low wave-energy conditions. The solid and dashed lines represent the beach profile at, respectively the start and at the end of the field period (modified from Kroon and Masselink, 2002).

The destructive effect of storms on ridge and runnel morphology has been widely acknowledged (e.g., King, 1972a; van den Berg, 1977; Navas et al., 2001), although the establishment of an entirely flat 'storm-profile' has never been described. Storm impact is mostly limited to a smoothing of the ridge and runnel relief and small individual ridges may vanish. Van den Berg (1977) suggested that, during storms, sediment is mainly redistributed within the ridge and runnel zone as he observed that the ridges eroded, but that the runnels filled in with the released sediment. This is also indicated by the studies of Wright (1976) and Levoy et al. (1998) as their sediment budget estimations revealed only a minor sediment loss in response to high wave-energy conditions. An example of an extreme storm surge in the North Sea occurred in February 1953, when a 3.3 m water level increase was measured on top of the normal tidal water level (Wemelsfelder, 1953, in Masselink and Hughes, 2003). The storm surge resulted in extensive flooding of the Lincolnshire coast and damage

ranged from minor dune cliffing in the north to the complete destruction of massive concrete defences in the south (King, 1972a). Ridge and runnel morphology along the north Lincolnshire coast became flatter, but only to a limited extent (Robinson, 1956; King, 1972a; Robinson, 1981).

The most comprehensive studies on the ridge and runnel dynamics over a lunar tidal cycle are presented by Kroon and Masselink (2002), Reichmüth (2003) and Anthony et al. (2004). Kroon and Masselink (2002) included an analysis of the spatial and temporal variation in the duration of swash and surf zone processes and concluded that the durations of these processes do not solely depend on the tide range, but also on the incident wave height. Reichmüth (2003) showed that the most significant changes under low energy wave conditions tended to occur on the seaward slope and crest of a ridge and that this only involved local redistributions of sediment, as volumetric changes were generally negligible. Anthony et al. (2004) were the first to quantify the vertical bed level change under high wave-energy conditions and found that it was similar to the maximum daily change under low to moderate wave-energy conditions. They further attributed the spatial patterns of morphological change to local morphodynamic feedback effects due to the breaks in slope associated with the presence of ridges and runnels.

Aim and objectives Chapter 6

This chapter aims to complement the findings above by monitoring the morphological change at smaller time-intervals. In previous investigations, beach profiles were generally surveyed once a day, i.e., over two tidal cycles, but in this study morphological measurements were conducted twice-daily. This intensive monitoring enables a more accurate link to be made between observed morphological change and tidal water levels and wave-energy conditions. Specifically, the objective of this chapter is to yield additional insight in:

(1) the spatial and temporal variability in ridge and runnel morphology over a lunar tidal cycle;
(2) the impact of varying wave-energy conditions;
(3) the extent to which the observed morphological change can be attributed to swash, surf and shoaling processes; and
(4) the occurrence and dynamics of drainage channels.

6.2 METHODOLOGY

Two three-week field experiments, both covering a spring-to-spring tidal cycle, were conducted at Theddlethorpe in June 2001 and September 2001. The methodology used during both field campaigns was identical, but different wave conditions were experienced. In June the inshore significant wave height was generally less than 0.5 m, representing prevailing low wave-energy conditions, while in September the inshore significant wave height frequently exceeded 1 m, representative for the intermediate to high wave-energy conditions that are more common towards winter.

The beach morphology was monitored each low tide using a transect of 150 fibreglass rods, spaced 2 m apart, incorporating four ridges and runnels. Once the tops of the rods were referenced to a temporary benchmark with known elevation in m ODN, the bed elevation at the rod locations was obtained by measuring the distance from the top of the rods to the sand level using a specially-designed ruler (Figure 6.2a). Additionally, the rods were surveyed daily using an electronic total station to ensure that the rods had remained in place (Figure 6.2b). The associated vertical accuracy of this method is considered better than 1 cm. The rod measurements were complemented with surveys of additional beach profiles, drainage channels and slipface positions. A second cross-shore transect was established at a distance of 50 m of the main transect line and surveyed on a daily basis during the daylight low tide. This allowed differentiation between local morphological changes (i.e., change in only one transect) and larger scale morphological changes (i.e., similar changes for both transects). Three-dimensional surveys, including additional cross-shore transects at 50, 100 and 150 m at either side of the main transect line, were conducted at the start, the middle and the end of the field periods. The set of profiles was used to create DEMs of the study area (refer to Section 5.2) and to compute differential maps that show the magnitude and patterns of bed level change.

During both field experiments, hydrodynamic data were obtained using a self-logging instrument station equipped with an acoustic current meter and a built-in pressure sensor (Figure 6.2c). The instrument station was deployed just above mean low water spring level and measured currents and water level at, respectively, 0.15 and 0.4 m above the bed. The station was programmed to sample at 4 Hz for 10 minutes every

half hour and mean water depth (tide level) and current velocity were computed for each of the data segments. Significant wave height H_s was estimated by $H_s = 4\sigma$ (Aagaard and Masselink, 1999), with σ the standard deviation of the detrended 10-min pressure records. Significant wave period T_s was determined spectrally ($T_s = M_0/M_1$, where M_0 and M_1 are the 0^{th} and 1^{st} spectral moments, respectively) (Lemm, 1999). The significant wave height was corrected for depth attenuation using linear wave theory (Bishop and Donelan, 1987). Occasional instrument failure during the June field period lead to data gaps, that were filled using tidal predictions from the Admiralty Tide Tables (2001) for Immingham (35 km to the north) and Skegness (25 km to the south).

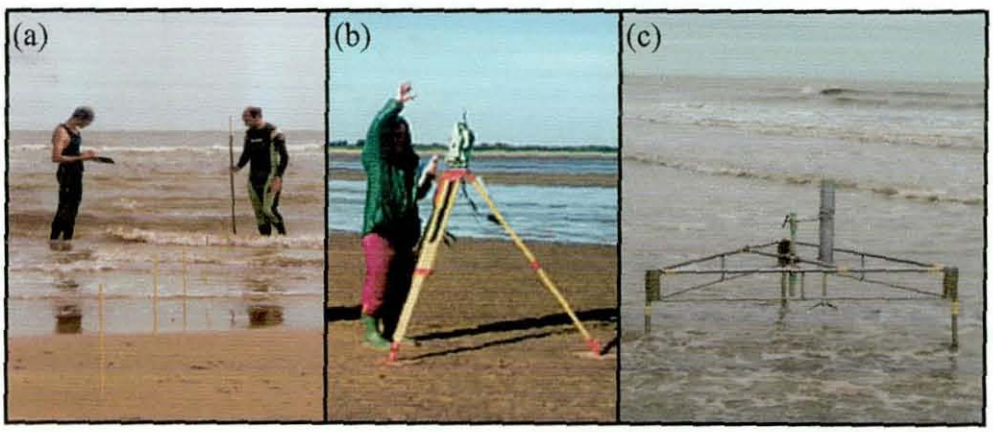

Figure 6.2 – Field measurement techniques: (a) bed level measurements using an array of fibreglass rods; (b) survey using an electronic total station; and (c) current and water level measurements by a self-logging instrument station.

The duration of swash, surf zone processes and shoaling waves on the ridge and runnel morphology was computed using a simple model based on water levels, as presented by Kroon and Masselink (2002). The local water levels on the intertidal beach were assumed to be composed of the tidal water level, the wave set-up and the wave run-up. The water-level record obtained from the instrument station was used as an estimation of the tidal water level, whereby interpolation was applied to fill the data gaps between bursts and extrapolation to extend the water level record to at least –1 m below MSL (the instrument station was usually emerged at low tide). The combined effect of wave set-up and wave run-up were computed using the equation (Holman, 1986, in Komar, 1998):

$$R = 0.69\, g^{0.5}\, H_0^{0.5}\, T \tan\beta \qquad \textbf{(6.1)}$$

where R is the wave run-up elevation exceeded by 2% of the run-up events (substitute of the maximum run-up elevation), H_0 is the deep-water wave height, T is the wave period and $\tan\beta$ is the beach gradient. The deep-water wave height H_0 and wave period T were extracted from the measured water level record and were assumed to be constant over one single tidal cycle. The model computed the local water levels by adding the tidal water level and the wave run-up elevation. Determination of the breaker depth is of crucial importance to differentiate between the surf zone and the shoaling wave zone, but, in reality, the division between the two zones is gradual and characterised by a mixture of breaking and shoaling waves (i.e., the outer surfzone; Svendsen, 1984). A wave breaker criterion γ of 0.35 was used to compute the breaker depth from the local wave height and this definition places the start of the modelled surf zone between that of the outer ($\gamma = 0.3$; Ruessink et al., 1998) and inner ($\gamma = 0.4$; Thornton and Guza, 1982) surf zone. A distinction between swash, surf zone processes and shoaling waves was subsequently made, based on the local water level in relation to the tidal water level and the breaker depth:

- swash action occurred when the local water level was between the tidal water level and the wave run-up level on the beach;
- surf zone processes prevailed when the local water level was smaller than the breaker depth and the beach was permanently inundated; and
- shoaling waves existed when the local water depth exceeded the breaker depth.

The model excluded the runnels for swash and surf zone processes. The number of hours per tidal cycle that the processes were operating were computed for the main transect line at a spatial interval of 2 m.

6.3 RIDGE AND RUNNEL DYNAMICS OVER LUNAR TIDAL CYCLES: RESULTS

June field period

An event summary of the wind, wave and tide conditions during the June field period is shown in Figure 6.3. Wind speeds were modest (< 7.5 m s^{-1}) most of the time and predominantly offshore. The field period covered a spring-to-spring lunar tidal cycle and was characterised by low wave-energy conditions. Significant wave heights were usually smaller than 0.5 m and significant wave periods were 4–7 s. Time-averaged

cross-shore and longshore currents indicate a strong tidal modulation. Onshore and southward currents occurred during the rising tide, whereas offshore and northward currents dominated during the falling tide. During the second half of the field experiment nearshore currents were more wind-dependent. The strong northerly winds between Tide 21 and 24 forced the currents to the south.

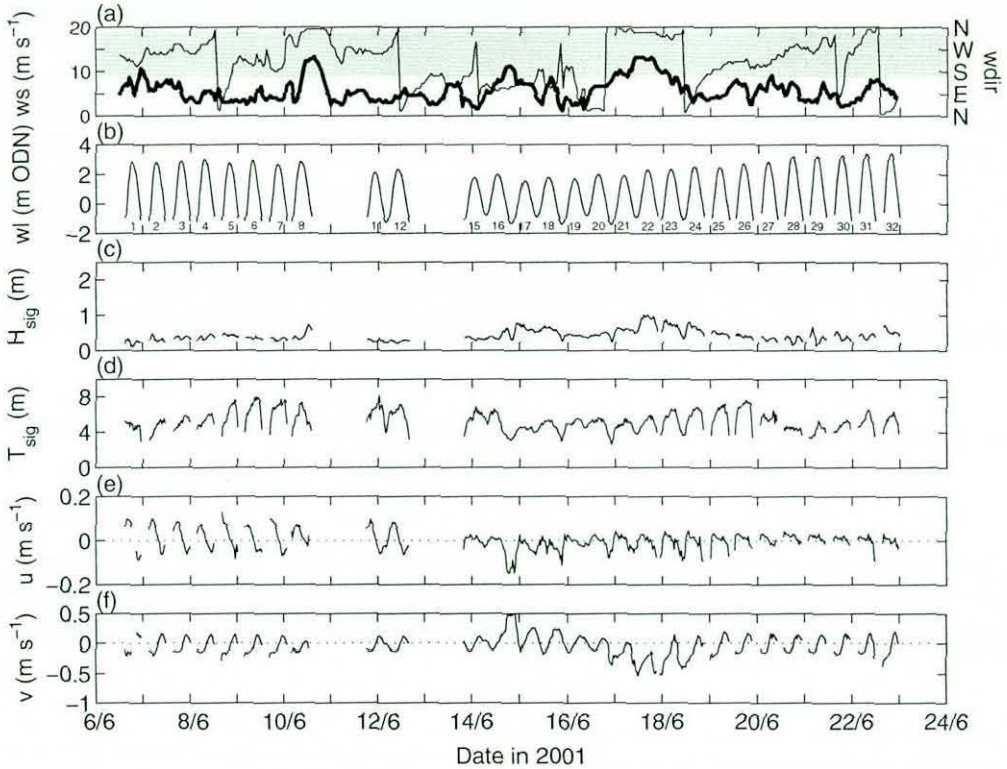

Figure 6.3 – Wind, wave and tide conditions during the June field experiment: (a) wind speed (thick line) and direction (thin line); (b) water level; (c) significant wave height; (d) significant wave period; (e) cross-shore current velocity; and (f) longshore current velocity. Positive values for cross-shore and longshore currents are onshore and northwards respectively. The grey patch in (a) marks offshore wind directions and tides are numbered in (b) for easy reference.

Figure 6.4 presents a three-dimensional view of the beach morphology and illustrates that four ridges were present, with the middle two ridges being best-developed. The morphological change over the lunar tidal cycle was limited. The number of ridges remained the same and none of the ridges were modified to any great extent. Bed level changes over the first half of the experiment were c. ± 0.1 m. Ridge 1 was rather inactive, whereas Ridge 2 and 3 were characterised by a light erosion of the seaward slopes. Ridge 2 showed accretion of the crest over the second half of the period.

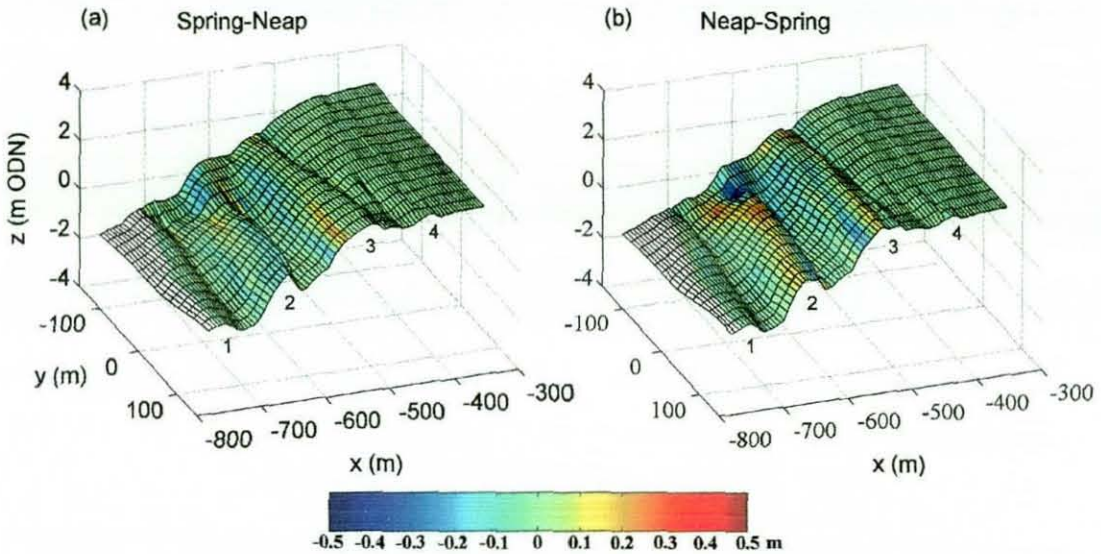

Figure 6.4 – Bed level change (colouring) over a lunar tidal cycle during the June field period: (a) from spring to neap tide; and (b) from neap to spring tide. Bed level change is plotted on top of the DEM at the start (a) and at the end (b) of the field period. The *y*-axis runs from south to north.

Smaller scale morphological changes are more apparent from the sequence of twice-daily beach profiles (Figure 6.5a). Ridge 2 migrated consistently onshore with an average rate of 0.3 m per tidal cycle. The ridge tended to become double-crested between Tide 23 and 26, but this trend did not persist and in the end one wide crest was present. This widening is clear when the first and last profiles are compared (Figure 6.5b). The profiles further show the development of two lobes on the seaward slope of the Ridge 3 after neap tide. Only the landward lobe developed further and migrated quickly onshore (1.2 m per tidal cycle). It had reached the crest of the ridge at the end of the field period and resulted in a local accretion of 0.15 m (Figure 6.5c).

The profile data were used to determine the morphological change between successive surveys, i.e., over each tidal cycle. The resulting morphological change profiles show that morphological changes like migration took place gradually, but that local accretion and lobe formation tended to occur in bursts (Figure 6.6). The rate of migration of Ridge 2 seemed independent of the stage in the lunar tidal cycle or the position of the breaker line (i.e., wave height). The accretion of the crest of Ridge 2, however, was directly linked to the occurrence of higher waves (Tide 17 and 22) and took place just landward of the breaker line.

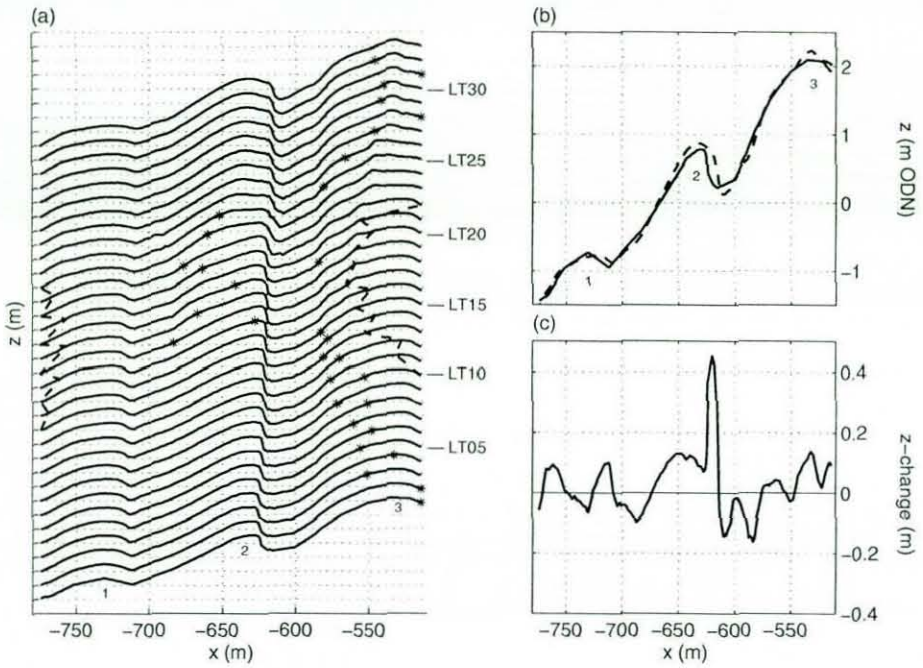

Figure 6.5 – (a) Twice-daily profiles of the main transect during the June 2001 field campaign. The profiles have been vertically offset by 0.5 m. The dashed lines on the left and right indicate the locations of the low tide and high tide marks, respectively. The asterixes on the low tide profiles indicate the location of the breaker line during the subsequent high tide. Labelling of the profiles is shown at the right-hand side of the graph, whereby 'LT' refers to 'Low Tide'. (b) Profiles measured at the start (solid line) and end (dashed line) of the field period. (c) Morphological change over the field period. Accretion is indicated by positive values and erosion by negative values.

September field period

An event summary for the wind, wave and tide conditions for the September field experiment is illustrated in Figure 6.7 and shows that hydrodynamic conditions during this field experiment were much more energetic then in June. The first half of the field campaign was characterised by stormy weather, with strong northerly winds (wind speed > 10 m s^{-1}) and significant wave heights exceeding 1 m. Offshore winds prevailed during the second half and suppressed the waves to such extent that significant wave heights remained below 0.5 m. The significant wave period was 4–7 s throughout the field experiment. Mean currents were strongly wave-driven during the first half of the field experiment. The mean cross-shore current was directed offshore with velocities up to 0.2 m s^{-1} and the longshore current was mainly to the south with velocities up to 0.9 m s^{-1}. During the second half of the field experiment, nearshore currents were mainly driven by the tide and reversed each tidal cycle.

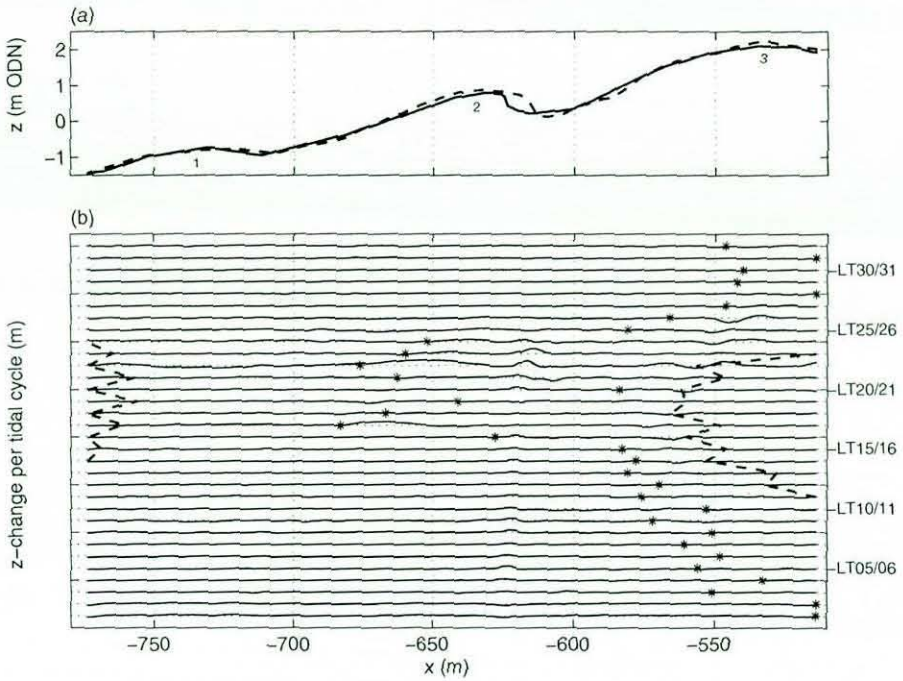

Figure 6.6 – (a) Profiles measured at the start (solid line) and end (dashed line) of the June field period. (b) Morphological change per tidal cycle. The profiles have been vertically offset by 0.3 m. Positive values indicate accretion, negative values indicate erosion. For meaning of additional lines, markers and labels refer to Figure 6.4.

The beach over the spring-to-spring tidal cycle in September was characterised by 4 ridges and, like in June, the middle ridges were most pronounced (Figure 6.8). It can be argued that Ridge 3 and 4 were in fact one double-crested ridge, but in this chapter they were taken as two separate ridges as they developed rather differently and evolved into two more individual units over the lunar tidal cycle. The morphological change over the September field experiment was remarkably larger than during the June field period. The most significant changes occurred during the start of the experiment under high wave-energy conditions and bed level changes were locally up to ± 0.5 m. The ridges eroded and deposition took place in the runnels. Bed level changes during the second half were much smaller and erosion of the seaward slope in combination with accretion on the landward slope resulted in onshore migration of the Ridges 2 and 3.

This onshore migration is more apparent from the consecutive beach profiles and they further reveal that the migration rate varied significantly across-shore and also through time (Figure 6.9). The upper ridges were observed to migrate fastest,

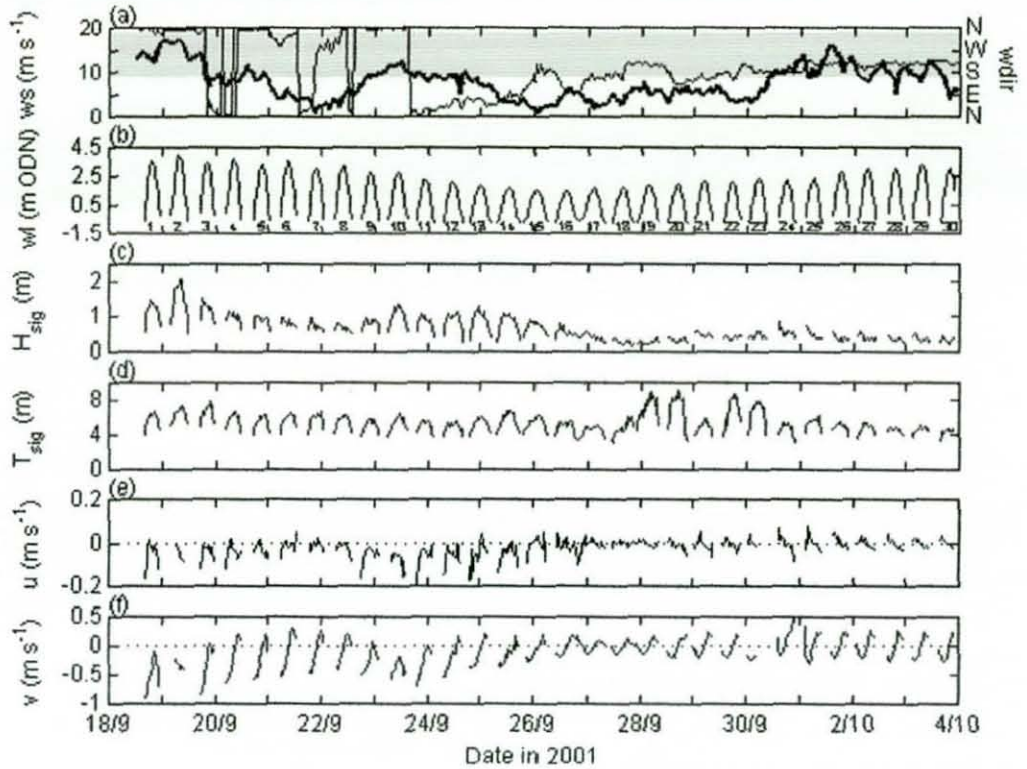

Figure 6.7 – Wind, wave and tide conditions during the September field experiment: (a) wind speed (thick line) and direction (thin line); (b) water level; (c) significant wave height; (d) significant wave period; (e) cross-shore current velocity and (f) longshore current velocity. Positive values for cross-shore and longshore currents are onshore and northwards respectively. The grey patch in (a) marks offshore wind directions and tides are numbered in (b) for easy reference.

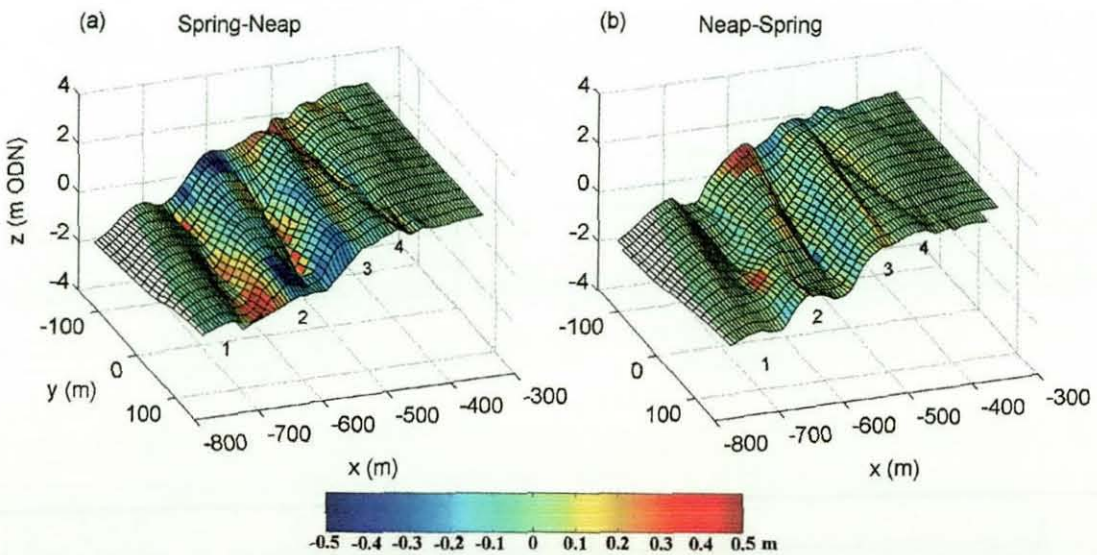

Figure 6.8 – Bed level change (colouring) over a lunar tidal cycle during the September field period: (a) from spring to neap tide and (b) from neap to spring tide. Bed level change is plotted on top of the DEM at the start (a) and at the end (b) of the field period. The *y*-axis runs from south to north.

particularly during the stormy conditions at the start of the field period, when Ridge 3 and 4 migrated, respectively, 1.6 and 0.9 m per tidal cycle. Ridge 2 was much bulkier and migrated significantly slower at a rate of 0.15 m per tidal cycle. The ridge started to become double-crested from Low Tide 10 onwards, but the distance between the crests had decreased significantly towards the end of the experiment as the new seaward crest migrated onshore at a much larger speed than the more landward crest (they probably merged, but after the monitoring period).

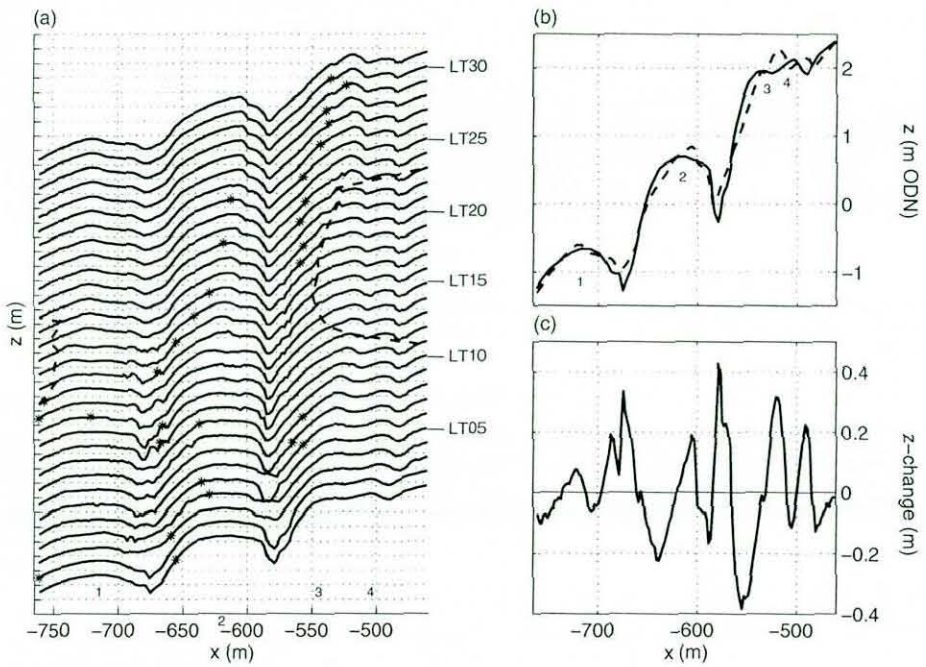

Figure 6.9 – (a) Twice-daily profiles of the main transect during the September 2001 field campaign. The profiles have been vertically offset by 0.5 m. (b) Profiles measured at the start (solid line) and end (dashed line) of the field period. (c) Morphological change over the field period. Accretion is indicated by positive values and erosion by negative values. For meaning of additional lines, markers and labels refer to Figure 6.4.

The morphological change profiles indicate that the most notable morphological change over a single tidal cycle occurred during Tide 2 when the wave height exceeded 2 m and the lower beach was flattened (Figure 6.10). The profiles further show the frequent development of small lobes, generally on the seaward slope of the ridges. These lobes were usually deposited over a single tidal cycle and often migrated onshore to join the crest of the ridge. This onshore migration was accomplished by erosion of the seaward slope and accretion of the landward slope. The lobes that develop on Ridges 3 and 4 can often be linked to the high water mark

and may, therefore, be considered as incipient swash bars. The relatively large morphological changes in the lowest runnel over Tides 10–17 was attributed to the formation and movement of high-energy dunes and megaripples.

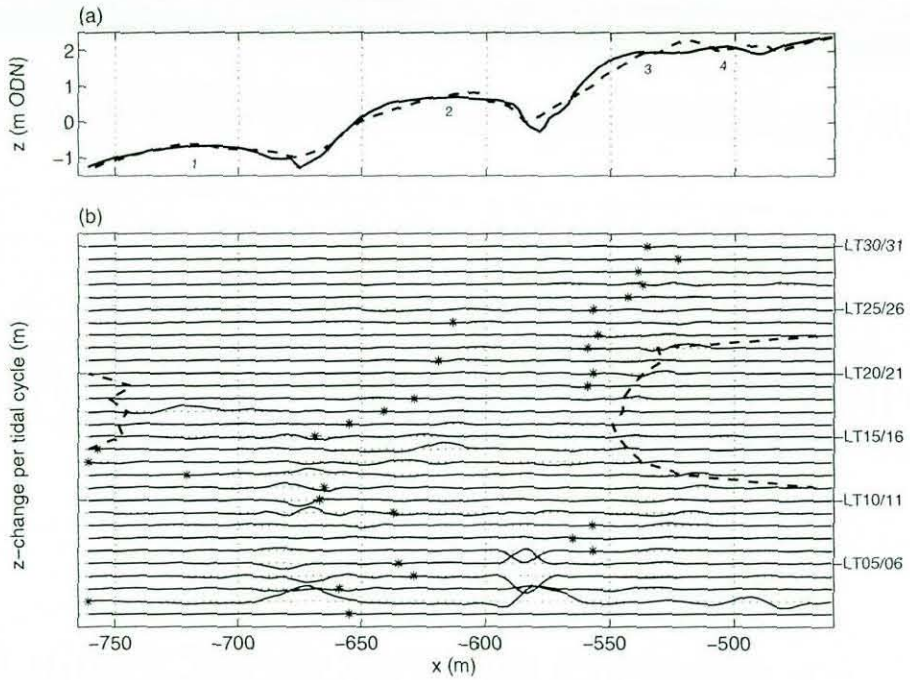

Figure 6.10 – (a) Profiles measured at the start (solid line) and end (dashed line) of the June field period. (b) Morphological change per tidal cycle. The profiles have been vertically offset by 0.3 m. Positive values indicate accretion, negative values indicate erosion. For meaning of additional lines, markers and labels refer to Figure 6.4.

6.4 ADDITIONAL MORPHOLOGICAL RESULTS

The morphological change due to the storm event in September (Tide 2) is shown in Figure 6.11a and b to evaluate the impact of high wave-energy conditions in more detail. As shown above, the high energy conditions had largest effects on the lower beach, where ridges eroded and runnels filled in. Ridge 2 in particular experienced severe sediment losses and eroded c. 0.05 m over its entire surface. Maximum bed level changes occurred in the runnels (accretion) and were 0.5 m. Figure 6.11a suggests that more sediment accreted in the runnels than was supplied across-shore from the ridges, and this indicates that longshore sediment transport processes may have played an important role in the redistribution of sediment during the storm. Ridges 3 and 4 remained intact and Ridge 4 even migrated 5 m onshore. The morphological changes under storm conditions were significantly larger than during

calm wave conditions, as bed level changes under such conditions were generally smaller than 0.1 m and maximum migration rates were 1.2 m per tidal cycle (Section 6.3).

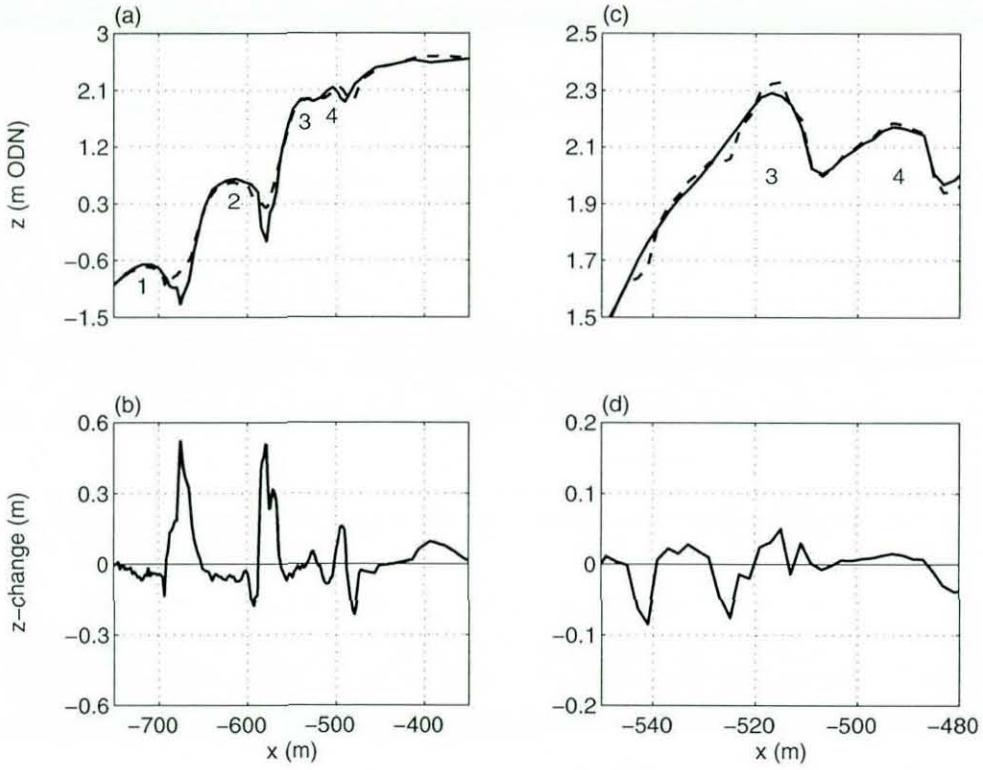

Figure 6.11 – Morphological change over (a, b) a surge event and (c, d) a 4-hour aeolian sediment transport event. (a) and (c) show the profiles before (solid line) and after (dashed line) the events. Positive values in (b) and (d) indicate accretion and negative values indicate erosion.

An example of morphological change due to aeolian sediment transport is shown in Figure 6.11 (c, d). Bed level change was monitored during an event of strong offshore winds and it was observed that changes up to 0.08 m occurred in only a few hours. Large amounts of sediment were trapped on the crests of the upper ridges and the seaward slope of Ridge 3 was reworked to form a small aeolian bar that subsequently survived submergence during the next few tidal cycles.

The position and migration of slipfaces over the second half of the September field period are shown in Figure 6.12 and it appears that slipfaces only formed on the landward slopes of the middle and upper ridges. The slipfaces of Ridges 3 and 4 could be traced for large distances alongshore (> 400 m), whereas the slipface on

Ridge 2 was only distinct in the southern part of the study area. The slipface pattern on the upper beach demonstrates that Ridge 4 merged with Ridge 3 in the south, but that a fifth ridge was present near the northern limit of the study area. The slipfaces of these upper ridges remained stable in time, whereas the slipface of Ridge 2 moved a distance of almost 7 m over 12 tidal cycles. The slipface migration rates were very similar to the crest migration rates as computed earlier from the twice-daily beach profiles.

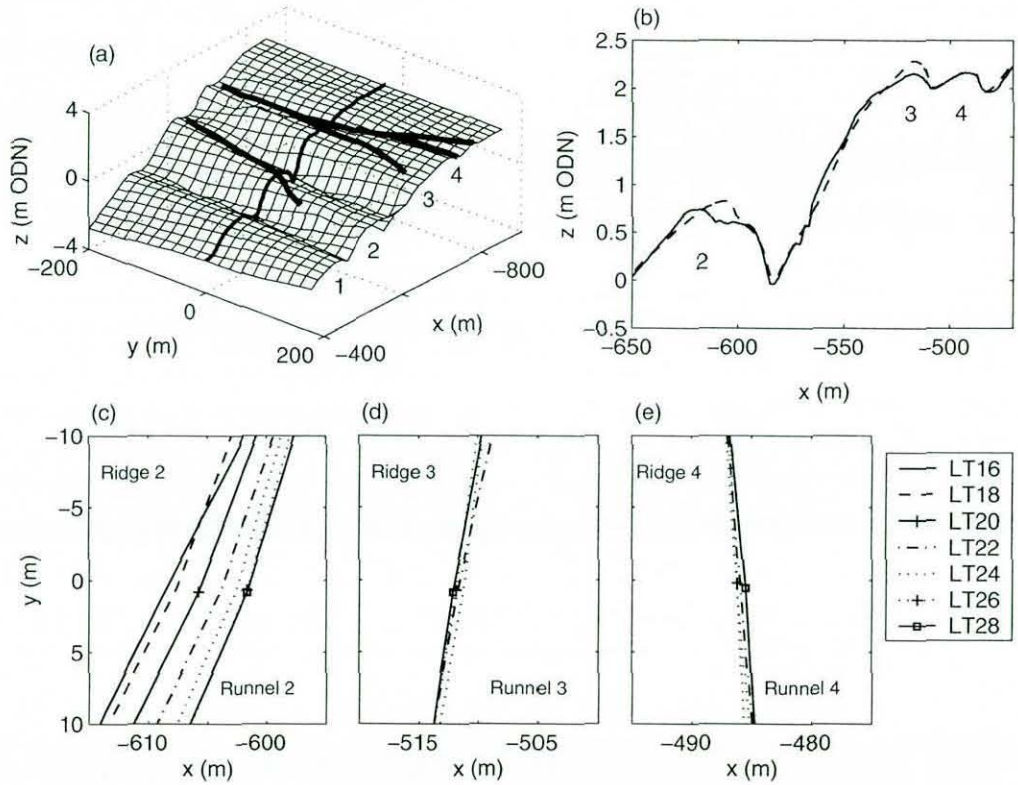

Figure 6.12 – (a) DEM of the ridges and runnels with locations of slipfaces (thick solid lines). The cross-shore line indicates the main transect. (b) Profiles at the start (solid line) and end (dashed line) of the slipface monitoring period (Tide 16–28). (c), (d) and (e) indicate slipface migration of, respectively, Ridge 2, 3 and 4.

The ridge and runnel morphology was regularly dissected by drainage channels and their occurrence and dynamics were investigated to get more insight in the importance of these features. The development of drainage channels over a lunar tidal cycle are discussed below, whereas drainage channels are further described in terms of their hydrodynamic characteristics in Chapter 7. Drainage channels form during the falling tide in attempt to drain trapped water from the upper sand flat and the runnels and vary in size from shallow sheet flow areas to incised channels up to 0.7 m

deep. The locations of drainage channels were surveyed using a total station and four types were identified to differentiate between drainage channels of various sizes (Table 6.1).

Table 6.1 – Drainage channel classification

Classes	Description
Type 1	Surface drainage without significant incision. Drainage 'channel' starts at crest, but does not cut through entire ridge. Width c. 1 m.
Type 2	Drainage channel with incision up to 0.2 m. No erosion cliffs at edges. Width 1–3 m.
Type 3	Drainage channel cutting through entire ridge with incision in middle of channel up to 0.4 m. Width 3–5 m. Erosion cliffs at edges up to 0.15 m in height.
Type 4	Drainage channel cutting through entire ridge with incision in middle of channel larger than 0.4 m. Width > 5 m. Erosion cliffs at edges larger than 0.15 m in height

A DEM of the study area with the location of drainage channels is shown in Figure 6.13a and demonstrates that the larger ridges were dissected by at least one well-developed drainage channel (Type 3/4). The orientation of most of the channels was towards the southeast and small deltas occurred where they discharged in the seaward-lying runnel. The upper drainage channels exhibited a distinct cyclic behaviour over the spring-to-spring tidal cycle. They were best-developed at spring tides when the largest amounts of water had to be drained from the sand flat, but were inactive and least-pronounced during neap tide. This alternation of filling in and deepening introduced an element of feedback into the system as the state of the upper drainage channels reciprocally affected the submergence of the sand flat. When high tide water levels dropped below the crest of Ridge 3 towards neap tide, flooding of the flat continued through the drainage channels and it was only at neap tide that the sand flat was emerged over the entire tidal cycle. After neap tide, however, the channels had filled in and the sand flat did not inundate till high tide levels reached over ridge 3 again. The drainage channels on the lower beach were active over the entire lunar tidal cycle and shifted mainly alongshore. For example, a well-defined drainage channel that dissected the middle ridge migrated southward over a distance of 40 m at the start of the field experiment when winds and waves were from the northeast and longshore currents from the south (Figure 6.13b). During the second half of the field experiment, the drainage channel migrated 20 m back to the north.

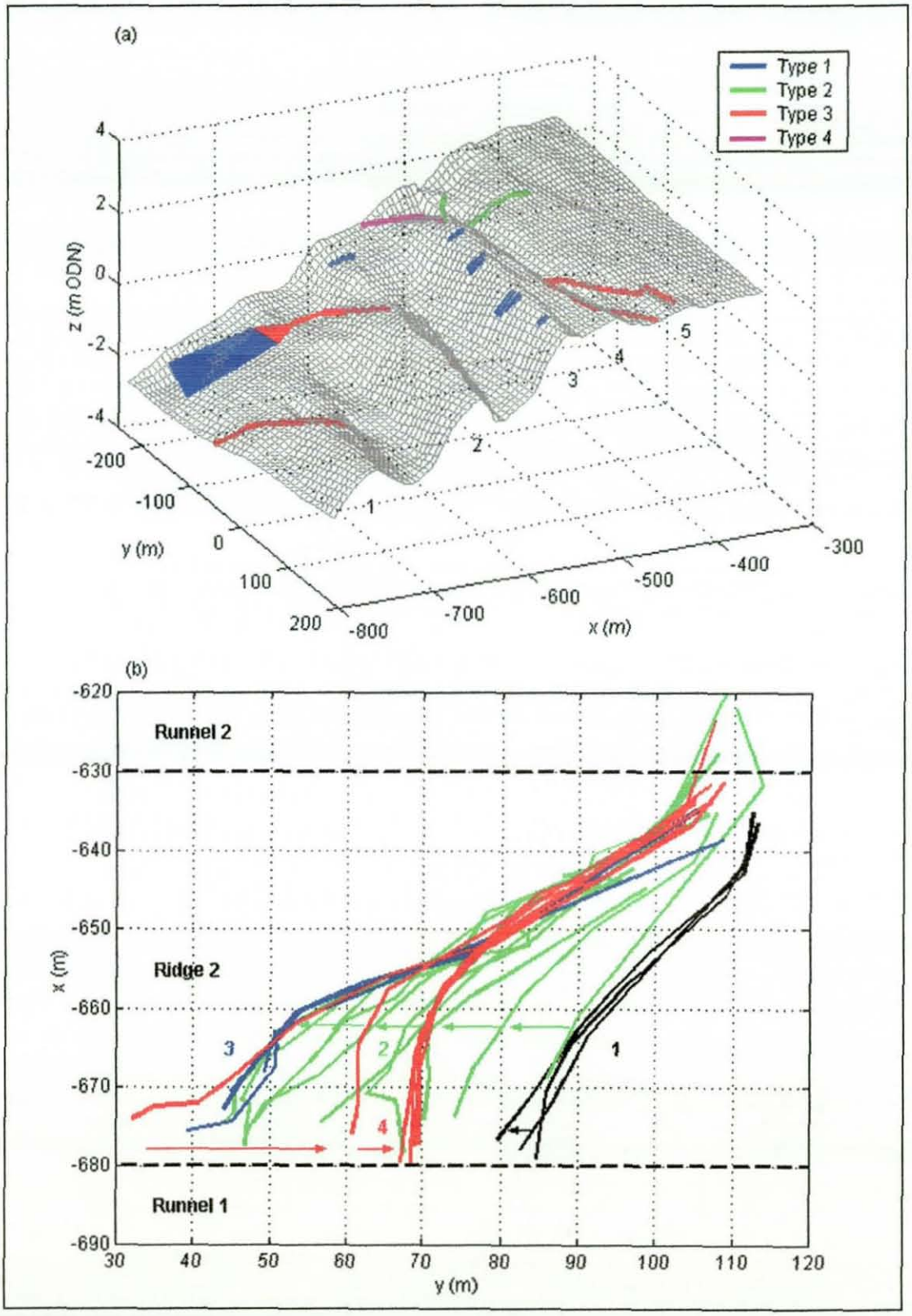

Figure 6.13 – (a) DEM with location of drainage channels (lines), August 2001. The triangle represents a drainage delta, the rectangle marks an area of closely-spaced drainage channels. Colours indicate channel type (refer to Table 6.1). (b) Alongshore drainage channel migration during the September field experiment (Tide 6–29). Colours represent consecutive sub-periods (1 = black, 2 = green, 3 = blue, 4 = red).

6.5 NUMERICAL SIMULATIONS OF WAVE PROCESSES

The numerical model described in section 6.2 was used to investigate the temporal and spatial variation in the duration of swash, surf and shoaling wave processes. The amount of time that these wave processes operated was computed for each ridge, and over every tidal cycle. Results are shown in Figures 6.14 and 6.15 for the field periods in, respectively, June and September 2001. The simulations show that shoaling waves predominated at Ridges 1 and 2 under calm wave conditions ($H_s < 0.5$ m), but that the influence of surf zone processes increased towards neap tide. Surf processes also acted longer when wave conditions became more energetic. Ridge 2, for example, was located in the surf zone for more than 5 hours when significant wave height exceeded 1 m. The duration of swash on the lower ridges was limited and did not exceed 30 minutes per tidal cycle. Ridge 3 was dominated by surf zone processes, particularly under energetic wave conditions. The duration of surf processes decreased towards neap tide, when the ridge became inundated for significantly shorter periods and swash action increased. Ridge 4 was intertidal during spring tides and subaerial during neap tides. The ridge experienced similar durations of wave processes as Ridge 3 at the start of the spring-to-spring tidal cycle, but wave processes after neap tide were remarkably different as the crest of Ridge 3 had become higher than Ridge 4. The sand flat was only flooded around spring tides and surf zone bores prevailed during inundation.

The low tide data described in Section 6.3 revealed that the ridge and runnel morphology undergoes significant changes over single tidal cycles. It is unclear, however, whether the morphological changes were accomplished by swash, surf and/or shoaling wave processes. Figures 6.16 shows the observed morphological change for four different tidal cycles, together with the modelled cross-shore distributions of swash, surf and shoaling wave processes. The selected tidal cycles represent:

(1) spring tide conditions with high waves (Figure 6.16a);
(2) spring tide conditions with low waves (Figure 6.16b);
(3) neap tide conditions with high waves (Figure 6.16c); and
(4) neap tide conditions with low waves(Figure 6.16d).

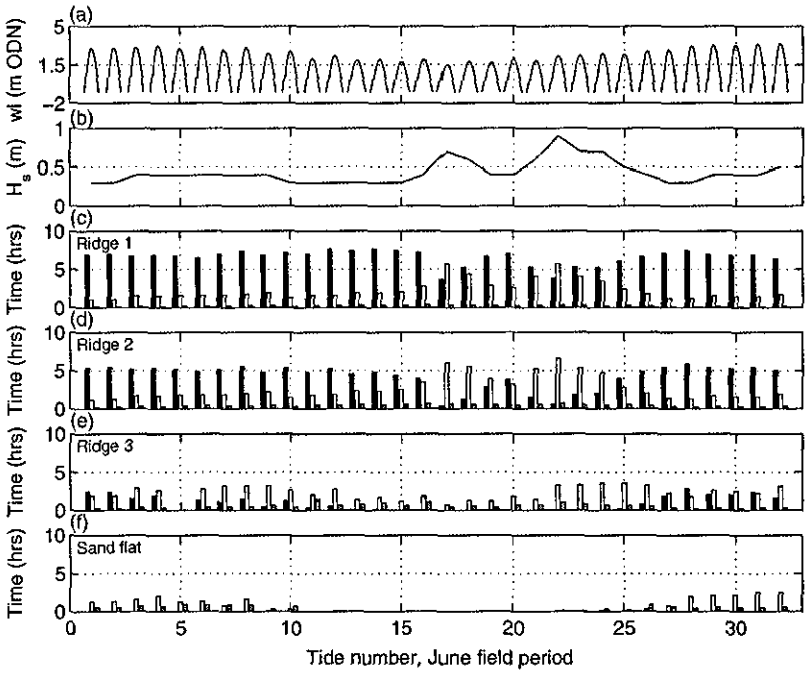

Figure 6.14 – (a) Measured tidal levels over the June field period. (b) Measured significant wave height at MLWN-level. (c–f) Modelled durations of swash (grey), surf (white) and shoaling wave (black) processes at the crests of ridges 1–3 and the sand flat. Duration of swash was doubled for better visualisation.

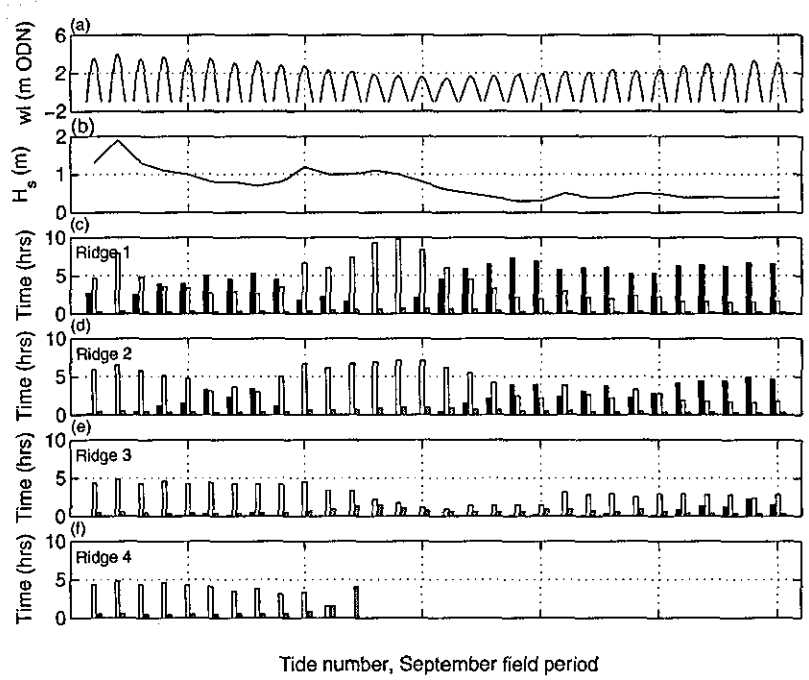

Figure 6.15 – (a) Measured tidal levels over the September field period. (b) Measured significant wave height at MLWN-level. (c–f) Modelled durations of swash (grey), surf (white) and shoaling wave (black) processes at the crests of ridges 1–4. Duration of swash was doubled for better visualisation.

Surf zone processes dominated over the entire intertidal zone during spring tide conditions with high wave-energy conditions (Figure 6.16a). The duration of the surf zone processes varied across-shore from 8 hours at the lowest ridge to 4 hours at the upper ridge, and these long durations induced significant morphological changes across the intertidal profile. Surf processes operated for much shorter periods during spring tides with low wave-energy conditions (Figure 6.16b). The surf zone rapidly shifted over the profile and surf processes only acted for more than 2 hours on the uppermost ridges. Shoaling waves predominated on the lower beach. The morphological change over this tidal cycle was very limited, and the largest changes occurred on the crest of ridge 3 where surf zone processes operated longest. The simulations for the neap tide scenarios (Figures 6.16c and d) show similar results, although two minor differences were observed: firstly, tidal translation rates were smaller and caused prolonged durations of the different wave processes across the ridge and runnel zone; and secondly, the swash curves showed some local peaks because the high tide mark during neap tide conditions was located at the seaward slope of ridge 3. This prolonged duration of swash induced local bed level changes of almost +0.1 m under high wave energy conditions (i.e., the formation of an incipient swash bar).

These results indicate that the quantity of morphological change is strongly related to the amount of time that surf processes operate. To check this hypothesis, the amount of time that swash, surf and shoaling waves acted on the different ridges was correlated to the 'ridge morphological change', defined as the absolute change in elevation averaged over the surface of the ridge (hence does not distinguish between erosion and accretion; Figure 6.17). Despite considerable scatter, not least because the results for different bars are combined, the results show that the amount of morphological change increases with the time that a ridge is subjected to swash and surf processes, and decreases with the time that shoaling waves operate.

6.6 DISCUSSION

Ridge and runnel morphology was monitored over spring-to-spring tidal cycles under a range of wave-energy conditions. The morphological changes during low wave-

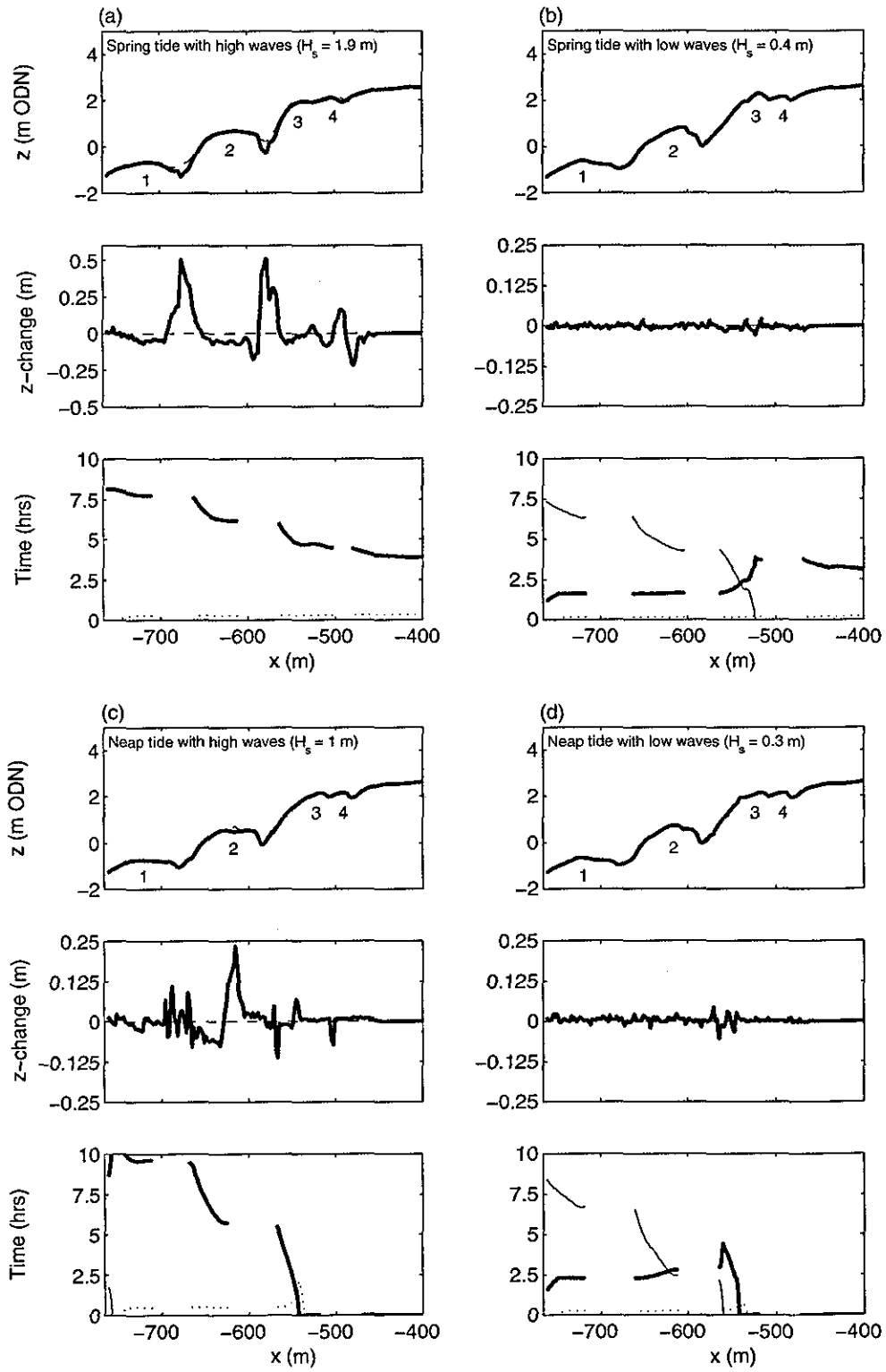

Figure 6.16 – Morphological change and duration profiles for swash, surf and shoaling wave processes for: (a) spring tide conditions with high waves; (b) spring tide conditions with low waves; (c) neap tide conditions with high waves; and (d) neap tide conditions with low waves. Each subplot shows the beach profiles before (solid line) and after (dashed line) the tidal cycle (top panels), the elevation change between these profiles (middle panels) and the cross-shore distribution of swash (dotted line), surf (thick solid line) and shoaling wave (thin solid line) processes (bottom panels).

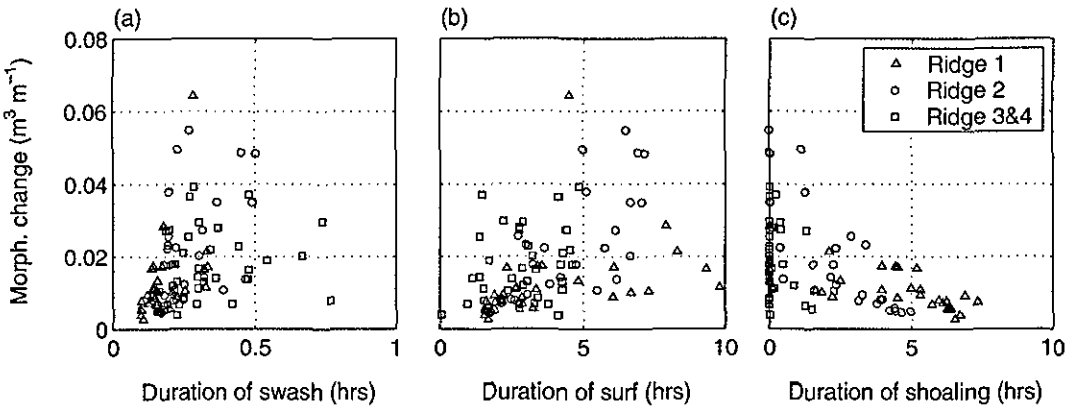

Figure 6.17 – Amount of absolute morphological change versus duration per tidal cycle of: (a) swash; (b) surf; and (c) shoaling wave processes. Different marker shapes represent different ridges.

energy conditions ($H_s < 0.5$) were small and generally did not exceed 0.01 m per tidal cycle (cf., King, 1972a; Voulgaris et al., 1998; Sipka and Anthony, 1999). Changes were limited to short sections of the cross-shore profile and were mostly related to the landward movement of the ridges through erosion of the seaward slope and deposition on the landward slope and slipface. The ridge migration rate ranged from insignificant to 1.6 m per tidal cycle and varied significantly across-shore and over the lunar tidal cycle. The lowest ridge was rather immobile, whereas the middle and upper ridges were migrating onshore (cf., King and Williams, 1949; Voulgaris et al., 1998). The rate of migration of the middle ridge was constant over the field experiment and seemed independent of wave level variations or the stage of the lunar tidal cycle (i.e., spring tide versus neap tide). The upper ridges were smaller and showed the largest migration rates, particularly under higher wave-energy conditions. The movement of these ridges was intermittent as they became subaerial during neap tide. Aeolian processes prevailed during these periods of prolonged emergence and it was observed that aeolian sediment transport induced local bed level changes up to 0.08 m in only a few hours. The observed migration rates are very similar to those in other studies (e.g., van den Berg, 1977; Voulgaris et al., 1998; Kroon and Masselink, 2002), although maximum migration rates in this study were slightly higher.

Morphological changes under high wave-energy conditions were much more significant. Bed level changes were not only larger, locally up to 0.5 m, but also more wide-spread across the entire beach profile. The impact of a 0.5-m surge on top of spring tide water levels was destructive on the lower beach, where the ridges eroded

and the released sediment was deposited in the runnels, but constructive on the upper beach. Here, the ridges remained intact and the most landward ridge migrated onshore. Although the storm event resulted in a flattening of the lower beach, ridges and runnels in this zone were still pronounced afterwards and even extreme storm events (i.e., the 1953 storm surge, refer to Section 6.1) did not destroy the ridges and runnels. This indicates that ridge and runnel morphology is rather resistant to complete destruction and it is therefore preferable to think of storm surges as events of larger morphological change rather than to label them as 'destructive'. Anthony et al. (2004), on the other hand, advocated that morphological change was as important during low wave-energy conditions as during storm events.

In addition to the migration of ridges, the formation of smaller lobes on the seaward slopes of the ridges was a commonly observed phenomenon. The lobes on the upper ridges often formed at the high tide mark and are, therefore, considered as incipient swash bars. The formation of the lobes on the middle ridges was more likely induced by surf zone processes as they formed at the position of the mid-surf at high tide, or just landward of the high tide breaker line. The lobes regularly survived tidal submergence over the successive tidal cycles and migrated onshore to join the crest. Such formation of lobes of sand and their onshore movement were also described by Greenwood et al. (2004) in a study of swash bar morphodynamics along the Danish coast. The development of secondary swash bars was further noted by Dabrio (1982), but he noted that their life span was limited as they formed at the low tide mark and were subsequently removed during the rising tide. Anthony et al. (2004) suggested that lobes of sand also displace alongshore, resulting in local morphological changes that can easily be misinterpreted as cross-shore profile adjustment

A numerical model was used to simulate the duration of swash, surf and shoaling wave processes across the intertidal profile under various tide and wave conditions. The results show that the duration of the different wave processes mainly depended on the wave-energy level. Surf zone processes prevailed across the entire ridge and runnel zone when waves were larger than 0.7 m and this is because larger waves are associated with wider surf zones and hence prolonged occurrence of surf processes. The stage of the lunar tidal cycle was also important, especially for the upper ridges as they became subaerial during neap tides. The simulations were further used to

explain the observed morphological changes and it appeared that the most important factor is the amount of time that swash and surf processes operate. It was, however, not possible to compute the rate of morphological change due to the individual processes as: (1) the net change derived from twice-daily profiles represents the cumulative effect of all three wave processes; and (2) the amount of change is not only related to the length of time that wave processes prevail, but also to their intensity. For example, 4 hours of surf zone processes under low-wave-energy conditions induced bed level changes up to 0.03 m, whereas high energetic surf processes induced a change of 0.2 m in the same amount of time. To determine the average rate of morphological change due to the three different wave processes, the model results were complemented by high-resolution (spatial and temporal) morphological measurements over a number of tidal cycles, and results of these are discussed in the next chapter (Section 7.4).

The occurrence and dynamics of drainage channels were investigated to gain more insight into their importance. All the larger ridges in the study area were dissected by at least one well-developed drainage channel and their presence altered the local ridge dynamics to a great extent. The drainage channels on the upper beach were intermittently active in relation to the spring-neap tidal cycle, whereas the drainage channels on the lower beach were dynamic all the time and migrated large distances alongshore. Small deltas formed where they drained into the landward-lying runnels and these may locally affect the flow dynamics.

On a daily to weekly time-scale (short-term), the ridges and runnels along the north Lincolnshire coast seem much less dynamic than nearshore bars on low-tidal beaches. In the latter environments, subtidal bars respond relatively rapidly to changing wave conditions and migrate offshore under rising wave conditions and move onshore under falling wave conditions at rates in the order of 10 m per day (Sallenger et al., 1985; Plant et al., 1999). Ridges and runnels are much less responsive and the large relaxation time is due to a combination of factors, including the relative stability of low-gradient, dissipative beaches (Wright and Short, 1984; Wright et al., 1982a, b), tidal residence times (Davis et al., 1972; van den Berg, 1977; Masselink, 1993) and morphodynamic feedback due to bar sheltering (Tucker et al., 1983; Ruessink and Kroon, 1994; Anthony et al., 2004; Masselink, in press). Relaxation time is an

important factor reducing the impact of storm events (cf. Wright, 1976) and this may explain the permanent character of ridge and runnel morphology.

6.7 CONCLUSIONS

- Ridges and runnels are very dynamic over a lunar tidal cycle. Morphological changes are mostly attributed to the onshore migration of ridges, but also the formation of smaller-scale lobes is important.
- Ridge migration rate ranges from insignificant to 1.6 m per tidal cycle and varies significantly across-shore. The lowest ridge was rather immobile, but rates of migration increased onshore. Migration rates of the upper ridges are further dependent on wave-conditions and stage of the lunar tidal cycle.
- Morphological changes during storms are much more significant than during low wave-energy conditions. Storm impact is destructive on the lower beach, resulting in a flattening of the morphology, but can be constructive on the upper beach (ridge migration).
- Well-developed drainage channels dissect the most pronounced ridges and cause a local disturbance in the ridge and runnel dynamics. The channels change significantly on a daily to weekly timescale and the state of the upper drainage channels affects the submergence of the sand flat, introducing an element of feedback in the system.
- Simulations of the occurrence of swash, surf, and shoaling wave processes suggest that the short-term response of ridges and runnels is mainly induced by surf zone processes.

Chapter seven

Ridge and Runnel Dynamics over Single Tidal Cycles

7.1 INTRODUCTION

This chapter deals with ridge and runnel dynamics on the smallest scale, that is the hydrodynamics and morphological evolution over a semi-diurnal tidal cycle. It is on this scale that beach morphological change can be associated with individual wave processes, such as swash, surf and shoaling waves on the one hand, and tidally induced currents on the other. Numerous hydrodynamic studies have shown that ridges tend to be dominated by flow velocities directed normal to the coast, whereas longshore currents prevail in the runnels (e.g., Voulgaris et al., 1996, 1998; Levoy et al., 1998; Sipka and Anthony, 1999).

Net longshore current speed and direction are generally tide-dominated, commonly with reversing directions (e.g., Reichmüth, 2003; Anthony et al., 2004), but further depend on the interaction of wave- and wind-induced longshore currents (Wright, 1976; Sipka and Anthony, 1999), as well as the longshore gradient of the runnel (Moore et al., 1984). Longshore current velocities not only vary throughout the tide, but also across the intertidal zone. Investigations by Levoy et al. (1998) and Anthony et al. (2004; Figure 7.1) showed that longshore current velocities during fair-weather conditions can reach values up to 0.4 m s^{-1} in the lower intertidal zone, but that they are significantly smaller on the mid-beach (maximum 0.3 m s^{-1}). Longshore current velocities increase during high wave-energy conditions, but interestingly the cross-shore variation shows a reverse trend. Levoy et al. (1998) recorded values of 0.8–1.2 m s^{-1} on the upper beach and 0.1–0.2 m s^{-1} on the lower beach, reflecting the decreasing influence of storm waves in the seaward direction.

Net cross-shore currents are also composed of wind-, wave- and tide-induced components. The tide-induced cross-shore flow results from the onshore and offshore migration of the water volume driven by, respectively, the flooding and ebbing over the beach topography. Vertical water level changes reach values up to 0.03 m min^{-1}, corresponding with tidal translation rates across the seaward slopes of ridges of 0.6–1.5 m min^{-1} (Masselink and Anthony, 2001). An analysis of the mean cross-shore current component by Voulgaris et al. (1998) showed that the cross-shore current consisted of a steady, offshore flowing undertow component of approximately 0.05 m s^{-1}, and a tidally driven component with an amplitude of also c. 0.05 m s^{-1}.

The interaction between the two causes a strong tidal asymmetry in the net cross-shore flow, as the tidal current opposes the undertow during the flood, whereas both cross-shore current components act in the same direction during the ebb. The relative importance of tidal versus wave processes varies across the intertidal zone. Tide-driven currents tend to occur when ridges experience shoaling waves and dominate on the lower parts of the intertidal zone, whereas the mid and upper intertidal zone usually reflect wave dominance (Parker, 1975; Levoy et al., 1998; Sipka and Anthony, 1999). King and Williams (1949) mentioned furthermore the effect of wind and they noted that onshore winds produce a landward movement of the surface water, that is subsequently compensated for by a seaward movement lower in the water column.

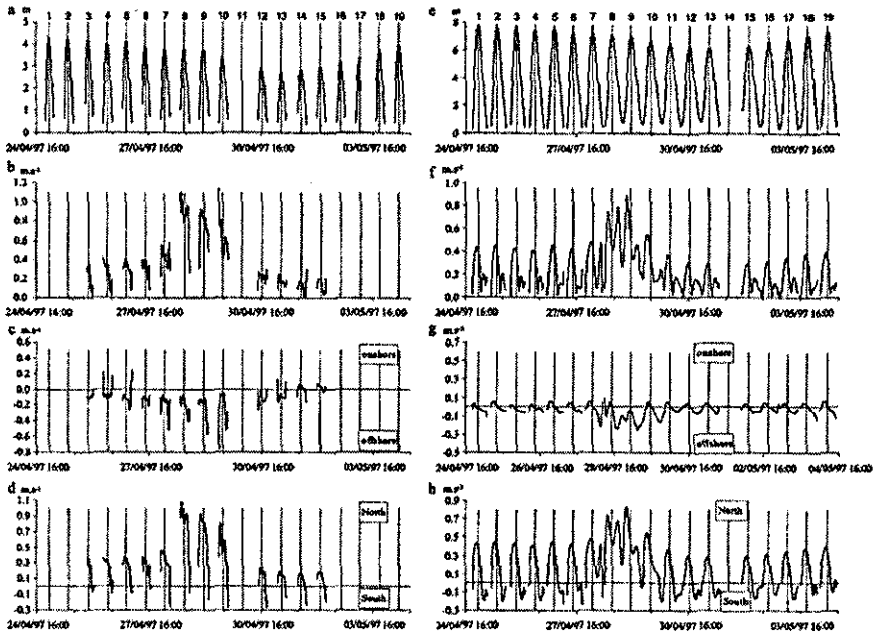

Figure 7.1 – Hydrodynamic conditions on a ridge and runnel beach in Northern France: (a) water level; (b) mean overall current velocity; (c) mean cross-shore current velocity; and (d) mean longshore current velocity. (e–f) represent same parameters as (a–d). Left and right panels show data for the mid and lower beach, respectively (from Anthony et al., 2004)

The pattern of cross-shore dominated flows across the ridges and longshore dominated currents in the runnels is further complicated by the presence of drainage channels. These channels cut through the ridges at regular intervals and drain the landward-lying runnel during the ebbing tide. The importance of drainage channels is mentioned previously in other ridge and runnel studies (e.g., Parker, 1975; Michel

and Howa, 1999), but a comprehensive hydrodynamic characterization of such channels has not been documented.

Sediment transport patterns on ridge and runnel beaches closely correspond to the spatial variation in the hydrodynamics. Cross-shore sediment transport prevails on ridges, whereas the sediment in runnels moves predominantly alongshore. The direction of sediment transport on the crest and landward slope of a ridge is predominantly directed onshore, induced by landward asymmetrical flow created by the passage of incident waves (Parker, 1975) and/or by unidirectional pulses of water overtopping the ridge crest and flowing into the runnel (Kroon and Masselink, 2002). The seaward ridge slope is characterised by either alongshore or offshore sediment transport (Parker, 1975). Voulgaris et al. (1998) noted that sediment transport rates are largest at the start and at the end of tidal flooding, when water depths are smallest.

Aim and objectives Chapter 7

The principal aim of this chapter is to describe and explain the dynamics of ridge and runnel topography over single tidal cycles. More specifically, the objectives are to:

(1) characterise the hydrodynamic processes in the different morphological settings of a ridge and runnel beach;
(2) document on the small-scale spatial and temporal variability in wave height and mean currents (i.e., across the intertidal zone and over a single tidal cycle);
(3) determine the importance of swash and surf zone processes to accomplish morphological change; and
(4) test the predictive capabilities of currently-existing cross-shore sediment transport models.

7.2 METHODOLOGY

Two three-week field experiments were conducted at Theddlethorpe beach in June 2001 and September 2001 to collect hydrodynamic data and monitor the beach morphology. The methodology used was identical for both field campaigns and has been largely described in Chapter 6. This section is supplementary and elaborates on the techniques that were used to collect data over a single tidal cycle.

The hydrodynamic data measured at the spring low water line, and used in the previous chapter to describe the wave climate during the field experiments, were complemented by data collected using three more instrument stations. One of these stations was equipped with an acoustic current meter with built-in pressure sensor and sampled at 0.15 m above the bed. The other two stations each consisted of a two-dimensional electromagnetic current meter and an individual pressure sensor. The current meters sampled at 0.15 m above the bed and the pressure sensors were located at bed level. The instrument stations were placed in such a way that the x and y axis of the current meters were aligned shore-normal and shore-parallel, respectively (i.e., directly measuring the cross-shore and longshore components of the flow). The positions and sampling routines of the three extra instrument stations were changed throughout the field campaign (Table 7.1). Tidal levels, significant wave height and mean cross-shore and longshore current velocities were computed for 10-minute data segments and this data was then used to: (1) visualise the variation over a single tidal cycle; (2) examine wave attenuation across the beach; (3) explore relationships between various hydrodynamic parameters; and (4) provide input for sediment transport models. The high-water wave conditions of the station at the spring low water line were used as an estimation of the offshore significant wave height H_0. This chapter presents hydrodynamic data for five tidal cycles with ranging conditions from low ($H_0 < 0.5$ m) to high ($H_0 > 1$ m) wave-energy.

Table 7.1 – Instrument station deployments.

Offshore station	
	At the spring low water line during the entire field experiment. 10 minutes per 30 minutes at 4 Hz
Onshore stations (3 in total)	
A	One station on each ridge 10 minutes per 30 minutes at 4 Hz*
B	All stations together on one ridge (middle ridge at neap tide, upper ridge at spring tide) 10 minutes per 30 minutes at 4 Hz*
C	One station in each runnel (6 tidal cycles only) 1 minute per 5 minutes at 4 Hz and 40 minutes per hour at 4 Hz**
D	One of the stations in a drainage channel (2 tidal cycles only) 10 minutes per 30 minutes at 4 Hz

*Instruments were sampling continuously at 8 Hz concurrent to high-resolution morphological monitoring

**different sampling strategies due to different types of instruments

An array of glass-fibre rods, placed across the ridge and runnel zone to monitor the bed level changes each low tide (Section 6.2), was used for high-frequent

morphological measurements during a number of tidal cycles (cf., Masselink et al., 1997; Kroon and Masselink, 2002). The bed level at the rods was obtained by measuring the distance from the top of the rods to the sand level and this was repeated at 10-minute intervals. The measurements commenced at low tide and at this stage only a few rods had to be measured because most of the rods were still emerged. Towards high tide, an increasing number of the rods on the lower beach became too deep to be sampled, but measurements at these rods were resumed as soon as this was possible again during the falling tide. Concurrent with the rod measurements, observations were made of the hydrodynamic conditions at each rod. The hydrodynamic processes that were identified are: swash and backwash, swash without backwash (at landward side of ridge), surf zone bores, breaking waves, shoaling waves, reformed waves and the presence of a longshore current. The rod measurements were checked for erroneous readings and converted to beach elevation. This resulted in a time series of elevation change for each single rod. In this chapter, morphological results are shown for four tidal cycles that are characterised by low to intermediate wave-energy conditions.

The bed morphology across the intertidal zone was mapped to indirectly address process dominance. A classification of bed forms was applied to characterise the bed structures across the ridge and runnels. The following bed types were identified (Figure 7.2): (1) plane bed; (2) washed-out wave ripples; (3) wave ripples; (4) ladders; (5) mixed wave and current ripples; (6) current ripples; (7) dunes; and (8) drainage channel structures. (Note: ladders are wave ripples superimposed with small current ripples). All observations were made when the intertidal zone was emerged and hence few, if any, of the bed forms due to flood were seen.

7.3 HYDRODYNAMIC CHARACTERISATION OF A RIDGE AND RUNNEL BEACH

On 23/09/01 (Tide 10), water levels and current velocities were recorded on the seaward slope of three consecutive ridges to investigate the hydrodynamic variability across the intertidal zone (Figure 7.3). The offshore significant wave height was 1.2 m, i.e., relatively high energetic conditions, and the high tide level was 2.8 m ODN. At all stages of the tide there was a clear attenuation of the wave energy levels

in the landward direction due to wave breaking, and over most of the tidal cycle, except occasionally at high tide, waves were breaking on at least two of the ridges at the same time (Figure 7.3c, d). Both the cross-shore and longshore current are tidally modulated to some degree, but the prevailing southward longshore current is primarily wave-driven (Figure 7.3e, f). Longshore current velocities ranged from 0.1 to 0.6 m s^{-1}, whereas cross-shore current speeds were much lower (< 0.1 m s^{-1}) and mainly offshore.

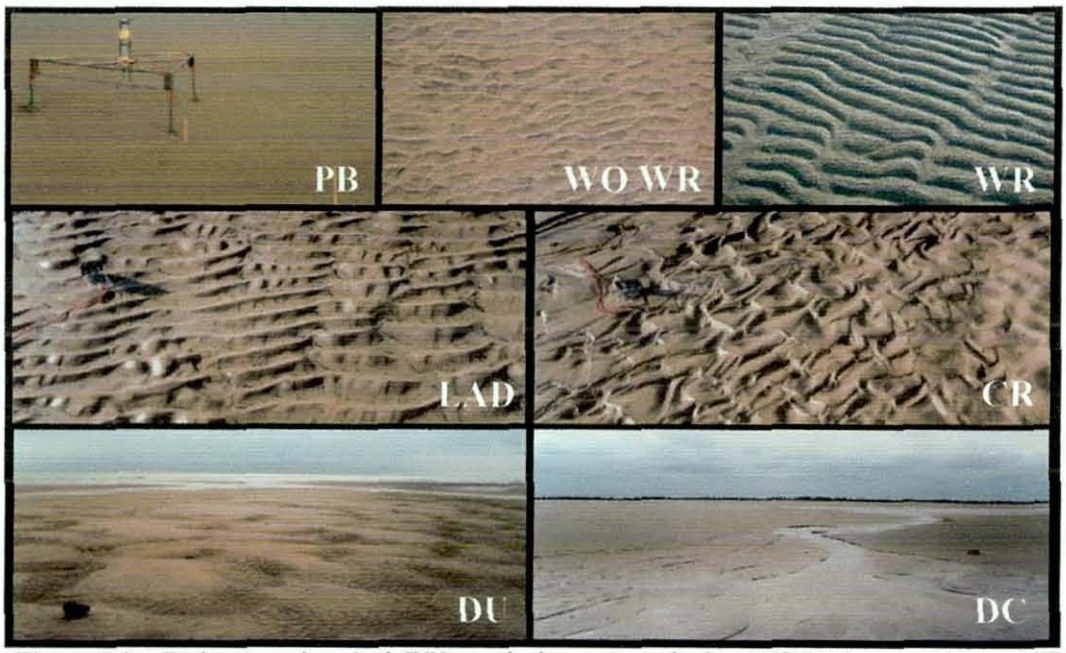

Figure 7.2 – Bed types: plane bed (PB), washed-out wave ripples (WO WR), wave ripples (WR), ladders (LAD), current ripples (CR), dunes (DU) and drainage channel patterns (DC).

The instrument stations were placed across one single ridge to examine the effect of local beach gradient on nearshore waves and currents (Figure 7.4). The offshore significant wave height over Tide 7 (21/09/01) was 0.8 m, i.e., intermediate wave-energy conditions, and the high tide level was at 3.1 m ODN. The breaker depth was 2.3 m, so the ridge was just in the shoaling zone around high tide. All three stations recorded similar magnitudes and trends for the various hydrodynamic parameters and this implies that the variation within a ridge due to varying local gradient is smaller than the variability across the different ridges. The current velocities further show a strong tidal dominance and both cross-shore and longshore currents reversed at high tide (Figure 7.4c and d). During the rising tide, cross-shore currents were offshore under surfzone zone processes, but become onshore towards high tide when shoaling waves prevail.

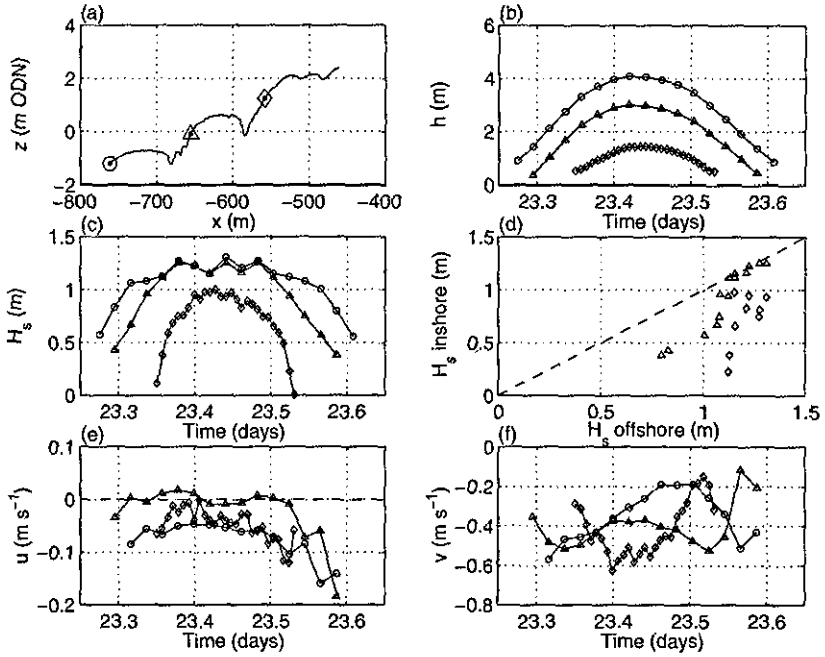

Figure 7.3 – Hydrodynamic conditions on 23/09/'01 (Tide 10): (a) beach profile with locations of stations; (b) water depth; (c) significant wave height; (d) relationship between significant wave height at offshore station and inshore stations; (e) mean cross-shore current velocity; and (f) mean longshore current velocity. Different markers are used to indicate the stations and their respective data. Positive cross-shore and longshore currents are onshore and toward the north, respectively.

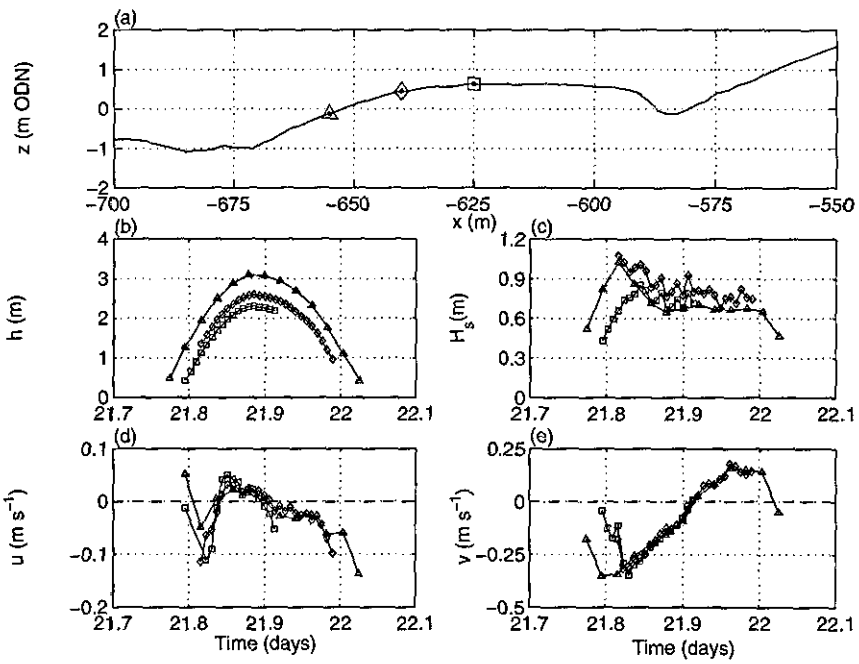

Figure 7.4 – Hydrodynamic conditions on 21/09/'01 (Tide 7): (a) beach profile with locations of stations; (b) water depth; (c) significant wave height; (d) mean cross-shore current velocity; and (e) mean longshore current velocity. Different markers are used to indicate the stations and their respective data.

Three instruments were also employed in three consecutive runnels (Figure 7.5). The offshore significant wave height over Tide 22 (29/09/01) was 0.4 m, i.e., representing low wave-energy conditions, and the high tide level was at 2.1 m ODN. The flow in the runnels was prevailingly parallel to the shoreline and was characterised by values up to 0.2 m s^{-1}. The runnels on the lower beach were tide-dominated, whereas the currents in the upper runnel were also affected by wave- and wind conditions. The wind was blowing from the south (refer to Figure 6.7) and forced the flow in the upper runnel to the north.

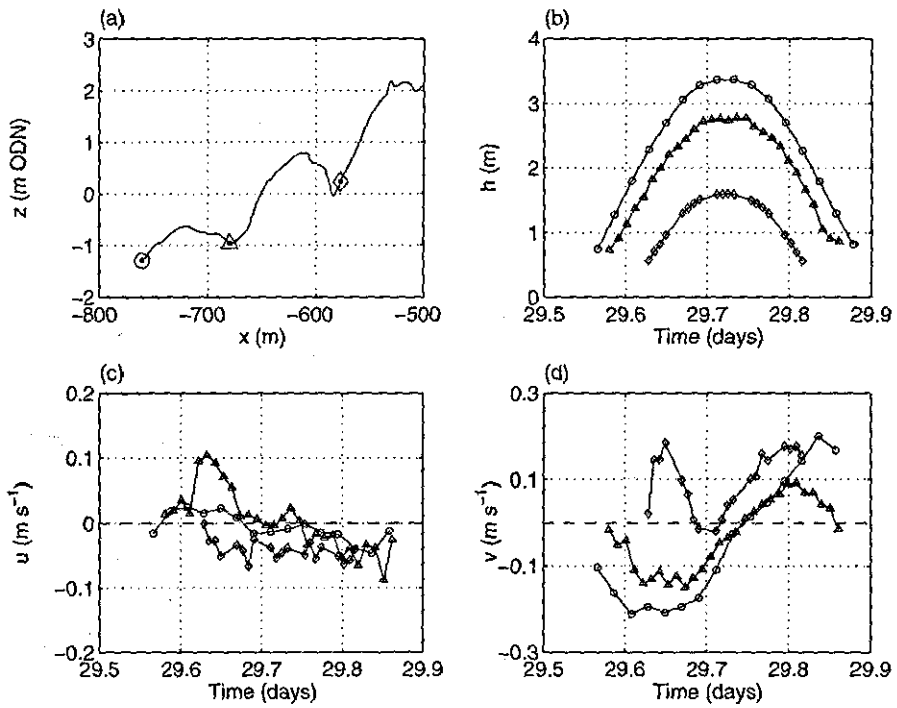

Figure 7.5 – Hydrodynamic conditions on 29/09/'01 (Tide 22): (a) beach profile with locations of stations; (b) water depth; (c) mean cross-shore current velocity; and (e) mean longshore current velocity. Different markers are used to indicate the stations and their respective data. Positive cross-shore and longshore currents are onshore and toward the north, respectively.

One of the instrument stations was placed at the head of a drainage channel over two tidal cycles under low wave-energy conditions (Figure 7.6). The drainage channel cut through the middle ridge from NW to SE, was c. 6 m wide and featured erosion cliffs that were c. 0.3 m high. During the rising tide, water entered the drainage channel as soon as the seaward-lying runnel filled up and this resulted in flows with speeds up to 0.25 m s^{-1} (Figure 7.6c, d). The drainage channel functioned as an inlet for the landward-lying runnel until swashes and waves started to reach over the crest. At this

point, a longshore current started to develop in the runnel and opposed the flow in the drainage channel, resulting in the current direction in the channel to reverse. The occurrence of strongly-asymmetric reforming/shoaling waves at this stage caused small peaks in the curves of significant wave height (Figure 7.6e, f). Current velocities ceased towards high tide and picked up again half way the falling tide when the channel started to drain the landward-lying runnel. The outflowing current reached values up to 0.8 m s^{-1}.

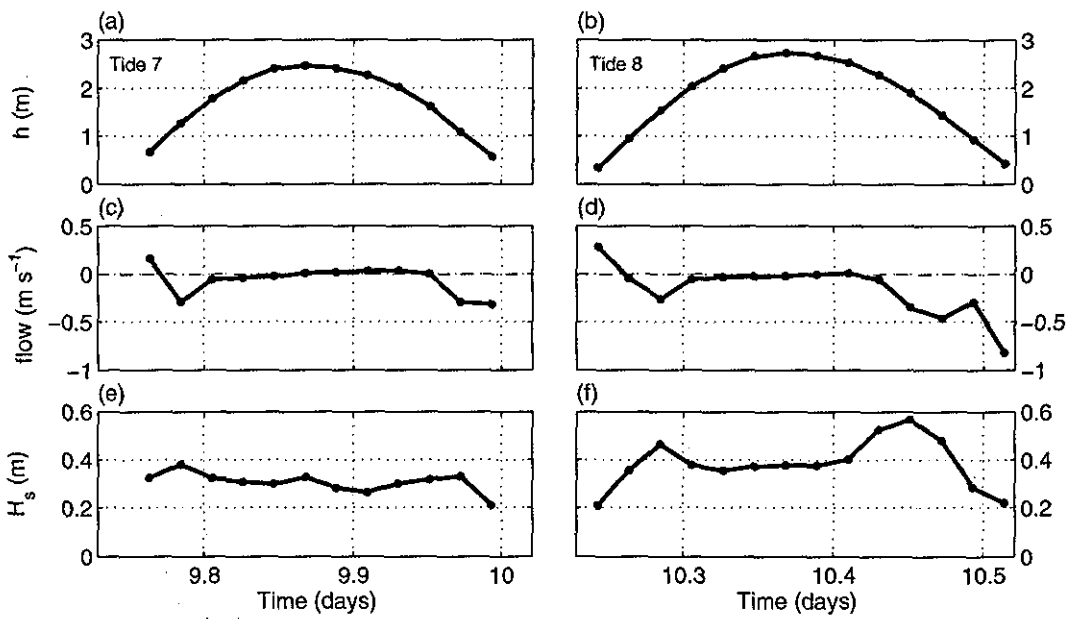

Figure 7.6 – Hydrodynamic conditions in a drainage channel over two tidal cycles: (a, b) water depth; (c, d) mean flow velocity; and (e, f) significant wave height. Left and right panels show data for, respectively, Tide 7 (09/06/'01) and Tide 8 (10/06/'01). Positive flow velocities indicate a landward flow, negative velocities indicate a seaward flow.

The tidal modulation of local significant wave height and current velocities was explored in more detail using all the hydrodynamic data of both field campaigns (Figure 7.7). The local wave height was dependent on the tidal stage in such a way that wave height was larger during the flood than during the ebb, regardless of wave energy level (Figure 7.7a). Tidal control on wave height further manifested itself in the constraint of local significant wave height in shallow water depths (Figure 7.7b). Wave height attained maximum values at high water when energy losses over the nearshore zone are least. Maximum wave height in the runnels was significantly lower than on the ridges due to the sheltering effect of ridges.

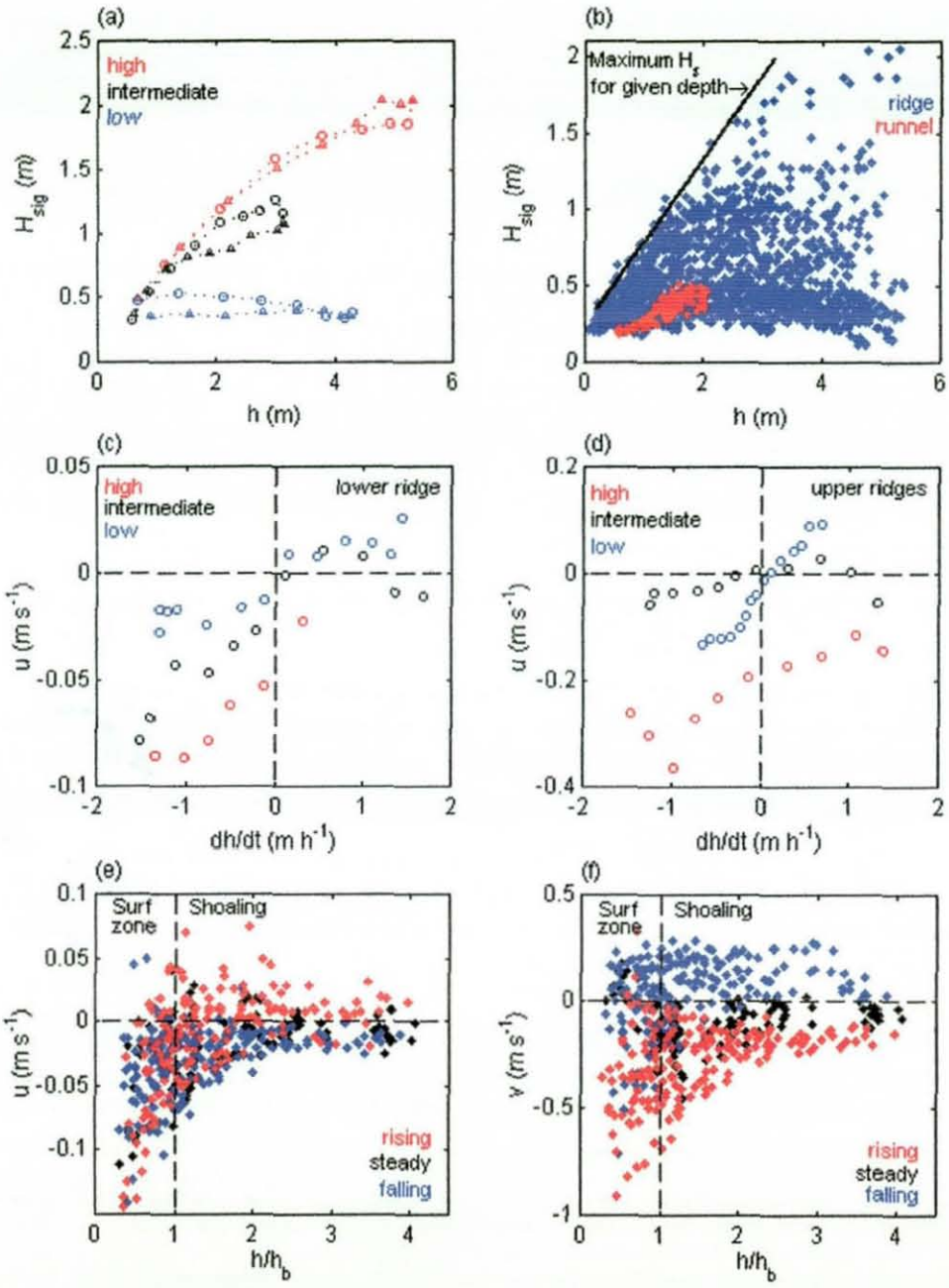

Figure 7.7 – Relationships between various hydrodynamic parameters: (a) local significant wave height against water depth under varying wave-energy conditions (circle = rising tide, triangle = falling tide); (b) control of tidal water level on local wave height; (c) and (d) mean cross-shore current velocity against local water level gradient (dh/dt) for lower ridge and upper ridges, respectively; (e) and (f) tidal control on, respectively, mean cross-shore and longshore current velocity in the surf ($h/h_b < 1$) and shoaling ($h/h_b > 1$) zones. An irregular wave breaker criterion γ of 0.35 was used to compute the breaker depth h_b (Kroon and Masselink, 2002).

Current velocities were also strongly modulated by the tide and the degree of modulation is similar for lower and upper ridges (Figure 7.7c, d). Cross-shore flows were mainly onshore during the rising tide and offshore during the falling tide, except under high wave-energy conditions when flow was continuously offshore. The net cross-shore flow during moderate to high wave-energy was the result of a combined steady offshore directed undertow and a tidally-varying current and it was possible to separate them as the tidal component of the current should equal zero at high tide ($dh/dt = 0$). Using the high-energy data for the upper ridge (Figure 7.7d), it appeared that undertow velocity was -0.2 m s^{-1} and, therefore, the tidal cross-shore component equalled c. $\pm$ 0.1 m s^{-1}. Tidal currents opposed the undertow during the flood, causing the net cross-shore current to tend towards zero, whereas during the ebb, both currents acted in the same direction. Under intermediate wave conditions, bed return flow contributed to the net flow just a limited amount of time as surfzone conditions just prevailed at the start and the end of inundation. Net cross-shore currents were fully tide-dominated during low wave-energy conditions. Figure 7.7e further illustrates that cross-shore currents were more tidally modulated in the shoaling wave zone than in the surfzone, where the undertow outbalanced the onshore tidal flow during the rising tide. The net longshore current also shows a strong tidal dependence, generally with southward currents occurring during flood and northward flows during ebb (Figure 7.7f). Wave-induced longshore currents only dominated during steady tide and were mostly towards the south due to northerly winds.

7.4 MORPHOLOGICAL CHANGE DURING A SINGLE TIDAL CYCLE

In Section 6.5, the outcome of a numerical model that simulated wave processes over a tidal cycle was used to explain the morphological changes over a tidal cycle. It was suggested that the longer a ridge was subject to swash and surf zone processes, the greater the morphological response. It was, however, not possible to link the observed morphological changes to the individual processes. High-resolution (temporal and spatial) morphological measurements were conducted over a number of tidal cycles to complement the model results and to determine the average rate of morphological change due to swash, surf (bores and breakers) and shoaling wave processes. Results are shown for two tidal cycles (Figures 7.8–7.10).

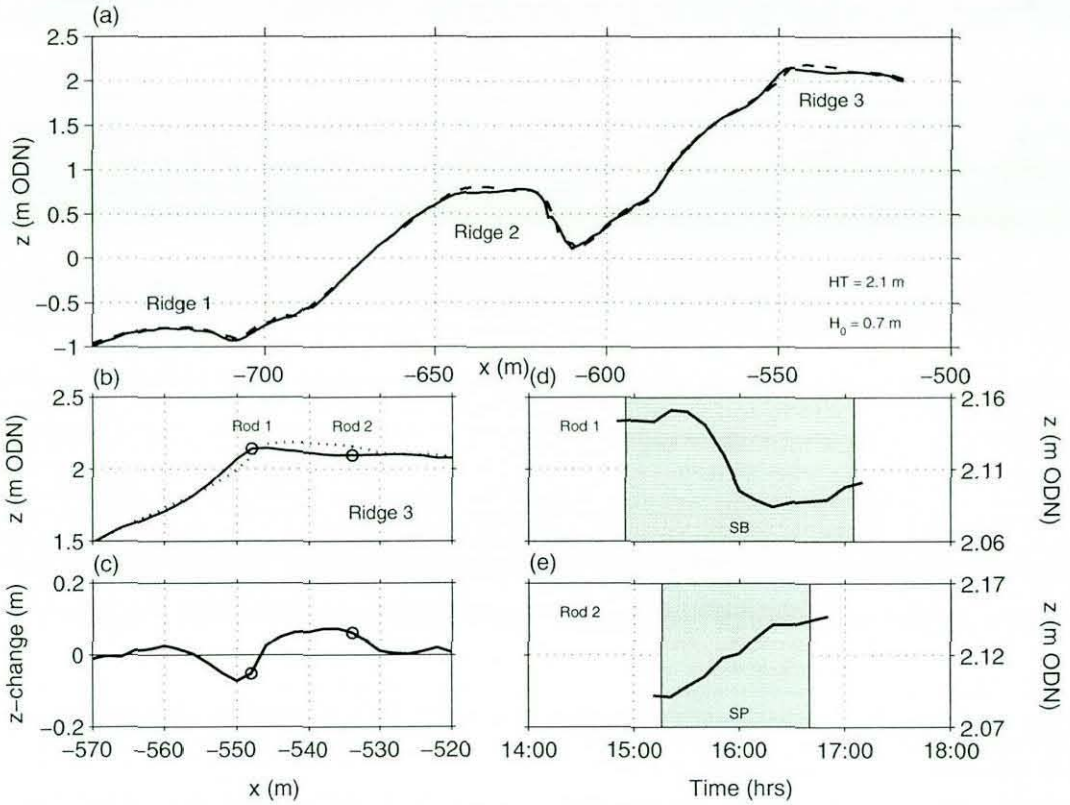

Figure 7.8 – Morphological change over Tide 24 (18/06/'01): (a) beach profiles at start (solid line) and end (dashed line) of tidal cycle; (b) same profiles as in (a), but zoomed in at ridge 3; (c) elevation change for ridge 3; (d) and (e) bed level change at, respectively, rod 1 and rod 2. In (c) positive values indicate accretion and negative values indicate erosion. In (d) and (e) shading labelled with 'SB' and 'SP' indicate the action of swash-backwash and uni-directional swash pulses, respectively.

Significant morphological changes were observed on Ridge 2 and Ridge 3 over Tide 24 (18/06/01), showing, respectively, offshore and onshore movement of the crest (Figure 7.8a). Offshore significant wave height was 0.7 m (i.e., intermediate wave-energy conditions) and the water level at high tide reached 2.1 m ODN, equal to the elevation of the crest of Ridge 3. This ridge experienced c. 2 hours of continuous swash action, which resulted in onshore migration of the crest over a distance of 5 m (Figure 7.8b–e). Local bed level changes were up to 0.08 m. Ridge 2 was mainly subjected to surf zone bores with short periods of swash action when water depth was shallow (Figure 7.9). Over the tidal cycle, the crest position of the ridge changed, but this seems not to have been accomplished by the offshore migration of the initial crest because: (1) the sediment budget over the tidal cycle revealed that the total amount of erosion and accretion were not in balance (Figure 7.9b), implying that part of the sediment was supplied alongshore; and (2) the initial crest was still present at the end

of the tidal cycle and, in fact, migrated 4 m onshore. The morphological change on this ridge was mainly induced by surfzone bores, with net accretion or erosion in the order of 0.05 m. Uni-directional pulses of swashes overtopping the newly-formed wave crest caused significant accretion at rods 5 and 6 near the end of tidal inundation (Figures 7.9e, f).

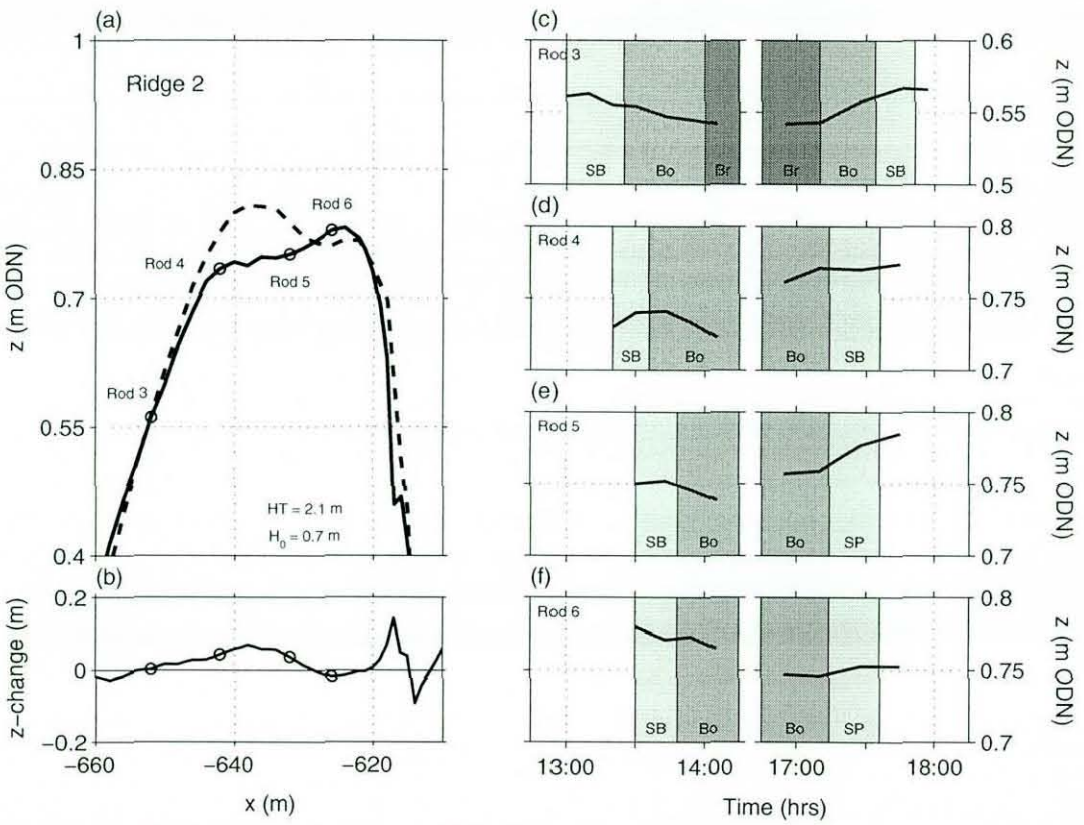

Figure 7.9 – Morphological change over Tide 24 (continued from Figure 7.8): (a) beach profiles at start (solid line) and end (dashed line) of tidal cycle zoomed in at ridge 2; (b) elevation change for ridge 2; (c–f) bed level change at rods 3–6. In (b) positive values indicate accretion and negative values indicate erosion. In (d–f) shading labelled with 'SB', 'SP', 'Bo' and 'Br' indicate the action of swash-backwash, uni-directional swash pulses, bores and breakers, respectively.

Another example of the morphological change at ridge 2 is shown in Figure 7.10. Offshore significant wave height over Tide 16 (26/09/'01) was 0.6 m (i.e., low to intermediate wave-energy conditions) and the high tide level was at 1.4 m ODN. The ridge crest migrated onshore over a distance of 3.8 m through transfer of sediment from the seaward slope (erosion) to the landward slope (accretion). In this case, however, the morphological change was accomplished by the combination of swash, surfzone bores and breakers (Figure 7.10c–f).

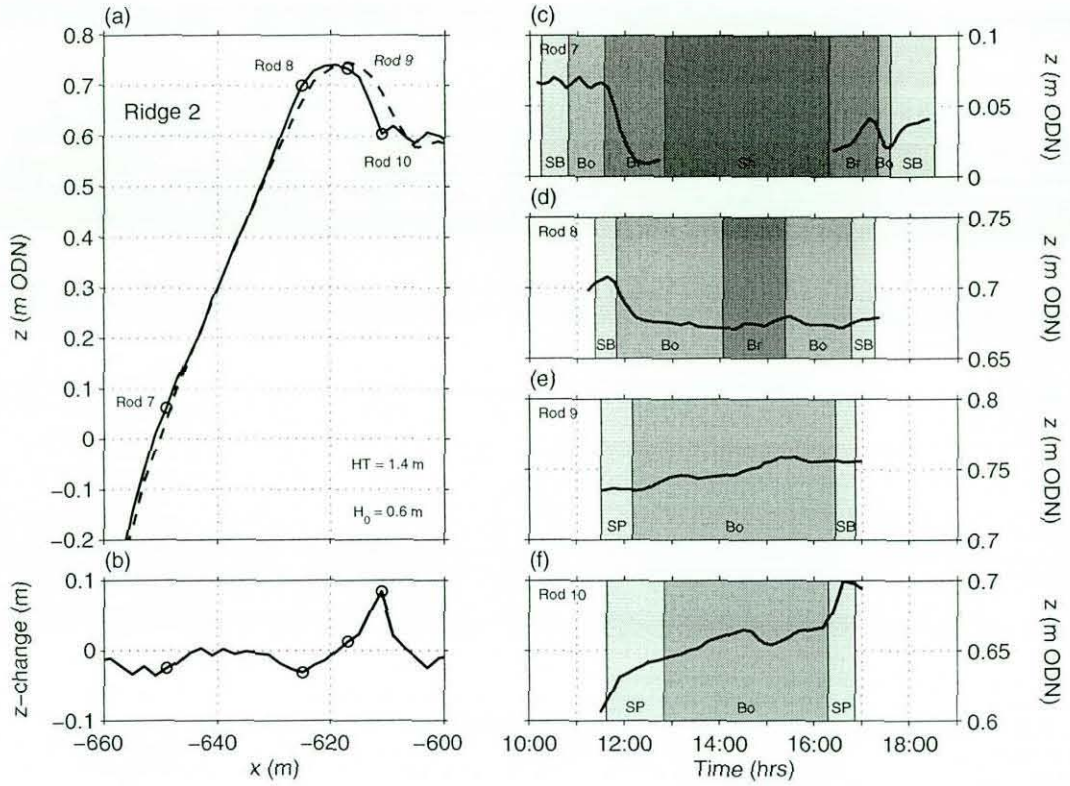

Figure 7.10 – Morphological change over Tide 22 (26/09/'01): (a) beach profiles at start (solid line) and end (dashed line) of tidal cycle zoomed in at ridge 2; (b) elevation change for ridge 2; (c–f) bed level change at rods 7–10. In (b) positive values indicate accretion and negative values indicate erosion. In (d–f) shading labelled with 'SB', 'SP', 'Bo', 'Br' and 'Sh' indicate the action of swash-backwash, uni-directional swash pulses, bores, breakers and shoaling waves, respectively.

The high-resolution morphological data were subsequently used to investigate the rate of morphological change due to swash and surf processes (Table 7.2). Results indicate that the rate of morphological change is relatively independent of the type of wave process and this implies that the morphological change due to a certain wave process is more related to the amount of time that the process operates. The analysis further demonstrated that bores during the rising tide were erosive, in contrast to the falling tide, when bores also induced accretion. Rates of morphological change were generally larger on the seaward slope than on the crest.

Table 7.2 – Rate of morphological change dz/dt in (m hr^{-1}) due to swash, bores and breakers. Values in brackets indicate minimum (erosive) and maximum (accretive) rates.

	Rising tide			Falling tide		
	Swash	Bores	Breakers	Swash	Bores	Breakers
Slope	[–0.03 0.04]	[–0.04 0.00]	[–0.06 0.00]	[0.00 0.04]	[–0.08 0.05]	[0.00 0.02]
Crest	[–0.07 0.06]	[-0.01 0.01]	no data	[0.00 0.01]	[0.00 0.01]	no data

The morphological change in a drainage channel was monitored during the falling stage of Tide 8 (10/06/'01) from the moment that the channel started to drain to the seaward-lying runnel (Figure 7.11). Water depth at this point was approximately 0.5 m and flow velocity was c. 0.8 m s^{-1} (refer to Section 7.2).

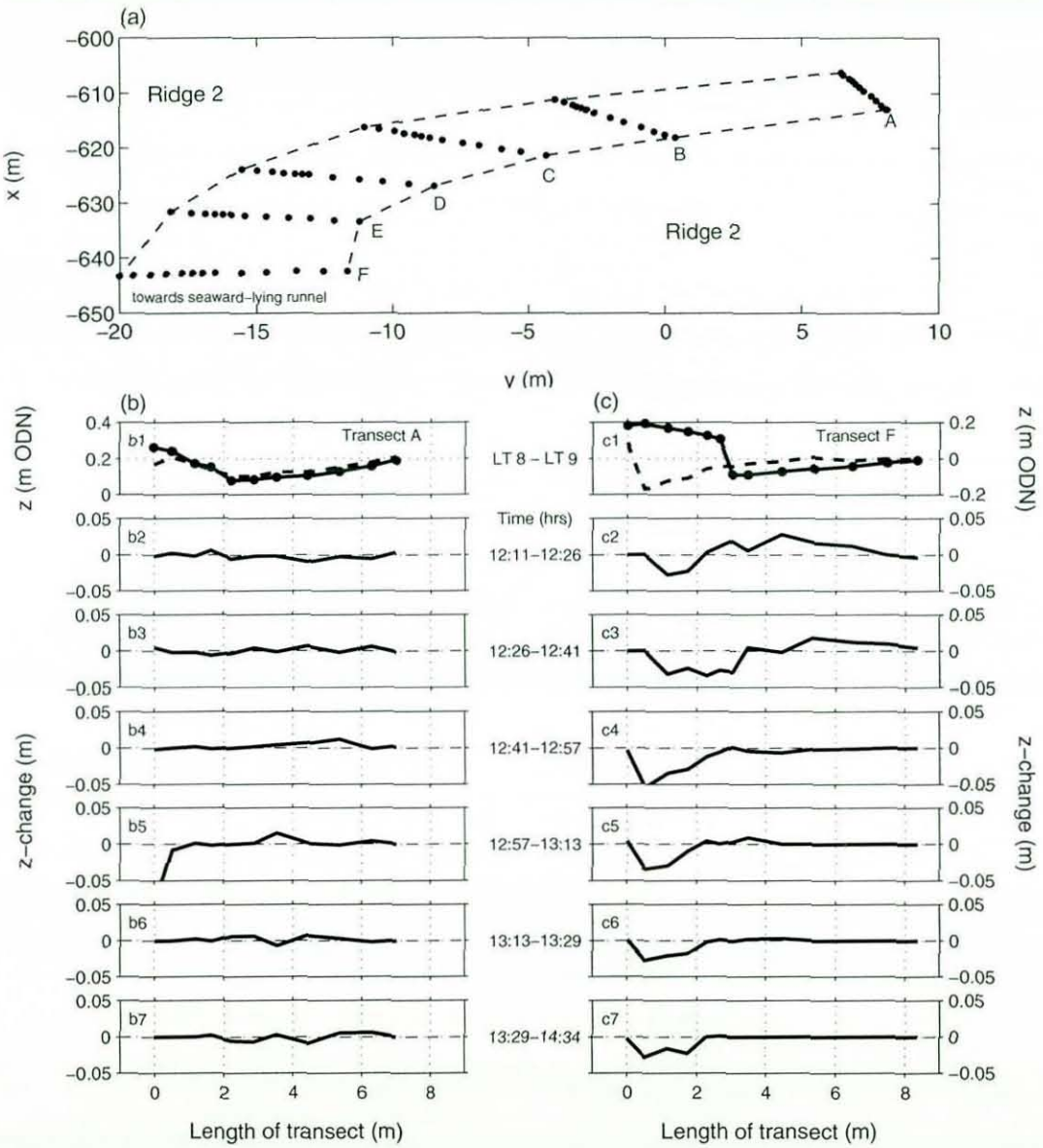

Figure 7.11 – Morphological change of a drainage channel over Tide 8 (10/06/'01): (a) plan view of the channel with monitoring points (transects A–F); (b_1) and (c_1) transect profiles before (solid line) and after (dashed line) tidal cycle for, respectively, transect A and F; and (b_{2-7}) and (c_{2-7}) elevation change at subsequent intervals during the falling tide. Positive values indicate accretion and negative values indicate erosion. The arrows in (a) indicate the flow patterns during ebb.

Figure 7.11a shows a plan view of the drainage channel with the locations of the transects along which morphological change was monitored. The morphological

changes were most different at the two outermost transects (A and F), whereas the transect in between showed a gradual change between those two extremes. At the head of the drainage channel (Transect A), the channel had a symmetrical U-shape and net morphological change over the tidal cycle was negligible (Figure 7.11b). The seaward end of the channel (Transect F) was characterised by a 0.2-m high erosion-cliff. When flows ceased towards the end of the tidal cycle, this cliff had heightened to 0.3 m and had moved southward just over 2 m (Figure 7.11c). The erosion of the outer bend was induced by non-uniform flow in the drainage channel with much larger current velocities in the outer bend than in the inner bend and the inner bend was subject to accretion as a result (similar to the formation of point bars in river meanders).

7.5 BED MORPHOLOGY

Observations of the bed morphology (refer to Figure 7.2) concurrent with the high-resolution morphological measurements showed that swash action caused plane bed, whereas wave ripples and dunes were present when surf zone bores prevailed. Bed forms were, however, difficult to observe when the bed was submerged and these observations were complemented by the mapping of the bed morphology every low tide (Figure 7.12a). The runnels were generally found to be covered with wave and/or current ripples or transient between them, whereas bed morphology on the ridges was mostly swash-dominated. The seaward slopes of the ridges were characterised by plane bed whilst washed-out wave ripples became more common toward the crest of the ridge. Here, the swash action was not strong enough to completely flatten the wave ripples that had formed previously at larger water depths. Occasionally, the ridge crest and landward slope of the middle ridge were covered with dunes. Megaripples were generally present in the deeper runnels.

A three-dimensional map of the bed morphology along nine cross-shore transects is presented in Figure 7.12b. Significant areas were affected by the presence of drainage channels as they not only caused deep trenches through a ridge, but also formed deltas where they terminated in the seaward-lying runnels. The bed forms in the drainage channels and on the deltas were a mixture of current ripples and plane bed, both, however, formed by strong outflowing currents, as opposed to longshore

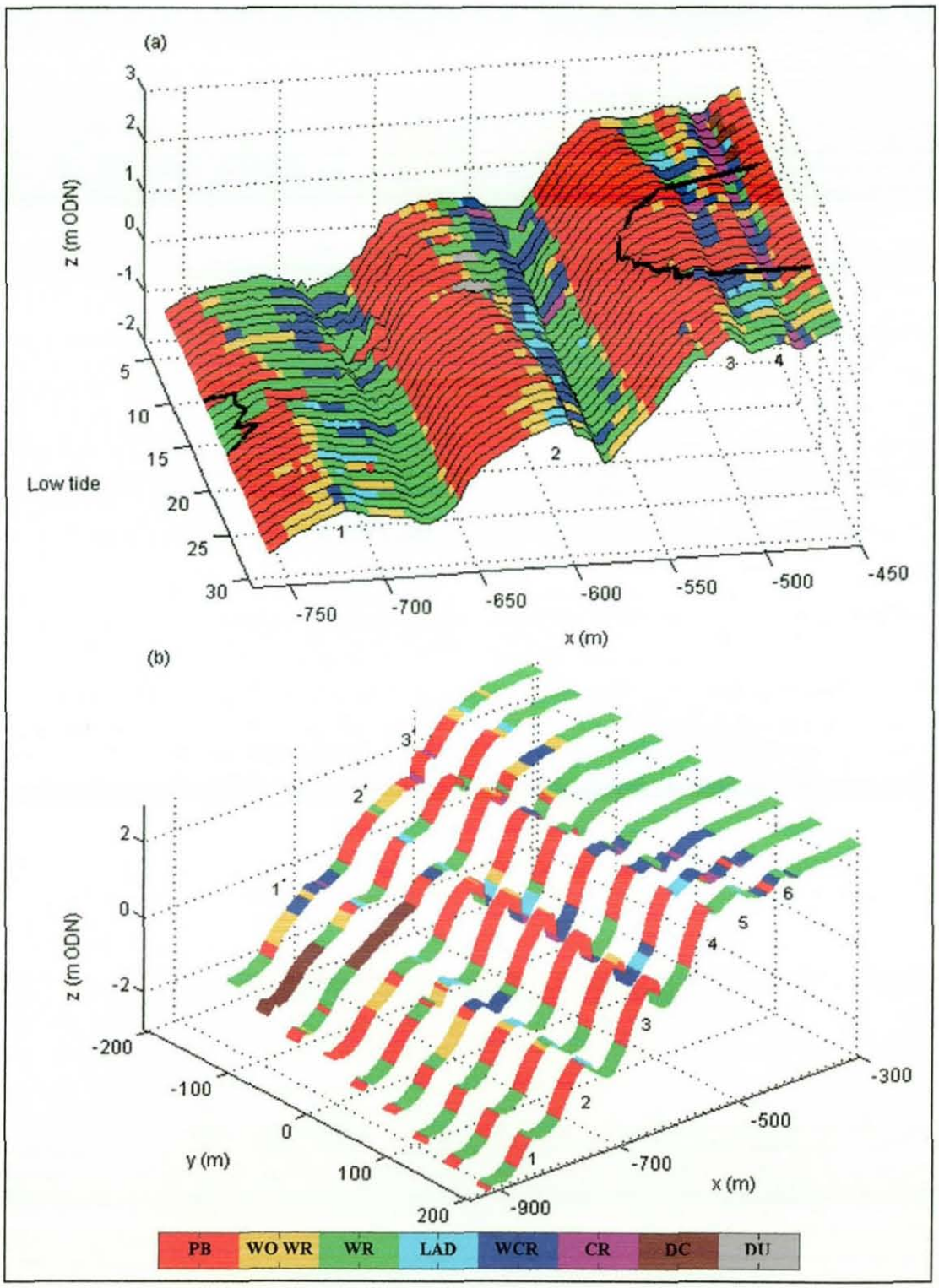

Figure 7.12 – Bed morphology at low tide: (a) bed morphology along one cross-shore transect over a spring-to-spring tidal cycle; (b) three-dimensional view along nine cross-shore transects. Bed types are: plane bed (PB), washed-out wave ripples (WO WR), wave ripples (WR), ladders (LAD), mixed wave and current ripples (WCR), current ripples (CR), drainage channel structures (DC) and dunes (DU). Bed morphology is plotted on top of simultaneously-taken beach profiles. In (a), 'slices' represent the bed morphology at successive low tides and the thick solid black lines mark the high tide levels (right) and low tide levels (left).

currents and swash elsewhere on the ridges and runnels. The map further shows that a small difference in local gradient can result in different bed types to emerge at low tide, implying a subtle relationship between gradient, flow and bed morphology. For example, plane bed prevailed on the steeper parts of the seaward slope, whereas washed-out wave ripples dominated on flatter parts with a gradient smaller than 0.015 (Figure 7.13).

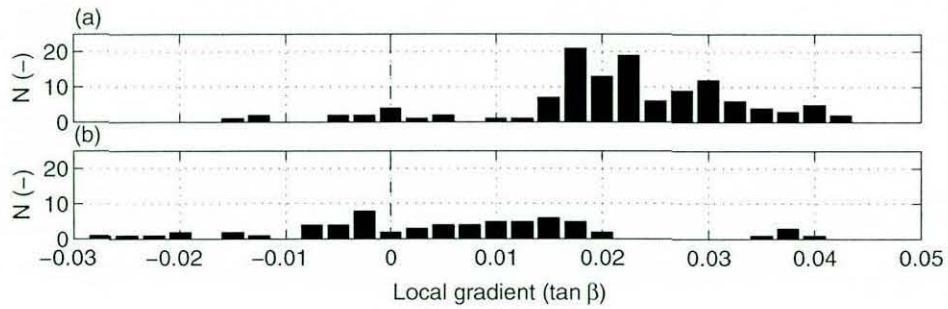

Figure 7.13 – Occurrence of (a) plane bed and (b) washed-out wave ripples in relation to local gradient. The bars indicate number of observations per gradient class.

7.6 SEDIMENT TRANSPORT MODELLING: THEORETICAL REVIEW

It seems appropriate to consider intertidal and subtidal bars as part of a spectrum of bar morphologies, rather than distinctly different bar types, with one of the discriminating factors being the tide-induced non-stationarity in the hydrodynamic processes (Masselink et al., submitted). It follows therefore, that concepts and models pertaining to subtidal bar behaviour should be applicable to intertidal bars. Cross-shore sediment transport and subtidal bar dynamics are primarily controlled by two processes, each dominating over different parts of the nearshore zone: (1) outside the surf zone the wave skewness associated with shoaling waves causes onshore sediment transport; and (2) inside the surf zone sediment transport is mainly directed offshore due to sediment suspension by breaking waves and the subsequent advection by the bed return flow (e.g., Osborne and Greenwood, 1992a, 1992b).

There have been various attempts to model the morphological evolution of nearshore bar systems. One of the most successful approaches has been the application of the energetics expression for sediment transport, originally derived by Bagnold (1963,

1966) for steady flow, and extended by Bailard (1981) and Bailard and Inman (1981) to combined (oscillatory and steady) flows:

$$Q_x = K_b\left\{\left\langle|\underline{u}|^2\tilde{u}\right\rangle + \left\langle|\underline{u}|^2\bar{u}\right\rangle - \frac{\tan\beta}{\tan\phi}\left\langle|\underline{u}|^3\right\rangle\right\} + K_s\left\{\left\langle|\underline{u}|^3\tilde{u}\right\rangle + \left\langle|\underline{u}|^3\bar{u}\right\rangle - \frac{\varepsilon_s}{w_s}\tan\beta\left\langle|\underline{u}|^5\right\rangle\right\} \quad \textbf{(1)}$$

where Q_x is the time-averaged, cross-shore volume sediment transport per unit width per unit time (positive in the offshore direction), $|\underline{u}|$ is the total (i.e., cross-shore and longshore) nearshore velocity vector, $\bar{u}$ and $\tilde{u}$ are the mean and oscillatory components of the cross-shore near-bottom velocity, respectively, ϕ is the angle of internal friction of the sediment, $\tan\beta$ is the bed slope and angle brackets denote time averaging. The coefficients K_b and K_s are:

$$K_b = \frac{\rho_w}{g(\rho_s - \rho_w)} c_f \frac{\varepsilon_b}{\tan\phi} \quad \textbf{(2a)}$$

$$K_s = \frac{\rho_w}{g(\rho_s - \rho_w)} c_f \frac{\varepsilon_s}{w_s} \quad \textbf{(2b)}$$

where g is gravity, ρ_w is the fluid density, ρ_s is the density of quartz sand, c_f is the friction coefficient, ε_b and ε_s are the bedload and suspended load efficiencies, respectively, and w_s is the sediment fall velocity. According to Church and Thornton (1993), $\varepsilon_b = 0.135$, $\varepsilon_s = 0.015$ and $c_f = 0.003$. It is emphasised that the cross-shore sediment transport Q_x depends on longshore as well as cross-shore currents, because both contribute to the total stress that mobilises sediment for steady flow.

Application of the energetics approach to predicting cross-shore beach change by Thornton et al. (1996) and Gallagher et al. (1998) has revealed that the approach works well under energetic conditions, when strong breaking-wave-driven mean flows prevail. Under such conditions, the approach adequately models the offshore movement of nearshore bar systems. However, energetics-based sediment transport models do not perform well under mild wave conditions, when breaking-wave-driven mean flows are weak, and when nearshore bars migrate onshore.

Recently, Elgar et al. (2001) suggested that onshore bar migration, observed under mild wave conditions, may be related to the skewed fluid accelerations associated with the orbital velocities of non-linear surface waves. As waves shoal and break, they evolve from profiles with sharp peaks and wide troughs outside the surf zone

(horizontally-asymmetric Stokes waves), to pitched-forward shapes with steep front faces inside the surf zone (vertically-asymmetric saw-tooth bores). If accelerations increase the potential for sediment transport, as clearly demonstrated by Canlantoni (2002), then there will be more onshore than offshore transport under pitched-forward waves. To quantify acceleration effects in pitched-forward waves, Elgar et al. (2001) proposed the following dimensional form of acceleration skewness (i.e., the difference in the magnitudes of accelerations under the front and the rear wave faces):

$$a_{spike} = \frac{\langle a^3 \rangle}{\langle a^2 \rangle} \qquad \textbf{(3)}$$

where a is the time series of acceleration (derivative of the velocity time series) and angle brackets denote time averaging. Subsequently, Hoefel and Elgar (2003) formulated the following expression for cross-shore, acceleration-driven sediment transport Q_x:

$$Q_x = K_a \left(a_{spike} - \mathrm{sgn}\left[a_{spike} \right] a_{crit} \right) \qquad \text{for } \left| a_{spike} \right| \geq a_{crit} \qquad \textbf{(4a)}$$

$$Q_x = 0 \qquad \text{for } \left| a_{spike} \right| \leq a_{crit} \qquad \textbf{(4b)}$$

where K_a is a constant, sgn[ ] is the sign of the argument and a_{crit} is a threshold that must be exceeded for initiation of transport (cf., Drake and Callantoni, 2001).

Hoefel and Elgar (2003) presented a cross-shore sediment transport model based on Equations (3) and (4) and forced the model with cross-shore velocity data from a large array of current meters deployed across a nearshore bar system. During a 5-day period with approximately 0.75-m high waves and cross-shore mean currents less than 0.3 m s^{-1}, the observed bar migration of about 30 m was predicted accurately using the model (K_a = 1.4 x 10^{-4} m s; a_{crit} = 0.2 m s^{-2}). Application of the energetics-based model (Eq. 1) failed to reproduce the observed onshore movement of the nearshore bar system. Moreover, inclusion of the effects of skewed accelerations in the energetics-based sediment transport model resulted in improved predictive skill during storms, when mean cross-shore currents were strong.

7.7 APPLICATION OF ENERGETICS- AND ACCELERATION-BASED SEDIMENT TRANSPORT MODELS

The amount of sediment transport over a tidal cycle was predicted using both the energetics and acceleration approach. The models were forced using measured hydrodynamic data and sediment transport was calculated over 10-minute intervals. Figure 7.14 shows that the acceleration model always predicted onshore sediment transport, whereas the energetics approach mainly resulted in sediment transport predictions that are directed offshore, particularly under high wave-energy conditions. These trends were omnipresent on any part of the ridge, implying that the models were rather insensitive to changes in the local gradient (Figure 7.14a–c).

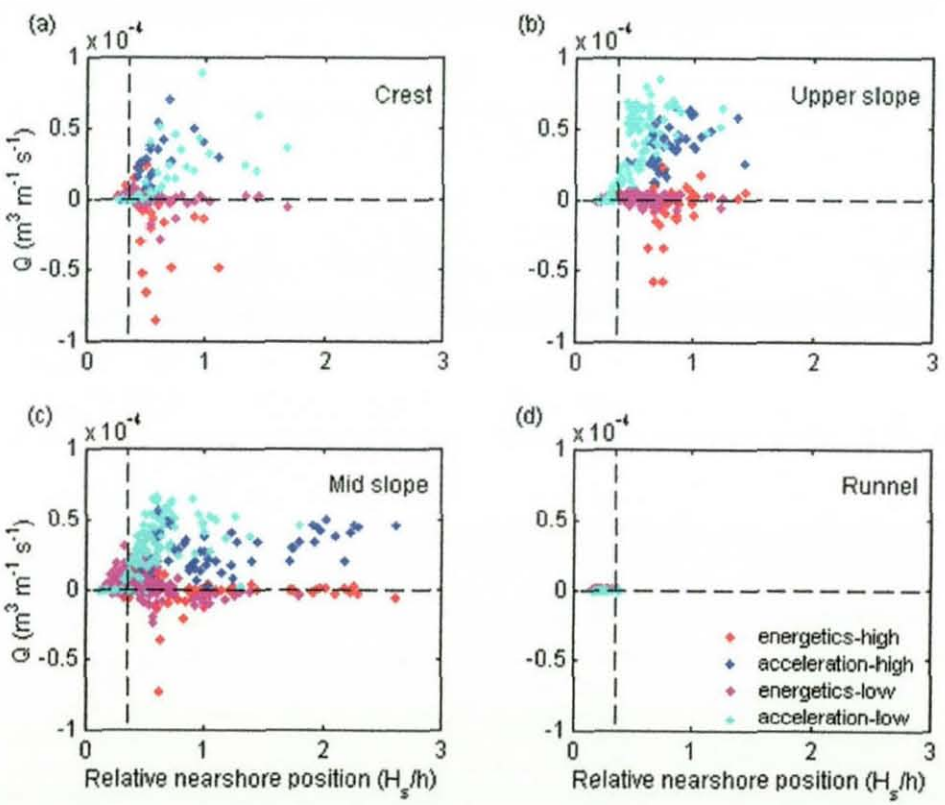

Figure 7.14 – Sediment transport predictions across the nearshore zone according to the energetics and acceleration approach. Data points are further grouped on the basis of location (a–d) and according to wave-energy level (low: $H_0 < 0.8$ m, high: $H_0 > 0.8$ m; Masselink, in press). Vertical dashed lines indicate transition from shoaling zone (left) to surf zone (right) using $H_s/h = 0.35$ as the criterion (Kroon and Masselink, 2002).

The main achievement of the acceleration model is the prediction of onshore sediment transport in the surf zone under low to intermediate wave-energy

conditions. This is a common observation for subtidal bars (e.g., Thornton et al., 1996; Gallagher et al., 1998) and is only estimated correctly by the acceleration approach. Cross-shore sediment transport in the runnels was virtually absent and this was predicted properly by both sediment transport models (Figure 7.14d).

The sediment transport models were further used to compute the net amount of sediment transport over a number of tidal cycles. Due to the collection of hydrodynamic data in bursts, the sediment transport record had gaps and these were filled using linear interpolation. Figure 7.15 shows the results for three tidal cycles characterised by: (1) onshore ridge migration; (2) offshore ridge migration; and (3) insignificant morphological change. Neither of the models was able to predict accurately the amount of sediment transport over a tidal cycle. Onshore ridge migration was most-closely predicted by the acceleration approach (Figure 7.15a), but results were not as promising as for onshore migrating subtidal bars (Hoefel and Elgar, 2003). The model predicted a net sediment transport equal to just half of the observed net sediment transport, and the approach performed yet poorer for the case with offshore ridge migration (Figure 7.15b). Surprisingly, also the energetics approach failed to predict the amount of sediment transport under offshore migrating ridges. Although offshore current velocities reached values up to 0.25 m s^{-1} during the falling tide (Figure 7.15b_5), predicted sediment transport rates according to the energetics model were negligible (Figure 7.15b_3). The observed sediment transport was best-predicted for the third tidal cycle, when morphological change was limited (Figure 7.15c).

7.8 DISCUSSION

The ridges, runnels and drainage channels form three distinct sub-environments of a ridge and runnel beach, each with different hydrodynamic conditions, sediment transport processes and bed morphology. The characteristics of each of these sub-environments are discussed in the following three paragraphs.

Ridges are subjected to the most diverse range of wave processes, often experiencing swash, surf zone bores, breakers and shoaling waves over a single tidal cycle. These wave processes acted on the bed, forming plane bed under swash, and wave ripples

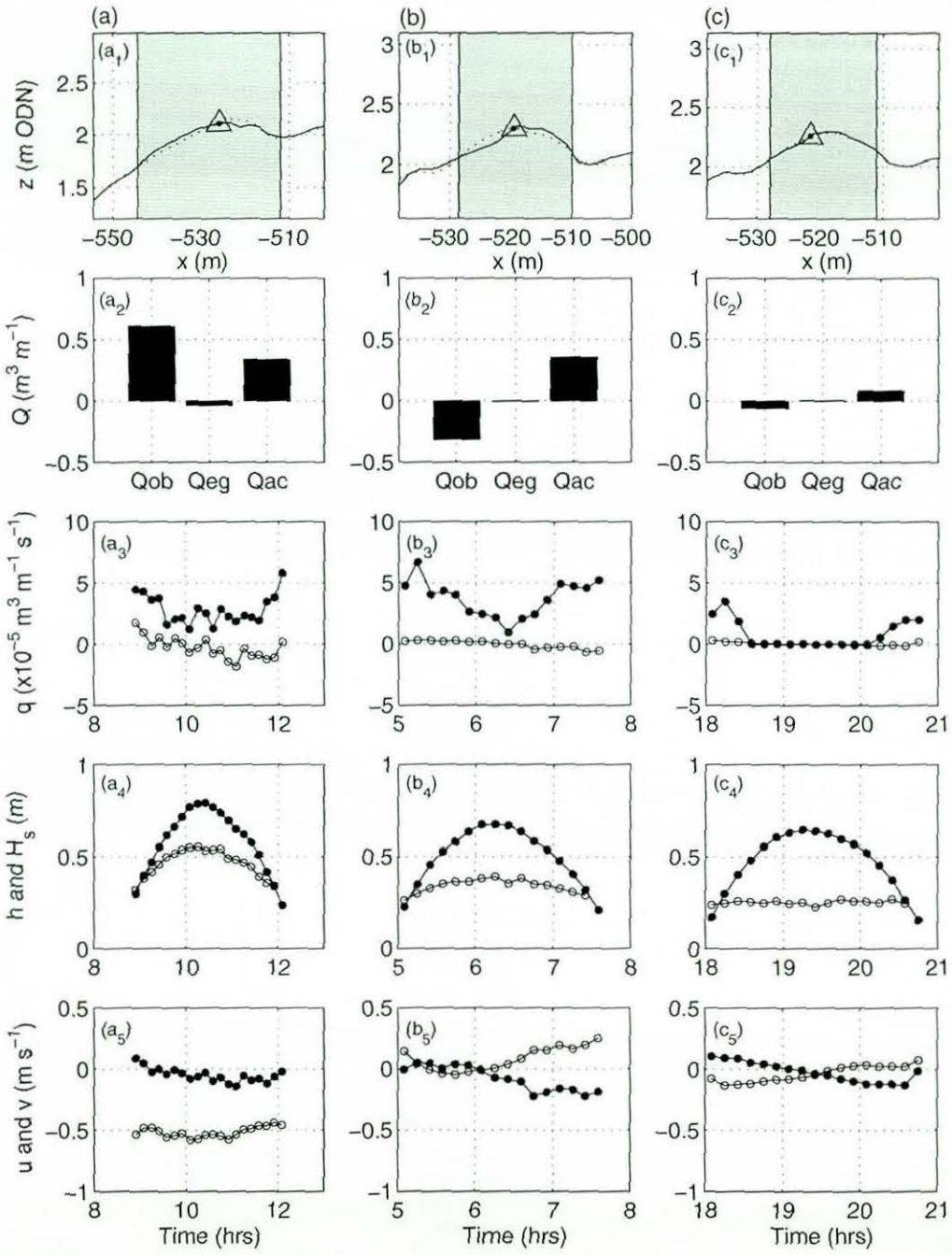

Figure 7.15 – Sediment transport predictions and hydrodynamic conditions over (a) Tide 10 (23/09/'01); (b) Tide 27 (02/10/'01); and (c) Tide 30 (03/10/'01). Panels from top to bottom are: (1) beach profiles before (solid line) and after (dashed line) the tidal cycle (with location of instrument station); (2) observed (Qob) and predicted sediment transport over tidal cycle (Qeg = energetics model, Qac = acceleration model); (3) predicted sediment transport rates (filled marker = acceleration model, open marker = energetics model); (4) water depth (filled marker) and significant wave height (open marker); and (5) mean cross-shore (filled marker) and longshore (open marker) current velocity. The grey boxes in the top panels mark the areas over which the sediment budgets were calculated.

and dunes under surf zone bores. Surf zone bed forms, however, were normally being flattened completely by swash during the falling tide, particularly on parts of the seaward slope with a local gradient > 0.015. This was also observed by Kroon and Masselink (2002), though they suggested a threshold gradient of 0.025. Morphological change was mostly concentrated near the summit of the ridge, often characterised by a distinct onshore or offshore migration of the crest. When a ridge was fully inundated, morphological change on the seaward slope and crest was predominantly induced by surf zone processes (bores and breakers), whereas uni-directional swash pulses played an important role on the landward slope of the ridge. The power of swash was demonstrated by a ridge crest migrating onshore over a distance of 4 m in a couple of hours solely due to the action of swash. An analysis of the rate of morphological change under swash action and surf zone processes suggested that the rate of morphological change is rather independent of the type of wave process, implying that the morphological change induced by a certain process is strongly related to the amount of time that the process operates.

The runnels were characterised by the prevalence of longshore currents. Tidally induced longshore currents were typically 0.4 m s^{-1}, with flow toward the south during flood and toward the north during ebb. Longshore currents in the lower runnels tended to be tide-dominated, but wave-induced longshore currents started to dominate higher up the beach (cf., Parker 1975; Levoy et al., 1998; Sipka and Anthony, 1999; Kroon and Masselink, 2002; Anthony et al., 2004). Sediment in the runnels was predominatly transported alongshore and mainly accomplished by the migration of small-scale bed forms such as current ripples and dunes (cf., Chauhan, 2000). Megaripples form in the runnels under high wave-energy conditions and their migration caused significant local morphological change (cf., Parker, 1975; Anthony et al., 2004).

Drainage channels form the third sub-environment of a ridge and runnel beach and are the sites where runnel flows change direction and drain through the channels into the more seaward-lying runnel. During the falling tide, currents in the channels reached values up to 0.7 m s^{-1} and large amounts of sediment were transported seaward. The formation of extensive deltas where the drainage channels flowed in the seaward-lying runnel indicate the importance of drainage channels in establishing a

three-dimensional flow of water and sediment across a ridge and runnel couplet and this may in turn result in slower ridge migration rates (cf., Antony et al. 2004). Longshore currents regularly caused erosion of the landward ridge slope and the released sediment was rather likely transported to the seaward-lying runnel through the drainage channel.

The hydrodynamic data were further used to investigate variations across the intertidal beach and over a single tidal cycle. A comparison of the local wave height on three consecutive ridges showed a clear attenuation of the wave-energy levels in the landward direction (due to wave breaking) and this indicates that the sheltering effect by the lower ridges was significant. Mean longshore and cross-shore current velocities did not vary across-shore, in contrast to earlier findings demonstrating an onshore decrease in mean longshore velocities under low wave energy conditions (Levoy et al., 1998; Antony et al., 2004).

Local significant wave height and mean current velocities were strongly modulated by the tide. Local wave height was limited in shallow water depths, but attained maximum values at high tide when energy losses across the ridge and runnel profile were least. Similar analyses by Reichmüth (2003) and Anthony et al. (2004) for the northern beaches of France revealed smaller maximum wave heights at a given water depth. Additionally, local wave heights were larger during the rising than falling tides. This was noticed previously by Voulgaris et al. (1996) and they suggested that this was due to the interaction of the waves with the tidally-induced *longshore* currents, whereby opposition of the waves and currents during the rising tide resulted in increased wave height. This seems, however, not the case in this study as waves generally approached from the same direction as the flood current. It is more likely that the tidal modulation of the wave height was attributed to the *cross-shore* component of the tidal current, with onshore flows during the rising tide reinforcing the waves and the effects of offshore tidal flow during ebb resulting in lower wave heights.

Mean cross-shore currents were tide-dominated during low wave-energy conditions and wave-dominated during high wave-energy conditions. Analysis of the mean cross-shore current over a tidal cycle with high wave-energy levels revealed that the

wave-induced undertow velocity was -0.2 m s^{-1} and that the tidal cross-shore component equalled c. $\pm$ 0.1 m s^{-1}. Tidal currents opposed the undertow during the flood, causing the net cross-shore current to tend towards zero, whereas during the ebb both currents acted in the same direction. Voulgaris et al. (1996) found a similar tidal variation under slightly lower wave-energy conditions, with values of 0.05 m s^{-1} for both, the mean wave- and tide-induced current velocity. Kroon and Masselink (2002), however, did not observe a significant tidal variation in the cross-shore current velocity under low wave energy conditions.

Although it seems appropriate not to consider ridges and subtidal bars as distinctly different bar types, some concepts and sediment transport models pertaining to subtidal bar behaviour appeared not applicable to ridge and runnel morphology. For subtidal bars, the energetics expression for sediment transport under combined and steady flows (Bailard, 1981; Bailard and Inman, 1981) works well to predict offshore bar migration under high wave-energy conditions (Thornton et al, 1996; Gallagher et al, 1998), whereas the acceleration-based approach (Hoefel and Elgar, 2003) performs better under low wave-energy conditions when bars move onshore. For ridges and runnels, however, both models are incapable of predicting the morphological change over a tidal cycle. For onshore ridge migration, the acceleration approach approximated the observations best, but largely underestimated the total amount of sediment transport. Predictions were even less accurate for offshore ridge migration, but in that case also the energetics model failed. This suggests that the currently-available sediment transport models need further adjustment to enhance the capacity to predict morphological change on intertidal bars.

7.9 CONCLUSIONS

- Hydrodynamic characterisation of ridges, runnels and drainage channels show that these form three distinctly different sub-environments on a ridge and runnel beach. Mean currents are predominantly cross-shore on the ridges, longshore in the runnels and seaward in drainage channels, establishing complex three-dimensional sediment transport patterns across the ridge and runnel morphology.

- Mean current velocity and direction are the result of a subtle balance between tide- and wave-induced currents, with wave-dominance increasing onshore and with higher wave-energy levels.
- A clear attenuation of wave-energy level in the landward direction is present during all stages of a tidal cycle, indicating the importance of wave-sheltering by the lower ridges. Local significant wave height is further strongly modulated by the tide.
- The rate of morphological change is similar under swash and surf zone processes, and the morphological change due to the individual processes is therefore strongly related to the amount of time that the process operates.
- Energetics- and acceleration-based sediment transport models, that were developed to predict morphological changes on subtidal bars, do not perform well for ridge and runnel morphology and need further adjustment to enhance the capacity to predict morphological change at intertidal bars.

Chapter eight

Synthesis and General Conclusion

8.1 INTRODUCTION

In Section 1.2, the idea was discussed that insight into coastal behaviour can be gained by considering the coast as a geomorphic system (Kroon, 1994). Within such systems, a multitude of processes, operating at a range of temporal and spatial scales, has to be considered to understand morphological behaviour. At the smallest temporal scale, turbulent fluctuations of about 1 second are important, but at the other extreme, processes with typical durations of several decades (10^{10} s) are essential to investigate large-scale coastal behaviour (LSCB; Terwindt and Battjes, 1990). Similarly, spatial scales range in the order of 10^9, from the length scale of a sand grain (10^{-4} m) to that of a coastal stretch (10^5 m). The form and functioning of a coastal geomorphic system is the end product of the interaction of processes at all scale levels and is therefore the result of sediment transport due to all waves and currents that impacted the coast over the considered time span (e.g., De Boer, 1992; Wijnberg, 2002).

It is common in coastal research to investigate problems using a reductionist approach, i.e., considering the geomorphic systems as a hierarchy of nested compartments, each with its own temporal and spatial scale according to the primary scale relationship (refer to Figure 1.4; e.g., De Vriend, 1992; Cowell and Thom, 1994; Kroon, 1994). Hydrodynamic processes, sediment transport and morphology at corresponding scales interact mutually and morphodynamic systems can be identified within each compartment (Figure 1.5). Using scale as a framework for analysis is thought to facilitate the investigation of coastal geomorphic systems, because by focussing on morphodynamic systems at a particular compartment, one can consider smaller-scale processes as noise and larger-scale processes as boundary conditions (Terwindt and Wijnberg, 1991).

The next step to enhancing insight into geomorphic systems is to develop an understanding of the rules linking process and form at the different temporal and spatial scales. This has been one of the major challenges in geomorphological research over the last decades (e.g., Bauer et al., 1999a, b; Rhoads, 1999; Terwindt and Wijnberg, 1991) and still forms the principal limitation of the reductionist approach, because to understand the geomorphic system as a whole often requires a larger understanding than just the sum of its components (De Boer, 1992). A key question in this respect is

whether larger scale coastal behaviour is 'just' the net result of smaller-scale processes, or whether autonomous larger scale processes are also at work (Terwindt and Battjes, 1990). To upscale the morphodynamic behaviour of a smaller compartment to a larger compartment, Kroon (1994) suggests defining a new coastal parameter at each successive compartment that schematises all the process variables and explains the morphological behaviour at that level. Another approach may be the upscaling to larger-scale processes by filtering the processes at smaller scales (Wijnberg, 1995).

8.2 APPLICATION OF THEORETICAL CONCEPTS TO RIDGE AND RUNNEL MORPHOLOGY – METHODOLOGY

In the present study, ridge and runnel morphology was investigated according to the reductionist approach, i.e., considering the ridge and runnel morphology as a geomorphic system that comprises a hierarchy of ever smaller, lower-level morphodynamic systems, but that is at the same time part of a hierarchy of ever larger, higher-level morphodynamic systems. Ridge and runnel morphology was investigated over temporal scales ranging from a single tidal cycle (10^3 s) to a decade (10^9 s) and corresponding spatial scales covered a single ridge and runnel couplet (10^1 m) to the ridge and runnel morphology along the entire north Lincolnshire coast (10^4 m). Within this temporal and spatial scale range, five compartments were identified (Figure 1.6 and Table 8.1) and although boundaries between temporal scales are straightforward, the spatial boundaries are more arbitrary.

Table 8.1 – Temporal and spatial scales of identified compartments.

	Time-scale	Spatial scale
1	Inter-annual	Ridge and runnel morphology along entire north Lincolnshire coast
2	Summer versus winter	Ridge and runnel morphology along entire north Lincolnshire coast
3	Monthly	Multiple ridges and runnels
4	Lunar tidal cycle	Multiple ridges and runnels
5	Single tidal cycle	One ridge and runnel couplet

Chapters 3–7 presented results of the analysis of ridge and runnel behaviour, focussing on one compartment per chapter. The results of these previous chapters will now be compiled and the dominant processes and morphological changes at each scale level will be identified (Section 8.3). These results will then be interpreted in the light of

compartment integration, addressing the filter approach as suggested by Wijnberg, 1995, as well as the parameterisation method used by Kroon (1994). Regarding the size of the integration problem in geomorphology (e.g., De Boer, 1992; Bauer et al., 1999a, b; Rhoads, 1999; Terwindt and Wijnberg, 1991), a complete integration of temporal and spatial scales and a total understanding of ridge and runnel morphology as a geomorphic system is beyond the scope of this thesis.

Applying the reductionist approach as a basis for the investigation of ridges and runnels, it is thought that the first step is to identify the dominant processes and morphological changes at each scale level, i.e., labelling the components of the morphodynamic system that can be recognised within each compartment (Figure 8.1).

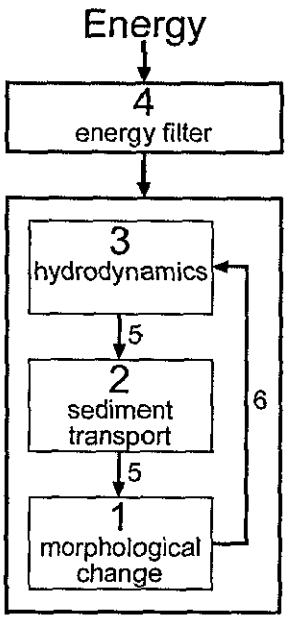

Figure 8.1 – Schematic representation of a morphodynamic system (numbers are explained in the text).

The strategy to do this was to first identify the dominant morphologic development at each compartment level (No. 1 in Figure 8.1). This was then followed by a consideration of local sediment budgets, bed morphology and field observations to determine the sediment transport patterns that induced the morphological change (No. 2 in Figure 8.1). These observed morphological and sediment transport patterns were subsequently compared to the temporal change in forcing conditions and a hypothesis was formed about the relevant forcing process (No. 3 in Figure 8.1). In this last step, the

most important component of the total energy input (sea level, offshore waves, tides, currents and wind) at each scale level was determined and this component was then used as the energy filter at that scale level (No. 4 in Figure 8.1).

After the analysis of forcing-driven morphological responses, the analysis further involves the identification of relaxation time- and feedback-dominated responses (respectively, No. 5 and 6 in Figure 8.1). Wijnberg and Kroon (2002) indicated the importance of relaxation time and feedback in nearshore bar dynamics and characterised the responses in terms of the degree of correlation between morphological change and external forcing conditions. Relaxation time-responses are characterised by a lagged and filtered correlation between the morphology and the forcing signal, and are expected on the basis of rapid tidal migration rates and the limited tidal residence times of the different hydrodynamic processes (Masselink et al., submitted). Feedback-dominated responses are indicated by the weak correlation between the external forcing signal and the morphological response and are difficult to convincingly demonstrate, as a lack of correlation between forcing and morphological response may be because the link between forcing and response is complex and not all processes are accounted for.

8.3 CHARACTERISATION OF RIDGE AND RUNNEL DYNAMICS OVER A RANGE OF SPATIAL AND TEMPORAL SCALES

Figure 8.2 summarises the morphodynamic analysis for each ridge and runnel compartment and the following paragraphs discuss the results for each compartment, commencing at the smallest scale.

Ridge and runnel characterisation at the single-tidal-cycle timescale (Figure 8.3): Hydrodynamic measurements and high-resolution (spatial and temporal) morphological monitoring over numerous single tidal cycles showed that morphological change over a tidal cycle was very local (cf., Levoy et al., 1998) and mainly induced by swash and surfzone processes (cf., Kroon and Masselink, 2002). The presence of the ridges and runnels as undulating beach morphology was important in controlling the hydrodynamic processes across the intertidal zone. Hydrodynamic measurements showed that ridges, runnels and drainage channels form three sub-environments of a ridge and runnel beach,

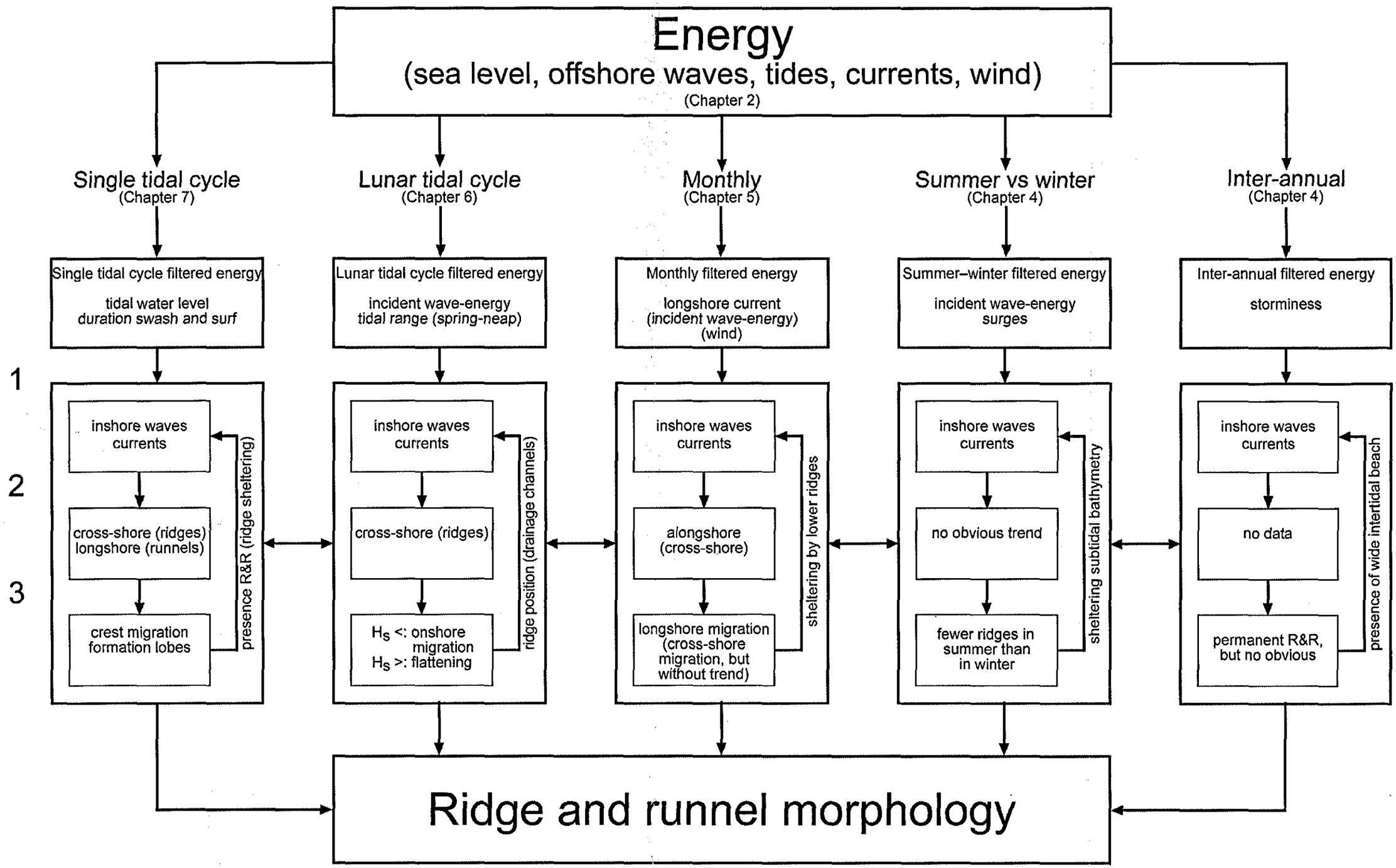

Figure 8.2 – Primary components of ridge and runnel morphology as a geomorphic system. Small boxes within the morphodynamic system box refer to: (1) hydrodynamic processes; (2) sediment transport; and (3) morphological change. R&R and H_s stand for 'ridges and runnels' and 'significant wave height', respectively.

each characterised by distinctly different hydrodynamic processes, sediment transport processes and bed morphology. This has been mentioned in numerous previous studies (e.g., Parker, 1975; Voulgaris et al., 1996, 1998), but not argued on the basis of in-situ hydrodynamic measurements, because instrument stations are usually placed solely on the ridges. Mean currents were predominantly cross-shore on the ridges, longshore in the runnels and seaward in drainage channels, establishing complex three-dimensional sediment transport patterns across the ridge and runnel morphology (Figure 8.3). The mean current velocity and direction were the result of a subtle balance between tide- and wave-induced currents (cf., Wright, 1976; Sipka and Anthony, 1999) and wave-dominance generally increased onshore, and with higher wave-energy levels (cf., Parker, 1975; Levoy et al., 1998).

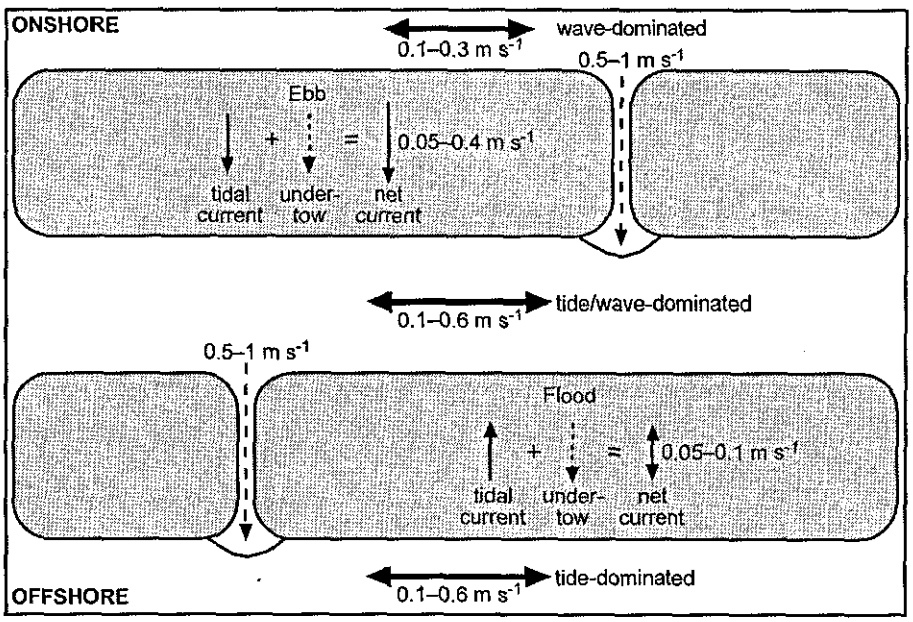

Figure 8.3 – Schematic characterisation of ridge and runnel dynamics at a single tidal cycle time-scale. Dashed arrows mean that the current is not always present: undertow is only present under moderate to high wave energy conditions an drainage channel flow predominates during the falling tide

Like in the studies of Reichmüth (2003) and Anthony et al. (2004), a clear attenuation of the wave height in the landward direction was observed during all stages of a tidal cycle and this indicates the importance of wave-sheltering by the lower ridges (i.e., morphodynamic feedback). Local significant wave height was further strongly modulated by the tide, with higher wave heights occurring during the rising stage, when waves were reinforced by the onshore-directed component of the tidal current. This was

also observed by Voulgaris et al. (1996), but they attributed this to the interaction of waves with the longshore component of the tidal current.

After tidal inundation, the runnels were characterised by a mixture of wave- and current ripples, whereas the surface of the ridges had been reworked to plane bed, demonstrating the power of the swash during the last stages of submergence. Bed morphology observations by Chauhan (2000) and Kroon and Masselink (2002) showed very similar bed form patterns. The drainage channels were characterised by current ripples and small deltas formed where they drained into the seaward-lying runnel.

Morphological change over a tidal cycle was limited to cross-shore sediment redistribution over short sections of the beach profile and was mostly concentrated near the summit of the ridge, (cf., Reichmüth, 2003), either resulting in onshore or offshore migration of the crest. In addition, smaller lobes commonly developed on the seaward slopes of the ridges. The lobes on the upper ridges were mostly formed by swash, whereas the formation of the lobes on the middle ridge was attributed to surf zone processes. Formation of such lobes has been mentioned previously (e.g., Kroon and Masselink, 2002; Anthony et al., 2004), but their significance has not been fully acknowledged. These lobes regularly survived tidal submergence over successive tidal cycles and migrated onshore to join the crest (e.g., Greenwood et al., 2004), thereby forming an important mechanism for vertical growth of the ridge crest. The present study confirmed the findings of Kroon and Masselink (2002) that swash and surf zone processes play significant morphodynamic roles, but further showed that the rate of morphological change is similar for both these processes. There is, however, more scope for surf zone processes to act, because the surf zone is much wider than the swash zone, and therefore surf zone processes are more prevalent. Aeolian events were also found to occasionally cause local morphological change over a single tidal cycle.

Energetics- and acceleration-based sediment transport models, originally applied to simulate the development of subtidal bars (Thornton et al., 1996; Gallagher et al., 1998; Hoefel and Elgar, 2003), were applied using measured hydrodynamic data, but failed to predict the changes in the ridge and runnel morphology. The energetics approach was applied to ridges and runnels previously by Voulgaris et al. (1996, 1998), but with limited success due to the lack of hydrodynamic measurements near the bed.

Hydrodynamic equipment has improved, however, over the last years and it would be very useful to re-focus on the small-scale hydrodynamic and sediment transport processes to provide more comprehensive input data. The application of the acceleration approach in this study was innovative and resulted in better predictions than for the energetics approach, particularly when onshore sediment transport prevailed.

Although it seems inappropriate to consider intertidal and subtidal bars as distinctly different bar types (Masselink et al., submitted), it is clear that sediment transport models pertaining to subtidal bar morphology need further adjustment to enhance the capacity to predict morphological change on ridge and runnel beaches. On the short-term time scale, subtidal bars respond relatively rapidly to changing wave conditions (Sallenger et al., 1985; Plant et al., 1999), but ridges and runnels are much less responsive and the large relaxation time is due to a combination of factors, including the relative stability of low-gradient, dissipative beaches (Wright and Short, 1984; Wright et al., 1982a, b), tidal residence times (Davis et al., 1972; van den Berg, 1977; Masselink, 1993) and morphodynamic feedback due to bar sheltering (Tucker et al., 1983; Ruessink and Kroon, 1994; Anthony et al., 2004; Masselink, in press).

Ridge and runnel characterisation at the lunar-tidal-cycle time scale (Figure 8.4):
Two three-week field campaigns were conducted at Theddlethorpe to collect wave- and current data and to monitor the evolution of ridge and runnel morphology over a lunar tidal cycle. Beach profiles were measured twice-daily (i.e., at each low tide) and this resulted in the most comprehensive data set that currently exists at the scale of lunar tidal cycles, as morphological surveying in previous studies was limited to once a day (i.e., over two tidal cycles). This enabled more accurate linking between observed morphological change and tidal water levels and wave-energy conditions.

Morphological changes over a lunar tidal cycle mostly involved onshore migration of the ridges, like in the study by Kroon and Masselink (2002), and formation and development of smaller-scale depositional lobes. Migration rates were similar to those observed in previous investigations (e.g., van den Berg, 1977; Voulgaris et al., 1998) and ranged from insignificant to 1.6 m per tidal cycle, dependent on the cross-shore position of the ridge (cf., Reichmüth, 2003). The lowest ridge was relatively immobile because of relaxation time effects on the lower beach due to the limited availability of

swash and surf zone processes. The middle ridge migrated at a constant rate of 0.3 m per tidal cycle, whereas the upper ridges were even more dynamic, but their migration rate also depended on wave-conditions and the stage of the lunar tidal cycle (they were emerged at neap tide).

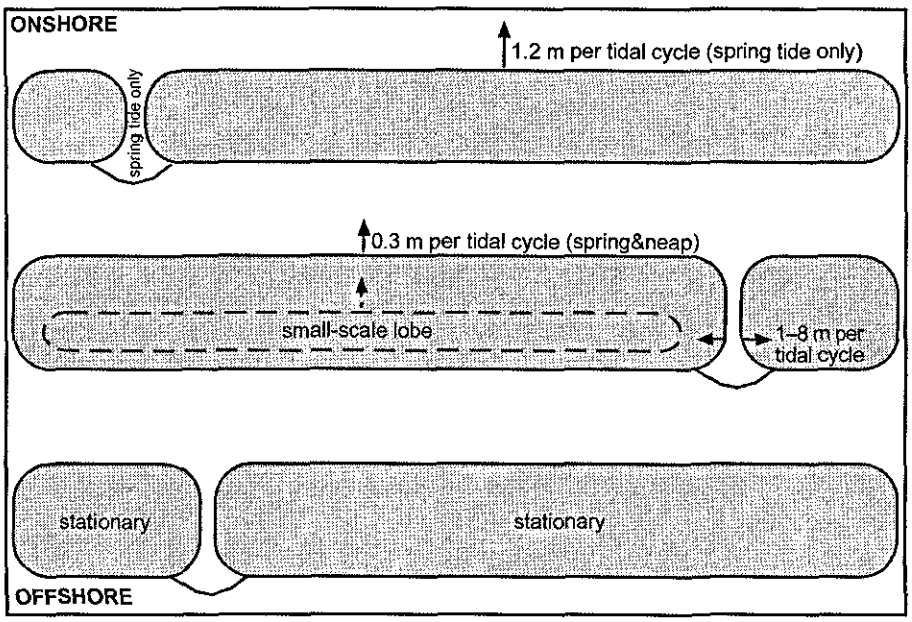

Figure 8.4 – Schematic characterisation of ridge and runnel dynamics at a lunar tidal cycle time-scale. Dashed borders indicate a temporary lobe.

Morphological changes during storm events were much larger than during low wave-energy conditions and it was found that storm impact was destructive on the lower beach, but constructive on the upper beach (onshore migration). In previous studies, the destructive effect of storms has been observed (King and Williams, 1949; King, 1972a), but morphological changes taking place under high wave-energy conditions have only recently been quantified for the first time. For example, data presented by Anthony et al. (2004) suggest that morphological change can be as important during low wave-energy conditions as during storm events. This contradicts the findings in this study, although some differences may be accounted for by the use of different data analysis techniques. It would therefore be useful to investigate the effect of high wave-energy conditions in more detail, analysing both data sets identically. The storm impact analysis presented in this study showed furthermore that the cross-shore variability in storm impact is significant.

Simulations of the occurrence of swash, surf and shoaling wave processes, applying a numerical model as developed by Kroon and Masselink (2002), suggested that the response of ridges and runnels on this time-scale was mainly induced by surf zone processes. The amount of morphological change was strongly related to the duration of surf zone processes, hence such response is considered mainly forcing-dominated. The position of the ridge in relation to tidal levels was, however, important in controlling relaxation-time effects and feedback processes (mainly ridge sheltering). A further element of feedback was brought into the system by the presence of drainage channels, particularly on the upper beach. It was found that the cycles of inactivation and reactivation of the upper drainage channels played a significant role in the frequency and degree of flooding of the upper intertidal sand flat. The role of drainage channels has been largely neglected in previous ridge and runnel studies. In future studies, sediment transport measurements in drainage channels will be essential to determine their importance as sediment transfer paths for offshore sediment transport and the degree to which this decelerates onshore ridge migration.

Ridge and runnel characterisation at the monthly time scale (Figure 8.5):

Monthly three-dimensional survey data for Donna Nook, Theddlethorpe and Mablethorpe revealed that ridge and runnel morphology was very dynamic on this time-scale, as illustrated as well by Mulrennan (1992) and Reichmüth (2003). Morphological changes were accomplished by ridge migration, build-up, flattening, appearance and disappearance. The dominant morphologic behaviour was the longshore migration of ridges and this response is considered to be forced by the littoral drift induced by the prevailing northeasterly waves. The movement of the ridges was toward the south and at rates estimated at 30 m per month. The importance of longshore migration has so far only been mentioned by King and Williams (1949) for the ridges and runnels near Gibraltar Point, south Lincolnshire, but the rate of movement was never quantified. Longshore ridge migration on other beaches is either absent, as at Blackpool beach where the net littoral drift is insignificant (BBC, 2000), or has never been documented due to the lack of regular three-dimensional surveys over periods more than six months.

At the monthly time scale, cross-shore ridge migration was of secondary importance and systematic trends were not apparent. Ridge migration rates and directions varied greatly depending on the location of the ridge in the cross-shore and also between the

different beaches. Despite a similar external forcing (waves, tides and wind), some ridges migrated onshore, whilst others remained stationary or even migrated in the offshore direction and this disparate behaviour of the different ridges may be attributed to feedback effects. Cross-shore migration probably varied across-shore due to wave-sheltering by the lower bar, and between the sites because the degree of this sheltering varied with the size and exact location of the lower bar. The prominence of the ridge and runnel morphology, however, reflected seasonally-driven changes in the wind-, wave- and surge conditions and this is clearly a forcing-dominated response. A distinct correlation between external forcing conditions and ridge and runnel prominence was also observed by Mulrennan (1992) and Reichmüth, 2003.

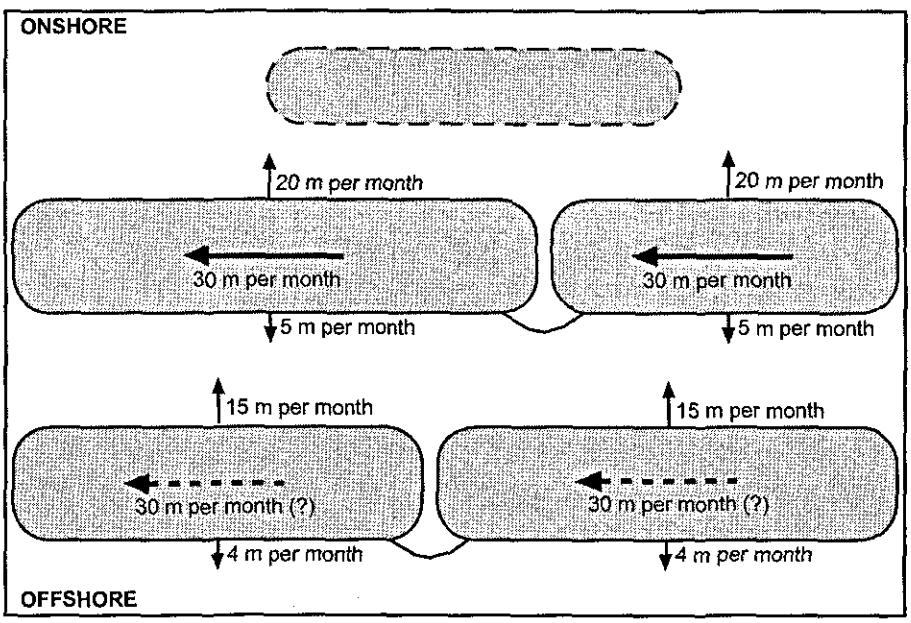

Figure 8.5 – Schematic characterisation of ridge and runnel dynamics at a monthly time-scale. Dashed ridge borders indicate that the ridge is temporary. Dashed arrows indicate that the process was difficult to determine due to lack of data for the lowest ridge.

Ridge and runnel characterisation at summer-versus-winter and inter-annual time scales (Figure 8.6):

Aerial photographs collected in 1977, 1983 and from 1991 to 2003, in combination with profile data dating back to 1953 (King 1972a), suggested that ridge and runnel morphology has characterised the north Lincolnshire coast for at least the last 50 years and ridges and runnels also seemed permanent features on numerous other beaches in the United Kingdom, for example, at Formby Point, Blackpool and Gibraltar Point (King and Williams, 1949; Wright, 1976; Masselink and Anthony, 2001; Burgess et al.,

2002). Individual ridge and runnel couplets, however, are not permanent and form, evolve and disappear within a year. The life span of an individual ridge and runnel couplet is related to the occurrence and frequency of storms, although the wide intertidal zone, in combination with short tidal residence times (Masselink, 1993) strongly filters storm impact (i.e., respectively feedback- and relaxation time effects).

An analysis of twice-yearly profile data covering the last 13 years revealed that more ridges were generally present in summer than in winter, confirming observations by Masselink and Anthony (2001). The seasonality in the morphological development indicates that ridges and runnels can be considered forcing-responsive on this time-scale. Particularly variation in wave energy level and the frequency of surges is thought to be important. One factor believed to contribute to the spatial variation along the coast is the different degree of beach sheltering due to the subtidal bathymetry (i.e., feedback effects). A subtidal bank is present in the southern part of the study area, whereas a low gradient shelf fronts the intertidal zone in the northern part of the study area.

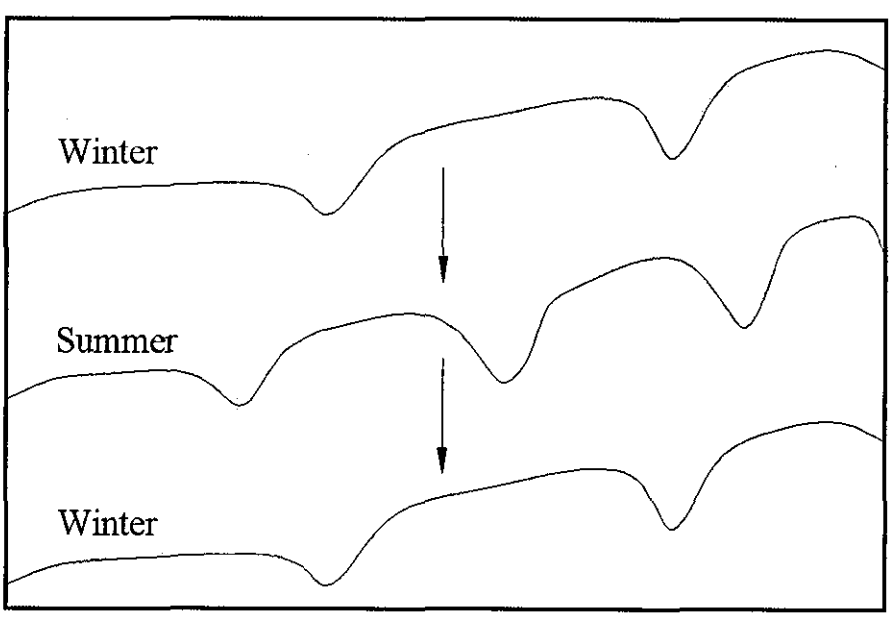

Figure 8.6 – Schematic characterisation of ridge and runnel profiles to illustrate ridge and runnel dynamics at a summer versus winter time-scale.

The profiles further demonstrated that ridge and runnel configuration changed to such an extent that individual ridges could generally not be tracked from year to year and distinct inter-annual trends in the morphological expression of the ridges and runnels

were not obvious (not least because they may be masked by the strong intra-annual variability).

This is one of the few studies to have quantified morphological changes using long-term profile data and to have demonstrated the permanency of ridge and runnel morphology. Investigation of ridge and runnel dynamics at this time-scale is scarce, mainly due to the lack of profile data covering periods longer than 5 years. Long-term profile data for subtidal bar morphology, however, is much more extensive and numerous studies have examined the long-term behaviour of these bars, for example along the Dutch coast (Ruessink and Kroon, 1994; Wijnberg and Terwindt, 1995), in New Zealand (Shand et al., 1999) and at Duck, USA (Lippmann et al., 1993; Plant et al., 1999). These coasts are characterised by double or multiple subtidal bar systems and show long-term cyclic behaviour with bars passing through three stages during their existence: generation close to the shoreline, net seaward migration through the surf zone, and decay at the outer margin of the nearshore zone. Such cyclic behaviour was not observed at the Lincolnshire coast possibly because it is not present, or because the intra-annual variability is too strong and masks long-term variation.

Investigation of the initial formation of ridge and runnel morphology is beyond the scope of this thesis, but has formed a major point of debate in recent studies on ridges and runnels (Mulrennan, 1992; Masselink and Anthony, 2001; Kroon and Masselink, 2002; Reichmuth, 2003; Anthony et al. 2004; Masselink, in press). The mechanism involved in the formation of ridge and runnel morphology remains elusive and the permanency of the morphology is the major obstacle for progress. Future work can, however, focus on the construction of individual ridge and runnel couplets. This occurs regularly within a year, as more ridges were present in summer than in winter. To capture the appearance (and disappearance) of individual ridges and runnels, the conduction of weekly (or at least twice-monthly) beach surveys is essential, concurrent with continuous inshore wave and water level measurements. Complementary data from an ARGUS station (i.e., a camera monitoring the beach several times per day or per hour; e.g., Lippmann and Holman, 1989, 1990) would be helpful to determine the occurrence of swash, surf and shoaling wave processes across the profile.

Spatial variability in ridge and runnel morphology along the north Lincolnshire coast (Figure 8.7):

A detailed DEM of the intertidal zone derived from LIDAR was used to examine the spatial variability of the ridges and runnels along the north Lincolnshire coast. The application of LIDAR for ridge and runnel morphology was innovative and enabled the investigation of the spatial (alongshore and cross-shore) variability in much greater detail than documented previously.

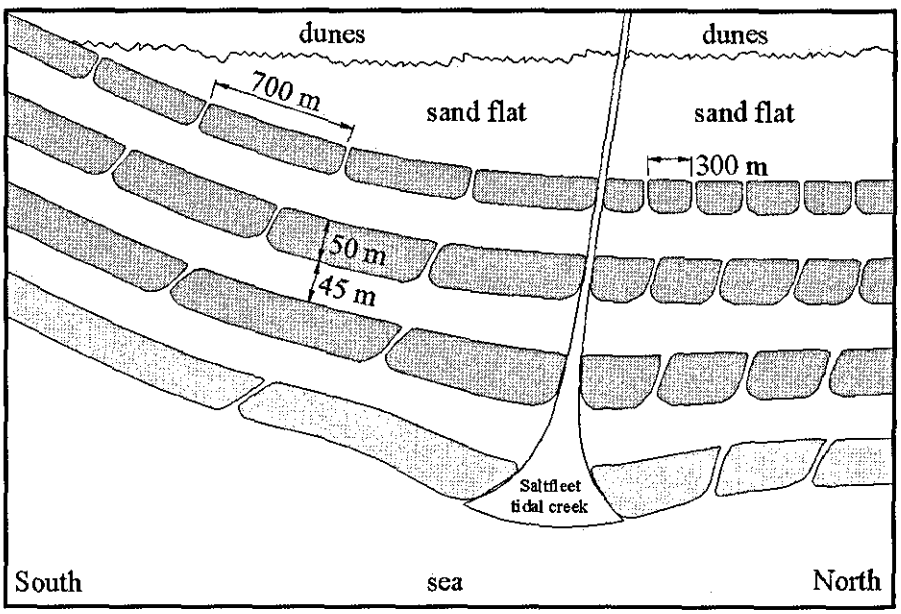

Figure 8.7 – Schematic characterisation of the spatial variability in ridge and runnel morphology along the north Lincolnshire coast. Ridges are represented in grey, whereby darker shading indicates higher ridges.

Three to five ridges and runnels were present along the north Lincolnshire coast, and this is generally more than on other ridge and runnel beaches (e.g., King, 1972a; Mulrennan, 1992; Chauhan, 2000; Anthony et al., 2004). The ridges and runnels were distributed fairly evenly across the intertidal profile, as illustrated before by Masselink and Anthony (2001), but investigation of the cross-shore variation in the dimensions of the ridges clearly demonstrated that the largest ridges (in volume) occurred around MSL (cf., Kroon and Masselink, 2002; Reichmüth, 2003), whereas the smallest ridges were found in the lower intertidal zone. The height of the upper ridges was similar to those found around MSL, but they were considerably narrower.

Inspection of the longshore variation in ridge and runnel morphology suggested that the spacing of the drainage channels that dissect the ridges is related to the amount of water

that needs to be drained during the falling tide. A wide upper intertidal flat and salt marsh region is present along most of the study area and the ridges are frequently dissected by drainage channels. The morphology is distinctly three-dimensional as a result. In the southern part of the study area, where the sand flat tapers out and the ridges and runnels are ultimately backed by dunes, the drainage channels are less numerous and the morphology is more two-dimensional. Although the spatial variation in drainage channel density is rather site-specific, it is thought that the relation between the density of drainage channels and the amount of water that needs to be drained from the upper beach may be general.

Geographic distribution of ridge and runnel morphology

A video of the whole coastline of England and Wales (taken as part of DEFRA's Futurecoast project; Burgess et al., 2002), complemented by aerial photographs and field visits, was used to identify all sites in England and Wales with ridge and runnel morphology. Multiple intertidal bars are common along the predominantly macrotidal coastline of England and Wales, but as suggested by King and Williams (1949) and King (1972), they tend to be restricted to fetch-limited settings with low gradient nearshore profiles. The most extensive ridge and runnel beaches are found in association with estuaries (cf., Parker, 1975; Wright, 1976; Mulrennan, 1992; Levoy et al., 1998; Chauhan, 2000; Masselink and Anthony, 2002) and this is attributed to the low nearshore gradient characteristic of such coasts, perhaps compounded by an abundance of sandy sediments.

How exactly the nearshore gradient controls the occurrence of multiple intertidal bars is not known. Previous investigations into the characteristics of multiple subtidal bar morphology have demonstrated a strong negative correlation between the number of bars and the nearshore gradient (Davidson-Arnott, 1988; Short and Aagaard, 1993). Clearly, a gentle intertidal gradient can accommodate more bars than a steep gradient due to the increased width of the intertidal zone, but this does not explain why the occurrence of multiple intertidal bar morphology is limited to very flat beaches. Along the north Lincolnshire coast, a critical intertidal gradient of around 0.015 appears to exist beyond which multiple intertidal bars do not develop. Perhaps fortuitously, Davidson-Arnott (1988) and Short and Aagaard (1993) established that the maximum nearshore gradient for beaches with more than three subtidal bars was similar, namely

0.012 and 0.015, respectively. Ridge occurrence is also controlled by forcing conditions and, for example, the rather limited number of ridges (2–3) on the 'megatidal' (mean spring tide range > 8 m) Merlimont beach, northern France, has been attributed to relatively energetic wave conditions at this location (Anthony et al., 2004). Clearly, to explain the occurrence of ridge and runnel morphology, more work is required.

8.4 UPSCALING BETWEEN SCALE LEVELS

The previous section provided a detailed description of the morphodynamic systems that can be identified within each scale level, i.e., compartment. The following step is to describe how one compartment links to the next. This is not a straight forward process and involves the consideration of many aspects. As mentioned above, there are two common approaches to link the morphodynamic behaviour between compartments: (1) upscaling to larger-scale processes by filtering the processes at smaller scales (Wijnberg, 1995); and (2) definition of a new coastal parameter at each successive compartment that schematises all the process variables (Kroon, 1994).

The upscaling approach by filtering the processes at smaller scales involves the averaging over time and space of hydrodynamic and sediment transport processes from one scale level to the next. One disadvantage of this approach is that it only considers the processes that are important on the smallest-scale. This implies that the approach should not be applied for geomorphic systems that are also characterised by processes that dominate on larger scale levels only. Ridge and runnel morphology seems such a system. For example, individual waves were important over a single tidal cycle, but larger-scale morphological behaviour of ridges and runnels was better explained by the occurrence of wave-induced longshore currents and variations in the incident wave-energy level. As wave-induced longshore currents were relatively insignificant at smaller time-scales, they would have been neglected using the filtering approach and most likely the long-shore migration of the ridges at a monthly time-scale would be incorrectly related to other hydrodynamic processes.

In a similar way, morphological responses that are dominant at smaller scales do not necessarily correspond to large-scale coastal behaviour. In Chapter 5 it was shown that morphological change over a lunar tidal cycle was mainly accomplished by cross-shore

migration of the ridges. The net result over longer periods is, however, insignificant due to the bi-directionality of the change. Longshore ridge migration on the other hand, is irrelevant at smaller time scales, but as this process is highly unidirectional, this adds up to be the dominant behaviour at the monthly time-scale.

De Boer (1992), in a review on hierarchies and 'spatial scale transference' indicated furthermore that differences between the characteristics of input and output of a geomorphic system increase with spatial scale. This not only means that the energy input by waves and currents has to 'travel' longer and over larger distances to be expressed in large-scale morphological change, but also that the scope for internal forcing processes increases and hence filters out the forcing-dominated responses. This effect is not accounted for in the filtering approach and hence it is increasingly difficult to apply this upscaling technique at larger compartment levels. De Boer (1992) further states that low-magnitude, high-frequency processes can be studied at a relatively small scale, though that high-magnitude, low-frequency processes should be studied at a relatively large-scale. This is an important concept because it implies that short-term processes such as storm events influence the morphology at much larger spatial scales then according to the primary scale relationship. This imbalance between spatial and temporal scales complicates the morphodynamic behaviour of ridges and runnels and is difficult to incorporate in upscaling.

The other approach to scale up is to define a new coastal parameter at each compartment that correlates the dominant hydrodynamic processes to the net morphological responses (Terwindt and Battjes, 1990; Kroon, 1994). When this approach is applied to ridges and runnels, it appears that to some degree, the observed morphological changes can be explained by rather simple parameters (Figure 8.8).

(1) At the smallest scale level, it was observed that local morphological change over a single tidal cycle was mainly induced by surf zone processes (Chapter 7). The total morphological change during inundation was found to be strongly related to the amount of time that surf zone processes operate (t_{surf}). The morphological response may further depend on the exact location within the surf zone, parameterised as H_s/h, because sediment transport rates are likely to be less in the outer surf zone ($0.35 < H_s/h < 0.5$), than in the inner surf zone ($H_s/h > 0.5$).

(2) Over a lunar tidal cycle, morphological changes were manifest over the entire cross-shore profile and the rate and character of the changes were dependent on the tidal range and the wave-energy level. Masselink (1993) introduced the relative tide range *RTR*, which is the ratio of the tide range to the wave height, and this seems an appropriate parameterisation at this scale level. Kroon and Masselink (2002) suggested that significant morphological changes to ridge and runnel morphology require wave/tide conditions characterised by $RTR < 30$. The amount of morphological change increases with decreasing *RTR* values and in the present study, morphological change particularly took place when *RTR* values were below 10.

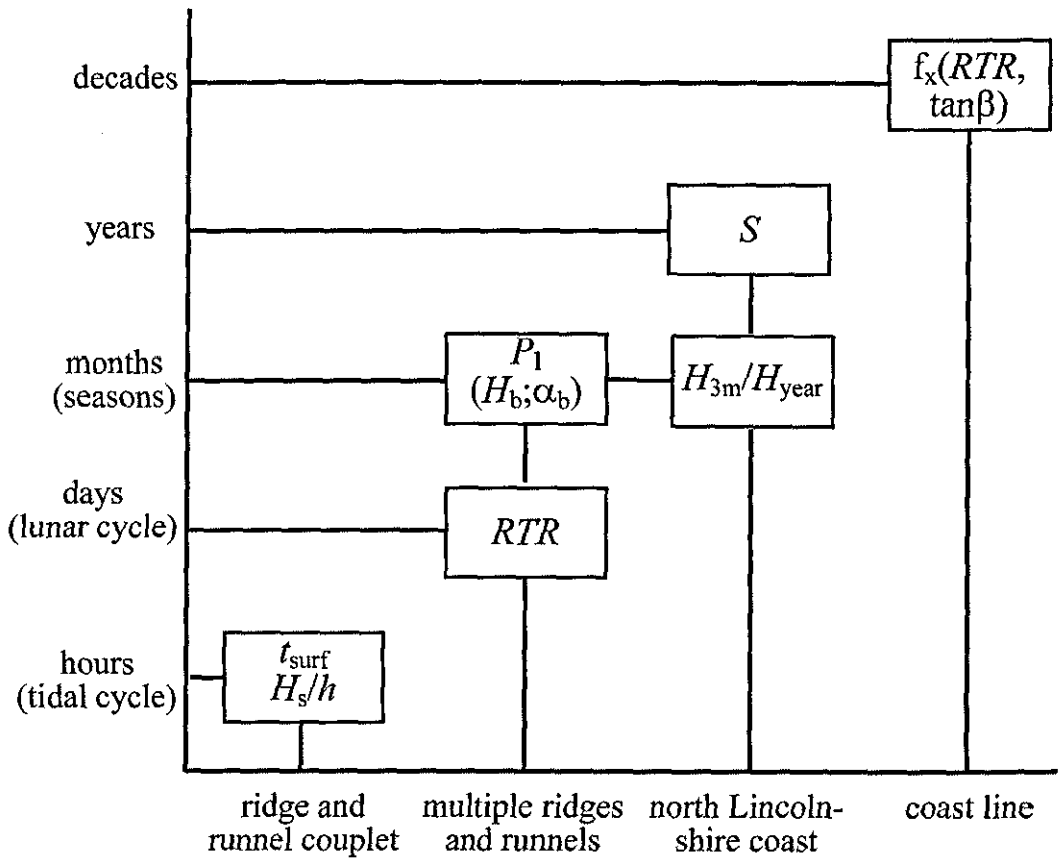

Figure 8.8 – Scale diagram including suggested parameterisations to explain morphological behaviour at each scale level.

(3) On a monthly time-scale, the morphological changes were highly three-dimensional and particularly the longshore migration of the ridges was significant. The migration was forced by the southward littoral drift and hence is controlled by the

long-shore component of the wave energy flux P_l, which is in turn a function of the breaker height H_b and the wave breaker angle α_b (CERC, 1984).

(4) The summer-versus-winter variation in ridge and runnel prominence and the number of ridges and runnels was directly related to the incident wave energy level. A critical wave height is likely to exist so that ridges and runnels become more numerous and more prominent if wave-height conditions are below this value. A parameterisation could perhaps be defined as the ratio of the average significant wave height over a three-month period to the average wave height over the year H_{3m}/H_{year}, whereby values above 1 indicate that ridge and runnel morphology becomes flatter and values below 1 indicate that ridges and runnels become more prominent. The contrast between the summer and winter state of the ridge and runnel morphology can further be expressed by the difference between summer and winter average significant wave heights (H_{winter} minus H_{summer}).

(5) Storminess is thought to be important on the intra-annual time-scale and hence the definition of a storminess parameter S seems appropriate. Kroon (1994) used the duration of storm events and the duration of the interval between storm events (i.e., a measure of the storm recurrence interval) to comprise such a parameter, but it may further be essential to incorporate the storm intensity. In this study, storm events were identified using the offshore significant wave height, but this raises problems at the intra-annual time-scale due to the lack of long-term wave data. Wind data, particularly the occurrence and velocity of onshore winds may be the best substitute.

(6) On the largest spatial scale, a coast line, it would be interesting to find a parameterisation that would indicate whether a sandy beach is characterised by ridge and runnel morphology or not. Ridge and runnel morphology tend to be restricted to fetch-limited settings (i.e., reduced wave heights and absence of ocean swell) with low gradient nearshore profiles and meso- to mega-tidal regimes (e.g., King and Williams, 1949; Mulrennan, 1992; Anthony et al., 2004). This suggests that parameters of importance are the relative tide range *RTR* and the beach slope $\tan\beta$.

Two aspects should be kept in mind with parameterisation when scaling up: (1) at the smaller scales, it should be considered whether the application of locally derived

parameters at the seaward boundary (i.e., offshore hydrodynamic conditions) is more appropriate; and (2) parameterisation at larger scales is increasingly difficult due to internal forcing processes (feedback and relaxation time effects). An in-depth analysis of coastal parameterisations that include feedback processes and relaxation time effects will be a challenging step in future research.

Integration of compartments is a difficult process and within this thesis was only a secondary aim. The above-sections should be regarded as an preliminary attempt to contribute to the understanding of ridge and runnel morphology as a geomorphic system.

8.5 GENERAL CONCLUSION

The overall aim of this research was to investigate the morphodynamics of ridge and runnel morphology at a range of nested spatial and temporal scales, drawing upon the theoretical concept of a coastal geomorphic system with a hierarchy of compartments (Section 1.4). According to Kroon and Wijnberg (2002), little is known about the generation, evolution and decay of ridge and runnel morphology and this thesis contributes significantly to the existing literature by presenting an in-depth characterisation of the ridge and runnel morphology and addressing its dynamics at various spatial and temporal scales, ranging from small-scale bed level change over a single tidal cycle to large-scale development of the ridge and runnel morphology over the last decade. Observations were combined to propose a morphodynamic model for ridge and runnel morphology as a geomorphic system and results showed that the interaction of processes at different temporal and spatial scales, in addition to the mixture of forcing-, relaxation time- and feedback-dominated morphological responses, greatly complicates the dynamics of ridge and runnel systems.

More specifically, the defined objectives and conclusions regarding these objectives are:

(1) "to document the longshore morphological variability in ridge and runnel morphology" – The large-scale spatial variability along the coast is manifest in the density of drainage channels. Extensive upper intertidal flats in the north drain substantive amounts of water during the falling tide and here, the ridge and runnel morphology is highly three-dimensional. The sand flats taper out toward the south and ridges and runnels ultimately cover the entire intertidal zone. Concurrently, drainage channels occur less frequently.

(2) "to improve insight into the inter- and intra-annual behaviour of the ridges and runnels" – Ridge and runnel morphology seems permanent along the north Lincolnshire coast and is very dynamic, particularly on intra-annual time-scales. More ridges are present in winter than in summer and the ridges migrate alongshore, onshore and offshore on a monthly time-scale.

(3) "to describe and explain temporal and spatial variability in ridge and runnel dynamics under varying tidal and wave-energy conditions" – On a lunar tidal cycle time-scale, onshore ridge migration is the dominant morphological development

during low-wave energy conditions, whereas the ridge and runnel morphology becomes flatter during storm events, particularly lower on the beach.

(4) "to yield additional insight into the controlling processes for maintenance and evolution of ridge and runnel topography" – The short-term response of ridges and runnels is mainly induced by swash and surf zone processes. Both processes appear to be equally effective in accomplishing morphological change, but there is more scope for surf zone processes to act, because the surf zone is much wider than the swash zone.

References

Aagaard, T., Davidson-Arnott, R.G.D., Greenwood, B. and Nielsen, J. 2004. Sediment supply from shoreface to dunes: linking sediment transport measurements and long-term morphological evolution. Geomorphology, 60, 205–224.

Aagaard, T. and Masselink, G. 1999. The surf zone. In: Short, A.D. (Ed). Handbook of Beach and Shoreface Morphodynamics. John Wiley & Sons Ltd., 72–118.

ABP Research and Consultancy Ltd. 1996. Southern North Sea sediment transport study, literature review and conceptual sediment transport model. Southampton. Report No. R.546, 80 p.

Ackermann, F. 1999. Airborne laser scanning-present status and future expectations. ISPRS Journal of Photogrammetry and Remote Sensing, 54, 164–198.

Adams, J.C. and Chandler, J.H. 2002. Evaluation of LIDAR and medium-scale photogrammetry for detecting soft-cliff coastal change. Photogrammic record, 17, 99, 405–418.

Admiralty Tide Tables. 2001. United Kingdom and Ireland (including European Channel Ports). Hydrographic Office, Taunton, United Kingdom, 440 p.

Admiralty Tide Tables. 2004. United Kingdom and Ireland (including European Channel Ports). Hydrographic Office, Taunton, United Kingdom, 449 p.

Anthony, E.J., Levoy, F. and Monfort, O. 2004. Morphodynamics of intertidal bars on a megatidal beach, Merlimont, Northern France. Marine Geology, 208, 73–100.

Ashkenazi, V., Dumville, M., Bingley, R. and Dodson, A. 2000. The use of remote sensing in climate change. R&D Technical Report E82. Environment Agency R&D Dissemination Centre, Swindon, Uk, 24 p.

Bagnold, R.A. 1963. Mechanisms of marine sedimentation. In: Hill, M.N. (ed). The Sea. Interscience, New York, vol. 3.

Bagnold, R.A. 1966. An approach to sediment transport problem from general physics. Prof. Pap. 422-1, US Geol. Sur., Washington, D.C.

Bailard, J.A. 1981. An energetics total load sediment transport model for a plane sloping beach. Journal of Geophysical Research, 86, C11, 10938–10954.

Bailard, J.A. and Inman, D.L.1981. An energetics bedload model for a plane sloping beach: local transport. Journal of Geophysical Research, 86, C3, 2035–2043.

Bauer, B.O., Veblen, T.T. and Winkler, J.A. 1999a. Old methodological sneakers: fashion and function in a cross-training era. Annals of the Association of American Geographers, 89, 679–687.

Bauer, B.O., Winkler, J.A. and Veblen, T.T. 1999b. Afterword: a shoe for all occasions or shoes for every occasion: methodological diversity, normative fashions, and metaphysical unity in physical geography. Annals of the Association of American Geographers, 89, 771–778.

BBC. 2000. Blackpool Borough Council, Shoreline Strategy Plan, 1994–1999. Blackpool Borough Council. Blackpool.

Bird, E.C.F. 1985. Coastal changes: a global review. Wiley, Chichester.

Bishop, C.T. and Donelan, M.A.1987. Measuring waves with pressure transducers. Coastal Engineering, 11, 309–328.

Brander, R.W. and Cowell, P.J. 2003. A trend-surface technique for discrimination of surf-zone morphology: rip current channels. Earth Surface Processes and Landforms, 28, 905–918.

Brock, J.C., Wright, C.W., Sallenger, A.H., Krabill, W.B. and Swift R.N. 2002. Basis and methods of NASA Airborne Topographic Mapper LIDAR surveys for coastal studies. Journal of Coastal Research, 18, 1, 1–13.

Buonaiuto, F.S. and Craus, N.C. 2003. Limiting slopes and depths at ebb-tidal shoals. Coastal Engineering, 48, 51–65.

Burgess, K., Orford, J., Dyer, K., Townend, I. and Balson, B. 2002. FUTURECOAST - The integration of knowledge to assess future coastal evolution at a national scale. Proceedings 28th International Conference on Coastal Engineering, ASCE, 3221–3233.

Buscombe, D.D. 2002. The short-term morphodynamic response of a ridge-and-runnel system on a macrotidal beach. Lancaster, UK. BSc-thesis, University of Lancaster, 87 p.

Calantoni, J. 2002. Discrete particle model for bedload sediment transport in the surf zone. PhD-thesis, Graduate Faculty, North Carolina State University, 93 p.

Carter, R.W.G. 1988. Coastal Environments. Academic Press, London, 617 p.

CERC. 1984. Shore protection manual (4^{th} edition). Coastal Engineering Research Center, Waterway Experiment Station, Corps of Engineers, Vicksburg.

Chauhan, P.P.S. 2000. Bedform association on a ridge and runnel foreshore: Implications for the hydrography of a macrotidal estuarine beach. Journal of Coastal Research, 16, 1011–1021.

Church, J.C. and Thornton, E.B. 1993. Effects of breaking wave induced turbulence within a longshore current model. Coastal Engineering, 20, 1–28.

Coco, G., Huntley, D.A. and O'Hare, T.J. 2000. Investigation of a self-organising model for beach cusp formation and development. Journal of Geophysical Research, 105, C9, 21991–22002.

Corbau, C., Tessier, B. and Chamley, H.1999. Seasonal evolution of shoreface and beach system morphology in a macrotidal environment, Dunkerque area, Northern France. Journal of Coastal Research, 15, 97–110.

Cowell, P.J. and Thom, B.G. 1994. Morphodynamics of coastal eveolution. In: Carter, R.W.G. and Woodroffe, C.D. (eds), Coastal Evolution, Cambridge University Press, Cambridge, 33–86.

Cracknell, A.P. 2000. Remote sensing techniques in estuaries and coastal zones - an update. International Journal of Remote Sensing, 20, 3 (15 FE 1999), 485–496.

Dabrio, C.J. 1982. Sedimentary structures generated on the foreshore by migrating ridge and runnel systems on microtidal and mesotidal coast of Spain. Sedimentary Geology, 32, 141–151.

Darras, M. 1987. List of sea state parameters. IAHR Supplement to Bulletin 52, 11–43.

Davidson-Arnott, R.G.D. 1988. Controls on formation and form of barred nearshore profiles. Geographical Review, Vol. 78, No.2, 185–193.

Davies, J.L. 1964. A morphogenic approach to world shorelines. Zeitschrift für Geomorphologie, 8, 127–142.

Davis, R.A., Fox, W.T., Hayes, M.O., Boothroyd, J.C. 1972. Comparison of ridge and runnel systems in tidal and non-tidal environments. Journal of Sedimentary Petrology, 2, 413–421.

De Boer, D.H. 1992. Hierarchies and spatial scale in process geomorphology: a review. Geomorphology, 4, 303–318.

De Vriend, H.J., 1992. Mathematical modelling and large-scale coastal behaviour. Part1: Physical processes. Journal of Hydraulic Research, 29, 6, 727–740.

Drake, T.G. and Callantoni, J. 2001. Discrete-particle model for sheet flow sediment transport in the nearshore. transport in the nearshore. Journal of Geophysical Research-Oceans, 106, C9, 19859–19868.

Draper, L. 1991. Wave Climate Atlas of the British Isles. Department of Energy, Offshore Technology Report, OTH 89 303, HSMO, London, United Kingdom.

Elgar, S., Gallagher, E. and Guza, R. 2001. Nearshore sandbar migration. Journal of Geophysical Research, 106, 11623–11627.

French, J.R. 2003. Airborne LIDAR in support of geomorphologic and hydraulic modelling. Earth Surface Processes and Landforms, 28, 3, 321–335.

Gallagher, E.L., Elgar, S. and Guza, R.T. 1998. Observations of sand bar evolution on a natural beach. Journal of Geophysical Research, 103, C2, 3203–3215.

Greenwood, B., Aagaard, T. and Nielsen, J. 2004. Swash bar morphodynamics in the Danish Wadden Sea: sand bed oscillations and suspended sediment flux during and accretionary phase of the foreshore cycle. Danish Journal of Geography, 104, 1, 15–30.

Halcrow. 1988. The Sea Defence Management Study for the Anglian Region. Study report and Atlas. Sir William Halcrow&Partners Ltd. Swindon.

Hallermeier, R.J. 1981. Terminal settling velocity of commonly occurring sand grains. Sedimentology, 28, 859–865.

Hampton, M.A., Dingler J.R., Sallenger, A.H. (Jr.), and Richmond, B.M. 1999. Storm-related change of the northern San Mateo County coast, California. Proceedings Coastal Sediments '99, ASCE, 1311–1323.

Hayes, M.O. 1967. Hurricanes as geological agents: case study of hurricanes Carla 1961, and Cindy 1963. Bur. Econ. Geol., Rep. No. 61, Univ. Texas, 54 pp.

Hayes, M.O. and Boothroyd, J.C. 1969. Storms as modifying agents in the coastal environment. In: Eastern Section, S.E.P.M. Guidebook, May 9–11, 245–265.

Hoefel, F. and Elgar, S. 2003. Wave-induced sediment transport and sandbar migration. Science, 299, 1885–1887.

Huising, E.J. and Vaessen, E.M.J. 1997. Evaluating laser scanning and other techniques to obtain elevation data on the coastal zone. Proceedings of the Fourth International Conference on Remote Sensing for Marine and Coastal Environments, Orlando, 510–517.

Irish, J.L. and Lillycrop, W.J. 1997. Monitoring New Pass, Florida, with high density LIDAR bathymetry. Journal of Coastal Research, 13, 4, 1130–1140.

Irish, J.L. and Lillycrop, W.J. 1999. Scanning laser mapping of the coastal zone: the SHOALS system. ISPRS Journal of Photogrammetry and Remote Sensing, 54, 123–129.

Irish, J.L. and White, T.E. 1998. Coastal engineering applications of high-resolution LIDAR bathymetry. Coastal Engineering, 35, 47–71.

King, C.A.M. 1972a. Beaches and Coasts. Edward Arnold, London, 570p.

King, C.A.M. 1972b. Dynamics of beach accretion in south Lincolnshire, England. In Coastal Geomorphology, Coates, D.R. (ed.). Proceedings 3rd Annual Geomorphology Symposia Series, Binghampton, Allen&Unwin, London, 73–98.

King, C.A.M. and Barnes, F.A. 1964. Changes in the configuration of the inter-tidal beach zone of part of the Lincolnshire coast since 1951. Zeitschrift für Geomorphologie, 8, 105–126.

King, C.A.M. and Williams, W.E., 1949. The formation and movement of sand bars by wave action. Geographical Journal, 113, 70–85.

Komar, P.D. 1998. Beach processes and sedimentation, 2nd ed. Prentice Hall, Upper Saddle River, NJ, 544 p.

Krabill, W.B., Abdalati, W., Frederick, E.B., Manizade, S.S., Martin, C.F., Sonntag, J.G., Swift, R.N., Thomas, R.H. and Yungel, J.G. 2002. Aircraft laser altimetry measurement of elevation changes of the Greenland ice sheet: technique and accuracy assessment. Journal of Geodynamics, 34, 357–376.

Kroon, A. 1994. Sediment transport and morphodynamics of the beach and nearshore zone near Egmond, the Netherlands. PhD-thesis, Utrecht University, 275 p.

Kroon, A. and Masselink, G. 2002. Morphodynamics of intertidal bar morphology on a macrotidal beach under low-wave energy conditions, north Lincolnshire, England. Marine geology, 190, 591–608.

Lemm, A.J., Hegge, B.J. and Masselink, G. 1999. Offshore wave climate, Perth (Western Australia): 1994–1996. Marine and Freshwater Research, 50, 95–102.

Levoy, F., Anthony, E., Barusseau, J.-P., Howa, H., Tessier, B. 1998. Morphodynamics of a macrotidal ridge and runnel beach. Comptes Rendus Academie des Sciences, 327, 811–818.

Levoy, F., Anthony, E.J., Monfort, O. and Larsonneur, C. 2000. The morphodynamics of megatidal beaches in Normandy, France. Marine Geology, 171, 39–59.

Lillycrop, W.J., Irish, J.L. and Parson, L.E. 1999. SHOALS system. Sea technology, 38, 6 (1997), 17–25.

Lippmann, T.C. and Holman, R.A. 1989. Quantification of sand bar morphology: a video technique based on wave dissipation. Journal of Geophysical Research, 94, C1, 995–1011.

Lippmann, T.C. and Holman, R.A. 1990. The spatial and temporal variability of sand bar morphology. Journal of Geophysical Research, 95, C7, 11575–11590.

Lippmann, T.C., Holman, R.A. and Hathaway, K.K. 1993. Episodic, nonstationary behavior of a double bar system at Duck, North Carolina, U.S.A., 1986–1991. Journal of Coastal Research, 15, Special Issue, 49–75.

Mason, D.C., Gurney, C., and Kenneth, M. 2000. Beach topography mapping-a comparison of techniques. Journal of Coastal Conservation, 6, 1, 113–124.

Masselink, G. 1993. Simulating the effects of tides on beach morphodynamics. Journal of Coastal Research, Special Issue 15, 180–197.

Masselink, G. In press. Formation and evolution of multiple intertidal bars on macrotidal beaches: application of morphodynamic model. Coastal Engineering, article in press, 18p.

Masselink, G. and Anthony, E.J. 2001. Location and height of intertidal bars on macrotidal ridge and runnel beaches. Earth Surface Processes and Landforms, 26, 759–774.

Masselink, G. and Hughes, M.G. 2003. Introduction to coastal processes and geomorphology. Oxford University Press Inc, New York, 354p.

Masselink, G., Kroon, A., Davidson-Arnott, R.G.D. Submitted. Intertidal bar morphodynamics – a review. Geomorphology.

Masselink, G., Hegge, B.J. and Pattriarchi, C.B. 1997. Beach cusp morphodynamics. Earth Surface Processes and Landforms, 22, 1139–1155.

Mitasova, H., Bernstein, D., Drake, T.G., Harmon, R. and Miller, C. 2003. Spatio-temporal analysis of beach morphology using LIDAR, RTK-GPS and open source GRASS GIS. Coastal Sediments '03, proceedings, digital document. 11p.

Michel, D. and Howa, H.L. 1999. Short-term morphodynamic response of a ridge and runnel system on a mesotidal sandy beach. Journal of Coastal Research, 15, 428–437.

Moore, J.N., Fritz, W.J. and Futch, R.S. 1984. Occurrence of megaripples in a ridge and runnel system, Sapelo Island, Georgia: morphology and processes. Journal of Sedimentary petrology, Vol. 54, No. 2, 615–625.

Motyka, J.M. 1986, A macro review of the coastline of England and Wales, Volume 2: The East coast, the Tees to the Wash. Report SR107, HR Wallingford Ltd.

Mulrennan, M.E. 1992. Ridge and runnel beach morphodynamics: an example from the central east coast of Ireland. Journal of Coastal Research, 8, 906–918.

Navas, F. and Malvarez, G. 2002. Dundrum Bay: Coastal processes and modelling. In: Knight, J. (editor), Field guide to the coastal environments of northern Ireland, University of Ulster, Coleraine, Northern Ireland, 68–73.

Navas, F., Cooper, J.A.G., Malvarez, G.C. and Jackson, D.W.T. 2001. Theoretical approach to the investigation of ridge and runnel topography of a macrotidal beach: Dundrum Bay, Northern Ireland. Journal of Coastal Research, Special Issue 34, 183–193.

NCEDS (National Centre for Environmental Data and Surveillance). 1997. Evaluation of the LIDAR technique to produce elevation data for use within the Agency. R&D Technical Report of the National Centre for Environmental Data and Surveillance, Environment Agency, Bath, UK, 74p.

NOAA-USGS, 2004, LIDAR Missions, Electronic Document, http:\www.csc.noaa.gov/crs/tcm/missions.html

Odd, N.V., Baugh, J.V., Murphy, D.G., Cooper, A.J. and Oaks, A.M. 1995. Development and Application of NORPOLL (Mk1.1) to Predict the Effect of Load Reductions and Concentrations of Cadmium and Lead, Particulate Pollutants in the North Sea-PhaseII Final Report. Report SR383, HR Wallingford Ltd.

Orford, J.D. 1985. Murlough Spit, Dundrum Bay. In: Whalley, B., Smith, B.J., Orford, J.D. and Carter, R.W. (editors). Fieldguide to Northern Ireland. Queens University, Belfast, 68–76.

Orford, J. D. and Wright, P. 1978. What's in a name?-Descriptive or genetic implications of 'Ridge and Runnel' topography. Marine Geology, 28, M1–M8.

Orme, A. R and Orme A. J. 1988. Ridge-and-Runnel Enigma. The Geographical Review, American Geographical Society, 78, 169–184.

Osborne, P.D. and Greenwood, B.G. 1992a. Frequency dependent cross-shore, suspended sediment transport: 1. A non-barred shoreface. Marine Geology, 106, 1–24.

Osborne, P.D. and Greenwood, B.G. 1992b. Frequency dependent cross-shore, suspended sediment transport: 2. A barred shoreface. Marine Geology, 106, 25–51.

Owens, E.H. and Frobel, D.H. 1977. Ridge and runnel systems in the Magdalen Islands, Quebec. Journal if sedimentary Petrology, 47, 1, 191–198.

Parker, W. R. 1975. Sediment Mobility and Erosion on a Multibarred Foreshore (Southwest Lancashire, U.K.). In Nearshore Sediment Dynamics and Sedimentation, Hails, J. and Carr, A. (eds). Wiley and Sons, London, 151–179.

Parson, L.E., Lillycrop, W.J., Klein, C.J., Ives, R.C.P. and Orlando, S.P. 1997. Use of LIDAR technology for collecting shallow water bathymetry of Florida Bay. Journal of Coastal Research, 13, 4, 1173–1180.

Pethick, J. 2001. Coastal management and sea-level rise. Catena 42, 307–322.

Pettijohn, F.J., Potter, P.E. and Siever, R. 1987. Sand and sandstone. Springer-Verlag, New York. 553 p.

Phillips, J.D. 1992. The end of equilibrium?. Geomorphology, 5, 195–201.

Plant, N.G., Holman, R.A. Freilich, M.H. and Birkemeier, W.A. 1999. A simple model for interannual sandbar behavior. Journal of Geophysical Research, 104, C7, 15755–15776.

Plant, N.G., Freilich, M.H., Holman, R.A. 2001. Role of morphological feedback in surf zone sand bar response. Journal of Geophysical Research, 106, 973–989.

Posford-Duvivier, 1996. Lincolnshire shoreline management plan. Internal report of Environment Agency, Anglian Region. Rightwell House, Bretton Centre, Peterborough.

Pye, K. 1995. Controls on Long-term Saltmarsh Accretion and Erosion in the Wash, Eastern England. Journal of Coastal Research, 11, 337–356.

Reichmüth, B. 2003. Contribution a la connaissance de la morphodynamique des plages a barres intertidales: example de la Côte d'Opale, Nord de la France. PhD thesis in physical geography, University du littoral, Côte d'Opale, Dunkerque, France, 248 p.

Reichmüth, B. and Anthony, E.J. 2002. The variability of ridge and runnel beach morphology: Examples from Northern France. Journal of Coastal Research, Special Issue 36, 612–621.

Revell, D.L., Komar, P.D. and Sallenger, A.H. 2002. An application of LIDAR to analysis of El Niño erosion in the Netarts Littoral Cell, Oregon. Journal of Coastal Research, 18, 4, 792–801.

Rhoads, B.L. 1999. Beyond pragmatism: the value of philosophical discourse for physical geography. Annals of the Association of American Geographers, 89, 760–771.

Robinson, A.H.W. 1968. The Use of Sea Bed Drifter in Coastal Studies with Particular Reference to the Humber. Zeitschrift für Geomorphologie, volume 7.

Robinson, D.N. 1956. The North East coast of Lincolnshire, a study in coastal evolution. PhD-thesis, University of Nottingham, United Kingdom, 91 p.

Robinson, D.N. 1981. The book of the Lincolnshire Seaside, the story of the coastline from the Humber to the Wash. Barracuda Books Ltd, Buckingham, England, 172 p.

Ruessink, B.G. 1998. Infragravity waves in a dissipative multiple bar system. PhD-thesis, Utrecht University, 245 p.

Ruessink, B.G. and Kroon, A. 1994. The behaviour of a multiple bar system in the nearshore zone of Terschelling, the Netherlands: 1965–1993. Marine Geology, 121, 187–197.

Ruessink, B.G., Houwman, K.T. and Hoekstra, P. 1998. The systematic contribution of transporting mechanisms to the cross-shore sediment transport in water depths of 3 to 9 m. Marine Geology, 152, 295–324.

Sallenger, A.H., Holman, R.A. and Birkemeier, W.A. 1985. Storm-induced response of a nearshore-bar system. Marine Geology, 64, 237–257.

Sallenger, A.H., Krabill, W., Brock, J., Swipt, R., Jansen, M., Manizade, S., Richmond, B., Hampton, M. and Eslinger, D. 1999. Airborne laser study quantifies El Nino-induced coastal change. EOS, Transactions American Geophysical Union, 80, 89, 92–93.

Sallenger, A.H. (Jr.), Krabill, W.B., Swift, R.N., Brock, J., List, J., Hansen, M., Holman, R.A., Manizade, S., Sontag, J., Meredith, A., Morgan, K., Yunkel, J.K., Frederick, E.B. and Stockdon, H. 2003. Evaluation of airborne topographic LIDAR for quantifying beach changes. Journal of Coastal Research, 19, 1, 125–133.

Shand, R.D., Bailey, D.G., Shepard, M.J. 1999. An inter-site comparison of net offshore bar migration characteristics and environmental conditions. Journal of Coastal Research, 15, 750–765.

Shields, A. 1936. Anwendung der ahnlichkeits-mechanik und der turbulenz-forshung auf die geschiebebewegung. Preussische Versuchsanstalt fur Wasserbau und Schiffbau, 26.

Short, A.D. and Aagaard, T. 1993. Single and multi-bar beach change models. Journal of Coastal Research, Special Issue 15, 141–157.

Simpson, J.H. 1994. The North Sea Project: an overview and way forward. In: Chanock, H. et al. (eds). Understanding the North Sea System, Chapman & Hall, London, 207–218.

Sipka, V. and Anthony, E.J. 1999. Morphology and hydrodynamics of a macrotidal ridge and runnel beach under modal low wave conditions. Journal Recherche Oceanographique, 24, 24–31.

Southgate, H.N. and Beltran, L.M. 1998. Self-organisational processes in beach morphology. Proceedings of the 8th International Bi-ennial Conference on Physics of Estuaries and Coastal Seas. Balkema, Rotterdam, 409–416.

Stockdon, H.F., Sallenger, A.H. (Jr.), List, J.H. and Holman, R.A. 2002. Estimation of shoreline position and change using airborne topographic LIDAR data. Journal of Coastal Research, 18, 3, 502–513.

Svendsen, L.A.1984. Wave heights and set-up in a surf zone. Coastal Engineering, 8, 303–329.

Terwindt, J.H.J. and Battjes, J.A. 1990. Research on large-scale coastal behaviour. Proceedings 22nd International Conference on Coastal Engineering, ASCE, 1975–1983.

Terwindt, J.H.J. and Wijnberg, K.M. 1991. Thoughts on large scale coastal behaviour. Proceedings Coastal Sediments '91, ASCE, 1476–1487.

Thornton, E.B. and Guza, R.T. 1982. Energy saturation and phase speeds measured on a natural beach. Journal of Geophysical Research, 97, 9499–9508.

Thornton, E.B. Humiston, R.T. and Birkemeier, W. 1996. Bar/trough generation on a natural beach. Journal of Geophysical Research, 101, 12097–12110.

TU Delft. 1997. Hand-out of course on aircraft laser altimetry held on 1–2 April.

Tucker, M.J., Carr, A.P. and Pitt, E.G. 1983. The effect of an offshore bank in attenuating waves. Coastal Engineering, 7, 133–144.

Van den Berg, J.H. 1977. Morphodynamic development and preservation of physical sedimentary structures in two prograding recent ridge and runnel beaches along the Dutch coast. Geologie en Mijnbouw, 56, 185–202.

Van Enckevort, I.M.J. and Ruessink, B.G. 2003a. Video observations of nearshore bar behaviour. Part 1: alongshore uniform variability. Continental Shelf Research, 23, 501–512.

Van Enckevort, I.M.J. and Ruessink, B.G. 2003b. Video observations of nearshore bar behaviour. Part 2: alongshore non-uniform variability. Continental Shelf Research, 23, 513–532.

Van Houwelingen, S.T., Masselink, G., and Bullard, J.E. submitted. Dynamics of multiple intertidal bars, north Lincolnshire, England. Earth surface processes and landforms.

Voulgaris, G., Mason, T. and Collins, M.B. 1996. An energetics approach for suspended sand transport on macrotidal ridge and runnel beaches. Proceedings of 25th International Confeence on Coastal Engineering. ASCE, 3948–3961.

Voulgaris, G., Simmonds, D., Michel, D., Howa, H., Collins, M.B. and Huntley, D.A. 1998. Measuring and modelling sediment transport on a macrotidal ridge and runnel beach: An intercomparison. Journal of Coastal Research, 14, 315–330.

Wehr, A. and Lohr, U. 1999. Airborne laser scanning-an introduction and overview. ISPRS Journal of Photogrammetry and Remote Sensing, 54, 68–82.

Wemelsfelder, P.J. 1953. The disaster in the Netherlands caused by the storm flood of February 1, 1953. Proceedings of the 4th Coastal Engineering Conference, ASCE, 256–271.

White, S.A. and Wang, Y. 2003. Utilizing DEMs derived from LIDAR data to analyze morphologic change in the North Carolina coastline. Remote Sensing of Environment, 85, 39–47.

Wijnberg, K.M. 1995. Morphologic behaviour of a barred coast over a period of decades. PhD-thesis, Utrecht University, 245 p.

Wijnberg, K.M. 1996. On the systematic offshore decay of breaker bars. Proceedings of the 25th International Conference on Coastal Engineering, ASCE, 3600–3613.

Wijnberg, K.M. 2002. Environmental controls on decadal morphologic behaviour of the Holland coast. Marine Geology, 189, 227–247.

Wijnberg, K.M., Kroon, A. 2002. Barred beaches. Geomorphology, 48, 103–120.

Wijnberg, K.M. and Terwindt, J.H.J. 1995. Extracting decadal morphological behavior from high-resolution, long-term bathymetric surveys along the Holland coast using eigenfunction analysis. Marine Geology, 126, 301–330.

Woolard, J.W. and Colby, J.D. 2002. Spatial characterization, resolution, and volumetric change of coastal dunes using airborne LIDAR: Cape Hatteras, North Carolina. Geomorphology, 48, 269–287.

Wright, P. 1976. The Morphology, Sedimentary Structures and Processes of the Foreshore at Ainsdale. PhD thesis, University of Reading, 367p.

Wright L.D. and Short A.D. 1984. Morphodynamic variability of surf zones and beaches: a synthesis. Marine Geology, 56, 93–118.

Wright, L.D., Guza, R.T and Short, A.D. 1982a. Dynamics of a high-energy dissipative surf zone. Marine Geology, 45, 41–62.

Wright, L.D., Nielsen, P., Short, A.D. and Green, M.O. 1982b. Morphodynamics of a macrotidal beach. Marine Geology, 50, 97–128.

Zhang, K., Leatherman, S., Whitman, D. and Robertson, W. 2003. Quantification of overwash deposition and post-storm recovery along Assateague Island, Maryland-Virginia using airborne LIDAR surveys. Coastal Sediment '03, Book of Abstracts, 371–372.